Investigating the feasibility of utilizing AUV and Glider technology for mapping and monitoring of the UK MPA network

Final report for Defra project MB0118

Project Leader: Dr Russell B Wynn (NOC)

Report published and delivered in September 2012 by the National Oceanography Centre and the UK Marine Environmental Mapping Programme (MAREMAP) of the Natural Environment Research Council (NERC)

This report has been prepared by the Natural Environment Research Council (the Council) as represented by the National Oceanography Centre, with reasonable skill and care within the terms of the Contract with the Customer, as defined in the Scope of Work.

No responsibility or liability is accepted for any use which may be made of the Work or results produced, nor for any reliance which may be placed on such Work or results, other than that use or reliance to which the Council has expressly consented to in writing.

This report should be referenced as follows:

Wynn, R.B., Bett, B.J., Evans, A.J, Griffiths, G., Huvenne, V.A.I., Jones, A.R., Palmer, M.R, Dove, D., Howe, J.A, Boyd, T.J. and MAREMAP partners (2012) *Investigating the feasibility of utilizing AUV and Glider technology for mapping and monitoring of the UK MPA network*. Final report for Defra project MB0118. National Oceanography Centre, Southampton. 244 pp.

Executive summary

- This report investigates the potential benefits of increased use of **propeller-driven Autonomous Underwater Vehicles** and **buoyancy-driven Gliders** for mapping and monitoring of UK waters, with specific reference to the developing **Marine Protected Area (MPA)** network.

- A total of **about 40 AUVs and Gliders are currently operating within the public sector**, with major users including the Natural Environment Research Council (NERC), its Delivery Partners, UK universities, and the Ministry of Defence. A range of vehicles is also operated by the international commercial sector, mainly for use by the hydrocarbons industry.

- AUVs such as the NERC Autosub vehicles can access **water depths to 6000 m** and typically undertake missions lasting from hours to a few days; they are capable of collecting geophysical, biological and oceanographic data from **both the seafloor and water column**. Gliders are used to collect **water column hydrographic and biological data** and, due to their lower energy demands, can be deployed on **missions lasting several weeks**. New acoustic sensors such as echo-sounders and cetacean monitors are currently being integrated, making them increasingly suitable for **multi-trophic-level surveys**.

- New developments such as **Autosub Long Range**, with an endurance of several months, will see AUVs increasingly being used for mapping and **long-term monitoring** of distant deep-water sites. **Air-launched AUVs** may become viable in future, and could be useful in situations requiring a **rapid response**, e.g. Harmful Algal Blooms or oil spills.

- AUVs and Gliders operate independently of a research vessel and can be deployed in most areas of the UK EEZ. However, their ability to collect certain data, e.g. seafloor photos, and undertake spatially accurate repeat transects, may be compromised in areas of **strong tidal currents and/or high turbidity**, e.g. near coastal headlands and in areas of high plankton biomass. In some areas their missions may have an elevated risk of disruption through **entanglement** with fishing gear or other marine debris, and **collision** with shipping traffic or offshore structures. These constraints need to be taken into account during mission planning.

- Within the **UK EEZ only about 26% of the seafloor has been mapped with multibeam,** which is the typical base layer for habitat mapping. This figure drops to **less than 20% for the EEZs of the UK Overseas Territories (OTs), which c**ollectively amount to about 5.8 million km^2 of marine area (whereas the land area amounts to just 20,000 km^2, or 0.3% of the marine area). The UK also has **two of the largest MPAs** on the planet within OTs, including the EEZ of the British Indian Ocean Territory (BIOT, covering 630,000 km^2) and South Georigia and the South Sandwich Islands (covering 1,000,000 km^2).

- Seafloor multibeam bathymetry mapping with AUVs is currently focussed on small areas where **high-resolution data** are required, but future technological developments may see them deployed for routine mapping (especially in hostile or relatively inaccessible regions) to help fill some of the gaps in coverage. It is also clear that **effective co-ordination of effort and application of appropriate technologies** will be required to address this gross under-sampling of UK waters.

- A series of **case studies** were produced for this report, in order to highlight the **capabilities and limitations** of AUVs and Gliders for marine mapping and monitoring in both shallow and deep-water environments. Equivalent vessel-based case studies were also included, to enable comparison of costs and data quality.

- Case Study 1 saw NERCs **Autosub6000 AUV** undertake detailed **habitat mapping off northwest UK** in partnership with JNCC, with a particular focus on existing and proposed Special Areas of Conservation (SAC). Flying the vehicle close to the seabed allowed collection of **higher-resolution bathymetry and sidescan sonar data than is possible with a research vessel**, providing important new insights into the condition and boundaries of SACs for cold-water coral communities at water depths >1000 m.

- Case Study 2 saw **Autosub6000** deployed over the Greater Haig Fras SAC and rMCZ off southwest UK in 100 m water depth. High-resolution multibeam bathymetry and sidescan sonar data **compared well** with equivalent Cefas vessel-based data from the same area, and the instrument also collected valuable water column data and a total of **15,000 full-colour seafloor photos**. The integrated dataset illustrates the potential of the vehicle for producing **ground-truthed habitat maps**.

- Case Study 3 involved two deployments of the SAMS **Seaglider 'Talisker'** across the Rockall Trough off northwest UK, in order to collect oceanographic transect data to depths of up to 1000 m. The Glider collected **hundreds of vertical profiles** of temperature, salinity, dissolved oxygen, chlorophyll-a fluorescence, and optical backscatter, allowing characterisation of different water masses. Both missions were successful, and underline the ability of Gliders to collect data in **hostile conditions at high spatial and temporal resolution**.

- Case Study 4 involved two successful deployments of a NERC **shallow-water Slocum Glider** in the Irish Sea, one looking at the Western Irish Sea (WIS) gyre and the other the Mersey Plume (MP). Both missions demonstrated the ability of Gliders to collect data in areas of relatively **strong tidal flow and busy shipping and fishing activity**. They also showed how Gliders can monitor development of **temporally and spatially variable oceanographic features**, and the influence of these features on plankton biomass.

- Case Study 5 is based upon a habitat-mapping cruise to the deep-water Whittard Canyon off southwest UK, on the **NERC vessel RRS *James Cook***. A total of >700 km of track-lines were surveyed with sidescan sonar, and 6130 km^2 of hull-mounted multibeam data were collected. This base mapping helped guide detailed ground-truthing, including ROV dives and coring. The results showed the importance of a **nested approach to mapping of complex habitats**, and that steep canyon-wall environments are important refuges for vulnerable cold-water coral communities.

- Case Study 6 includes data from new **high-resolution multibeam bathymetry mapping** of the shallow Sea of the Hebrides, most of which was undertaken on small inshore vessels as part of the **MCA Civil Hydrography Programme** to order 1a standards (metre-scale resolution). The high quality of multibeam imagery obtained from this bedrock-dominated terrain mean that **the results can be used for navigational purposes**, as well as for geological and habitat mapping purposes.

- Case Study 7 saw the **BGS inshore vessel, *White Ribbon*,** conduct seafloor mapping and sampling around the Isle of May (which has MPA status). High-resolution multibeam and sidescan sonar data were subsequently ground-truthed with 256 seafloor photographs, with the latter also being used for **novel grain size assessment**. The results reveal a variety of habitat types, while repeat survey of one area showed no significant difference in seabed character over a four-year period.

- The increasing cost of research vessel operations, and rapid developments in AUV and Glider technology, mean that these instruments are inevitably going to play an increasing role in marine mapping and monitoring of UK waters. **Gliders are particularly cost-effective** for long-term monitoring of hydrography and pelagic ecosystems, while AUVs can provide seafloor mapping and water column data at **higher resolution** than vessels (especially important in areas of complex habitats). However, research vessels are still an optimal platform in nearshore environments and/or where direct sampling is required.

- **Integration of AUV and Glider technology into routine surveys, combined with improved co-ordination and sharing of expensive marine infrastructure (e.g. research vessels), has the potential to generate significant cost savings to UK Government in the future.**

Contents

Contributors

Mr Chris Balfour (National Oceanography Centre)
Dr Brian Bett (National Oceanography Centre)**
Dr David Billett (National Oceanography Centre)
Mr Alan Evans (National Oceanography Centre)*
Prof Gwyn Griffiths (National Oceanography Centre)*
Dr Veerle Huvenne (National Oceanography Centre)**
Miss Alice Jones (National Oceanography Centre)*
Mr Phil Knight (National Oceanography Centre)
Mr Andrew Lane (National Oceanography Centre)
Dr Tim Le Bas (National Oceanography Centre)
Mr Steve McPhail (National Oceanography Centre)
Miss Clare O'Neill (National Oceanography Centre)
Dr Matthew Palmer (National Oceanography Centre)**
Dr Henry Ruhl (National Oceanography Centre)
Dr Russell Wynn (National Oceanography Centre)*

Mr Dayton Dove (British Geological Survey)**
Mr Simon Ritson (British Geological Survey)
Mr Nick Smart (British Geological Survey)

Dr John Howe (Scottish Association for Marine Science)**
Dr Tim Boyd (Scottish Association for Marine Science)**

*Work Package leader
**Case Study Leader

Introduction

The UK is committed to establishment of an ecologically coherent network of Marine Protected Areas (MPAs) in the coming years. The network will require initial high-resolution seafloor mapping to provide a baseline for future monitoring. This baseline mapping and subsequent long-term monitoring will generate significant costs to Government, especially as many proposed sites are far offshore in outer shelf or deep-water locations. The aim of this project is to assess whether propeller-driven Autonomous Underwater Vehicles (AUVs) and buoyancy-driven Gliders can provide a fit-for-purpose and cost-effective method for mapping and monitoring the future UK MPA network.

The project will initially establish the current and future capabilities of the Government-owned AUV and Glider fleet, and provide comparison with commercially available systems in the UK/EU and elsewhere. The spatial and temporal limits of AUV and Glider deployment in UK waters will then be investigated, including the effects of high tidal flow, turbidity and commercial shipping/fishing activity. The potential application of AUV and Glider technology to mapping of UK Overseas Territories will also be explored.

Provision of several case studies from UK waters will allow comparison of the resolution, spatial extent, calibration/repeatability and quality of data collected with different survey methods, including deep- and shallow-water AUV and Glider deployments, and deep- and shallow-water boat-based mapping in a variety of environments. These case studies will come from locations in English and Scottish waters, including existing cSACs and rMCZs. It should be noted that existing case study data have been collected by NERC at a total cost of >£2M (including £1M in summer 2011), therefore providing significant added value to this project.

Finally, the project will explore the cost-benefit, advantages/disadvantages and operational risks of different survey methods, e.g. cost/time per unit area, data handling requirements etc. A series of conclusions and recommendations will be provided, e.g. the potential for proof-of-concept case studies in the future, such as integrated bio-physical AUV/Glider surveys incorporating new acoustic sensors.

The project team comprises the Lead Partners of the UK Marine Environmental Mapping Programme (MAREMAP), i.e. National Oceanography Centre (NOC), British Geological Survey (BGS) and Scottish Association for Marine Science (SAMS). NOC are the lead organization for this project. Note that NOC and BGS are both component bodies of the Natural Environment Research Council (NERC), and are therefore treated as the same legal entity. SAMS have been sub-contracted by NOC for the purposes of this project.

Work Package 1: Introduction to the UK Government AUV and Glider fleet

WP Leader: Prof Gwyn Griffiths (NOC)

1.1. The WP1 task

As set out in the proposal this task's remit was as follows:

"*The NERC-owned AUV and Glider fleet is based at two centres: the Marine Autonomous and Robotic Systems facility (MARS) at NOC, and the North Atlantic Glider Base (NAGB) at SAMS. This WP will include an inventory of the AUV and Glider capability within MARS and NAGB. Future developments, e.g. Autosub Long-Range and aerial deployment of mini AUV/Glider devices will also be considered. Comparison will be made with commercial systems in UK/Europe and elsewhere*."

While the scope of the task has not changed, the wording has been altered to reflect:

a) Organisational developments in NERC to May 2012;
b) Clarification on the ownership of vehicles and;
c) To align with the title of this work-package, reference needs to be made to assets owned by the Ministry of Defence.

Consequently, the following is the revised remit for this work package's task:

"*The NERC-owned AUV and Glider fleet is managed by the Marine Autonomous and Robotic Systems facility (MARS) at NOC. The North Atlantic Glider Base (NAGB) at SAMS and the Glider activity at the BAS are delivery partners of MARS. This WP will include an inventory of the AUV and Glider capability within MARS, its partners, UK Universities and the Royal Navy. Future developments, e.g. Autosub Long-Range and aerial deployment of mini AUV/Glider devices will also be considered. Comparison will be made with commercial systems in UK/Europe and elsewhere*.

This WP will be undertaken by NOC (with limited input from SAMS) between 1 March and 31 May 2012."

1.2. Outline of relevant organisations owning AUVs and Gliders

This section outlines the glider and AUV capability and assets within the Natural Environment Research Council, its delivery partners, UK universities and the Ministry of Defence. A summary table is available in Appendix 1.

1.2.1. Natural Environment Research Council

Marine Autonomous and Robotic Systems (MARS) at the NOC

The National Oceanography Centre has been at the forefront of designing, developing and operating autonomous underwater vehicles since 1989. The result has been the Autosub family of vehicles, which currently comprises Autosub3 (1600 m depth rated), Autosub6000 (6000 m depth rated) and Autosub Long Range (6000 m depth rated and endurance of up to 6000 km). More details are provided in section 1.4. Since 2006 the NOC has owned and operated commercial-off-the-shelf (COTS) undersea gliders. These were procured to support specific research projects, and so were under the control of individual Principal Investigators within the science groups. By early 2011 it was clear that a more effective

organisation of the NOC's eleven gliders and three AUV assets (Fig. 1.1) was required, and a review led to the formation of the Marine Autonomous and Robotic Systems (MARS) facility within the National Marine Facilities Division at NOC.

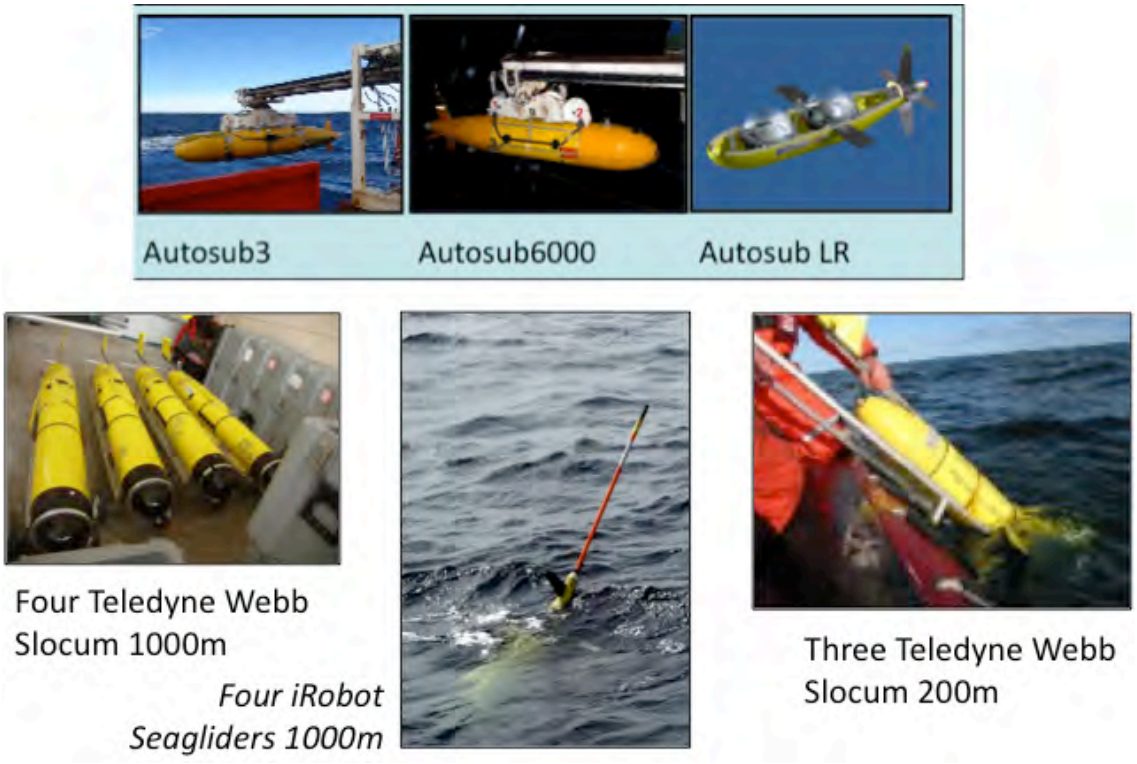

Figure 1.1: The NOC AUV and Glider fleet

The mission for MARS is:
"*To deliver National Capability in Autonomous Vehicles in an impartial and transparent manner to the UK's marine science community, incorporating operations, research and development and to provide a focal point and champion for this community, raising its profile and impact with key stakeholders, research funding bodies and the public*."

MARS has the following vision:
"*Our vision is that by 2016 we will be recognised as the world leader in the integrated provision of autonomous vehicles for marine science, with effective deployments, novel capabilities and strong partnerships*."

One of the internationally distinctive aspects of MARS is that it combines expertise in all forms of autonomous undersea vehicles within one group, and that it supports operations as well as development of new capability.

While MARS is an activity of the NOC, it currently has two delivery partners, each with Glider and AUV activity and their own assets. The delivery partners are BAS and SAMS.

PHysical Oceanographic and Biogeochemical Observations of the Southern Ocean (PHOBOS) at BAS

The PHysical Oceanographic and Biogeochemical Observations of the Southern Ocean (PHOBOS) activity at BAS is a delivery partner of MARS at NOC. By the very nature of the research activity of BAS in the Southern Ocean and Antarctica, the servicing and logistics requirements for their vehicles are best met from teams embedded within BAS programmes.

However, very close technical and scientific links exist with MARS to ensure exchange of knowledge and experience and to reduce costs wherever possible.

BAS operates two Teledyne Webb Research 1000 m depth rated G2 Slocum Gliders, Swallow and Amazon, and took delivery of an iRobot Seaglider in March 2012. The two Slocum Gliders were tested successfully in Oban in early October 2011. From late 2012 they will be deployed from Rothera on the Antarctic Peninsula each summer to give spatial context to the Rothera oceanographic and biological Time Series (RaTS) and to investigate flows of warm Circumpolar Deep Water onto the shelf[1]. The Seaglider will contribute to ecosystem studies in the Southern Ocean and will be fitted with acoustic instrumentation for krill swarm detection and abundance estimates.

For matters connected with Gliders at BAS the contact is Dr Mike Meredith: mmm@bas.ac.uk, and Dr Sophie Fielding for detailed knowledge on acoustics on Gliders: sof@bas.ac.uk.

1.2.2. Scottish Association for Marine Science

The SAMS Marine Physics Group announced the formation of the North Atlantic Glider Base (NAGB) in January 2012. The NAGB is located at the Scottish Marine Institute's campus in Oban, northwest Scotland (SMI is the home of SAMS). It will be a delivery partner of MARS and became operational in April 2012, supported by the realignment of part of SMI's NERC National Capability funding.

NAGB welcomes scientists from all over the world to bring Gliders to SMI for deep water testing, launch and recovery for North Atlantic missions, and for instruction on operations and real-time data delivery. The NAGB can also provide access to iRobot Seagliders and a Hydroid Inc. REMUS 600 AUV for development and trial of new sensors. SMI has been operating gliders and AUVs in the North Atlantic since 2009, and has provided support to many UK groups for Glider and AUV development trials, dating back to Autosub 1 trials in 1997.

The NAGB offers the following to visitors:

- Access to laboratory space for pre-mission, post-service Glider preparation (including buoyancy correction).
- Access to SAMS two coastal research vessels[2] for sheltered deep water testing (to 200m).
- Arrangement of fast vessel hire for deployment and recovery for North Atlantic missions.
- Advice on scientific and operational aspects of North Atlantic Glider missions.
- Advice and software for real-time Glider data delivery to GTS or to data centres.

As part of SMI's NERC National Capability all of the above are offered on a free-at-the-point-of-use basis to NERC-funded applicants using the National MARS facility housed at NOC, to a maximum of one month per year[3]. To non NERC-funded groups SMI offers the above on an appropriately costed basis.

---

[1] http://www.antarctica.ac.uk//staff-profiles/webspace/mmm/RaTS/RaTS.html Accessed 11 April 2012
[2] http://www.samsrsl.co.uk/renewable-energy/vessel-equipment-hire/ Accessed 11 April 2011
[3] Fast boat hire costs excluded – circa £800 per day all-in

The NAGB is currently home to:

- Two iRobot Seagliders: Talisker, acquired in 2008, and Ardbeg, acquired in 2012. The Gliders are equipped with CTD, dissolved oxygen, optical backscatter and chlorophyll fluorescence sensors[4].

- One Hydroid REMUS 600 propeller-driven AUV (Fig. 1.2). This 600 m rated COTS vehicle is 2 m long, and has an endurance of around 70 km (12 hours). It carries a CTD, an ADCP for current profiling and navigation, a fluorometer for chlorophyll estimation and a turbulence sensor suite[5]. Named Rebus, this vehicle has been used on coastal missions around Scotland (e.g. Boyd et al., 2010) and in the Arctic.

Figure 1.2: REMUS 600 AUV Rebus based at the Scottish Marine Institute, showing the turbulence sensor cluster on its nose (Courtesy SMI).

For all matters connected with the North Atlantic Glider Base, the contact is Prof Mark Inall: Mark.Inall@sams.ac.uk. For matters specific to the REMUS AUV, the contact is Dr Tim Boyd: Tim.Boyd@sams.ac.uk.

1.2.3. University of East Anglia

The University of East Anglia has used capital funding from HEFCE to acquire iRobot Seagliders for the research group led by Prof. Karen Heywood. While NERC has supported the use of these Gliders in competitively awarded research projects, it does not own the assets.

[4] http://www.smi.ac.uk/smart-observation-techniques Accessed 12 April 2012
[5] http://www.smi.ac.uk/smart-observation-techniques/auv/?searchterm=REMUS Accessed 12 April 2012

Prof. Heywood's group, and collaborators, have extensive glider experience, with missions completed in the North Sea (with Dr Liam Fernand of CEFAS), off northern Spain, in the Indian Ocean, and in the Ross and Weddell Seas, Antarctica[6]. Within the NERC GENTOO project, Prof. Heywood has worked with Dr Fielding at BAS and Prof. Griffiths at NOC to fit a new echo-sounder to an iRobot Seaglider for krill studies.

The UEA fleet currently has three iRobot Seagliders (SG502, SG510 and SG537), after losing one vehicle when on trials at Oban (probably due to ship collision) and one Glider is missing in the Southern Ocean (SG522, and it is very unlikely to now be recovered as its ARGOS beacon battery has expired). All have CTD, dissolved oxygen using the Aanderaa optode, and optical backscatter and fluorescence sensors. It is intended that SG537 will be fitted with an Imagenex zooplankton echosounder (see section 1.5.1) in 2012. It is also intended to fit SG510 (and possibly SG502) with a Photosynthetically Active Radiation (PAR) sensor (section 1.5.1) in 2012.

Contact Prof. Karen Heywood at K.Heywood@uea.ac.uk

1.2.4. Heriot-Watt University

The Oceans Systems Laboratory (OSL[7]) at Heriot-Watt University is a world-leader in the engineering and design of autonomous underwater systems. Together with a spinout company SeeByte[8], which specialises in software for handling and presenting data from autonomous systems, the OSL has an extensive track record of working with industry and the military on seabed surveys.

As well as a Hydroid Inc. REMUS 100 AUV, the OSL's facilities include vehicles they have developed, such as the hover-capable RAUVER (Remote/Autonomous Underwater Vehicle for Experimentation and Research; Fig. 1.3).

[6] Data from these missions is available at http://ueaglider.uea.ac.uk/DIVES/ Accessed 11 April 2012

[7] http://osl.eps.hw.ac.uk/index.php Accessed 11 April 2012

[8] http://www.seebyte.com/ Accessed 11 April 2012

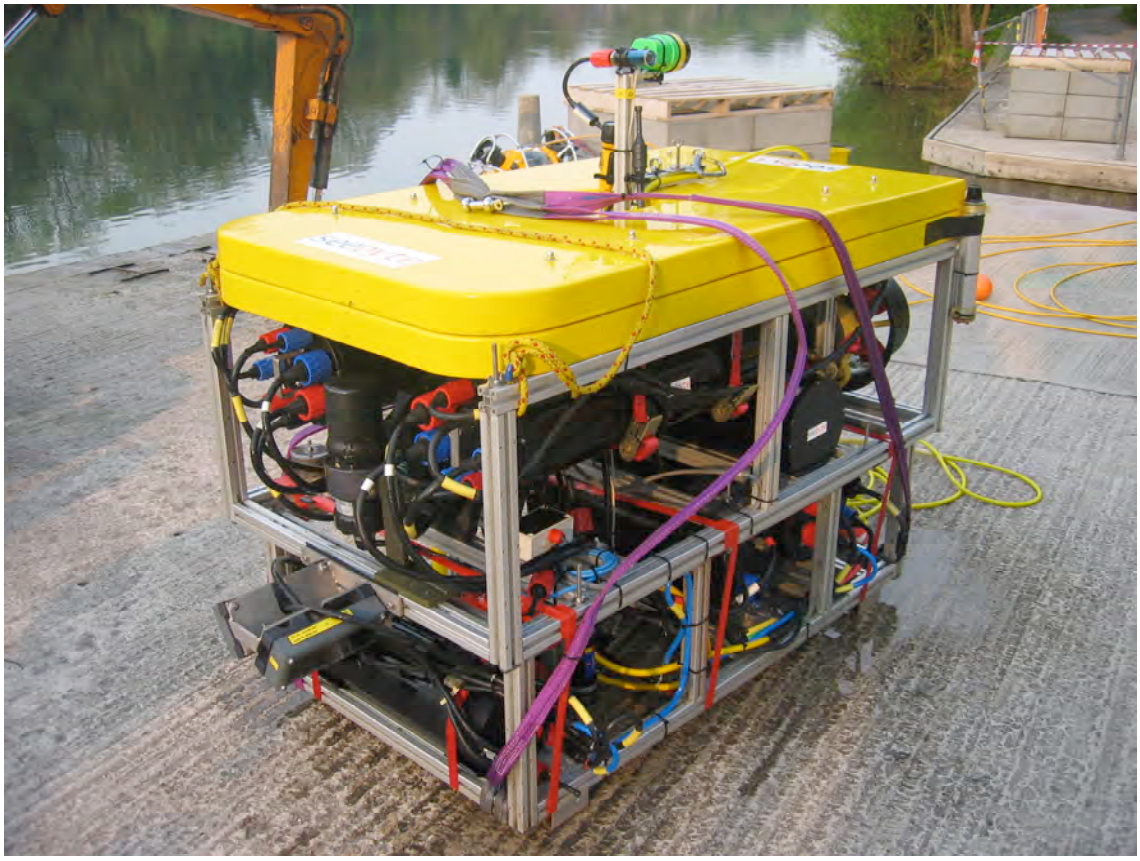

Figure 1.3: Designed for scientific experimentation and testing ideas for proof of concept, the RAUVER has been used for seabed and navigation studies. It is currently decommissioned awaiting redevelopment.

Contact Prof. David Lane: D.M.Lane@hw.ac.uk

1.2.5. Ministry of Defence

Undersea Gliders

To the best of our knowledge the Ministry of Defence Royal Navy) does not own or operate any undersea Gliders. However, we understand that two US Navy owned Gliders have recently been given over to the Royal Navy for training in launch and recovery and tasking. NOC Southampton has worked under contract with Dstl to:

- Evaluate the potential of undersea Gliders for military data gathering, producing a report in 2009, and an associated two-day awareness workshop delivered to a range of Royal Navy and allied staff at HMS Drake.

- Carry out a demonstration Glider mission from a Royal Navy vessel in 2011, with data telemetry to the UK Met Office.

An appropriate contact is Dr Tim Clarke at Dstl Porton Down: TCLARKE@mail.dstl.gov.uk

AUVs

The Ministry of Defence owns and operates a number of propeller-driven autonomous underwater vehicles for specialist purposes, centred on mine countermeasures (MCM) and hydrographic applications. Assets known to the author comprise:

- A fleet of 12 Hydroid REMUS 100 vehicles rated to 100 m depth (Fig. 1.4). Some of these vehicles have been in use since 2006, and a major refurbishment is expected in 2012. This refurbishment will add new sonar capabilities to the vehicles both to aid bathymetric mapping on the sub-metre scale (microbathymetry), using BlueView technologies' 3D MB2250 MicroBathymetry system, and wider swath bathymetry using GeoAcoustics' GeoSwath. With these extensive systems on board, the likely endurance is less than 12 hours or less than 70 km.

- From the initial fleet of four vehicles, the Royal Navy currently has three REMUS 600 vehicles for "mine reconnaissance, hydrographic surveys and environmental assessments"[9]. The initial £5.5m contract for two vehicles and their support systems was delivered in 2009.

Contacts in this area rotate; it would be appropriate to first contact either Dr Tim Clarke at Dstl (details above) or the general contact at the Maritime Warfare Centre (Tactical Development) at mwc.td@gtnet.gov.uk. The current team leader is Richard Hill, until September 2012.

Figure 1.4: REMUS 100 AUV owned by the Royal Navy (www.defpro.com/daily/details/970/)

1.3. Undersea Gliders

Undersea Gliders are propelled using buoyancy change engines. It is a common misconception that, like gliding aircraft, they extract energy from the environment and that this is the source of their long endurance. The reality is more prosaic. In an undersea Glider an electric motor drives a hydraulic pump (the working liquid may be water or oil), which moves fluid from the inside of the Glider body to an external bladder, thereby doing work against the hydrostatic pressure. In doing so, the volume of the Glider is increased, its density reduces, and it rises. Wings (lift surfaces) convert that rise to forward motion. The mechanics are exactly analogous to a propeller driven vehicle, where an electric motor is coupled to a lift surface, the propeller. However, by their very nature, pure buoyancy driven vehicles are compelled to undulate, they cannot fly horizontally, neither can they follow

[9] http://tinyurl.com/cwa74be Accessed 12 April 2012

terrain[10]. Their long endurance is solely down to two design compromises: a) they travel slowly, and b) they are very frugal on their energy consumption for control of the vehicle and for sensors. The aphorism for the Seaglider is "Half a year, at half a knot, with half a Watt". If the science need can be met within, or close to, these parameters, then Gliders may be a good choice for ocean monitoring. A simple explanation of their long endurance is included in Appendix 2, reproduced from the May 2012 MARS Newsletter.

A history of the technological development, and early use, of the current generation of undersea Gliders can be found in Davis et al. (2003). Three commercial Gliders, variants on the original concept, whose development was funded by the US Office of Naval Research, started to become available from the mid 2000s (Griffiths et al., 2007).

NOC Southampton took delivery of their first three Gliders in early 2006, after a competitive tender exercise between the supplier companies or organisations, namely:

- Webb Research Corporation (now Teledyne Webb Research) of Falmouth Massachusetts, USA, had been manufacturing Slocum Gliders with a 200 m depth limit for some years. However, as our interest was in deep ocean physics, we awaited their 1000 m rated product. The company's founder, Doug Webb, was the inventor of the concept, and the company was, and is, a leader in buoyancy-controlled instruments for ocean science, being by far the largest manufacturer of APEX (ARGO) floats.

- Seaglider Fabrication Centre, University of Washington, was manufacturing a variant on the Webb Glider with lower power consumption, a purportedly lower drag hull, and a simpler operator's interface.

- Bluefin Robotics, Cambridge, Massachusetts, held the licence from the University of California San Diego (Scripps Institution of Oceanography) for the Spray, another variant on the Webb concept.

Bluefin's unit price for Spray was far higher than that of Webb Research for the Slocum, and the operator interface was not as well developed or as comprehensive. The customer base was also much smaller. At the time of our procurement, the Seaglider Fabrication Centre was not in a position to supply us. Consequently, NOC's first three Gliders were Webb Research Slocums. A fourth was added subsequently to the Southampton deep Slocum fleet to service the needs of the RAPID Watch project for long endurance missions off the Morocco continental shelf.

Shallow-diving Slocum Gliders were procured at NOC Liverpool from 2008 as part of the NERC Oceans 2025 programme, for work in the Irish Sea. In 2010, with increasing take-up of Seagliders by the science community, with proven endurance beyond the 86 days we were achieving with deep Slocums, and their commercial manufacture by iRobot Corporation, NOC Southampton procured two Seagliders for its own science programmes and two for an upcoming NERC programme "Sensors on Undersea Gliders".

The characteristics of the NOC's current fleet, which encompasses the great majority of variants used by the community in Europe and elsewhere, are set out in section 1.3.1.

[10] There are vehicles in development that combine propeller and buoyancy engines to remove these constraints.

1.3.1. Characteristics of the Undersea Gliders at NOC

Teledyne Webb Research 1000m Slocum Gliders

Ammonite, Bellamite and Coprolite were NOC's first Gliders, the second order to be delivered in Europe at the time, and are based at Southampton. All three are early examples of the first generation (G1) of deep Webb Gliders. As there has been substantial technical progress since their manufacture, while these Gliders have field-proven sub-systems, many components have been changed by the manufacturer. Bellamite and Coprolite are both scheduled to be deployed for up to three months from June to September 2012 as part of the NERC FASTNEt programme off the Celtic Sea shelf break.

These Gliders carry a non-pumped Seabird CTD and have a proven endurance of up to 86 days using primary lithium batteries. Due to stringent transportation regulations and safety concerns over large, custom-made, lithium primary batteries the manufacturer only provided alkaline battery packs for these Gliders as original equipment. These give a typical endurance of about 30 days with a few days reserve. Collaboration with colleagues in Germany and France has enabled us to source lithium battery packs from a German manufacturer using SAFT cells from France, and we now have a battery pack design with a UK-based supplier using South Korean cells. This reduces lead times, and can make transportation easier. We will conduct a comparison of these two battery packs in the gliders we will deploy on FASTNEt in June 2012. These Gliders do not carry optical sensors or a fluorometer. Subject to capital funding from BIS/NERC being available in 2012/13 these Gliders are planned to undergo a major upgrade to the current G2 specification at the factory in 2012-13.

The Dolomite Glider carries a non-pumped Seabird CTD. It is a 'G1.5' version, and was purchased to carry out demonstration missions for the RAPID-MOC programme. It too is planned to undergo a major upgrade to G2 specification at the factory in 2012-13.

Teledyne Webb Research 200m Slocum Gliders

Three shallow-water Gliders were bought for Liverpool-based projects within NERC's Ocean 2025 programme, but since 1 April 2012 are within the MARS fleet. These have been used for short duration missions in the Irish Sea. The current deployment of Unit 117 is with a lithium battery pack and should give us the first long deployment with this glider. The expected duration is ~42 days.

Unit 117 is a G1 type and has a non-pumped Seabird CTD. In addition, the Glider has an Aanderaa oxygen optode, and a Wetlabs triplet sensor for CDOM, Chl-a and turbidity. Consequently, its endurance is less than for Gliders with only a CTD.

Unit 175 is G1 and has a non-pumped Seabird CTD and a Rockland Scientific MicroRider turbulence probe (microconductivity, shear and temperature at up to 512 Hz). While both the Glider and turbulence probe are commercial instruments, and used by a number of groups, the combination is still novel. A great deal has been learnt about the nuances of setting up this combination, e.g. in ballasting, and on obtaining quality turbulence measurement from a Glider. Currently, this has to be considered experimental, but our aim is to bring this Glider into full service for users (rather than specialists) during 2012/13.

Unit 194 is NOC's most recent Slocum Glider, is a G2 and is our only Glider with a pumped Seabird CTD. It also has an Aanderaa oxygen optode, and a Wetlabs triplet sensor for CDOM, Chl-a and turbidity.

iRobot 1000m Seagliders

MARS has four Seagliders within its fleet, two for general science use, and two dedicated to the NERC 'Sensors on Autonomous Undersea Gliders' programme until June 2015. All carry a Seabird CTD and a Wetlabs BBFL2-VMT 650/CDOM/Chl-a puck and an Aanderaa 4330 oxygen optode:

- Altair was lost in service off El Hierro in the Canary Islands in October 2011. This was most likely due to a fault with its Iridium satellite modem.

- Bellatrix has been used on the RAPID Watch Morocco station in 2011. Its mission was curtailed due to increasing internal humidity, indicative of a slow leak. On return to NOC it was clear that the Glider had impacted with the seabed at some time during its deployment and (probably) a fishing line moved across its upper body, pushing back very slightly the CT sensor, sufficient to cause the small leak. The Glider is now back from a manufacturer service, and an upgrade to 'ogive' fairings to provide a greater sensor volume for the Sensors on Gliders programme.

- Canopus will be fitted with a Photosynthetically Available Radiation (PAR) sensor for its first mission, a deployment on the NERC Osmosis cruise in September 2012.

- Denebola will be fitted with 'ogive' fairings for the Sensors on Gliders programme.

- Eltanin is the replacement for the lost Altair.

1.3.2. NOC capability in sensor integration onto Gliders

Whereas the Gliders described above come with a suite of standard sensors, there are often requirements from users to carry additional sensors and instruments, for example, a selection from those described in section 1.5.1. To facilitate sensor integration, MARS staff at NOC have the facilities, training and knowledge to add new sensors to Gliders and to our Autosub family of vehicles.

For the COTS Gliders, this has involved developing relationships with the manufacturers for access to Glider simulators (for Teledyne Webb Research Slocums), to the interface code needed to integrate these payloads into the Glider data streams, and the energy use planning tools to fully understand the effect of adding sensors on the endurance of the vehicles.

This capability will be fully utilised in 2012-2014 for the NERC 'Sensors on Autonomous Undersea Gliders' programme, where nitrate, phosphate, fast conductivity and temperature sensors developed elsewhere in NOC will be incorporated into two Seagliders, and where MARS will assist St Andrews University researchers to add Passive Acoustic Monitoring systems to gliders.

1.4. The MARS fleet of autonomous underwater vehicles

The Autosub family of vehicles has been developed at the NOC to meet the needs of the NERC marine science community. Consequently, they are generally larger than many of the vehicles available commercially, as scientists wish to carry extensive instrument payloads, some of which, in prototype form, can be large and heavy. Generally, larger AUVs also have

longer endurance, and can carry more accurate and capable navigation instruments, essential for example, for under ice missions in high latitudes.

1.4.1 Autosub3 and Autosub6000

The key characteristics of these vehicles, which share many common features, are given in Table 1.1.

	AUTOSUB 3	AUTOSUB 6000
Physical	6.8 m, 2400 kg (dry)	5.5 m long, 1800 kg (dry)
Depth Rating	1600 m	6000 m
Range. Endurance	400 km, 80 hours at 5 km/hour	150 km, 30 hours at 5 km (at minimal)
Energy Supply	Primary batteries. 12 hours to change.	Secondary rechargeable batteries. 7 hours to recharge.
Navigation	150 kHz DVL bottom track range 400 m. Accuracy is 0.1 % of distance travelled since last fix	300 kHz DVL bottom track range 200 m. Accuracy is 0.1 % of distance travelled since last fix. Range only acoustic positioning to within 15 m when at 5000 m operating depth at the start and end of the mission.
Collision Avoidance	Forward look single beam for ice berg and grounding line avoidance when under ice sheet.	Scanning Tritech Seaking sonar for near seabed optimised collision avoidance in rough terrains.
Communications	Acoustic Modem. Range 2 km. WiFi radio link when on surface, giving access to vehicle data.	Acoustic Modem. Range 7km. WiFi radio link when on surface, giving access to vehicle data.
Control	Constant depth, Constant Altitude, Constant distance below a surface overhead, depth profiling. Track following, holding station.	Constant depth, Constant Altitude, depth profiling. Track following, holding station. Box survey with configurable line spading, altitude, orientation and extents.
Launch and Recovery	Dedicated LARS needing hydraulic power (210 bar)	Dedicated LARS needing hydraulic power
Special Features	Optimised for under ice operations. Heated container system for polar operating conditions.	Optimised for seabed survey.
SENSORS		
Multibeam	EM2000. 400 m swath at 3 m resolution. 1.75 km^2 /hour. Can be configured to look upwards.	EM 2000. 400 m swath at 3 m resolution. 2 m resolution. 1.75 km^2 / hour.
Sidescan	NONE	Edgetech 2200. 410/120 kHz Sidescan Sonar: 0.3 m resolution at 0.8 km2/hour (410 kHz) 1.5 m resolution at 3.0 km2/hour (120 kHz)
Sub Bottom Profiler	Planned 2013	Edgetech 2 to 16 kHz sub bottom profiler
ADCP	Down (150 kHz), Up (300 kHz)	Down (300kHz)
Magnetometer		Applied Physics tri axis
CTD	Seabird 911, with pumped twin CTD sensors. Dissolved Oxygen Transmissometer, Light Scattering Sensor, Fluorometer also available.	Seabird 911, with pumped twin CTD sensors. Dissolved Oxygen Transmissometer, Light Scattering Sensor, Fluorometer also available.
Camera	NONE	Long range 1.4M pixel mono. Close range 5m pixel, dual colour system.
Additional sensors interfaces	Power: 48 volt, up to 2 00 Watt. Communications: RS232, Ethernet. Sensors accommodated in free flooded front section.	Power: 48 volt, up to 200 Watt. Communications: RS232, Ethernet. Sensors accommodated in free flooded front section.

Table 1.1: Comparison of the specifications and sensor and instrument capabilities of the NOC's Autosub6000 and Autosub3 propeller-driven AUVs

Autosub3 with a 1600 m depth capability has been fitted with extensive acoustic instrumentation (see section 1.5.4) relevant to surveys of higher trophic levels (zooplankton and fish). Its predecessor, Autosub2 demonstrated the use of a submersible flow cytometer

on an AUV, in combination with a multispectral spectrophotometer, in 2001. This enabled quantification of the populations of phytoplankton in two communities (one comprising coccolithophores, flagellates and dinoflagellates; the other dominated by diatoms and flagellates; Cunningham et al., 2003; Fig. 1.5).

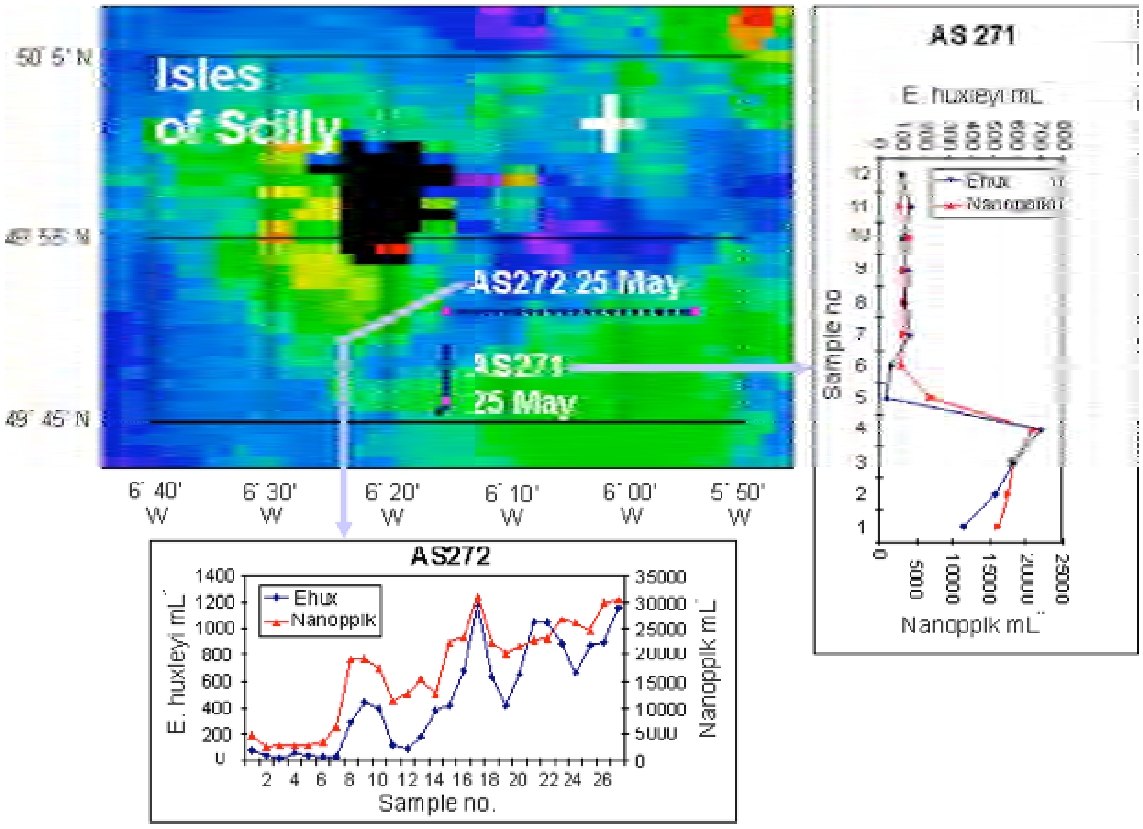

Figure 1.5: Main image shows a SeaWifs satellite image from 24 May 2001 off the Scilly Isles. The tracks of two Autosub2 missions (dotted dark blue lines), when carrying a submersible flow cytometer (Cytosub), are shown. The two graphs show the different populations of phytoplankton from the Cytosub along the track; they demonstrate qualitative agreement with the satellite bulk data, but add quantitative information. Courtesy Dr G. Tarran, PML.

Autosub6000 uses different battery and buoyancy technologies in order to achieve a 6000 m depth rating, but otherwise is similar to Autosub3. The vehicle has primarily seen service for the geological, geophysical and benthic biology communities to date, with its precision navigation, extensive suite of acoustic and optical seafloor mapping instruments, and terrain following and collision avoidance systems. Examples of the sonar and camera images obtainable with this vehicle are shown in Fig. 1.6.

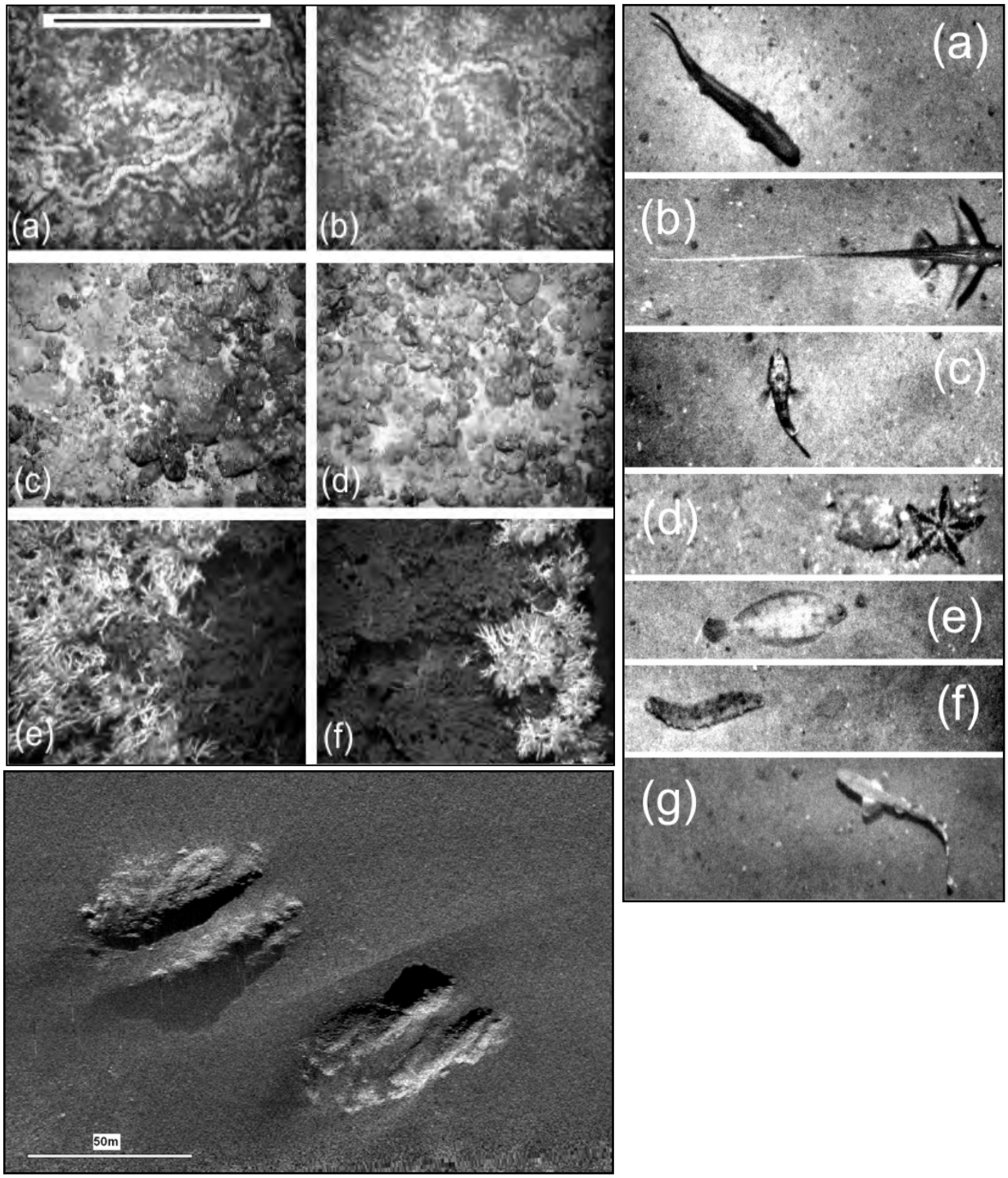

Figure 1.6: Panels a-f and a-g show images captured from the monochrome camera on Autosub6000 when traversing at a height of ~15 m over the North Rockall Bank in 2011. The above sidescan sonar image is in the area of the Darwin Mounds.

1.4.2. Autosub Long Range

Not until very recently has technology made it possible to tackle the design of an AUV that would combine a 6000 m depth rating with a long endurance (to 6000 km or ~6 months). This target range exceeds that of the longest-endurance propelled underwater vehicles of today - the buoyancy-engined undersea Gliders.

Some of the sub-systems for Autosub-Long Range could have been sourced in the mid 1990s. For example, there has been virtually no useful progress with readily available, high specific energy, primary lithium metal batteries. Perhaps surprisingly, after an exhaustive review of technical options and cost, the main pressure vessels for Autosub Long Range comprise two forged aluminium spheres of a type used from the late 1970s for deep-ocean seismometers. With these constraints, it is only because modern electronics, mechanical and electrical systems can deliver the engineering and data acquisition performance required, at minimal power consumption, that the vehicle performance envelope of 6000 m diving depth and 6000 km range becomes feasible.

There are limitations necessary in achieving this performance envelope. The key limitation is maintaining low average energy consumption. While instruments that consume high power are not ruled out (for example those using short-pulse-duration active acoustics with pings at relatively infrequent intervals) the average energy used must be sufficiently low if the full range of the vehicle is to be achieved. Long endurance missions also mean that the instruments should show minimal changes to their calibration. *In situ* platforms such as profiling Lagrangian floats, with endurance of several years, have shown what is possible with specially designed sensors.

The Autosub Long Range vehicle (Fig. 1.7) underwent its first oceanic engineering trials off the Canary Islands in January 2011. There followed the addition of key sub-systems, and essential changes to communications systems, and the vehicle (as of April 2012) is undergoing shore-based trials at NOC prior to the next oceanic trials in January 2013.

Figure 1.7: Autosub Long Range during its sea trials in January 2011.

The technical features of the vehicle are given in Table 1.2, while Fig. 1.8 shows the expected endurance. The specified range will be achieved if the average power consumption of the onboard control systems and sensors is kept to 1 W (blue line), and the speed is 0.4 m s^{-1} or less. However, a useful range of over 2000 km would be obtained with control and sensor power of up to 5 W, and maintained over a greater speed range, up to 0.8 m s^{-1}.

Table 1.2 Autosub Long Range Technical Features:

Propulsion Motor: Magnetically coupled d.c. electric motor with gearbox housed at 1 bar pressure. Operating from 2 W to 50 W output with overall ~ 50% efficiency over full power range.

Main Pressure Vessels: 2 of 711 mm diameter forged aluminium sphere with equatorial ring for connector ports. Mass to displacement ratio of 730 kg m^{-3} with an internal volume of 0.142 m^3.

Energy and Power Source: 40 kg of primary lithium thionyl chloride cells, delivering 68 M Joule at the operating power. Cost of £7000 per pack.

Additional buoyancy: High performance syntactic foam with a density of 570 kg m^{-3} as on the Isis ROV.

Control system hardware: Magnetically coupled DC motor driven stern plane and rudder. Vehicle is highly directionally stable, hence motors can have low duty cycle, saving energy.

Control system software: Main control, navigation data handling and communications modules hosted on Marvel PXA270 running at 104 MHz, with Windows CE operating system. Low-level control system using PIC controllers and RS485 bus.

Fitted sensors: Seabird SBE 52 CTD. RDI Teledyne 300 kHz ADCP.

Navigation: GPS on surface. Dead Reckoning using TCM5 flux gate compass, RDI Teledyne 300 kHz ADCP. Seabird strain gauge pressure sensor used for depth sensing. ADCP beams used for constant altitude mode operation and collision avoidance.

Communications: Two way Iridium satellite communications for science data download, mission and configuration upload.

Relocation backup: ARGOS beacon (in addition to Iridium system).

Table 1.2: Autosub Long Range technical features.

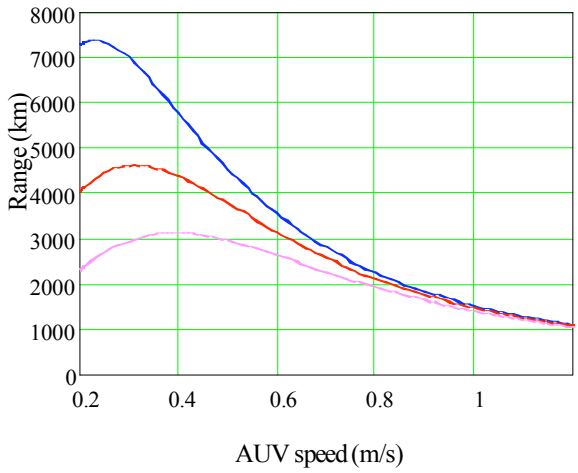

Figure 1.8: Range predictions of Autosub Long Range based on outline design (km) vs. speed (ms^{-1}) with hotel powers of 1 W (blue trace), 2.5 W (red trace) and 5 W (magenta). At moderate speeds the range is strongly sensitive to the AUV speed, and at lower speeds it has a high sensitivity to the hotel power used. Ranges in excess of 6000 km are possible with tight control over sensor power.

1.4.3. The concept of air-launched underwater vehicles

The following section is from a report by Peter Stevenson[11], NOC, on the concept of air-launched AUVs:

"*The concept of Autonomous Underwater Vehicles (AUVs) being launched from aircraft was funded as a feasibility study through the NERC Oceans 2025 programme running from 2008 to 2011. The original concept was to have a more economical means of seeding wide swaths of ocean with sensors for carrying out wide scale, synoptic physical oceanographic surveys. The means considered for achieving this was to launch multiple AUVs from high altitude and have them glide 100 km or more, navigating themselves to specific locations. Upon hitting the water, they would begin their AUV missions. As well as applications for wide spatial surveys, opportunities were seen for using aircraft of opportunity for supplementing existing surveys such as the Atlantic Meridional Transect (AMT), Porcupine Abyssal Plain (PAP), Meridional Overturning Circulation (MOC) as part of the NERC RAPID Watch programme. The faster response time of mobilising an aircraft compared with a ship opens possibilities for rapid response surveys, e.g. pollution spill and algal blooms. A unique application particularly well suited to Air-Launched AUVs (ALAUVs) is the survey of polynyas in the Polar Regions, which are uncharted and important to setting the conditions for circulation beneath the ice shelves. Beyond environmental research and civil survey work, the concept also has naval applications for sound velocity profiles, bioluminescence, and, with the ALAUV being much smaller and semi disposable compared with existing vehicles, covert surveys. Key to the overall success is creating an economical AUV so they could be considered to be semi disposable; crucial to this is keeping a small overall size to simplify the design, and minimise the sub systems and manufacturing costs. With the developments of miniaturisation and lower power requirements of computing systems, Global Positioning System (GPS) receivers and antennae, advancement of satellite communications and, to a lesser extent, battery technologies, there exists an opportunity for developing an AUV very much smaller and cheaper than AUVs to date but which still has a practical range. A number of small sensors in the market place used for tagging fish and mammals, and the research work at the National Oceanography Centre (NOC) on miniaturised sensors, all help support the case for further development*".

Figure 1.9: Air-launched AUV concept

An outline design for an 82 mm diameter, air-launched AUV has been produced (Fig. 1.9), with a target maximum operating depth of 500 m, and an endurance of 200 km at 1 W

[11] http://eprints.soton.ac.uk/188105/ Accessed 12 April 2012

control system and sensor power. A proposal to NERC to design such a vehicle coupled with science missions to study Antarctic coastal polynyas was not funded. However, there is active interest from industry, both as potential manufacturers and as potential users.

1.5. A summary of sensors for Gliders and AUVs relevant to DEFRA

The Slocum and Seagliders take very different approaches to sensor space available to users beyond the basic CTD. The manufacturers also take different approaches to helping users to interface new sensors. Teledyne Webb is more open than iRobot has been to date.

The Science Bay in the Slocum gliders (deep and shallow) is in the centre of the vehicle, Fig. 1.10. A hull section of 0.305 m by 0.212 m diameter is available to the user; it is also feasible to add an additional Science Bay. The usable volume within a single Science Bay is ~7 litres and the added mass must be less than 4 kg. Access points for external sensor mounting may be added in this hull section. It is possible to place some types of sensors within the rear, flooded, section of the glider, cabled to the Science Bay. Aanderaa oxygen optodes have been so used.

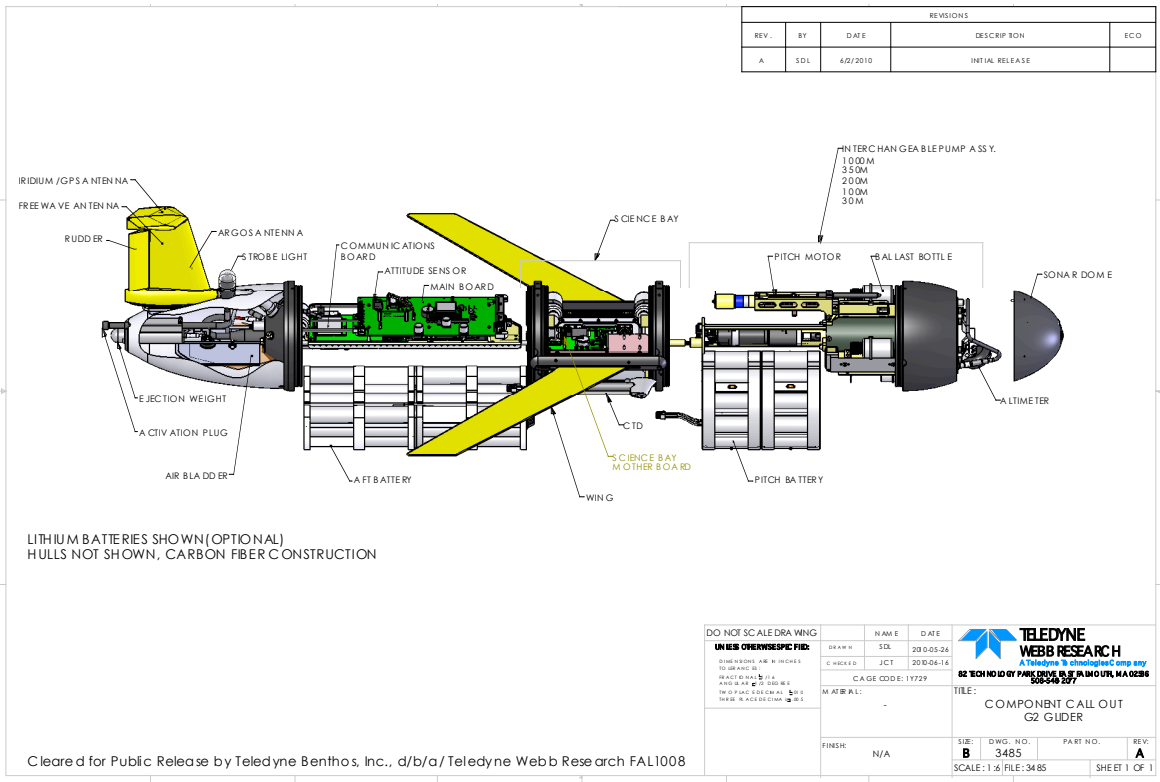

Figure 1.10: Exploded diagram of a Slocum G2 glider (e.g. Unit 194) showing the internal arrangement. The Science Bay where additional sensors can be located is in the centre of the glider; note that very little space is available in the flooded tail section (courtesy Teledyne Webb Research).

To date, the more complex nature of the Seaglider hull and fairing makes it advisable that additional sensor payloads be incorporated by the manufacturer, iRobot. Recently, this has been the case for a project led by the University of East Anglia (UEA) (in which Prof. Griffiths from NOC is a co-Principal Investigator) where a Nortek Acoustic Doppler Current Profiler and a small Imagenex 120 kHz scientific echo-sounder were added to an iRobot engineering test glider prior to fitting to a UEA glider. However, customer pressure for more flexible payload space has led iRobot to design retrofit 'ogive' fairings for the nose and tail of the vehicle that increase the payload space from ~3.2 litres and a weight in water of 2 kg to ~24

litres and a weight in water of 4 kg. However, there remain constraints, such as the external bladder, within this space (Fig.1.11).

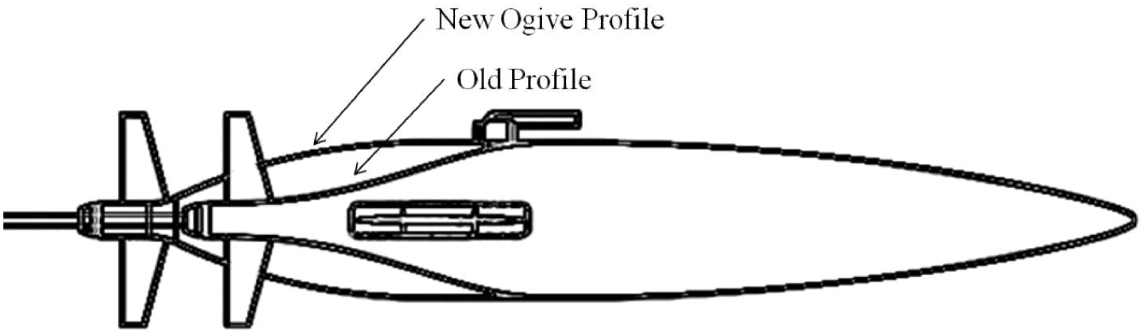

Figure 1.11: Sketch showing the payload space available in the standard iRobot Seaglider with the "Old Profile" fairing aft, compared with the new "Ogive" fairing. Two of NOC's gliders are being fitted with the new fairing. Non-disclosure agreements with iRobot mean we cannot present the more detailed drawings that we have for these vehicles (from C Yahnker, Overview of the development and advantages of new larger fairings for the iRobot Seaglider, Proc Oceans 2011, IEEE).

For all of the gliders it is necessary to ensure that additional sensors do not result in unacceptably high additional drag. Higher drag means that the stall angle of the glider increases, steeper dives then become necessary, expending additional energy and the distance that can be covered is less. Several of the suppliers of additional sensors for gliders have taken care to provide streamlined housings to ensure minimum added drag. Perhaps the most difficult sensor to integrate and maintain low drag would be the current-generation bathyphotometer for bioluminescence measurements.

1.5.1 Sensors currently used on gliders or long range AUVs

Conductivity, Temperature and Depth (Pressure)

The primary conductivity, temperature and depth sensors used in each of the COTS gliders are provided by the Sea-Bird SBE41CP[12] instrument. On the Seaglider and Slocum gliders this has until recently been a non-pumped custom variant as used on profiling floats. However, in 2011 Sea-Bird released a new CTD (the Glider Payload CTD) specifically for gliders[13]. This CTD includes a pump while consuming a maximum of 280 mW when sampling at 1Hz and providing real-time data. However, it can be operated in a number of modes that reduce power consumption; full details are on the specification page.

A purpose-designed CTD for use on gliders has also been designed at the Woods Hole Oceanographic Institution (Schmitt and Petit, 2006). Using a conductivity cell with four electrodes and an internal (thermistor) temperature sensor it combines a good dynamic response and high spatial resolution. The package has proven to be rugged, with low drag and resistant to fouling. The design does not call for a pump and the power consumption is ~420mW.

[12] http://www.seabird.com/alace.htm Accessed 8 April 2012
[13] http://www.seabird.com/products/spec_sheets/GliderPayloadCTDdata.htm Accessed 8 April 2012.

Dissolved oxygen sensors

Optical and electrochemical oxygen sensors have been used on various gliders; the fluorescence lifetime optode from Aanderaa[14] and a polarographic Clark electrode SBE43[15] sensor from Sea-Bird. Nicholson et al. (2008) showed that good quality oxygen data can be gathered in deep water. However, there are issues for long-term performance, such as photobleaching of the dyes used in the Optode, and long-term drift of the polarographic sensor. These, and other issues, have been studied by the ARGO community (Gruber et al., 2007). An example of oxygen sensor results from a Seaglider related to a mid-water chlorophyll maximum in the North Sea is shown in Fig. 1.12.

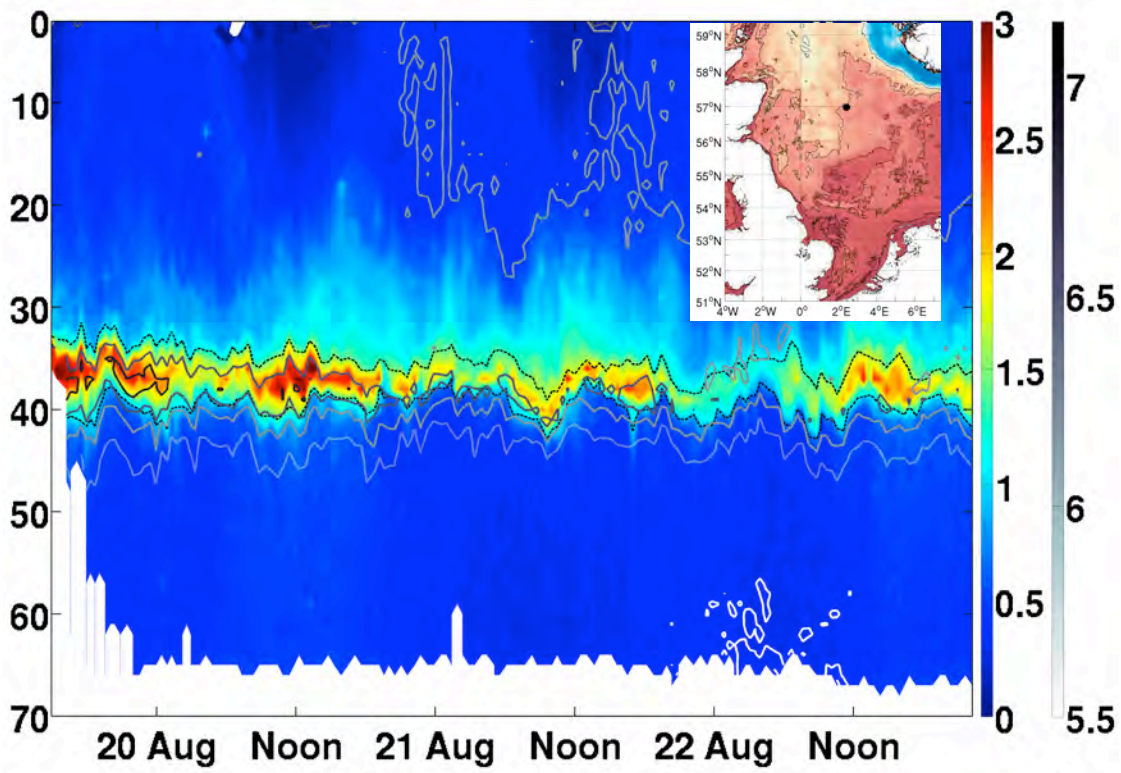

Figure 1.12: Hydrographic section (158 dives) of chlorophyll concentration (mg m^{-3}, left colour scale) calculated from chlorophyll fluorescence sensor onboard UEA's Seaglider SG510 ("Orca") during the joint UEA-Cefas North Sea Seaglider campaign in August 2010. The glider was deployed and recovered by the RV Cefas Endeavour. Dissolved oxygen (ml dm^{-3}, right colour scale) contours are indicated by the solid lines. Temperature contours for 7 and 13˚C are indicated by the dotted lines. Note the sharp deep chlorophyll maximum in the thermocline associated with a maximum in dissolved oxygen. The black dot on the inset map shows the position for this data set (courtesy Prof K. Heywood, UEA).

Optical sensors

Optical sensors have been used on gliders to measure chlorophyll fluorescence and backscatter (at one or more wavelengths and at one or more angles and optical proxies for coloured dissolved organic matter (CDOM), Perry et al. (2003), Niewiadomska et al. (2008)).

Several optical measurements can be made from one sensor cluster (referred to as a 'puck'), simplifying mounting the device to the glider, and giving a smaller form factor, and

[14] http://www.aadi.no/Aanderaa/Products/Sensors/OxygenOptode/default.aspx Accessed 8 April 2012
[15] http://www.seabird.com/products/spec_sheets/43data.htm Accessed 8 April 2012

simplified wiring. In addition, the measurements are in close physical proximity. One example is the Wetlabs BBFL2-VMT[16] that measures optical backscattering at a single angle (117˚) at a choice of wavelengths (470, 530, 660 or 700 nm), chlorophyll fluorescence at an excitation wavelength of 470 nm and an emission of 695 nm, and CDOM through excitation at 370 nm and emission at 460 nm. Wetlabs' FLNTU combines a fluorometer with a turbidity sensor that the manufacturer claims not to be affected by CDOM.

Other manufacturers supply broadly similar sensors, for example:

- HOBI Labs produce the Hydroscat2[17] a two-wavelength backscatter sensor and fluorometer (standard wavelengths of 420 and 700nm at 140˚, with 442 to 852 available to order).
- Seapoint Sensors Inc[18]. has a range of turbidity and fluorometers that have flown in gliders. Their ultraviolet fluorometer is specifically designed to measure CDOM and crude oil.
- Chelsea Technologies[19] have a range of small optical instruments such as the TriLux fluorometer for chlorophyll, phycoerythrin or phycocyanin, which can also behave as a nephelometer, and the UviLux fluorometer for refined hydrocarbons (365nm) or CDOM or crude hydrocarbons (450nm).

Photosynthetically Active Radiation: (PAR – the light flux between 400 and 700nm) has been measured from gliders using custom-designed sensors (Baumgartner and Fratantoni, 2008). The commercial instrument starting to be fitted to gliders is from Biospherical Instruments[20], including the QSP-2150. NOC is aware of data from one of the first deployments off South Africa in February-March 2012. This sensor will be fitted to a NOC Seaglider for a cruise in September 2012.

Radiometers: The OCR-500[21] series of radiometers from Satlantic has been used within gliders. Niewiadomska et al. (2008) used a four-wavelength (412, 443, 490 and 555 nm) OCR504I irradiance sensor looked upward, at 20˚ to the horizontal. An OCR504R radiance sensor looking down, angled at +20˚ to the horizontal, sampling on the upcast only, measured upwelling radiance at the same wavelengths.

Spectrophotometer: Kirkpatrick et al. (2003) described a liquid core waveguide spectrophotometer to measure absorbance over 380 to 750 nm, with the band at 440nm indicating CDOM. This device has been used in Slocum gliders, where it takes up the centre Science Bay[22]. This technique has been applied to detect red tides (Harmful Algal Blooms) off west coast Florida. Based on measurements of species-specific absorbance spectra in the laboratory, an instrument configured to detect *Karenia brevis* has been used on gliders (Kirkpatrick et al., 2006).

Bathyphotometer: This type of optical sensor is not sufficiently mature for routine use on gliders. Experimental devices have been flown, some of which have been evaluated on gliders. Fucile at Woods Hole Oceanographic Institution modified a free-drop bathyphotometer for use in gliders. The instrument was subsequently used on a REMUS

[16] http://www.wetlabs.com/products/eflcombo/triplet.htm Accessed 8 April 2012
[17] http://www.hobilabs.com/cms/index.cfm/37/152/1253/1260 Accessed 8 April 2012
[18] http://www.seapoint.com/products.htm Accessed 8 April 2012
[19] http://www.chelsea.co.uk/allproduct/marine/fluorimeters Accessed 8 April 2012
[20] http://www.biospherical.com/index.php?option=com_content&view=article&id=52&Itemid=125 Accessed 8 April 2012
[21] http://www.satlantic.com/details.asp?ID=23&CategoryID=1&SubCategoryID=0 Accessed 8 April 2012
[22] http://isurus.mote.org/~pederson/brevebuster.phtml Accessed 8 April 2012

AUV. A US Navy grant supported work by Fucile and Benthos on an expendable instrument, but progress is not known.

Wetlabs has a prototype instrument UBAT[23] in development, based on the MBBP-G3 instrument from J. Case at the University of California Santa Barbara. This instrument was used on a REMUS AUV by Moline (California Polytechnic State University)[24], but there has been no known use on a glider.

The Chelsea Technologies GLOWtracka bioluminescence sensor has been used on towed vehicles, including SeaSoar, and on profilers (with the addition of a pump to induce the organisms to bioluminesce). This sensor uses a large area photodiode rather than a photomultiplier, therefore its power consumption is lower than the UBAT.

Acoustic sensors

Acoustic Doppler Current Profiler: Baumgartner and Fratantoni (2008) reported on the use of a specially adapted 1MHz Nortek Aquadopp Acoustic Doppler Current Profiler on a Slocum coastal glider. A purpose-built acoustic transducer was used so that the ADCP was angled correctly to the vertical when the glider was descending. The instrument also provided acoustic backscatter estimates from zooplankton, in this case the copepod *Calanus finmarchicus*. The dynamic range of the backscatter was 90dB. A similar Nortek ADCP was fitted to an iRobot engineering Seaglider for use by UEA in January 2012 in the Weddell Sea, unfortunately, the integration programme took far longer than planned, and the instrument performed poorly, ascribed to "low backscatter". Investigations are in hand by the manufacturer and UEA. Nortek has also collaborated with scientists in Canada (Bachmayer and de Young, Memorial University of Newfoundland) to integrate a 400kHz Aquadopp ADCP onto a Slocum glider.

Teledyne RD Instruments and OASIS Inc. were funded by the US Office of Naval Research to integrate a 600kHz ADCP into a Slocum 200m glider[25]. This is now the instrument of choice to be fitted to the Slocum gliders for the coastal module of the US Ocean Observing Initiative Pioneer and Endurance arrays[26]

Doppler Velocity Log (DVL): This is a variant on the ADCP to provide speed over the ground. It is of limited usefulness on gliders unless the vehicle is continuously within range of the seabed. When this is the case, the result is improved navigation in areas of strong currents, as the glider can correct its heading in real time. This capability would be needed if it was important to keep (within set bounds) to a course, e.g. for repeat surveys of the same area. The 600 kHz Explorer DVL from Teledyne RD Instruments[27] is suitable for use on gliders, and has been used on a shallow Slocum (Woithe et al., 2011).

Passive Hydrophones: A number of passive acoustic instruments have been used on gliders for military and environmental science. Purpose-built digital acoustic recorders using HTI-96-MIN hydrophones covering 2–30 kHz were used by Woods Hole Oceanographic Institution (WHOI) to study whale vocalization (Baumgartner and Fratantoni, 2008). Under US Office of Navy Research support[28] Hurst and colleagues at WHOI produced 20 DMON passive acoustic monitors for marine mammal sounds for use on a variety of platforms, including

[23] http://www.wetlabs.com/Research/orrico/ubat.htm Accessed 8 April 2012
[24] Personal communication Mark Moline to GG March 2009.
[25] www.onr.navy.mil/reports/FY08/pocre.pdf Accessed 8 April 2012
[26] http://tinyurl.com/cj397mz Accessed 8 April 2012
[27] http://www.rdinstruments.com/explorer.aspx Accessed 9 April 2012
[28] www.onr.navy.mil/reports/FY11/mbhurst.pdf Accessed 8 April 2012

gliders. These provide recording of sounds over three selectable ranges from 10-150 kHz. Devices have been carried on Slocums (Fratantoni, WHOI), Seagliders (Nowacek, Duke University) and other vehicles.

Two of the WHOI pioneers of this programme, Mark Johnson (acoustics and signal processing) and Peter Tyack (marine mammal science) are now at St Andrews University, and have support from the NERC Sensors on AUG programme[29].

Active sonar: These are generally considered to be "high power" instruments, and therefore of limited use on gliders or low-power, long endurance AUVs; however, this need not be the case. The slow speed of these vehicles means that excellent spatial coverage along the track can be obtained at longer pulse-to-pulse settings than would be the case on ships. But, size and weight restrictions remain, and it is not surprising that manufacturers have been slow to produce active sonars specially tailored to these vehicles.

The NERC project GENTOO[30] required a well-calibrated 120 kHz echosounder for use on a Seaglider to detect and quantify krill (*Euphausia superba*) in the Weddell Sea in 2012. Imagenex was approached, because of their experience with low cost small sonars, and they produced to our specification a variant on an existing design that met the need for a self-logging instrument, with assured calibration, that could detect a single adult krill at 40 m range, would be compatible with the size, power availability and form factor of a glider, and could interface to the glider's data telemetry system. Initial results have been most encouraging, Fig.1.13. This is now a product on offer from Imagenex[31]. There are well-known limitations to the use of single frequency acoustics for zooplankton and fisheries studies, but this example shows what can be done. Sounders with other frequencies are needed, and confidence-building experiments with fisheries laboratories would be very beneficial.

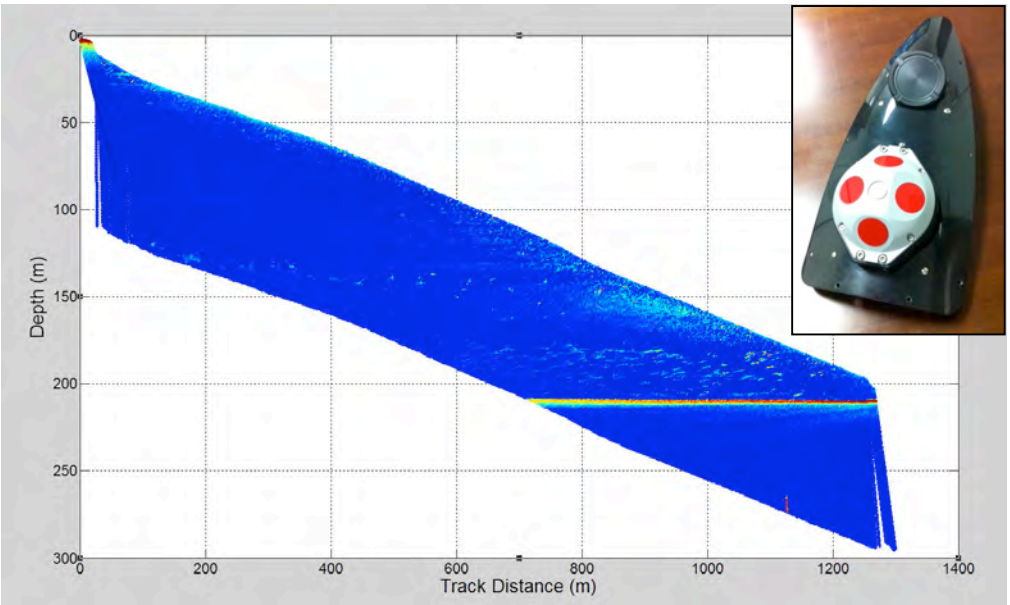

Figure 1.13: Example plot from the Imagenex 120 kHz sonar on a Seaglider from the GENTOO project (courtesy Karen Heywood (UEA) and Sophie Fielding (BAS)). The background blue colour indicates signals below the noise level of the sonar; as a band, it shows the motion of the glider on its decent. The continuous line at ~210 m is the seabed;

[29] http://gotw.nerc.ac.uk/list_med_pi.asp?pi=97157 Accessed 9 April 2012
[30] http://gotw.nerc.ac.uk/list_full.asp?pcode=NE%2FH01439X%2F1 Accessed 9 April 2012
[31] http://www.imagenex.com/html/853_echo_sounder.html Accessed 9 April 2012

discrete fish can be seen in the 30 m above the seabed, with weaker fish echoes at ~140m. The more continuous area at ~155 m depth at 900 m on the track is likely a patch of zooplankton. Inset: Photograph of a mock-up of the Seaglider hull with the four-transducer Nortek ADCP and the black single transducer Imagenex ES853 sonar.

Altimeter: An acoustic altimeter is standard on gliders as a primary sensor for seabed collision avoidance. Approach to <10m is usual and can be much less on shallow Slocum gliders whose buoyancy can be changed much faster than on deep gliders. Altimeters by Airmar and Tritech have been used. Although the in-use power of these units is ~0.5–2W, software minimises the active period. These altimeters can and do detect zooplankton layers. This can be a hindrance, for it is possible for the altimeter to mistake the zooplankton layer for the seabed, and for the turn-around inflexion to occur at the layer rather than the seabed.

Turbulence measurements

Rockland Scientific manufacture the microRider microstructure instrument, which incorporates two shear probes, two FP07 fast thermistors, a high-resolution pressure sensor and a 3-axis accelerometer. Initial results suggest that it is possible to resolve turbulent dissipation down to 5 x 10^{-11} W/kg. A group from IFM-GEOMAR in Germany deployed this instrument on a Slocum glider in 2009 in the equatorial Atlantic[32]. Numerous trials of this instrument mounted on a shallow Slocum glider (Fig. 1.14) have taken place at NOC Liverpool; a report[33] is available to registered users of e-prints at NOC (a copy can be provided on request). A September 2011 trial included comparison with turbulence sensors fitted on an AUV, and with a ship-deployed Vertical Microstructure Profiler. There have been many lessons learnt by Dr Matthew Palmer and his team at NOCL on this innovative (and rather ungainly) combination of sensor and platform (Fig. 1.14).

Figure 1.14: Rockland Scientific microRider turbulence package on a Slocum glider prior to trials in June 2011. Note the cover over the fragile sensors on the front of the turbulence probe, the black tube on the upper surface of the glider (courtesy Chris Balfour, NOCL).

[32] http://www.rocklandscientific.com/News/tabid/57/EntryID/532/Default.aspx Accessed 8 April 2012
[33] http://eprints.soton.ac.uk/200295/ Accessed 8 April 2012

1.5.2 Sensors in early adoption or development for gliders or low power AUVs.

pH and CO_2

The *in situ* measurement of pH by wet chemical or immobilized dye spectrophotometric techniques, and using solid-state ion-selective field effect transistors, is an active area of research. Early commercial devices are becoming available, such as the SeaFET pH sensor from Satlantic[34]. Many still have technical limitations, e.g. in drift, very slow response (minutes for the immobilized dye versions) or limited pressure tolerance. For example, the SeaFET is currently only for use in waters shallower than 70 m, and the drift is typically ~0.005 per month.

Microfluidic devices are also being developed, for example by Rao and colleagues at the University of Marland[35], and by Rerolle, Achterberg, Mowlem and colleagues at NOC[36]

Nutrients

Nitrate: The solid-state approach uses the absorption of ultra-violet light as the sensing method. A now-mature sensor based on this technique is the ISUS V3 instrument from Satlantic[37]. Its power consumption, at 7.5 W, is high, and would reduce severely the endurance of a glider, but is more readily handled within a long endurance AUV such as Autosub Long Range. The size also makes it more suitable for a larger vehicle; on a glider it would need to be carried externally as for the microRider turbulence probe.

Wet chemical approaches based on microfluidics have the potential to provide nitrate sensing with the size, form factor and power consumption suitable for use on gliders. One such implementation by Matthew Mowlem and colleagues at NOC (Sieben et al., 2010) will be fitted to Seagliders from December 2012 as part of the NERC Sensors on AUG programme for scientists at Plymouth (Dr Maeve Lohan), NOC Liverpool (Dr Claire Mahaffey) and NOC Southampton (Dr Adrian Martin).

Phosphate: Microfluidic and electrochemical approaches are being studied for measuring dissolved phosphate concentration. Mowlem's group, referenced above, are developing a phosphate sensor for glider use. A multiparameter analyser, including phosphate and ammonia, has been developed for use on the REMUS AUV by Sub-Chem[38].

Radionucleides

A Princeton Gamma-Tech Scintillation sensor has been fitted to a Seaglider (Fig. 1.15) for gamma spectroscopy in the range 100 keV to 5 MeV. This combination was purportedly used off Fukushima, Japan to look for I-131, Cs-134 and Cs-137[39].

[34] http://www.satlantic.com/seafet Accessed 9 April 2012
[35] www.onr.navy.mil/reports/FY10/eorao.pdf Accessed 9 April 2012
[36] http://meetingorganizer.copernicus.org/EGU2012/EGU2012-3012.pdf Accessed 9 April 2012
[37] http://www.satlantic.com/isus Accessed 9 April 2012
[38] http://www.subchem.com/products.htm Accessed 9 April 2012
[39] http://www.pgt.com/item/seaglider-uuv-pgt-scintillator-detector.html Accessed 9 April 2012

Figure 1.15: Princeton Gamma-Tech scintillation sensor fitted to an iRobot Seaglider (courtesy Edison Hudson, iRobot).

1.5.3 Summary of the impact of sensor energy use on endurance

The additional power drawn by the sensors reduce the available energy available for mission endurance. Table 1.3 illustrates the reduction of mission endurance for some of the sensors described above. These are indicative figures only, as energy saving measures may be implemented to minimise energy consumption by the sensors.

Sensor/instrument	Power consumption (mW)	Reduction in endurance (%)	Notes
Aanderaa optode 4330	120	9	2s sampling interval
Sea-Bird oxygen SBE43	60	4	
Wetlabs BB2F backscatter and fluorescence	70	5	1s sampling, interlaced with sleep.
Seapoint Ultraviolet fluorometer for CDOM	230	15	Average consumption.
Satlantic OCR504 radiometers	300	18	
Chelsea UviLux hydrocarbon or CDOM fluorometer	<1000	<43	Continuous use. Two needed for both hydrocarbons and CDOM.
MBBP Bathyphotometer	5500	80	As used on REMUS
Chelsea GLOWtracka	480	27	Without external pump.
WHOI digital acoustic recorder	230	15	Or can be self-powered.
Nortek Aquadopp ADCP	200-1000	7–22	Typical at 1Hz update rate, used on down glide only.
Airmar acoustic altimeter	50	4	At a typical 11% duty cycle with ~500mW in use.
Imagenex 853 120 kHz	<250	<15	With 4s sampling interval
Rockland microRider turbulence package	3000	54	At 15V continuous use on downcasts only

Table 1.3: Indicative power consumption of additional sensors a glider may carry and an indication of impact on mission endurance if the sensor is used on each up and down cast, except where another scenario is noted. Normal deep Slocum power consumption is assumed at 1.3W.

1.5.4 Sensors and instruments for high-power AUVs

On the Autosub3 and Autosub6000 vehicles far more power is available for sensors and instruments compared with gliders and Autosub Long Range. If required, several hundred watts can be sourced. Of course, the same principles apply, this power consumption will be at the expense of reduced range or endurance or speed.

Nevertheless, the acoustic instruments listed in Table 1.1 for Autosub3 and Autosub6000 are only possible because of this high power capacity and the payload volume and mass capabilities of these large vehicles. Thus, Autosub6000 can operate at the same time, a long-range swath bathymetric sonar (Kongsberg EM2000) to determine seabed morphology, a chirp sub-bottom profiler for sediment studies, and a high-frequency side-scan sonar for acoustic imagery of the seabed. In addition, there is sufficient energy available for high power flash units so that monochrome (proven on RRS *James Cook* cruise 60[40] in 2011) and colour (proven on RRS *Discovery* cruise 377 in July 2012) cameras can be deployed. It is on this latter cruise that Defra-funded time will be added to demonstrate this combination of capabilities on the UK continental shelf.

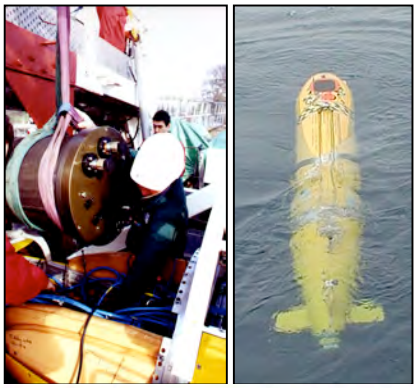

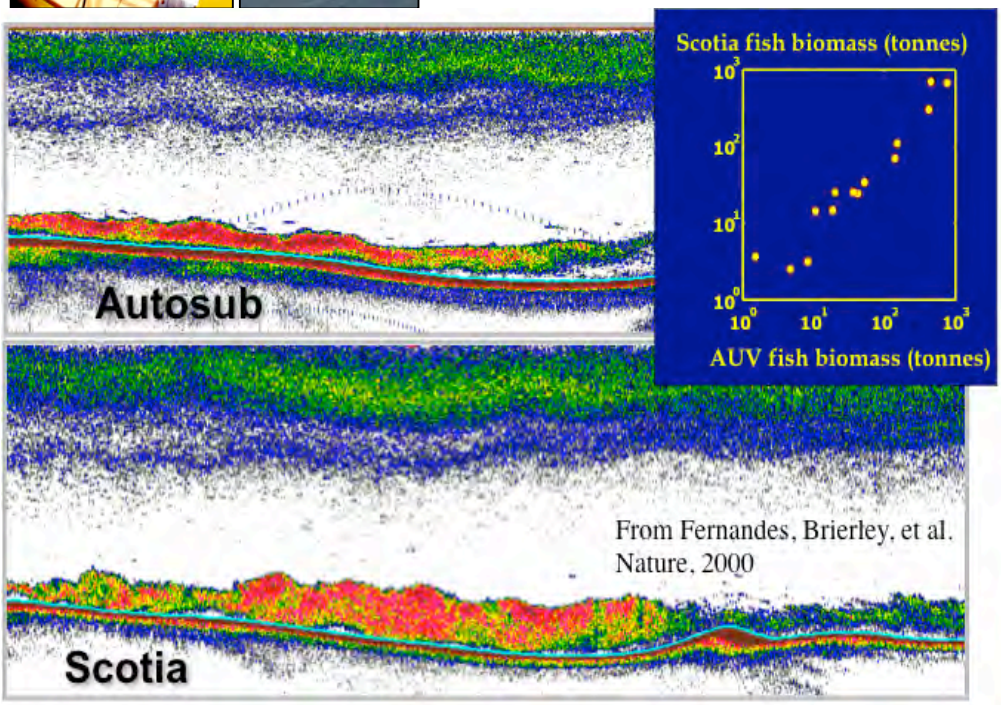

Figure 1.16: Left, the 112 kg enclosure with an EK500 echosounder being lowered into Autosub1 in July 1999. Right, the 38 kHz and 120 kHz transducers in the "upward-looking" mode on the vehicle. They could also be operated looking down, as for the data set below, taken from an acoustic survey of herring in the North Sea. Here Autosub travelled 200-800 m ahead of FRV Scotia, carrying exactly the same echosounder. A comparison of fish biomass from both systems is shown in the inset.

[40] http://www.eu-hermione.net/jc060-home Accessed 12 April 2012

The payload and power available on these large AUVs also makes them platforms suitable for carrying standard fisheries sonars. The *de facto* standard scientific fisheries echosounder, the EK60, could be carried, with transducers for multiple frequencies. The EK500, the precursor to the EK60, was carried on Autosub1 on missions in the North Sea in July 1999 (Fig. 1.16, acoustic surveys of Herring by the Marine Laboratory, Aberdeen, Fernandes et al., 2000) and in Antarctica (Fig. 1.17, zooplankton (krill) studies, Brierley et al., 2001).

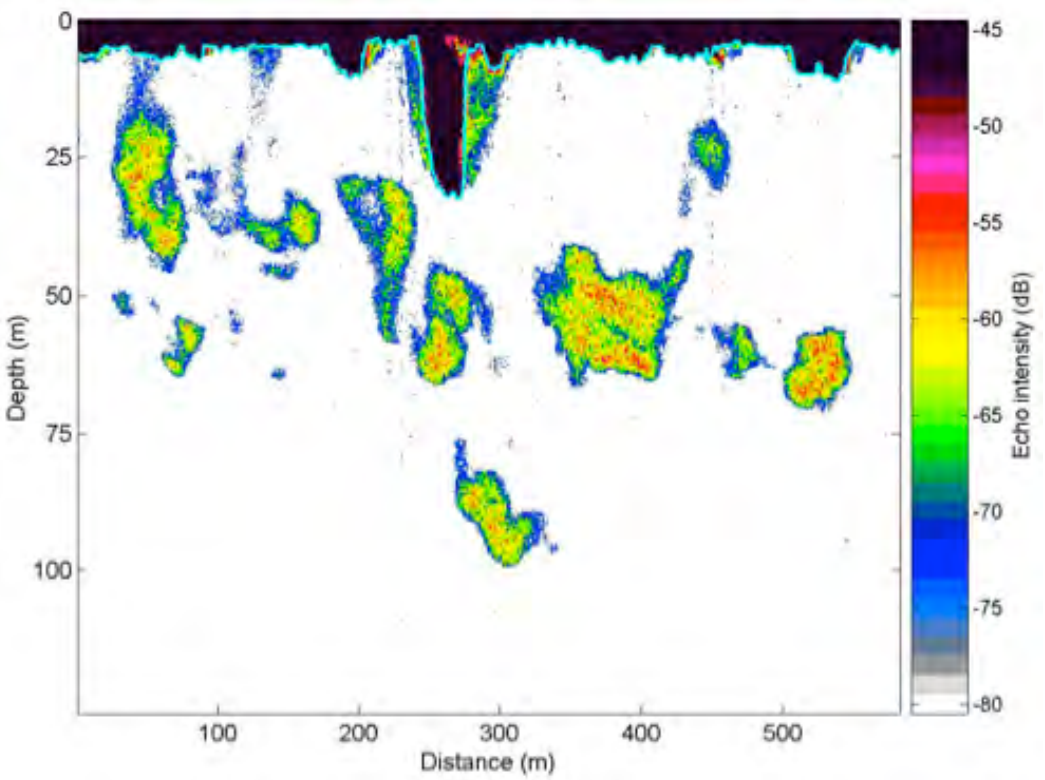

Figure 1.17: Acoustic record of krill swarms (associated with keels in the sea ice – upper black trace) taken with an EK500 echosounder in the northern Weddell Sea on Autosub1 in 2001.

1.6. Legal issues and Diplomatic Clearance

Legal issues and diplomatic clearance are increasingly important for autonomous vehicles, but poorly understood by many. Much of the experience to date has been in three areas of use, namely:

a) Marine Scientific Research (MSR), as understood in the UN Convention on the Law of the Sea.
b) Military Data Gathering (MDG).
c) Commercial surveys.

Obligations differ depending on the purpose of the data gathering programme. In the case of AUV programmes for MSR at Southampton, to avoid potential legal action in either public or private law, a wide-ranging report was commissioned in 2000 from two academic maritime lawyers. These informed our own operations, procedures and practice, and we subsequently made the reports available to the wider AUV community through the Society for Underwater Technology[41]. There remains to this day a great deal of uncertainty in maritime law as to whether an AUV is or is not a ship. The answer to that question is key to the laws and regulations that may or may not apply.

As an additional pragmatic initiative given this situation of uncertainty, we took part in a collective endeavour supported by the Society for Underwater Technology, involving AUV users from academic, commercial and defence backgrounds to develop a Code of Practice. This approach of self-determined good practice has worked well.

A summary of issues facing the US military in using unmanned maritime systems for military data gathering can be found in Kraska (2010)[42].

While it may be argued that AUVs gathering data in support of mapping and monitoring of the UK MPA/MCZ network would be Marine Scientific Research, some may well argue that it is not research but resource mapping. Note that the potential for an autonomous vehicle to inadvertently enter another nation's EEZ (e.g. due to a navigation fault) means that it is NOC practice (though not universal) to seek prior permission through the usual channels in case of an incursion.

It would be advisable for DEFRA to seek and obtain a legal opinion on these matter from a competent person. Advice on suitable persons, if required, can be given by Roland Rogers at NOC Southampton, contact: rxr@noc.ac.uk

[41] These reports are available for purchase via http://www.sut.org.uk/htmfoldr/books/TOOAU_pub.htm accessed 27 April 2012.
[42] See http://www.journalofoceantechnology.com/?page_id=73&id=24&jot_download_article=193 accessed 27 April 2012.

1.7. Comparisons with Commercial Systems and Providers

1.7.1 Manufacturers of commercial propeller-driven AUVs

There are a number of commercial AUVs in service with military, academic and commercial organisations world-wide. The representation of commercial vehicles in the UK fleet described in this report is very limited. Essentially, only one manufacturer is represented, Kongsberg Hydroid, and with only two vehicle types from the same family (REMUS 100 with the Royal Navy and at Heriot Watt University, and REMUS 600 at SAMS and the Royal Navy). A summary of some other leading commercial vehicles follows:

a) *Hugin 3000* from Kongsberg, Norway[43]
   - 3000 m depth rated, with a mass of ~1400 kg and a 470 km endurance at 1.5 m/s
   - Extensive proven sonar suite including dual sidescan (as for Autosub6000), conventional multibeam, synthetic aperture sonar for high, range-independent resolution, sub-bottom profiler.
   - Navigation by Inertial system with Doppler log or long baseline acoustics, or ultrashort baseline from an accompanying vessel.
   - Iridium satellite communications.
   - Purpose built launch and recovery system.
   - In use by major contractors based in the US, C&C Technologies[44] and Fugro[45]. C&C styles itself the world leader in commercial deepwater AUV surveys, and it is probably correct.

b) *Hugin 1000* from Kongsberg, Norway
   - 1000 m depth rated, a derivative of a vehicle first developed for mine hunting, with a mass of ~650 kg and a 250 km endurance at 1.5 m/s.
   - Same acoustic instrument suite and navigation capability as for Hugin 3000.

c) *Explorer* from International Submarine Engineering, Canada
   - Variants with up to 5000 m depth rating, has sold to research institutes in Europe and Japan, typical mass of 700 kg and 100 km range in minimalist configuration up to 350 km+ range with extended battery payload space.
   - Similar sonar capability to Hugin 3000 and Autosub6000.

d) *Bluefin21* from Bluefin Robotics, USA
   - Most common is the 300 m variant, but a depth rating of 3000 m is possible, mass of 360 kg, with a range of 120 km.
   - More restricted sonar suite given smaller size, typically a single high frequency sidescan and a small 200kHz multibeam, optional sub-bottom profiler.
   - The vehicle has a full capability inertial navigation system.
   - Only one known in Europe is an early version with the Alfred Wegener Institute, Germany. A smaller Bluefin 12 vehicle is owned by Global Marine, Portland, Dorset. Global Marine also act as UK agents for Bluefin.

[43] See http://tinyurl.com/cgmyrcc accessed 27 April 2012
[44] See http://www.cctechnol.com/site368.php accessed 27 April 2012
[45] See http://tinyurl.com/ct7zudp accessed 27 April 2012.

e) *SAAB Seaeye*[46], based in Fareham, UK although primarily known for its ROV product line, does build and sell the Sabertooth AUV.
   - This is a hover-capable deep water AUV, rated to 3000 m with a mass of 250 kg and a typical range of 20-40 km at 2 m/s.
   - It has an inertial measurement unit and can sprint at up to 10 knots.
   - Its instrument payload can include cameras and imaging sonars.
   - A fundamental difference with this vehicle from others is that it has been designed with a docking capability, and not as an add-on. Docking stations could be satellites of offshore platforms, for example. However, this is a concept of operations that is not yet entirely proven. There are certainly questions over having an expensive asset on standby in a seabed docking station.

f) *Gavia* from Teledyne Gavia, USA and Iceland
   - This is a small AUV somewhat similar in size and capability to the REMUS 100 from Hydroid. In its most capable Offshore Surveyor form the depth rating is 500-1000 m, with a mass of 80 kg and a typical endurance of 4-5 hours at 1.5 m/s. Extra batteries can double this endurance.
   - The vehicle can carry a GeoSwath interferometric swath bathymetric echo sounder, or a sidescan sonar and camera, or a sub-bottom profiler.
   - It has a full capability inertial navigation system with Doppler log.
   - As a relatively low cost vehicle, it is operated by several survey companies, ncluding Fugro Survey Perth, Australia and NCS Survey based in Aberdeen.

g) *Iver2* from OceanServer, USA
   - This is probably the lowest cost AUV currently available and in use by a number of organisations. In its 580-Extended Payload configuration it has a mass of 21 kg and an endurance of up to 14 hours at 1.2 m/s.
   - The vehicle has a mapping payload capability, based on new generation miniature sonars, which can give impressive short-range performance. These include the Imagenex Yellowfin triple-frequency sidescan sonar (260/330/770 kHz) and the Marine Sonics SeaScan HDS dual frequency sidescan (600/1200 or 900/1800 kHz).
   - Navigation is by dead reckoning, it does not have an inertial navigation system or precision heading or speed as standard.

1.7.2 Commercial gliders

All of the gliders described in this report are commercially manufactured. The UK academic community has gliders from the two main manufacturers, iRobot Corporation and Teledyne Webb Research, both based in the USA. A third US company, Bluefin Robotics, manufactures a glider – the Spray[47], but it has only been sold in small numbers. There is also a development in France, the SeaExplorer from the company ACSA[48].

[46] See http://www.seaeye.com/ accessed 3 May 2012.
[47] See http://www.bluefinrobotics.com/products/spray-glider/ accessed 27 April 2012.
[48] See http://www.underwater-gps.com/uk/product-detail.php?pr_id=8 accessed 27 April 2012.

1.7.3 AUV or Glider service providers

The offshore oil and gas industry is an extensive user of AUV services provided by survey companies. These survey companies have, in a number of cases, worked closely with vehicle manufacturers to develop an end-to-end capability to deliver data to clients. The survey companies act as full service contractors, to include providing the support ship and the initial data processing and mapping.

The leading survey company using AUVs is C&C Technologies. Based in Lafayette, Louisiana, USA, their Hugin AUVs are very closely integrated with their ships, which is an advantage in terms of reliability, but restricts operations to a "whole package" approach, in that operations from ships of opportunity is more difficult. In part this is a constraint due to these vehicles using an aluminium-hydrogen peroxide semi-fuel as an energy source, and hence refuelling is more complex than charging a battery.

Kongsberg Maritime / Hydroid has an Aberdeen-based pool of REMUS 100 vehicles for hire[49]. Their hire agreement requires the use of a Hydroid technician with the vehicles; this package is typically bought by a survey provider without its own AUV capability (e.g. the Gardline Group[50]). The client typically contracts with the survey provider that then sources the AUV capability from the Hydroid pool. There are no REMUS 600 or Hugin vehicles currently available in the rental pool.

Fugro Survey[51] also operate Hugin vehicles, in this case deep-water variants of the 1000 vehicle, thus without the limitations of the semi-fuel cell. They have five AUVs in their fleet and can operate on 3rd party ships as well as their own. The UK office of Fugro Survey acts as contact point for this capability.

Aberdeen-based NCS Survey[52] operates Teledyne Gavia vehicles. Rapid response is one of the areas where the company specialises.

There are a few companies providing operational oceanography services using gliders. We understand that iRobot, the manufacturer of Seaglider, is selling packages of data acquisition services using gliders. The US-based company Horizon Marine does sell glider-based data-gathering services to the offshore industry[53]. We are aware that the German company Optimare is likely to be a European partner for iRobot and may sell its services as a glider operator (a service it already delivers to the Alfred Wegener Institute). However, we are not aware of any UK-based companies (e.g. Gardline) that offer glider surveys.

When the research community has proven the feasibility and usefulness of MPA/MCZ survey options using AUVs or gliders, companies such as those listed here could well be able to undertake the routine operations.

[49] See http://tinyurl.com/ce3aznm accessed 3 May 2012.
[50] See http://www1.gardline.com/ accessed 3 May 2012.
[51] See http://www.fugrosurvey.co.uk/auv/ accessed 1 May 2012.
[52] See http://www.ncs-survey.com/services-4/auv-19 accessed 1 May 2012.
[53] See http://www.horizonmarine.com/services/ accessed 27 April 2012.

1.8. References

Baumgartner, M. F. and Fratantoni, D.M. (2008) Diel periodicity in both sei whale vocalization rates and the vertical migration of their copepod prey observed from ocean gliders. *Limnology and Oceanography*, 53, 2197–2209.

Boyd, T. et al. (2010) AUV observations of mixing in the tidal outflow from a Scottish sea loch. *Proc. AUV 2010, IEEE*.

Brierley, A.S., Fernandes, P.G., Brandon, M.A., Armstrong, F., Millard, N.W., McPhail, S.D., Stevenson, P., Pebody, M., Perrett, J.R., Squires, M., Bone, D.G. and Griffiths, G. (2002) Antarctic krill under sea ice: elevated abundance in a narrow band just south of ice edge. *Science*, 295, 1890-1892.

Cunningham, A., et al. (2003) Fine-scale variability in phytoplankton community structure and inherent optical properties measured from an autonomous underwater vehicle. *J. Marine Syst.*, 43, 51-59.

Davis, R.E., Eriksen, C.C. and Jones, C.P. (2003) Autonomous buoyancy-driven underwater gliders. In: Griffiths, G. (ed), *Technology and applications of autonomous underwater vehicles*. Taylor and Francis, London, p. 37-58.

Fernandes, P.G. et al. (2000) Fish do not avoid survey vessels. *Nature*, 404, 35-36.

Griffiths, G., Jones, C., Ferguson, J. and Bose, N. (2007) Undersea gliders. *Journal of Ocean Technology*, 2, 64–75.

Gruber, N. et al. (2007) The Argo-Oxygen program. White Paper available from http://www-argo.ucsd.edu/o2_white_paper_web.pdf. Accessed 8 April 2012.

Kirkpatrick, G.J., Orrico, C., Moline, M.A., Oliver, M.J. and Schofield, O. (2003) Continuous hyperspectral absorption measurements of colored dissolved organic material in aquatic systems. *Applied Optics*, 42, 6564-6568.

Kirkpatrick, G.J., Millie, D.F., Lohrenz S.E., Moline, M.A., Robbins, I. and Schofield, O.M. (2006) An in situ sensor of phytoplankton community structure based on light absorption. *EOS Trans. Am. Geophys Union*, 87, no. 36, suppl.

Nicholson D., Emerson, S. and Eriksen, C.C. (2008) Net community production in the deep euphotic zone of the subtropical North Pacific gyre from glider surveys. *Limnology and Oceanography*, 53, 2226–2236.

Niewiadomska, K., Claustre, H., Prieur, L. and d'Ortenzio, F. (2008) Submesoscale physical-biogeochemical coupling across the Ligurian current (northwestern Mediterranean) using a bio-optical glider. *Limnology and Oceanography*, 53, 2210-2225.

Perry, M.J., Eriksen, C.C. and Sackmann, B.S. (2003) Seaglider autonomous observations of phytoplankton abudance in waters off the Washington coast, USA, in Spring 2002. *Meeting Abstracts, American Society Limnology and Oceanography*, Salt Lake City, February 2003.

Schmitt, R.W. and Petitt, R.A. (2006) A fast response, stable CTD for gliders and AUVs. *Proc. IEEE/MTS oceans 2006*. doi: 10.1109/OCEANS.2006.306907

Sieben, V. et al. (2010) Autonomous microfluidic sensors for nutrient detection: Applied to nitrite, nitrate, phosphate, manganese and iron. *Analytical Methods*, 2, 484-491. doi:10.1039/c002672g

Woithe, H.C. et al. (2011) Improving Slocum glider dead reckoning using a Doppler Velocity Log. *Proc. Oceans 2011, IEEE*.

Work Package 2: Spatial and temporal limits of AUV and Glider technology in UK waters

WP Leader: Miss Alice Jones (NOC)

2.1. The WP2 task

As set out in the proposal this task's remit was as follows:

"*This WP will assess the spatial and temporal limitations of AUV and Glider technology in UK waters. The first task will be to gain input from staff at MARS and NAGB as to the perceived operational limits of their devices, especially relating to tidal flow and turbidity. Input from partners involved in compiling case study data will provide some 'real-world' examples. The aim will then be to map the known operational limits onto broad-scale maps of tidal flow (provided by NOC-L based upon tidal flow models) and turbidity (provided by PML NEODASS based on satellite remote-sensing data). The latter will also have a temporal aspect, relating to periods of high phytoplankton biomass (spring blooms) and fluvial run-off. In addition, an attempt will be made to identify zones of intense shipping and fishing activity, as these will be deemed high-risk areas that are largely unsuitable for AUV and Glider deployment. The final product will be a UK map delimiting areas where, either seasonally or throughout the year, it is considered that AUV and Glider deployments will not be possible. This will then be compared with the existing rMCZ network to assess what proportion of the network could potentially be mapped using AUVs and Gliders. The WP will be led by NOC with limited input from SAMS sub-contractors associated with NAGB*.

This WP will be undertaken by NOC (with limited input from SAMS) between 1 March and 31 May 2012, although additional information may be derived from new case study data, which will be delivered between 1 June and 31 August 2012."

2.2. Tidal currents

In areas with strong tidal currents, there is the potential for AUV and Glider missions to be jeopardised as a result of interference with the planned mission path course and speed. In addition, there may be increased vehicle energy costs associated with stronger current flow, as reported for the SAMS 'Talisker' Seaglider, which was found to use significantly more energy during periods spent in dynamic shallower seas than during dives in deeper water off the shelf (see section CS3.7.1).

Problems with AUV operations, which typically run at 3-4 knots (1.5–2 m sec^{-1}), can occur in currents peaking at around a third of this speed (greater than 1 knot, or 0.5–0.8 m sec^{-1}; S.McPhail, pers com). There will clearly be significant navigation problems if current speeds are comparable to, or greater than, the vehicle speed, and this is likely to affect the slower moving Gliders more than the AUVs (Seaglider typical speed is 0.5 knots/0.25 m sec^{-1}; section CS3.4.2).

Missions on the continental shelf (shallow water) are more likely to be negatively affected by tidal flow than those in deeper water off the shelf, because of the higher energy environment in the shallower shelf-seas (for example see section CS4.4.1) and the fact that the vehicles cannot take evasive action in the face of strong currents by moving deeper in the water column, where current speed tends to be reduced. However, Gliders have also been reported to be affected by meso-scale eddies and boundary currents in deeper water missions, where internal flow velocities associated with these hydrodynamic features may be higher than Glider speed (section CS3.8.2).

The effect of current flow on robotic vehicles is difficult to generalise, as the exact impact will depend on the specific operating speeds of each vehicle and the tidal conditions it encounters, in particular the direction of flow relative to vehicle movement; with side-on flow being potentially more difficult to deal with both during the mission and during post-mission processing of data.

The images below show peak neap and spring tidal current speeds (Fig. 2.1) and the percentage time with flows over 1 m sec and 2 m sec (Fig. 2.2) within the UK coastal seas. This information can be used to identify areas where conditions *may* be considered a potential risk factor to the successful operation of AUVs and gliders, and where they should at least be taken into account during mission planning.

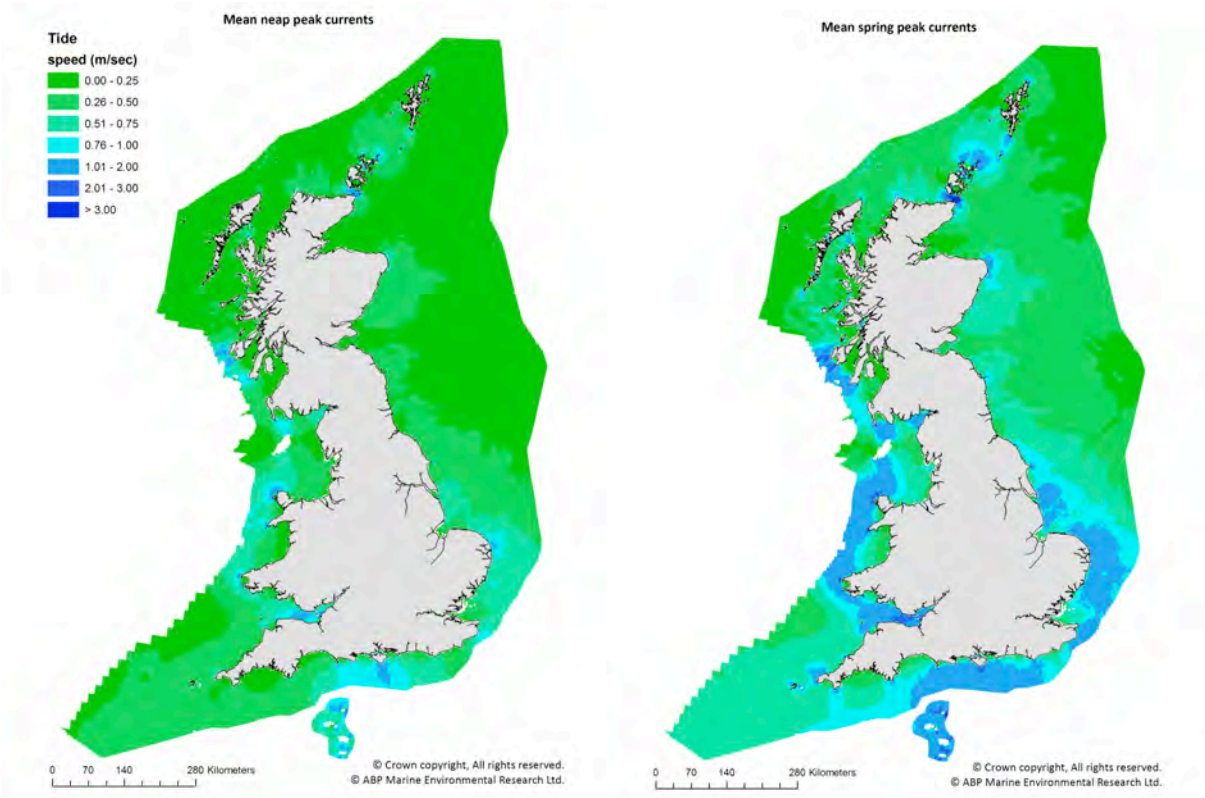

Figure 2.1: Peak current speed of mean neap (left) and spring (right) tides (m sec^{-1}), based on modelled data from the POL High Resolution Continental Shelf model. Data downloaded from the UK Marine Renewables Atlas (ABPmer, 2012) and subject to copyright as marked.

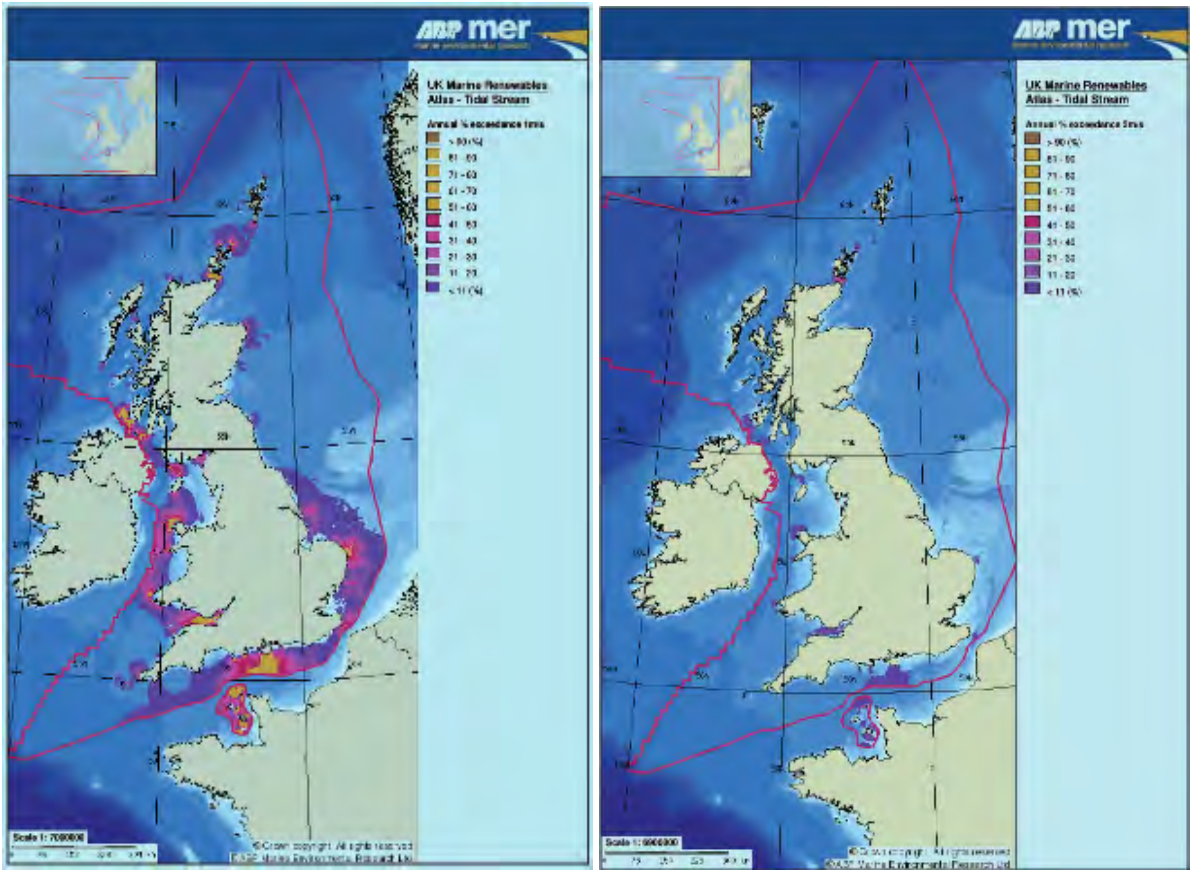

Figure 2.2: Tidal stream maps indicating percentage annual exceedance of 1 m sec^{-1} (left) and 2 m sec^{-1} (right), based on data from the POL High Resolution Continental Shelf (HRCS) model. Image downloaded from the UK Marine Renewables Atlas (ABP Marine Environmental Research Ltd. et al. 2008) and subject to copyright as marked.

The data in the maps in Fig. 2.1 and the images in Fig. 2.2 have been downloaded from the *ABPmer* Atlas of UK Marine Renewable Energy and are derived from the POL High Resolution Continental Shelf (HRCS) model. The HRCS modelled data has a horizontal resolution of approximately 1 nautical mile (1.8 km) and is based on a model prediction of a complete representative annual tidal event (therefore assumes that inter-annual variability is negligible).

Areas in the central English Channel, Bristol Channel and North Channel (between the Irish Sea and The Sea of the Hebrides) show high peak flows, with small areas experiencing currents greater than 1 m sec^{-1} during peak neap flow. This is also evident from some small channels between islands in the Hebridean and Orkney Islands, where flow is likely to be topographically restricted. Flows around headlands and promontories also tend to be higher (for example off the southwest Cornish peninsula, Pembrokeshire and the east coasts of Kent and East Anglia and Aberdeenshire). It is likely that tidal currents in these areas are being deflected by land, and this is concentrating flow into restricted areas.

2.3. Shipping traffic

There is a danger that underwater vehicles may become damaged or difficult to recover if they surface in areas of high shipping traffic, where boat-strikes would be an increased risk.
In accordance with the International Maritime Organisation regulations, vessel Automatic Identification System (AIS) must be fitted on all ships ≥ 300 gross tonnage undertaking international voyages, ≥ 500 gross tonnage undertaking domestic voyages, and on all

passenger vessels. AIS transmit information on vessel ID and location approximately once every 10 seconds while the ship is underway, or approximately once every few minutes while at anchor. The image in Fig. 2.4 shows AIS data collected from inshore waters around the UK over a period of four weeks during different months in 2008 (1st–7th Jan; 1st–7th March; 1st–7th June; 1st–7th Sept). This map of vessel density enables identification of high and low shipping traffic areas, with the highest density of traffic being indicated in red. It is worth noting that small inshore vessels will generally not have this system installed and therefore the map is not indicative of this type of marine traffic.

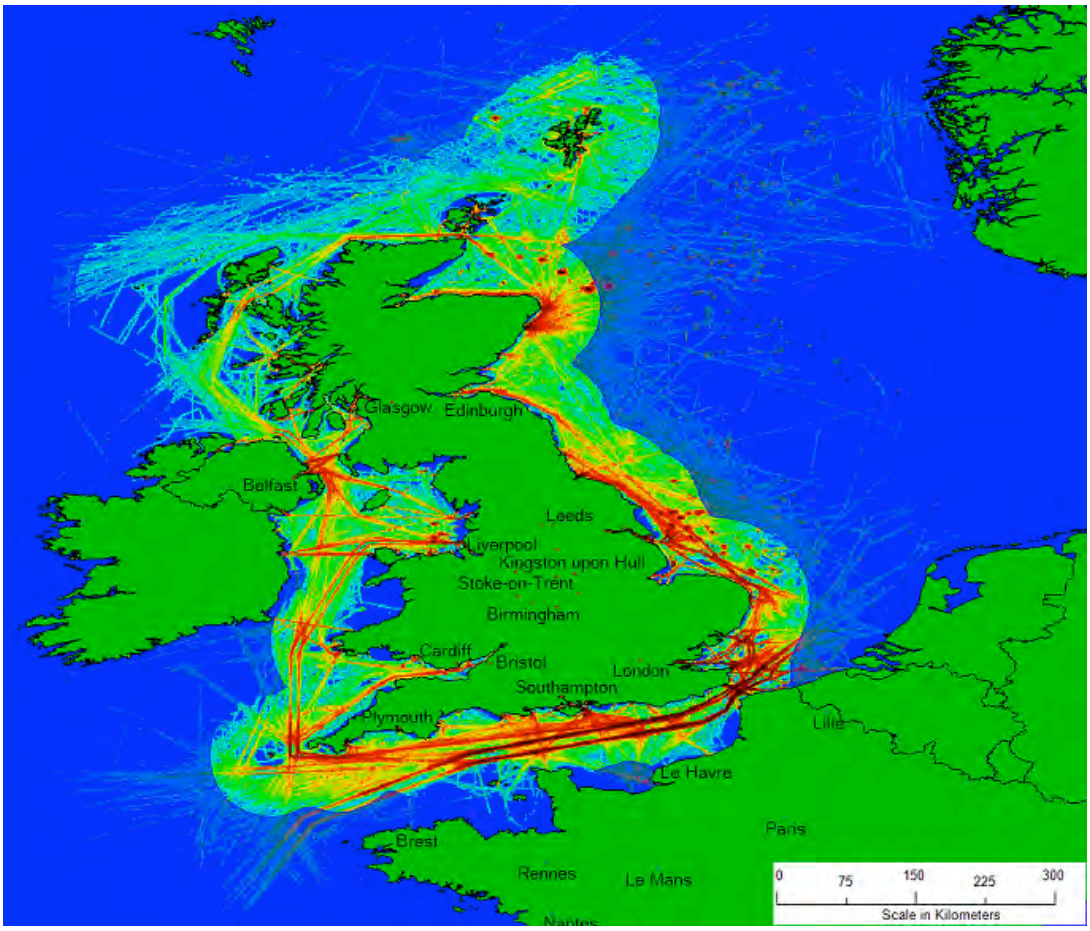

Figure 2.4: Analysis of Automatic Identification System (AIS) data from large vessels and passenger vessels within UK waters. Data are from four weeks in 2008: 1st–7th Jan; 1st–7th March; 1st–7th June; 1st–7th Sept. Amount of vessel traffic indicated by colour scale where red is highest density. Image courtesy of Luke Hankins, BMT Isis.

The shipping traffic data shows that most of the English Channel experiences high vessel traffic, with exceptional densities through the Straits of Dover and along the major shipping channels, which are clearly identifiable as parallel lines, indicating the traffic separation schemes (Fig. 2.4). The North Channel to the east of Belfast also has relatively high densities of large ship traffic as do the seas around the main ports along the east coast of the UK.

2.4. Fishing effort

The potential for entanglement or damage to underwater vehicles will be increased in areas with high levels of fishing activity, where there are increased densities of static or mobile fishing gear. The risks are likely to be higher in areas where trawling and gill-netting are prevalent, although longlines and pots/creel may also pose entanglement risks.

The images in Fig. 2.5 are from Witt and Godley (2007) and have been supplied in high resolution by Dr. Matthew Witt from the University of Exeter. They show patterns of fishing activity within the UK seas, using Vessel Monitoring Systems (VMS) data from UK registered vessels (Jan 2000 – Dec 2004). VMS is an automated system for recording data on fishing vessel locations at sea using GPS, and is mandatory on all EU member state fishing vessels ≥ 15 m overall length. The data represents fishing vessels using a range of gear types including dredging, beam trawling, pair trawling, gill netting and longlining. The data have been speed filtered, so should not show periods when boats are at anchor or in transit.

The maps in Fig. 2.5 indicate that fishing effort is not spread evenly throughout the UK seas, and is concentrated most heavily in areas in the western English Channel, Celtic Sea and at the shelf edge close to Goban Spur (GS on Fig. 2.5-a) and Porcupine Bank to the north. There are also very high-density areas to the northeast of Scotland and around the Orkney and Shetland Islands. There is a high level of consistency in the pattern of fishing activity, indicated by the low coefficient of variation of effort in the most fished areas (shown by dark colours on the maps in Fig. 2.5-c and d).

Looking specifically at the theoretically higher-risk fishing methods (trawls, gill netting and longlining) may provide more detailed information about the threats to AUVs and gliders in certain areas of the UK Sea. This data has been requested from the Marine Management Organisation and will be available for scrutiny during future operations.

Older data collected by the Fisheries Research Services (FRS) and the Centre for Environment, Fisheries and Aquaculture Science (CEFAS) during the period 1991–1996 (Coull et al., 1998) indicate that trawling for demersal species occured most frequently in the western Channel, Dover Strait and North Sea, with pelagic trawls also occurring frequently in the western Channel. Beam trawl effort (not shown) is similar to that of the pelagic fishing effort. Static gears (fixed nets, drift nets, long lines and traps) are used in high densities in inshore waters all along the coastline of the UK, apart from the Irish Sea, where effort is lower. There have been some significant changes in fisheries management structure and fishing boundaries since these data were collected, but it is assumed that the patterns in effort are still broadly indicative of the current situation (processed data for more recent years were not available).

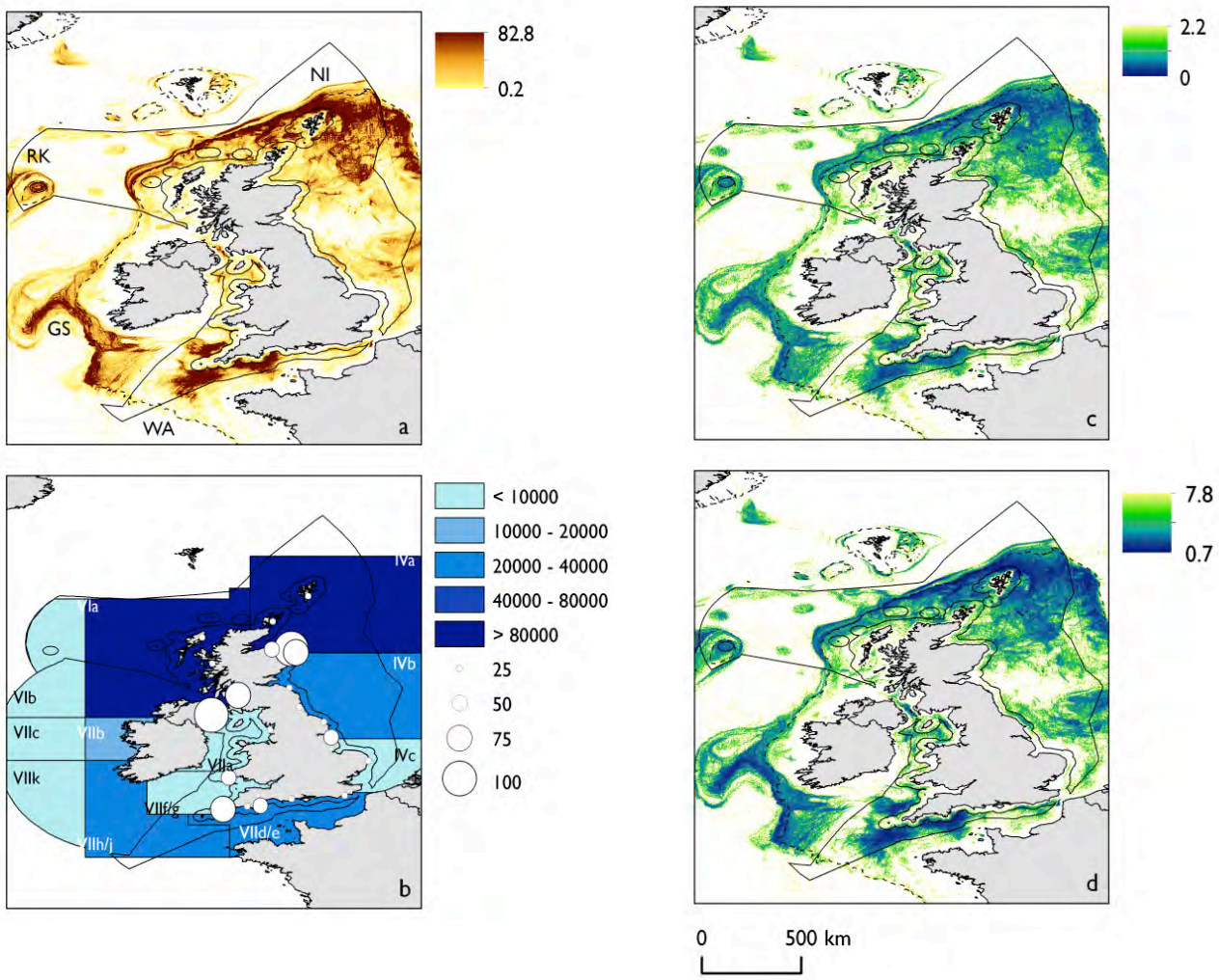

Figure 2.5: Mean annual spatial distribution of fisheries activity derived from VMS records using a simple speed filter. (a) Colour scale indicates mean annual number of VMS data points within 9km^2 pixels. WA = Western Channel, GS = Goban Spur, RK = Rockall, Northern North Sea = NI. (b) Tonnes of fish (demersal and pelagic) landed by UK registered vessels from the marked ICES statistical reporting boxes. White circles show the total number of vessels registered at main UK fishing ports (greater than 17 m length). (c) Coefficient of variation in the mean annual distribution, and (d) coefficient of variation of mean monthly distribution of fishing activity. For both (c) and (d) lighter colours = highest variability, darker colours = regions of consistent space-use. Image and caption reproduced with permission from Witt and Godley (2007).

2.5. Turbidity

Turbidity is a measure of the level of suspended particulate matter (SPM) in the water column. Turbidity levels can be highly variable spatially and temporally and are influenced by the interaction of physical marine forcing such as seabed currents, wind and waves, as well as seabed characteristics, river inputs, terrestrial runoff (affecting suspended sediment) and biological productivity (affecting levels of plankton and/or other organic particulate matter in the water). A high level of SPM will affect the clarity of the water by scattering and absorption of light, which in turn impacts on the quality of photographic data collected by AUVs.

Satellite-based Earth Observation (EO) data is presented in Figs. 2.6 and 2.7, which show Aqua-MODIS data through different seasons across multiple annual cycles (2003 – 2007). These images have been taken from Section 3.7 of DEFRA's Charting Progress 2 report

(UKMMAS, 2010) and highlight areas with constantly or seasonally high levels of suspended load. Measuring light attenuation (using the attenuation coefficient, k_d) provides information on the overall turbidity of the water (Fig. 2.6), whereas a measure called normalised water-leaving radiance at 551 nm, nLw(551), is used as an indication of the suspended sediment load in the surface waters (Fig. 2.7). Note that the data presented here are based on remote sensing from optical instruments, and are therefore only representative of the turbidity in the surface layers of the sea.

The results of the AUV survey presented in case study 2 (Section CS2) suggest that the amount of SPM in the water column can vary in shallow water environments on spatial scales relative to mission extent; both horizontally (Fig. CS2.6), and vertically (Fig. CS2.4). There was found to be a notable increase in turbidity below the thermocline, which would not be picked up by EO methods used to produce the images in Figs. 2.6 and 2.7, as these are only representative of surface turbidity.

The images in Fig. 2.6 highlight a tendency for increased turbidity in waters that are closer to shore and also where large rivers meet the coast, such as the Thames. The turbidity levels also tend to be high in parts of the UK coastal seas associated with strong tidal currents, and examination of finer temporal resolution images from NEODASS (NERC Earth and Observation Data Acquisition Service) indicate a visible difference between spring and neap flows (higher turbidity around spring tide periods). Turbidity is seasonally affected by phytoplankton blooms (usually highest in May) and weather, with winter turbidity influenced by high wind and waves (leading to increased mixing and sediment re-suspension), along with increased coastal and river runoff as a result of higher precipitation.

The Irish Sea, southern North Sea and northern English Channel are areas where high suspended-sediment loads are present throughout most of the year (Fig. 2.7), with a notable reduction in summer.

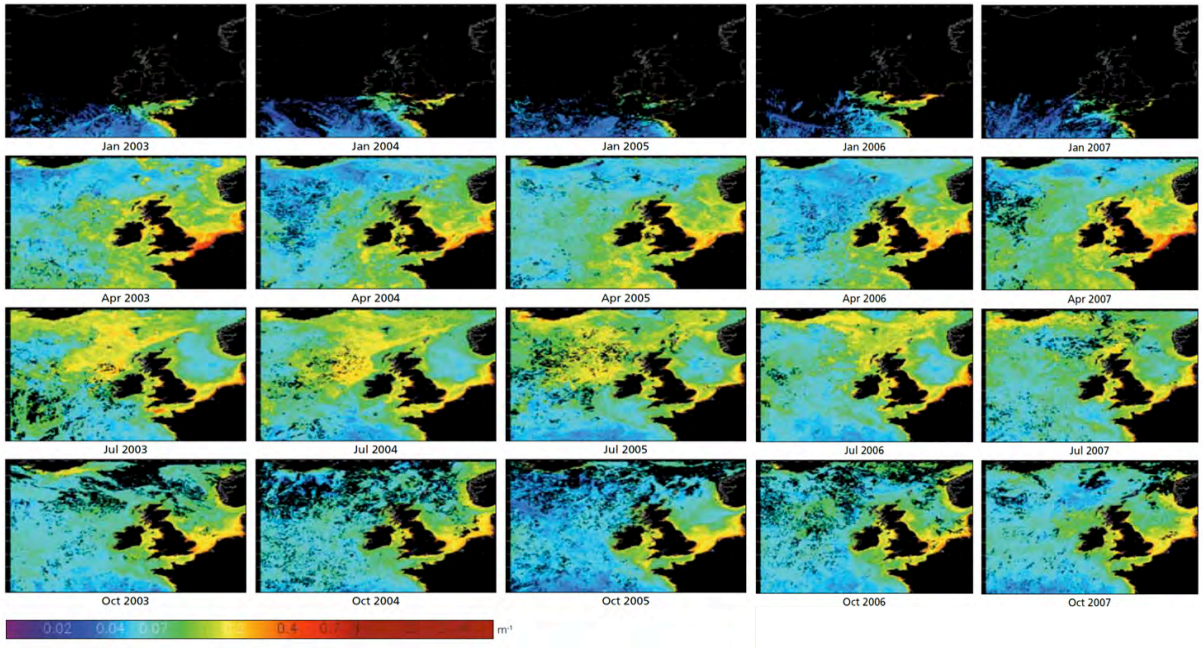

Figure 2.6: Turbidity maps from Earth Observation data for Jan, Apr, Jul and Oct 2003 – 2007. The maps show Aqua MODIS diffuse attenuation coefficient kd(490), which indicates the fraction of blue-green light that is attenuated per metre depth. The maps are representative of overall turbidity levels, therefore will include contributions from both suspended sediments and phytoplankton (the relative contributions of these components vary spatially and seasonally, with April and October being most influenced by suspended sediment load and July being most influenced by phytoplankton levels). There are no data from high latitudes in January because the low light at this time of year prevents the reliable use of the Aqua-MODIS data. Images are from the DEFRA Charting Progress 2 report (UKMMAS, 2010).

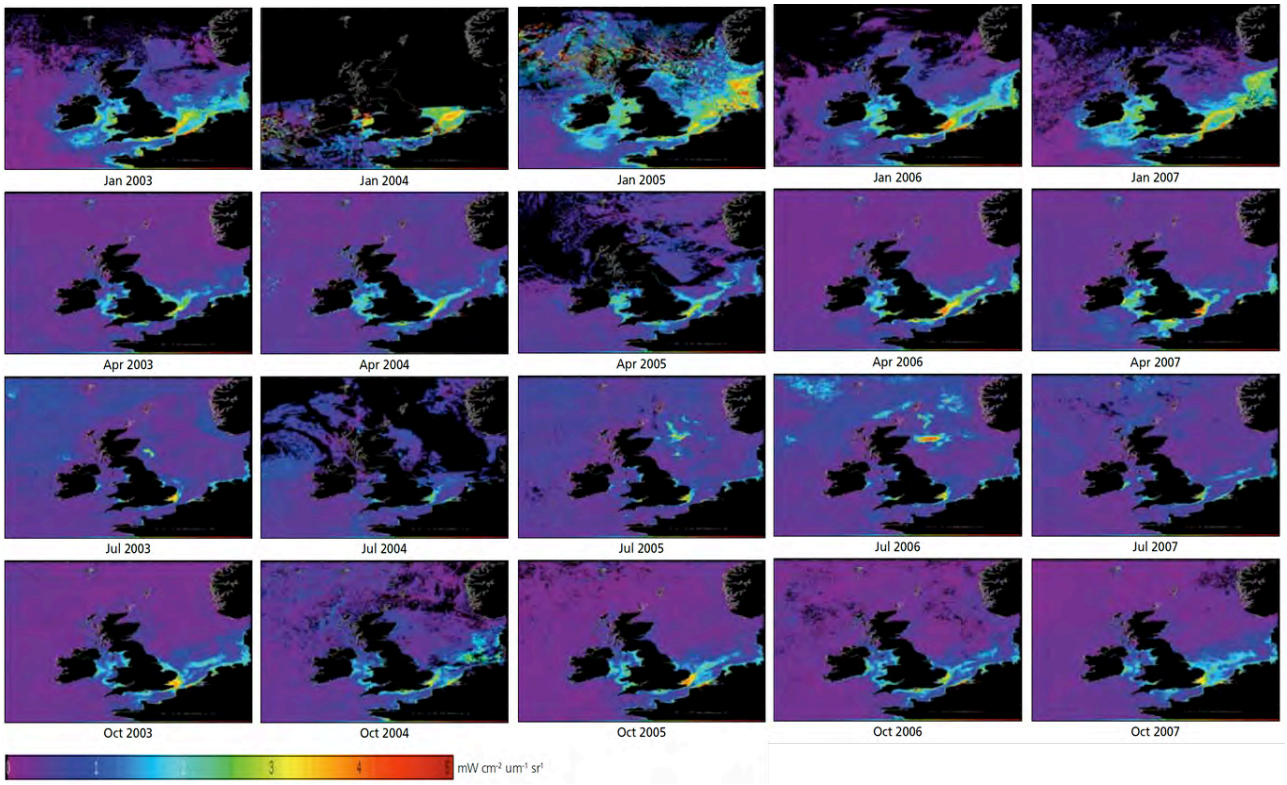

Figure 2.7: Maps of monthly suspended-sediment concentration from Earth Observation data for Jan, Apr, Jul and Oct 2003 – 2007. The maps show Aqua MODIS water-leaving radiance at 551 nm – nLw(551), which is used as a proxy for suspended sediment, although it will also pick up other scattering particulates such as coccoliths. The maps show that the seasonal pattern in the spatial distribution of suspended sediment in UK waters is consistent through the years. There are limited data from high latitudes in January because the low light at this time of year prevents the reliable use of the Aqua-MODIS data. Images are from the DEFRA Charting Progress 2 report (UKMMAS, 2010).

2.6. Offshore developments

The location of significant offshore development associated with oil and gas or marine renewable energy installations, may potentially cause obstruction to AUVs and Gliders. The map in Fig. 2.8 shows data layers from the Department of Energy and Climate Change (DECC) and Crown Estate (CE), which indicate the location of existing and proposed oil, gas, wind, wave and tidal energy developments within UK waters.

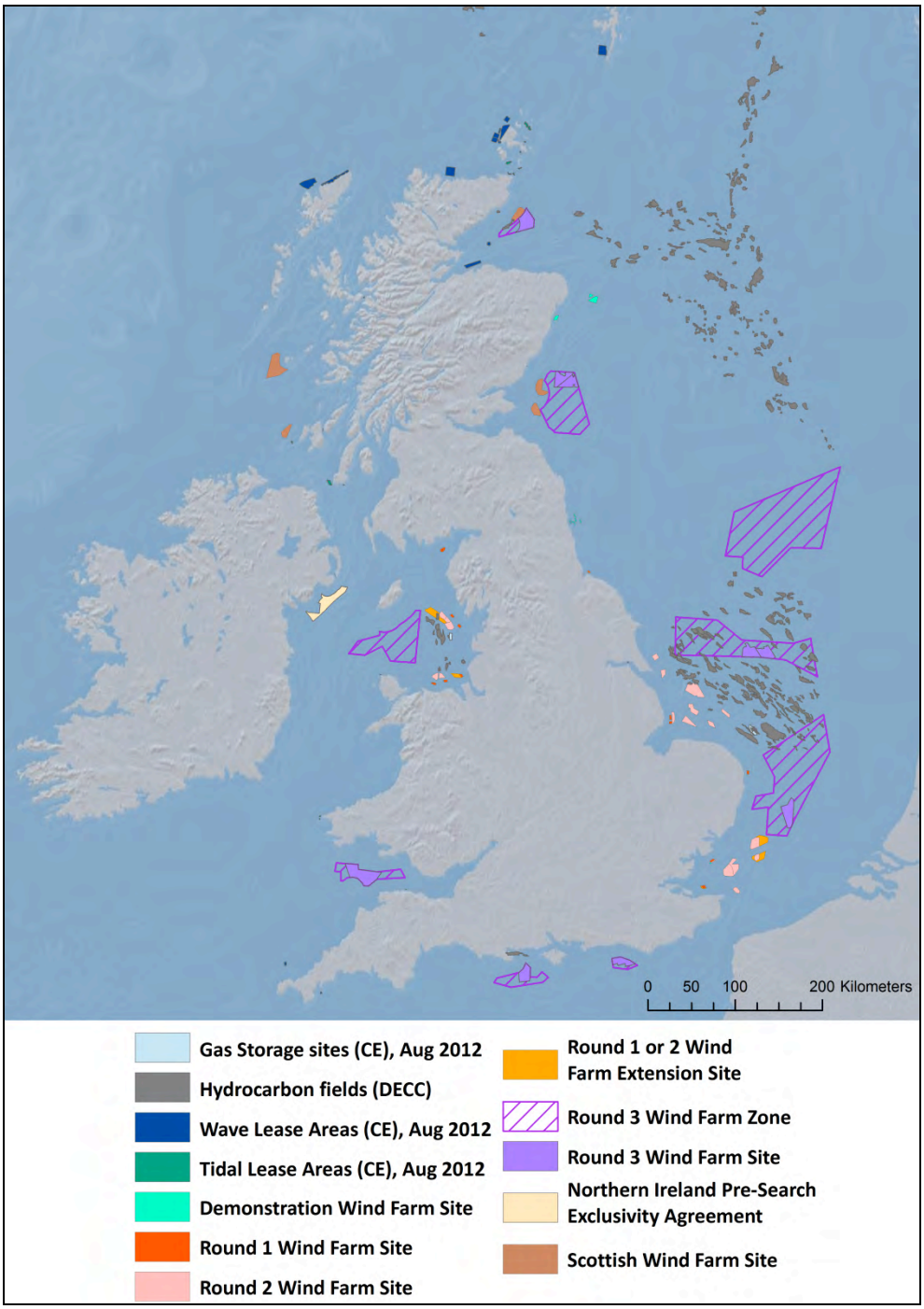

Figure 2.8: Map indicating the locations of various types of offshore energy activity including hydrocarbon fields (oil and gas; data from the Department of Energy and Climate Change DECC, 2012), wave and tidal energy lease areas (data from the Crown Estates, CE 2012), wind farm sites and potential development zones (data from CE 2012) and gas storage sites (data from CE 2012). Locations are based on the latest map layers available, as of Sept 2012.

It is clear from the map in Fig. 2.8 that activity related to offshore energy exists all around the UK, with the highest concentrations in the southern North Sea and northeastern Irish Sea. There is less offshore activity to the west of the UK, with noticeably little energy development existing or planned around the southwest peninsula, Celtic Sea and southern Irish Seas.

2.7. Summary of risk areas with reference to the location of marine protected areas in the UK seas

The map in Fig. 2.9 indicates the areas that are designated or proposed sites of marine conservation within the UK seas. These designations have been made in response to a range of national and European policies and represent sites containing habitats or species of conservation concern with some or all of their extent within marine environments.

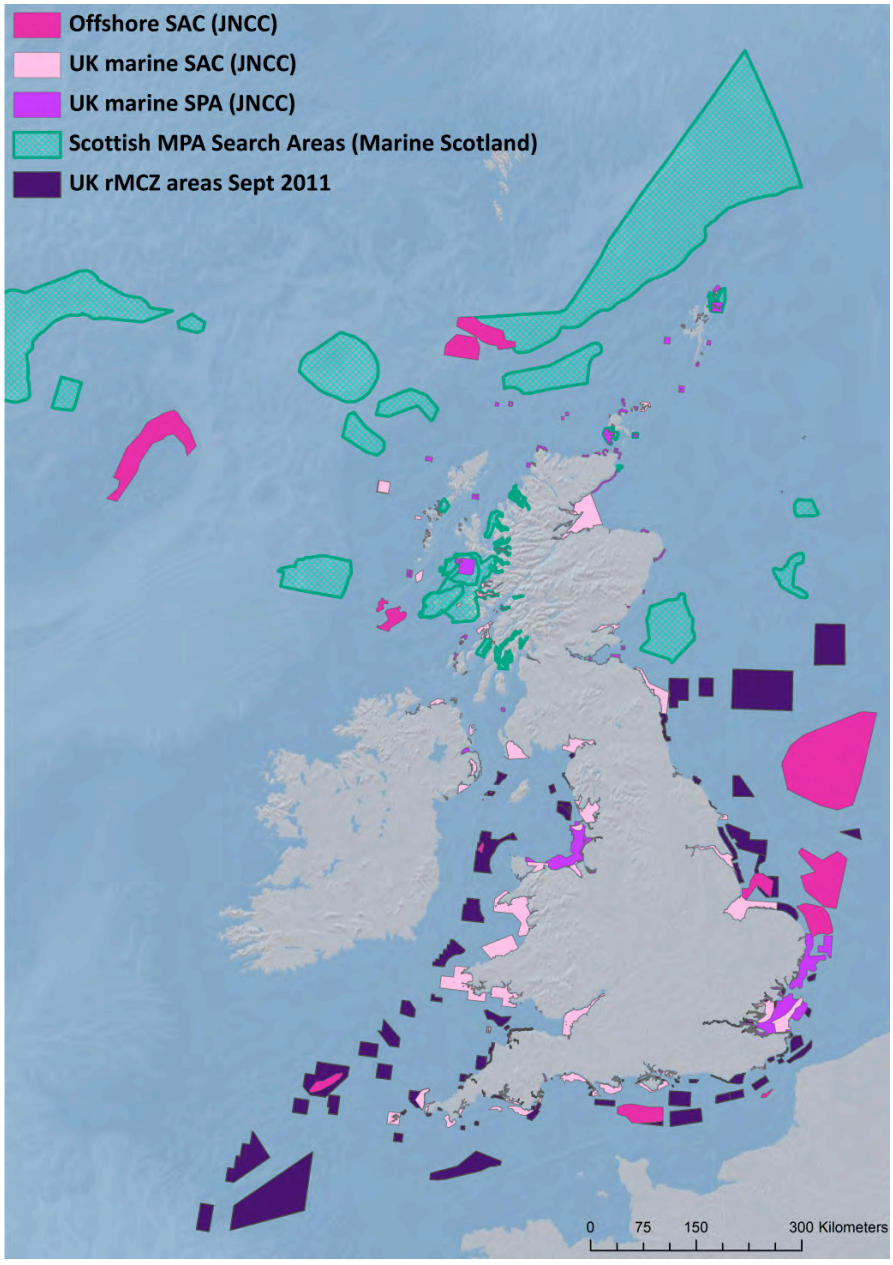

Figure 2.9: Location of designated (Offshore SAC, UK marine SAC and UK marine SPA) and proposed search areas for marine conservation site designation (Scottish MPA areas and UK rMCZ) within UK seas. Information sources are given in the map legend. Data are based on the latest map layers available, as of Sept 2012.

It is these areas that future AUV and Glider mapping and monitoring programmes, for MPA and MSFD purposes, are likely to be directed towards. Therefore it is pertinent to refer the risk areas highlighted in the previous sections to these protected areas, in order to broadly evaluate the ability of AUVs and Gliders to cover these key areas without risk to operations as a result of other activities and/or adverse conditions.

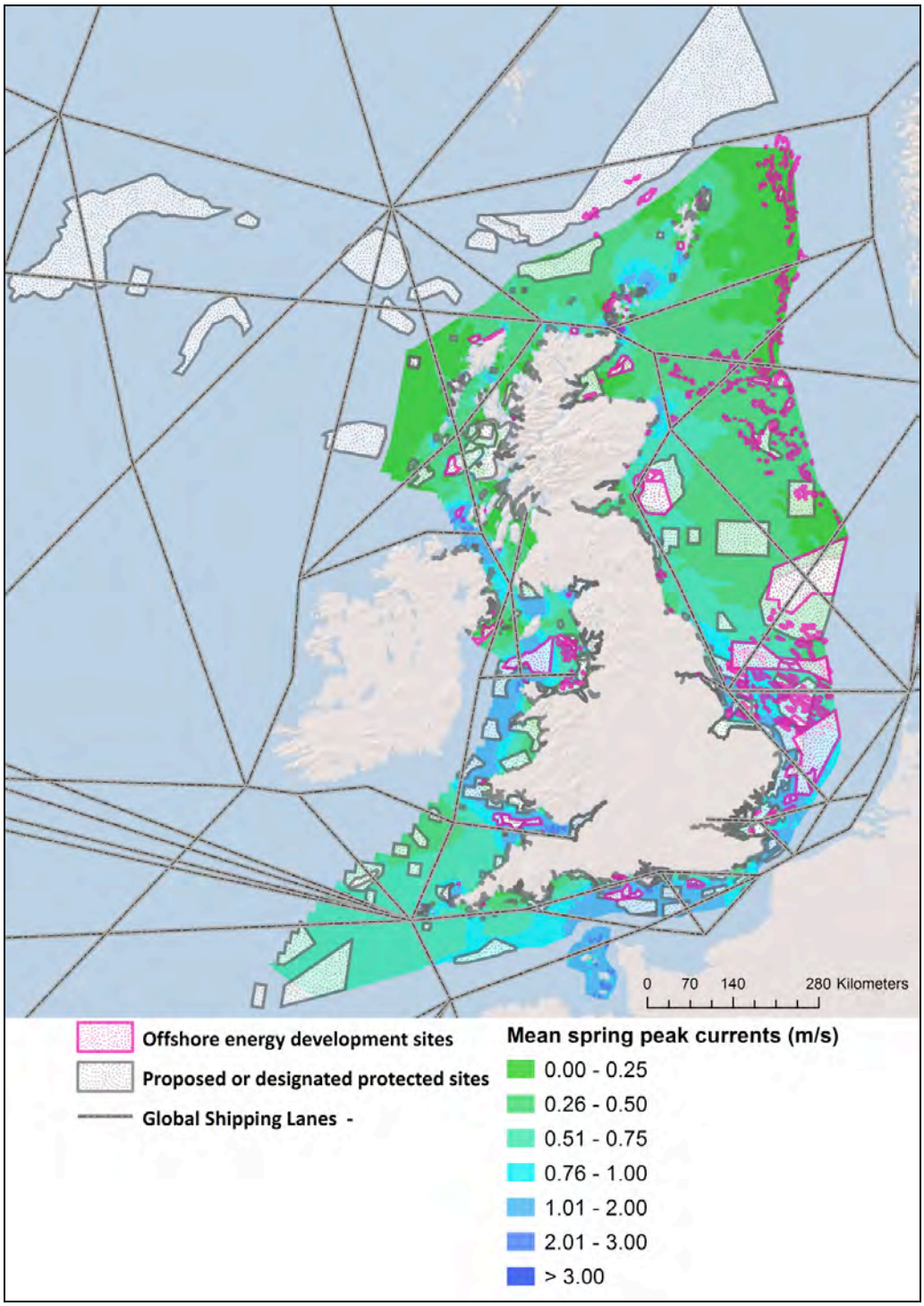

Figure 2.10: Map of UK proposed or designated marine protected sites (SACs, SPAs, rMCZs and Scottish MPA search areas) in the context of offshore energy development sites (oil, gas, wind, wave and tide), main shipping routes and mean peak spring tidal currents. Tide data downloaded from the UK Marine Renewables Atlas (ABPmer, 2012) and subject to copyright (reproduced with permission).

The map in Fig. 2.10 contains all available GIS layers from the previous sections and can be used to highlight areas of overlap between shipping traffic (indicated by shipping lanes), offshore development sites and high mean peak spring flows. This map does not contain information regarding turbidity or fishing activity (Figs. 2.5, 2.6 and 2.7), as these were not

available as processed GIS data layers within the timeframe of this report (although reference is made to the maps containing these data presented in the previous sections). Map layers for fishing and turbidity data will be made available for use in specific AUV and Glider mission planning.

Fig. 2.10 indicates that there are certain areas where high tidal flow, shipping lanes and offshore energy developments overlap, and may potentially affect the safe and successful application of AUVs and Gliders for the collection of monitoring data at marine protected sites. Regional summaries of the potential threats are given below:

2.7.1. Scottish proposed and protected areas in the northeast Atlantic and northern North Sea

Generally the Scottish MPA search areas and offshore SACs to the west of Scotland seem the least affected by potential risks assessed in this work package. There is little overlap of these areas with offshore development (Fig. 2.10) and high tidal flow (note that tidal data for much of this area are not available as a data layer for the GIS, but flow speeds are known to be generally slower in these deeper water areas; however, topographic restrictions such as the deep Faroe-Shetland Channel can experience local strong current flows). There is also less shipping activity (Fig. 2.4) and far lower fishing activity (Fig. 2.5) in these areas (although note that the shipping and fishing data presented relates only to vessels registered in the UK). Suspended sediment and overall turbidity levels are also low in these areas (Figs. 2.6 and 2.7).

2.7.2. Southern North Sea

The southern North Sea (offshore of Suffolk, Norfolk, Lincolnshire and east Yorkshire) has a particularly high level of offshore energy developments, which are relatively close, in some cases overlapping, to proposed or designated protected areas (Fig. 2.10). This area also experiences mean spring peak flows of greater than 1 m sec^{-1} (Fig. 2.10) and high levels of turbidity (related to suspended sediment load, see Figs. 2.6 and 2.7), although shipping traffic and fishing activities are relatively low. Further south in the North Sea, offshore of Kent and in the Thames Estuary and Dover Strait, there is a high concentration of proposed and designated SACs, SPAs and rMCZs (Fig. 2.10), which are within areas that experience consistently high levels of turbidity (associated with phytoplankton in the spring and autumn and suspended sediment in the winter, Fig. 2.7). Most of this area does not experience mean peak spring currents over 0.5 m sec (Fig. 2.10) and fishing levels are low (Fig. 2.5), although shipping traffic is considerable, particularly through the Dover Strait (Fig. 2.4).

2.7.3. The English Channel

The Central English Channel has consistently high tidal current flow (Figs 2.1–2.2) and shipping activity (Fig. 2.4), but the marine protected sites are far enough offshore to not suffer from the effects of high turbidity which are experienced closer to shore (Fig. 2.6). There is also relatively low fishing activity in this area (Fig. 2.5). Further west in the Channel, and into the Celtic Sea, tidal currents are generally slower and there is less shipping and offshore energy development (Figs. 2.10 and 2.4). Seasonal effects of plankton blooms (particularly in spring) may affect visibility in this area and there is high fishing activity in some parts, but these do not seem to overlap directly with the proposed or designated protected sites (Figs. 2.5, 2.7 and 2.9).

2.7.4. Bristol Channel

The proposed protected sites in the Bristol Channel are in areas of relatively high tidal currents (mean peak spring > 1 m sec^{-1}; Fig. 2.10). Shipping traffic tends to be higher in the southern part of the Bristol Channel (Fig. 2.4), and therefore high-density shipping is not closely associated with the designated (or proposed) sites, which are mainly along the northern parts of the Channel (Fig. 2.9). There is low fishing effort in the Bristol Channel and the main offshore development zone is not close to the protected sites (Fig. 2.10), therefore

unlikely to present a problem to monitoring. However there are high levels of turbidity in this area throughout the year (Figs. 2.6 and 2.7), which could potentially affect the collection of photographic data.

2.7.5. Irish Sea

Monitoring of the inshore protected areas in Cardigan Bay is unlikely to be significantly affected by tidal currents, shipping, fishing activity or offshore energy developments, although suspended sediment and seasonally high phytoplankton levels (in the autumn) may impede the collection of visual data from these sites at times (Figs. 2.6 and 2.7). Further offshore in the southern Irish Sea, tidal currents are stronger and could pose a risk to operations (Fig. 2.10); suspended sediment load is high in spring (likely to be associated with coccolith blooms) and overall turbidity is moderate through the year (Figs. 2.6 and 2.7). Fishing effort is low (Fig. 2.5), but shipping traffic in parts can be considerable (along the main shipping lanes; Fig. 2.4). There are no significant offshore developments in this area (Fig. 2.10). In the northern parts of the Irish Sea, the picture is similar, with inshore protected sites likely to be easier to monitor as a result of slower tidal currents (Fig. 2.10), but with the potential for seasonal peaks in turbidity to affect the successful collection of visual data (Fig. 2.6), particularly during the spring and autumn phytoplankton blooms. There are also a number of offshore energy developments in this region, some of which directly overlap with protected sites (hydrocarbon fields and Round 2 wind farm sites; Fig. 2.10). Fishing effort is low, as is shipping in most areas (apart from shipping lanes), therefore boat strike and/or net entanglement potential is low in this region (Figs. 2.4 and 2.5), although the Glider mission described in Case Study 4 of this report, in the deeper water of the Western Irish Sea, experienced an incident presumed to be the result of net entanglement, indicating that there is potential for interaction with fishing gear even in areas of relatively low fishing effort (Section CS4.3.1).

2.8. Summary

In conclusion, examination of the dynamic shelf sea environment and the level of human activity within the UK seas indicates that any future AUV and Glider monitoring missions will clearly have to be carefully planned with reference to tidal currents, turbidity, fishing, shipping and offshore energy activities.

The shallow-water deployment case studies (Sections CS3 and CS4) report successful extended deployments of Gliders in shallow, dynamic marine environments where human uses and strong tidal currents exist (CS4.2.2). In addition, although the image quality of the photographic data collected by the Autosub6000 AUV in CS2 was noticeably affected by SPM (CS2.4.3), the data were still of sufficient quality to characterise the seabed and census benthic fauna (CS2.5). It is also worth noting that methodological developments in image processing are underway at NOC (for removal of backscatter), which will enable improvements in the quality of images that are affected by turbidity.

There is high shipping traffic and fishing effort in many areas of the UK seas (Figs. 2.4 and 2.5), but this should not automatically preclude the use of AUVs and Gliders for monitoring protected marine sites; although clearly some sites are more amenable to this method of monitoring than others. In particular, the seas around Scotland, western English Channel and Western Approaches, Bristol Channel and southern Irish Sea show promising potential for AUV and Glider monitoring to be successful, dependent on exact location, careful mission planning and attention to seasonal issues with regard to the collection of photographic data.

2.9. References

ABP Marine Environmental Research Ltd. (2008) Atlas of UK Marine Renewable Energy Resources: Atlas pages, Southampton: ABPmer. Available at http://www.renewables-atlas.info/, accessed 5th September 2012.

BMT Isis, Automatic Identification System (AIS) data analysis. http://www.bmt-isis.com/?/1446/1312/2231, accessed 5th September 2012.

Coull, K. A., Johnstone, R. and Rogers, S.I. (1998) Fisheries sensitivity maps in British waters. Published and distributed by UKOOA Ltd. Available at http://www.Cefas.Defra.gov.uk/media/29947/sensi_maps.pdf, accessed 5th September 2012.

The Crown Estate (2012) Energy: Downloads: Maps and GIS data. http://www.thecrownestate.co.uk/energy/downloads/maps-and-gis-data/, accessed 11th September 2010.

Department for Energy and Climate Change (website), 2012. Oil and Gas; offshore maps and GIS shapefiles. http://og.decc.gov.uk/en/olgs/cms/data_maps/offshore_maps/offshore_maps.aspx, accessed 11th September 2012.

UKMMAS (United Kingdom Marine Monitoring and Assessment Strategy) (2010) Charting Progress 2 Feeder Report: Ocean Processes (Ed. Huthnance, J.), Department for Environment Food and Rural Affairs on behalf of UKMMAS. 279 pp. Available from http://chartingprogress.Defra.gov.uk/ocean-processes-feeder-report, accessed 6th September 2012.

Witt M. J. and Godley B. J. (2007) A step towards seascape scale conservation: using vessel monitoring systems (VMS) to map fishing activity. *PLoS One*, 10, e1111.

Work Package 3: Potential application of AUV and Glider technology to mapping of UK Overseas Territories

WP Leader: Alan Evans (NOC)

3.1. The WP3 task

As set out in the proposal this task's remit was as follows:

"*An outline of all UK Overseas Territories will be produced, highlighting those areas that have yet to be mapped using modern techniques, e.g. multibeam bathymetry. This WP will then explore how big each of those areas is, and how much it would cost to map them using AUV technology as opposed to conventional boat-based mapping. This will provide an initial idea of the total cost of mapping UK Overseas Territories with different survey methods.*

This WP will be undertaken by NOC between 1 March and 31 May 2012."

3.2. Introduction

The Exclusive Economic Zones (EEZs) of the United Kingdom's Overseas Territories (OTs) collectively amount to approximately 5.8 million km^2 of marine area (Fig. 3.1; Table 3.1). In comparison the land area amounts to less than 20,000 km^2, equivalent to just 0.3% of the marine area. Surveying the entire OT's EEZs would therefore be a costly and time-consuming undertaking. However, there are various ways to address how best to protect the marine environment in these regions. The UK has two of the largest Marine Protected Areas (MPAs) on the planet, one of which comprises the entire EEZ of the British Indian Ocean Territory (BIOT), an area of more than 630,000 km^2 (although excluding the area surrounding Diego Garcia). The second covers the entire EEZ of South Georgia and the South Sandwich Islands, north of 60° south, an area of just over 1,000,000 km^2. Neither of these EEZs have blanket coverage of data or evidence-based information that addresses all areas of the EEZs. This compares to the UK, where proposed Marine Conservation Zones (MCZs) are discrete, often isolated, relatively small areas that have been identified using a variety of environmental, biological and physical parameters.

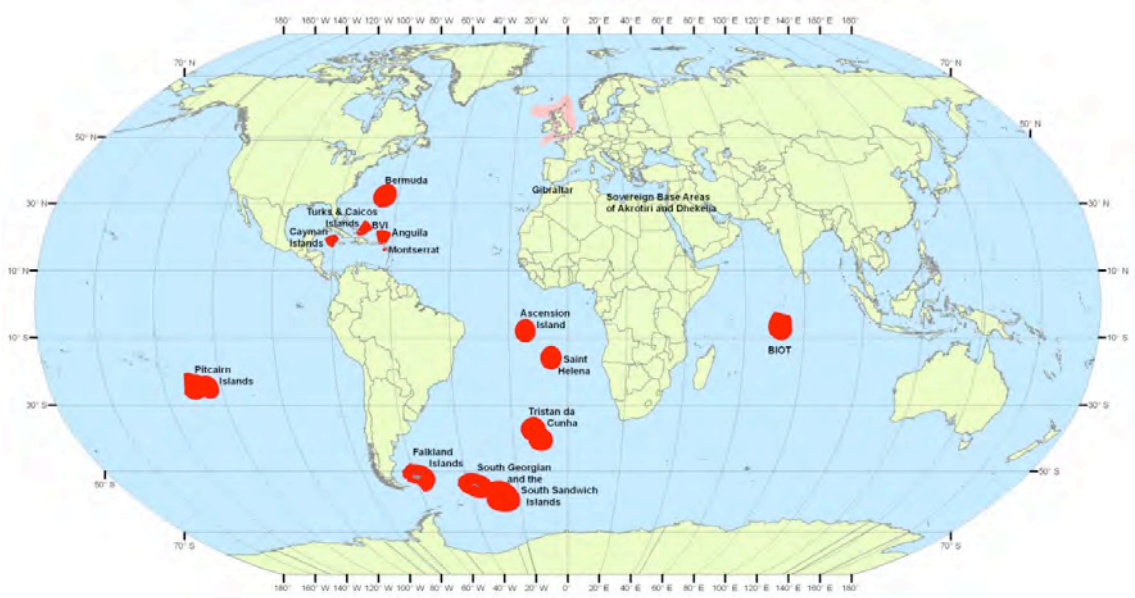

Figure 3.1: Location map showing all UK OT's EEZs (red)

Location	Land (km^2)	EEZ (km^2)
Anguilla	91	83500
Ascension	100	443,344
Bermuda	70	446,560
British Indian Ocean Territory	69	636,000
British Virgin Islands	153	87,847
Cayman Islands	288	119,000
Cyprus Sovereign Base of Akrotiri (to 3NM)	123	245
Cyprus Sovereign Base of Dhekelia (to 3NM)	130	115
Falkland Islands	12,173	545,800
Gibraltar (to 3NM)	6.5	82.5
Montserrat	100	8500
Pitcairn Islands (incl Ducie, Henderson & Oeno)	45	838,500
South Georgia and South Sandwich Islands	3900	1,240,500
St Helena	129	446,400
Tristan da Cunha	203	752,850
Turks and Caicos Islands	1000	148,700
Total	**18,581**	**5,797,944**

Table 3.1: Summary of the UK Overseas Territories land and marine areas.

In order to assess how best to approach the issue of protecting the marine environment of the OTs EEZs, e.g. through deployment of AUVs and Gliders for data collection, we firstly need to understand the physical environment that exists within each of these areas. Using the latest General Bathymetric Chart of the Oceans (GEBCO) digital terrain model (DTM), a comprehensive assessment of the physical environment in each OT has been made. This dataset provides bathymetry information globally at a resolution of 30 second of an arc of a degree, i.e. 926 m. With these data it has been possible to establish the varying depth ranges and geomorphological settings within each of the studied EEZs.

The GEBCO DTM allows us to establish not only an understanding of the general physical environment, but also the spatial extent of different depth ranges. Such information provides an initial appreciation of the effort that would be required to survey, for example, the area from the coastline to the 200m isobath, this being traditionally regarded as the shallow shelf seas area. Figure 3.2 illustrates how only data from within the EEZ is being used to generate the depth range values seen in Table 3.2, which provides the % coverage values.

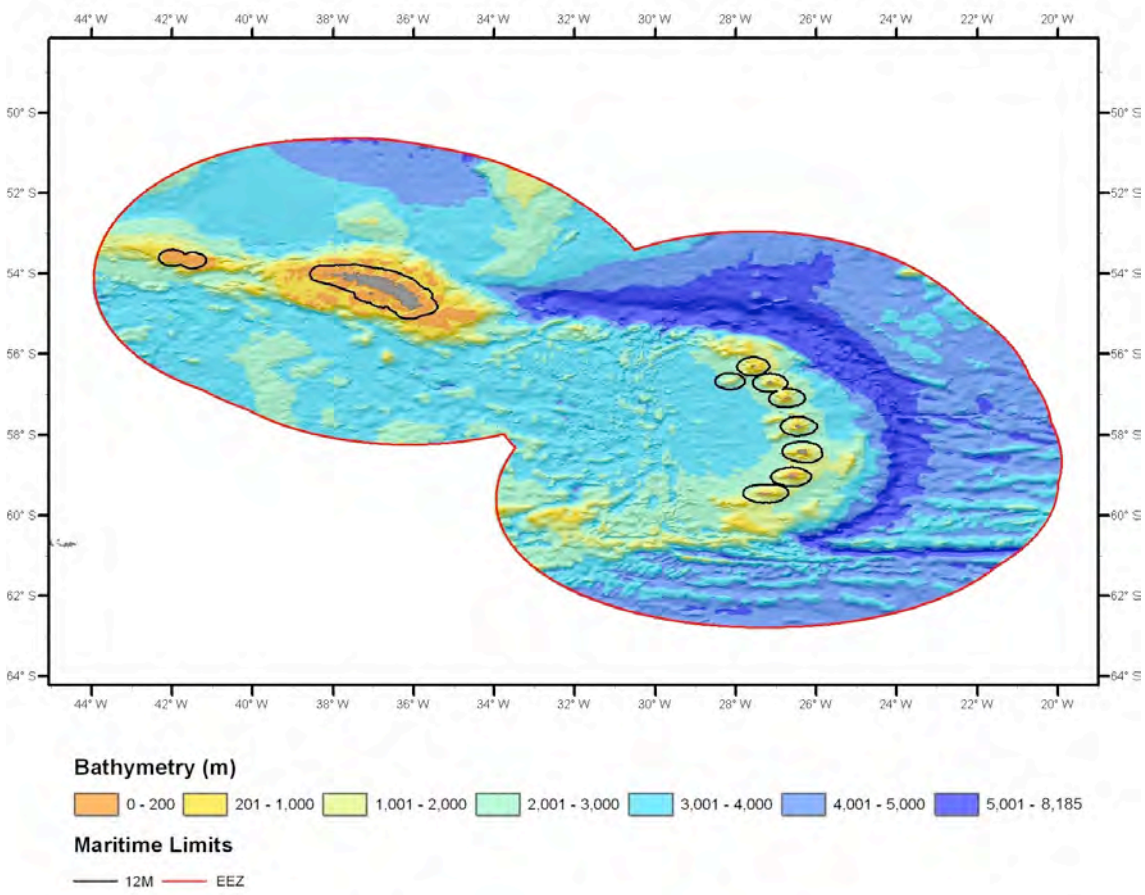

Figure 3.2: An example of the varying depth ranges within the EEZ of South Georgia and South Sandwich Island. Land is shown in grey.

Land area 4,000 km^2; EEZ 1,240,500 km^2

depth range (m)	**0-200**	**201-1000**	**1001-2000**	**2001-3000**	**3001-4000**	**>4001**
% of EEZ	1.81	3.021	5.576	17.596	39.4	32.594
depth range (m)	**0-200**	**0-1000**	**0-2000**	**0-3000**	**0-4000**	
cumulative %	1.81	4.831	10.407	28.003	67.403	

Table 3.2: An example of the depth range evaluation for the EEZ in Fig. 3.2. This shows that >70% of the EEZ is at water depths >3000 m, with only a small area (<2%) at <200 m depth (equivalent to shelf waters).

In addition to evaluating the general bathymetric context, GEBCO data also provide information on the varying types of geomorphological setting found within the UK'S OTs; this can provide an initial indication of the types of habitat that are likely to exist. There are two types of slope geomorphology typically found in UK OTs (Fig. 3.3): a dominantly shallow-water setting where access to the area and seafloor exploitation would be relatively easy, and a deep-water setting that is expensive to survey and monitor but is relatively protected from human activities.

The second aspect of this WP is an assessment of the coverage and availability of multibeam bathymetry data acquired within UK OT EEZ's. Due to time constraints only scientific survey data have been researched; additional commercial and military data undoubtedly exist but are not addressed here. It is also likely that there will be additional scientific data that are not readily identifiable or available, and as such the coverage values shown for each OT should be treated as minima (Fig. 3.4; Table 3.3).

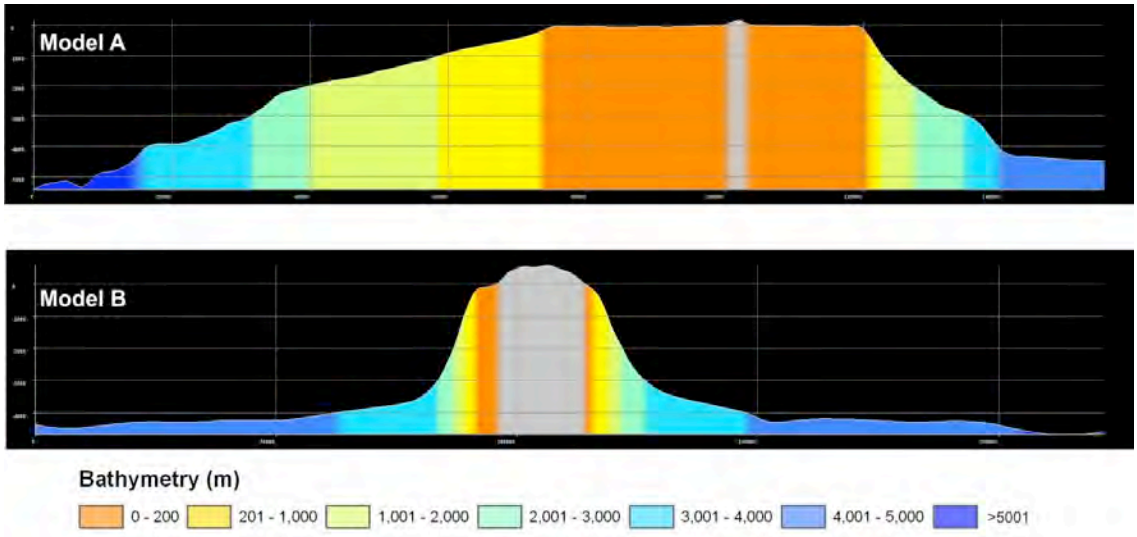

Figure 3.3: Typical bathymetric cross sections of the two dominant geomorphological settings found throughout the UK OTs. Model A displays a broad shelf and relatively restricted deep-water area, e.g. the Falkland Islands, whereas Model B has a narrow shelf and extensive deep-water area, e.g. volcanic archipelagos such as Montserrat.

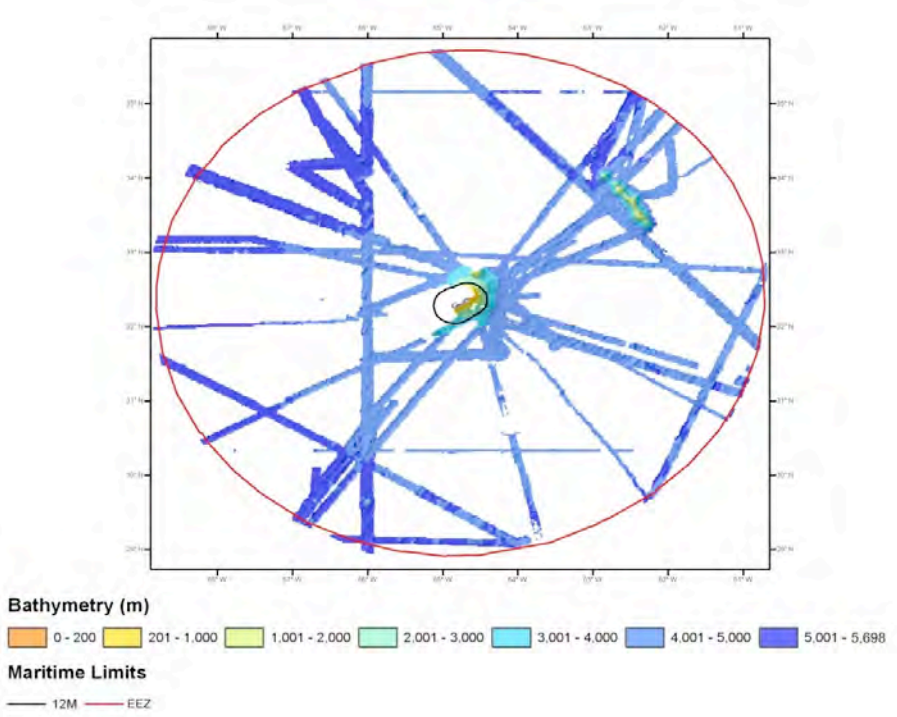

Figure 3.4: Map showing multibeam bathymetry coverage identified offshore Bermuda.

Multibeam coverage is 146,800 km^2 or 32.6% of EEZ

depth range (m)	0-200	201-1000	1001-2000	2001-3000	3001-4000	>4001
% of MB coverage	0.0760	0.1685	0.5980	1.3229	2.8500	94.9850
MB area (km^2)	111.57	247.36	877.86	1942.02	4183.80	139,437.98
% of EEZ	0.0248	0.0550	0.1953	0.4321	0.9309	31.0234

Table 3.3: Depth range analysis of the multibeam bathymetry data shown in Fig. 3.4. In this example about a third of the offshore area has been surveyed, 95% of which is at water depths >4000 m.

3.3. Anguilla

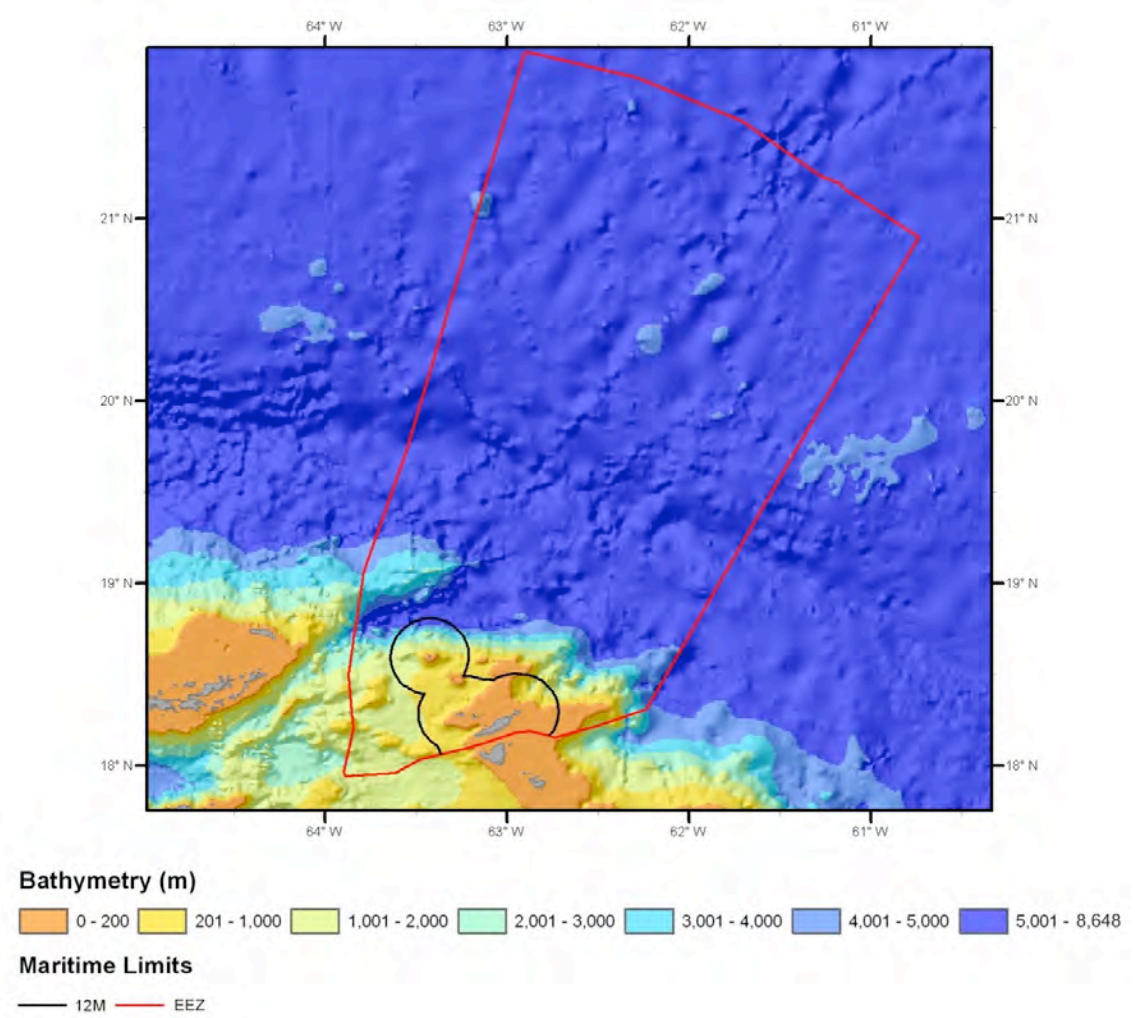

Figure 3.5: GEBCO bathymetry map of the Anguilla EEZ. Land is shown in grey.

Land area 91 km^2; EEZ 83,500 km^2

depth range (m)	**0-200**	**201-1000**	**1001-2000**	**2001-3000**	**3001-4000**	**>4001**
% of EEZ	2.5	3.78	3.99	1.29	2.31	86.1
depth range (m)	**0-200**	**0-1000**	**0-2000**	**0-3000**	**0-4000**	
cumulative %	2.5000	6.2800	10.2700	11.5600	13.8700	

Table 3.4: Depth range analysis of the Anguilla EEZ shown in Fig. 3.5. More than 86% is at water depths >4000 m, with just 2.5% at water depths <200 m.

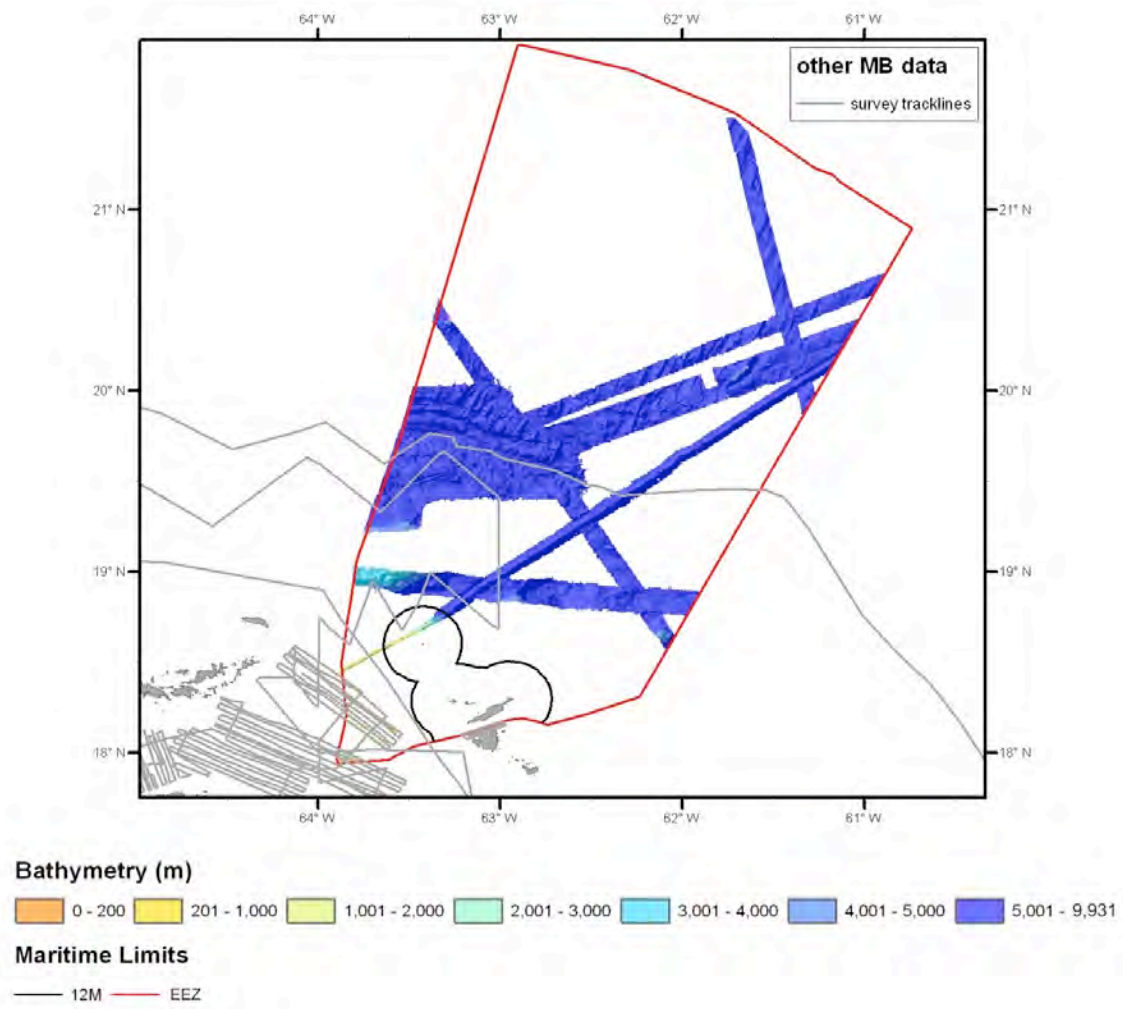

Figure 3.6: Map showing multibeam bathymetry coverage identified offshore Anguilla. Land is shown in grey shading. Grey lines indicate survey lines where additional data are potentially available.

Multibeam coverage is 28,427 km^2 or 34.04% of EEZ

depth range (m)	0-200	201-1000	1001-2000	2001-3000	3001-4000	>4001
% of MB coverage	0.0000	0.4600	2.3600	0.3300	1.4000	95.4200
MB area (km^2)	0.00	130.76	670.88	93.81	397.98	27125.04
% of EEZ	0.0000	0.1566	0.8034	0.1123	0.4766	32.4851

Table 3.5: Depth range analysis of the multibeam bathymetry data shown in Fig. 3.6. About a third of the offshore area has been surveyed, 95% of which is at water depths >4000 m.

There is potentially an additional 7000 km^2 of other multibeam data that have been identified (Fig. 3.6). This would result in a total of 35,427 km^2, equating to 42.4% of the EEZ.

Competent Institutions
Dept of Fisheries and Marine Resources http://www.gov.ai/department.php?id=3&dept=14

The Anguilla National Trust http://www.axanationaltrust.org/

MPA activity
Several small marine parks (The Marine Protected Areas Project)

3.4. Ascension

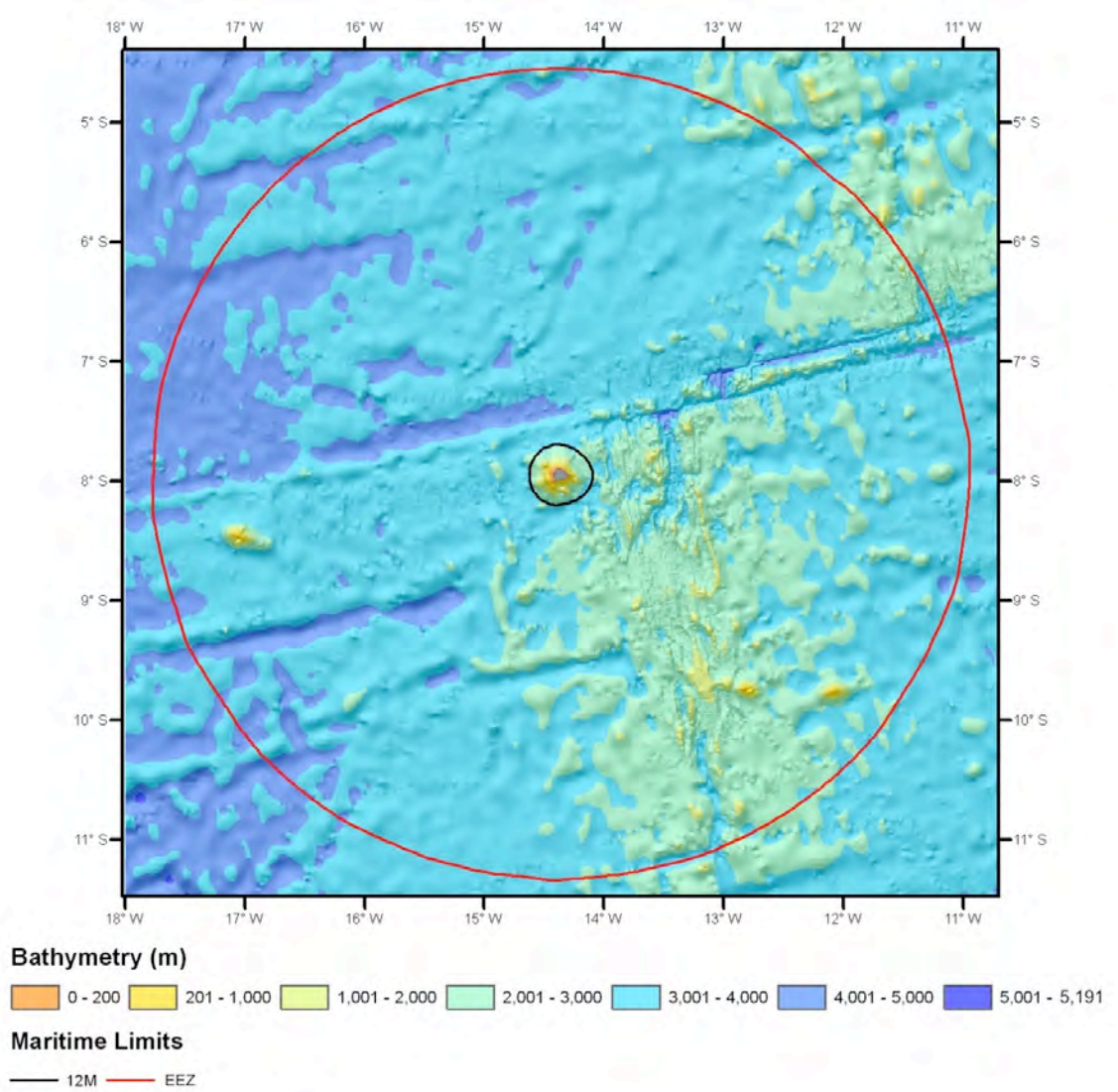

Figure 3.7: GEBCO bathymetry map of the Ascension EEZ. Land is shown in grey.

Land area 100 km^2; EEZ 443,344 km^2

depth range (m)	**0-200**	**201-1000**	**1001-2000**	**2001-3000**	**3001-4000**	**>4001**
% of EEZ	0.0243	0.128	0.9777	21.29	66.17	11.409
depth range (m)	**0-200**	**0-1000**	**0-2000**	**0-3000**	**0-4000**	
cumulative %	0.0243	0.1523	1.13	22.42	88.59	

Table 3.6: Depth range analysis of the Ascension EEZ shown in Fig. 3.7. More than 77% is at water depths >3000 m, with <1% at water depths <200 m.

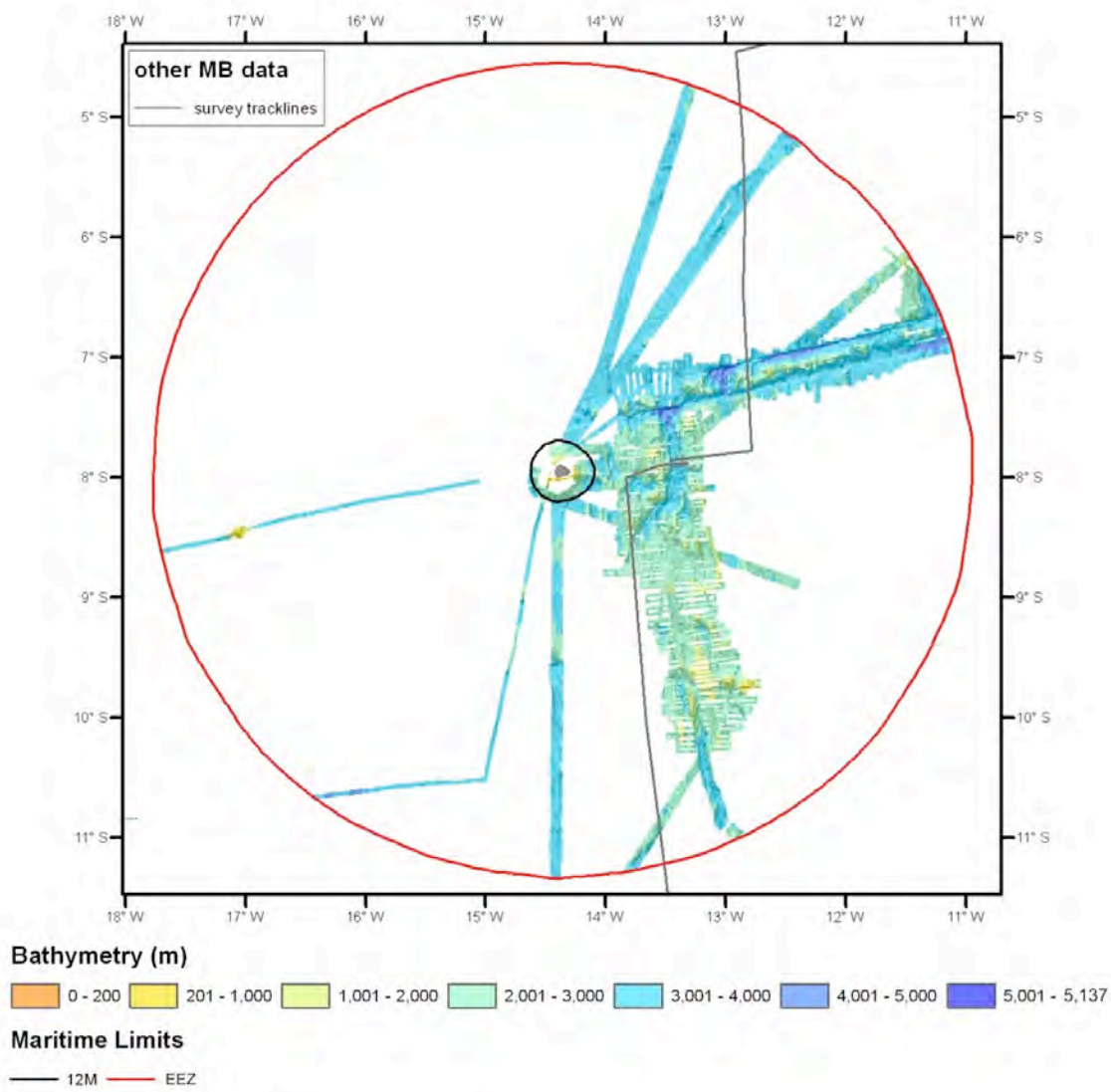

Figure 3.8: Map showing multibeam bathymetry coverage identified offshore Ascension. Land is shown in grey shading. Grey lines indicate survey lines where additional data are potentially available.

Multibeam coverage is 70,250 km^2 or 15.85% of EEZ

depth range (m)	0-200	201-1000	1001-2000	2001-3000	3001-4000	>4001
% of MB coverage	0.0083	0.3540	3.9840	41.0200	52.2100	2.4150
MB area (km^2)	5.83	248.69	2798.76	28816.55	36677.53	1696.54
% of EEZ	0.0013	0.0561	0.6313	6.4998	8.2729	0.3827

Table 3.7: Depth range analysis of the multibeam bathymetry data shown in Fig. 3.8. About 16% of the offshore area has been surveyed, 95% of which is at water depths >2000 m.

There is potentially an additional 13,000 km^2 of other multibeam data that have been identified. This would result in a total of 83,250 km^2, equating to 18.7% of the EEZ.

Competent Institutions
Unknown

MPA activity
Unknown

3.5. Bermuda

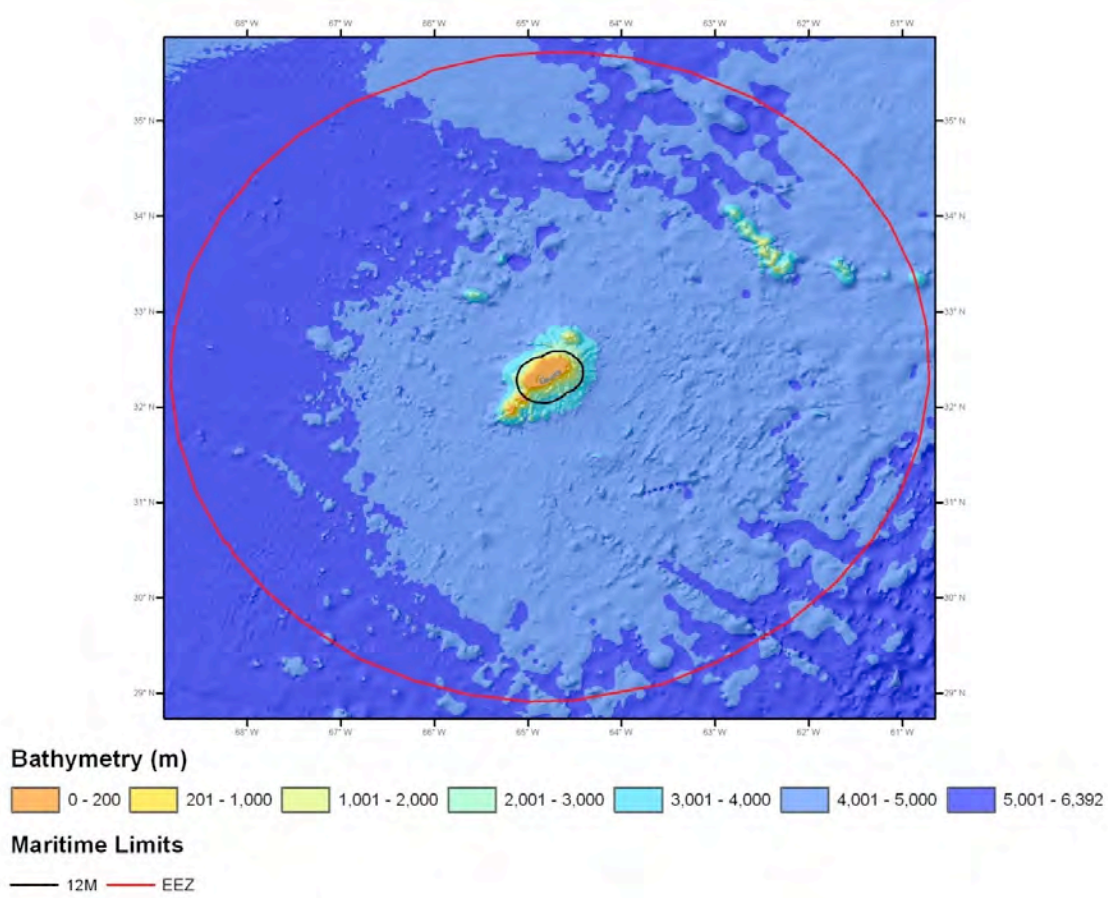

Figure 3.9: GEBCO bathymetry map of the Bermuda EEZ. Land is shown in grey.

Land area 70 km^2; EEZ 446,560 km^2

depth range (m)	**0-200**	**201-1000**	**1001-2000**	**2001-3000**	**3001-4000**	**>4001**
% of EEZ	0.24	0.11	0.275	0.596	1.183	97.5
depth range (m)	**0-200**	**0-1000**	**0-2000**	**0-3000**	**0-4000**	
cumulative %	0.2400	0.3500	0.6250	1.2210	2.4040	

Table 3.8: Depth range analysis of the Bermuda EEZ shown in Fig. 3.9. More than 97% is at water depths >4000 m, with <1% at water depths <200 m.

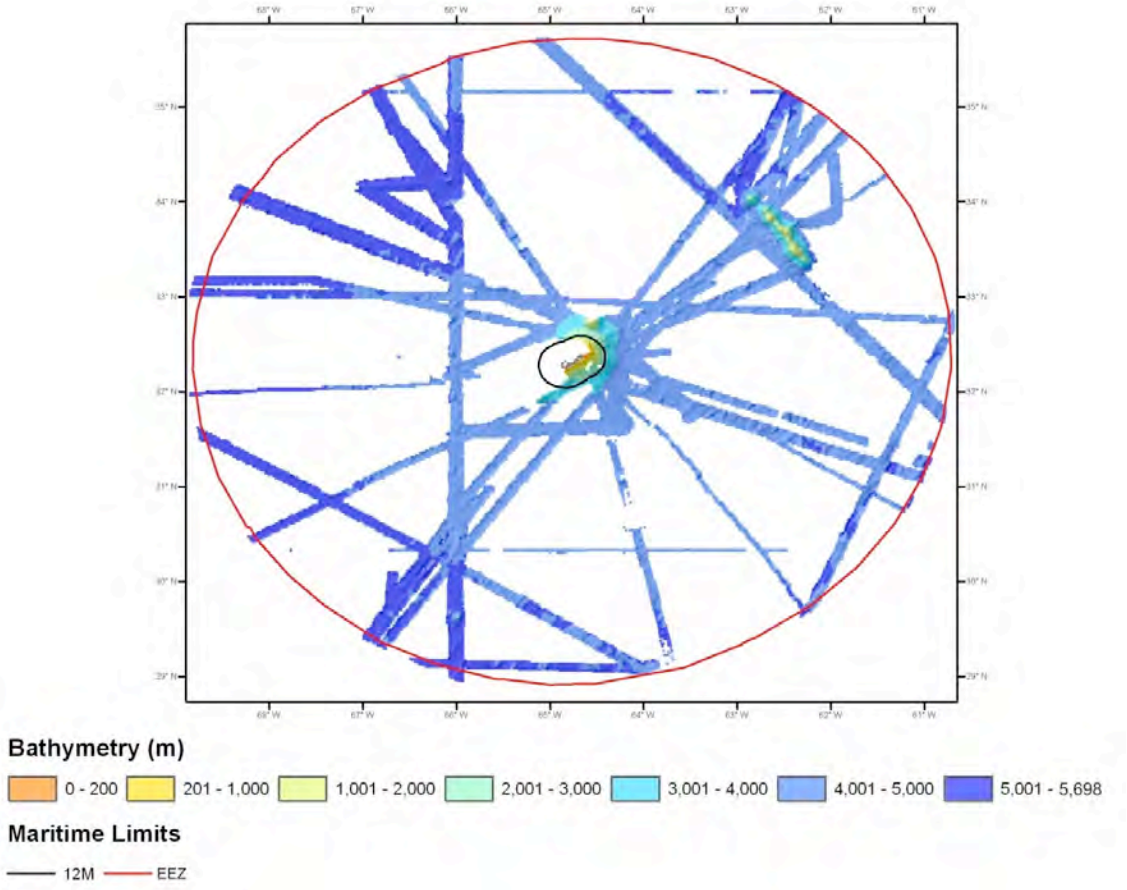

Figure 3.10: Map showing multibeam bathymetry coverage identified offshore Bermuda. Land is shown in grey shading.

Multibeam coverage is 146,800 km^2 or 32.6% of EEZ

depth range (m)	0-200	201-1000	1001-2000	2001-3000	3001-4000	>4001
% of MB coverage	0.0760	0.1685	0.5980	1.3229	2.8500	94.9850
MB area (km^2)	111.57	247.36	877.86	1942.02	4183.80	139437.98
% of EEZ	0.0250	0.0554	0.1966	0.4349	0.9369	31.2249

Table 3.9: Depth range analysis of the multibeam bathymetry data shown in Fig. 3.10. About a third of the offshore area has been surveyed, 95% of which is at water depths >4000 m.

Competent Institutions
The Bermuda Institute of Ocean Science (BIOS) - http://www.bios.edu/
The Bermuda Aquarium, Museum & Zoo (BAMZ) - https://bamz.org/home.php

MPA
There is a no-take zone that covers the inshore waters of the island. The Sargasso Sea Alliance (a partnership led by the Bermuda Government, in collaboration with scientists, international marine conservation groups and private donors) plans to protect a large part of the EEZ as part of the larger Sargasso Sea MPA. Which parts of the EEZ will be included is not yet known.

3.6. British Indian Ocean Territory (BIOT)

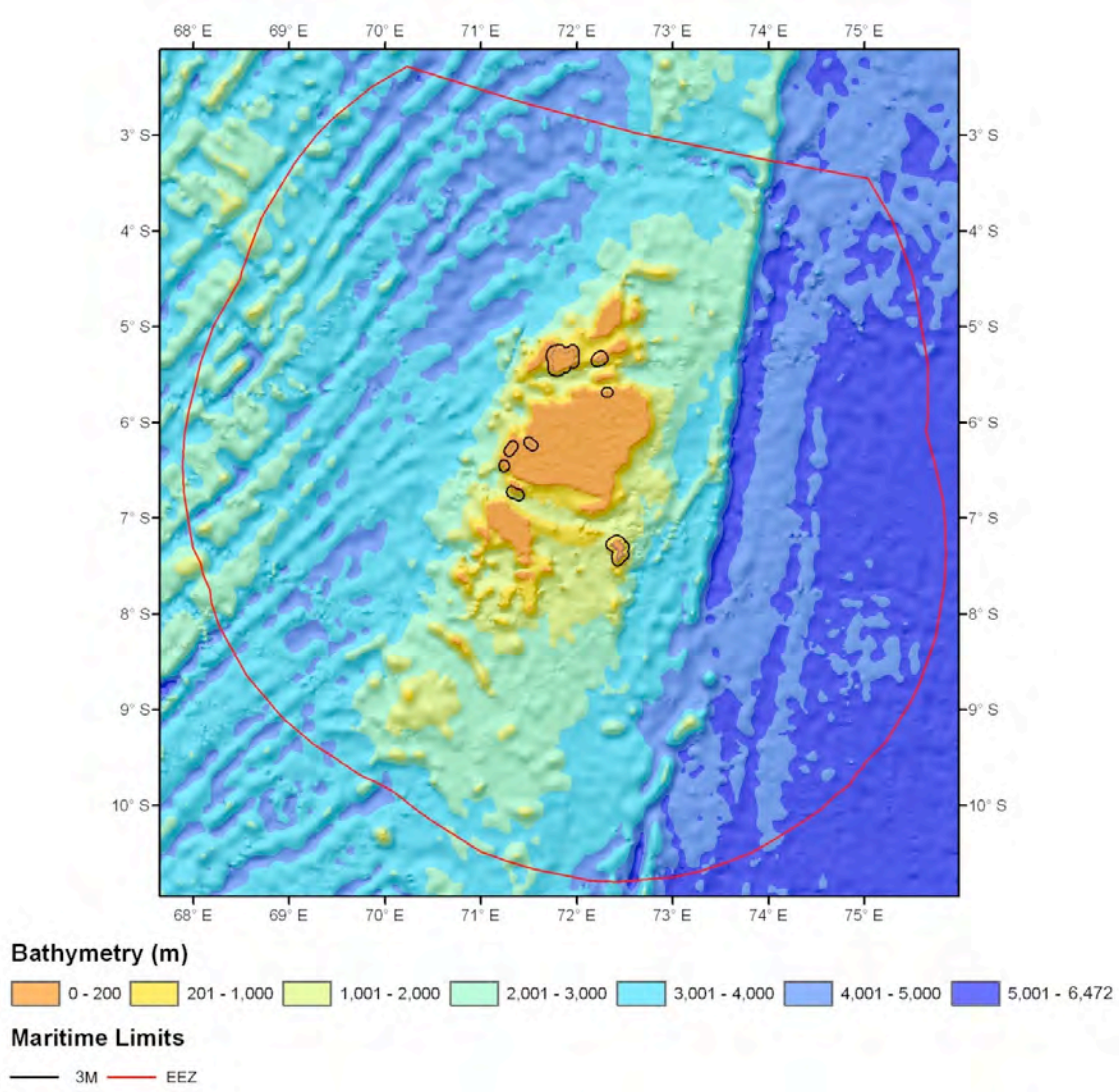

Figure 3.11: GEBCO bathymetry map of the BIOT EEZ. Land is shown in grey.

Land area 69 km^2; EEZ 636,000 km^2

depth range (m)	**0-200**	**201-1000**	**1001-2000**	**2001-3000**	**3001-4000**	**>4001**
% of EEZ	3.368	2.672	6.1766	17.205	32.99	37.58
depth range (m)	**0-200**	**0-1000**	**0-2000**	**0-3000**	**0-4000**	
cumulative %	3.368	6.04	12.2166	29.4216	62.4116	

Table 3.10: Depth range analysis of the BIOT EEZ shown in Fig. 3.11. More than 87% is at water depths >2000 m, with <4% at water depths <200 m.

There are no publicly available multibeam data currently accessible.

Competent Institutions
Chagos Conservation Trust - http://www.chagos-trust.org/

MPA
Since 1st April 2010, the entire EEZ is an MPA (no-take zone marine reserve).

3.7. British Virgin Islands (BVI)

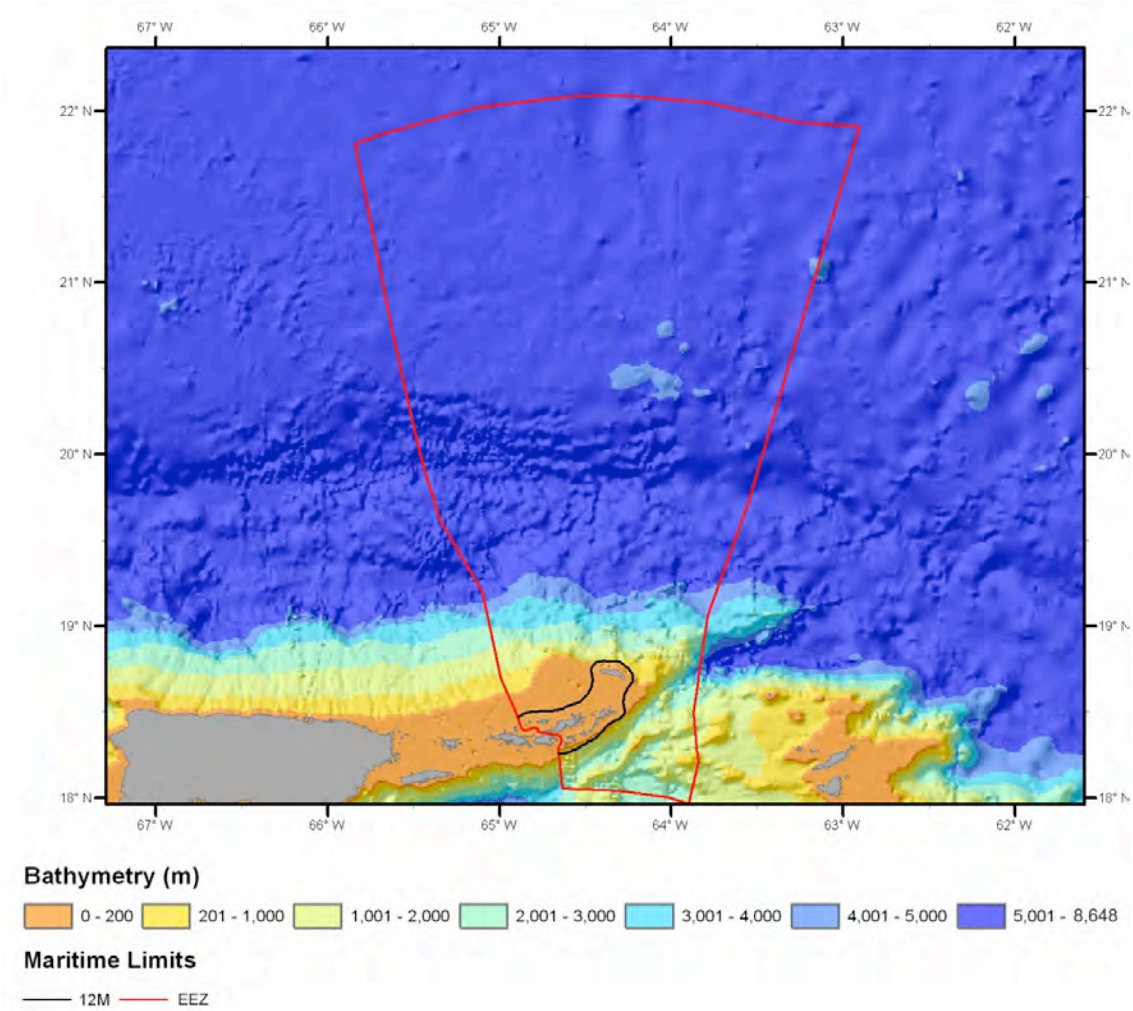

Figure 3.12: GEBCO bathymetry map of the BVI EEZ. Land is shown in grey.

Land area 176 km^2; EEZ 87,650 km^2

depth range (m)	**0-200**	**201-1000**	**1001-2000**	**2001-3000**	**3001-4000**	**>4001**
% of EEZ	3.44	1.51	3.93	3.5	2.3	85.3
depth range (m)	**0-200**	**0-1000**	**0-2000**	**0-3000**	**0-4000**	
cumulative %	3.44	4.95	8.88	12.38	14.68	

Table 3.11: Depth range analysis of the BVI EEZ shown in Fig. 3.12. More than 85% is at water depths >4000 m, with <4% at water depths <200 m.

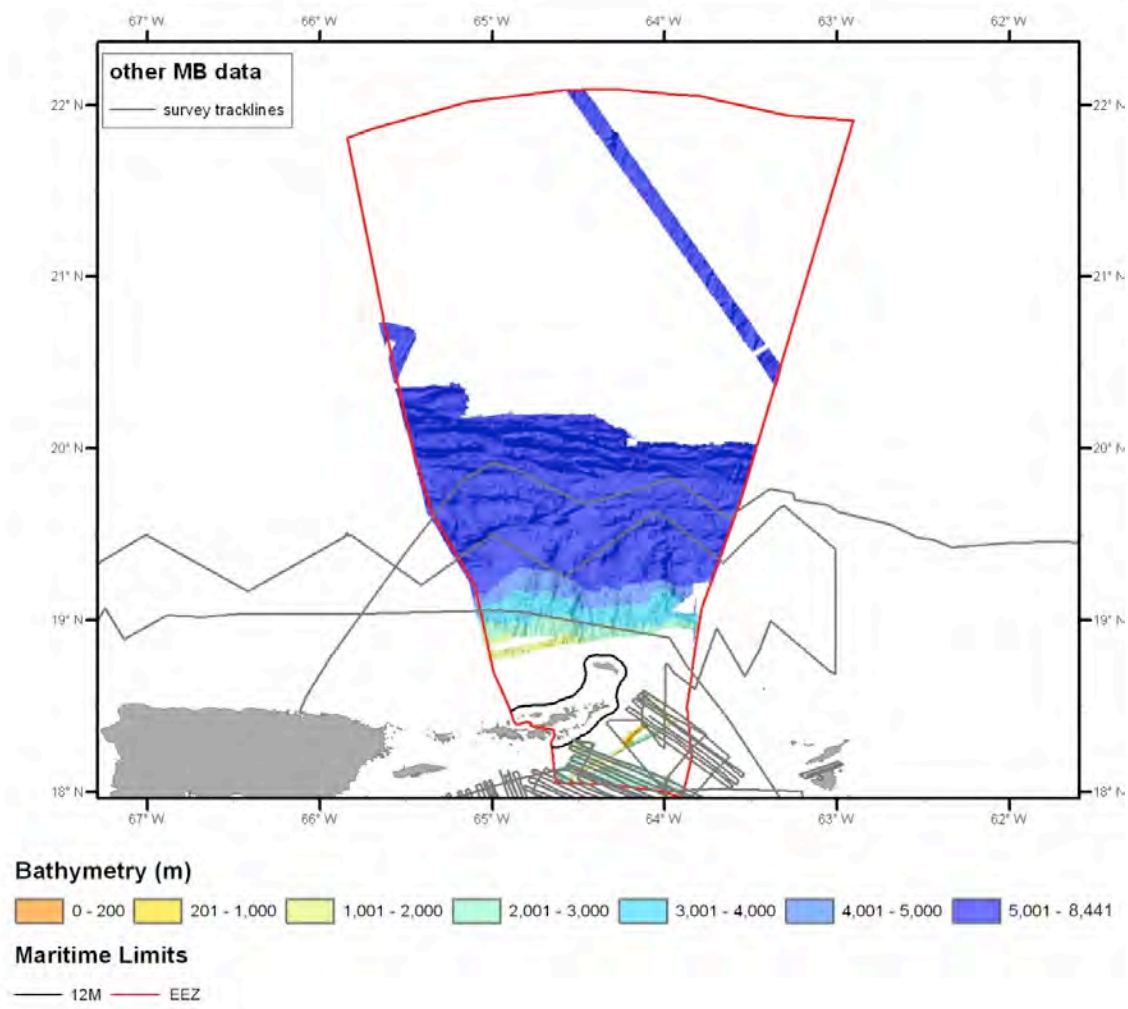

Figure 3.13: Map showing multibeam bathymetry coverage identified offshore BVI. Land is shown in grey shading. Grey lines indicate survey lines where additional data are potentially available.

Multibeam coverage is 31,000 km^2 or 35.4% of EEZ

depth range (m)	0-200	201-1000	1001-2000	2001-3000	3001-4000	>4001
% of MB coverage	0.046	0.42	3.39	7.39	6.56	82.17
MB area (km^2)	14.26	130.20	1050.90	2290.90	2033.60	25472.70
% of EEZ	0.0163	0.1485	1.1990	2.6137	2.3201	29.0618

Table 3.12: Depth range analysis of the multibeam bathymetry data shown in Fig. 3.13. About a third of the offshore area has been surveyed, >95% of which is at water depths >2000 m.

There are other multibeam data within the EEZ that need to be made available, although some of these overlap existing data seen (Fig. 3.13).

Competent Institutions

Conservation & Fisheries Department, Ministry of Natural Resources & Labour, British Virgin Islands http://www.bvidef.org/main/

National Parks Trust http://www.bvinationalparkstrust.org/

MPA

One marine park: the Wreck of the RMS Rhone.

3.8. Cayman

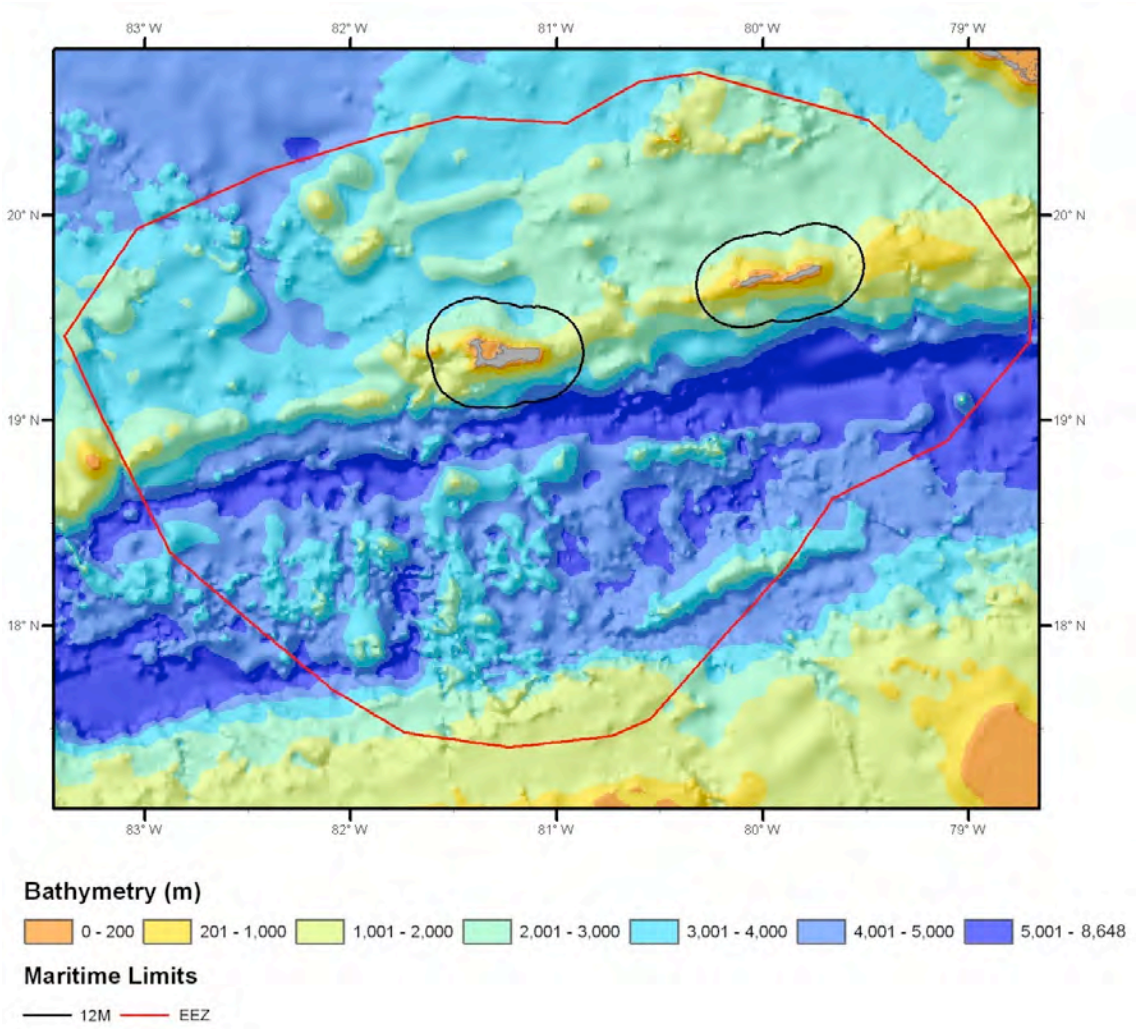

Figure 3.14: GEBCO bathymetry map of the Cayman EEZ. Land is shown in grey.

Land area 288 km^2; EEZ 119,000 km^2

depth range (m)	**0-200**	**201-1000**	**1001-2000**	**2001-3000**	**3001-4000**	**>4001**
% of EEZ	0.39	1.83	9.74	24.39	27.13	36.49
depth range (m)	**0-200**	**0-1000**	**0-2000**	**0-3000**	**0-4000**	
cumulative %	0.3900	2.2200	11.9600	36.3500	63.4800	

Table 3.13: Depth range analysis of the Cayman EEZ shown in Fig. 3.14. More than 87% is at water depths >2000 m, with <1% at water depths <200 m.

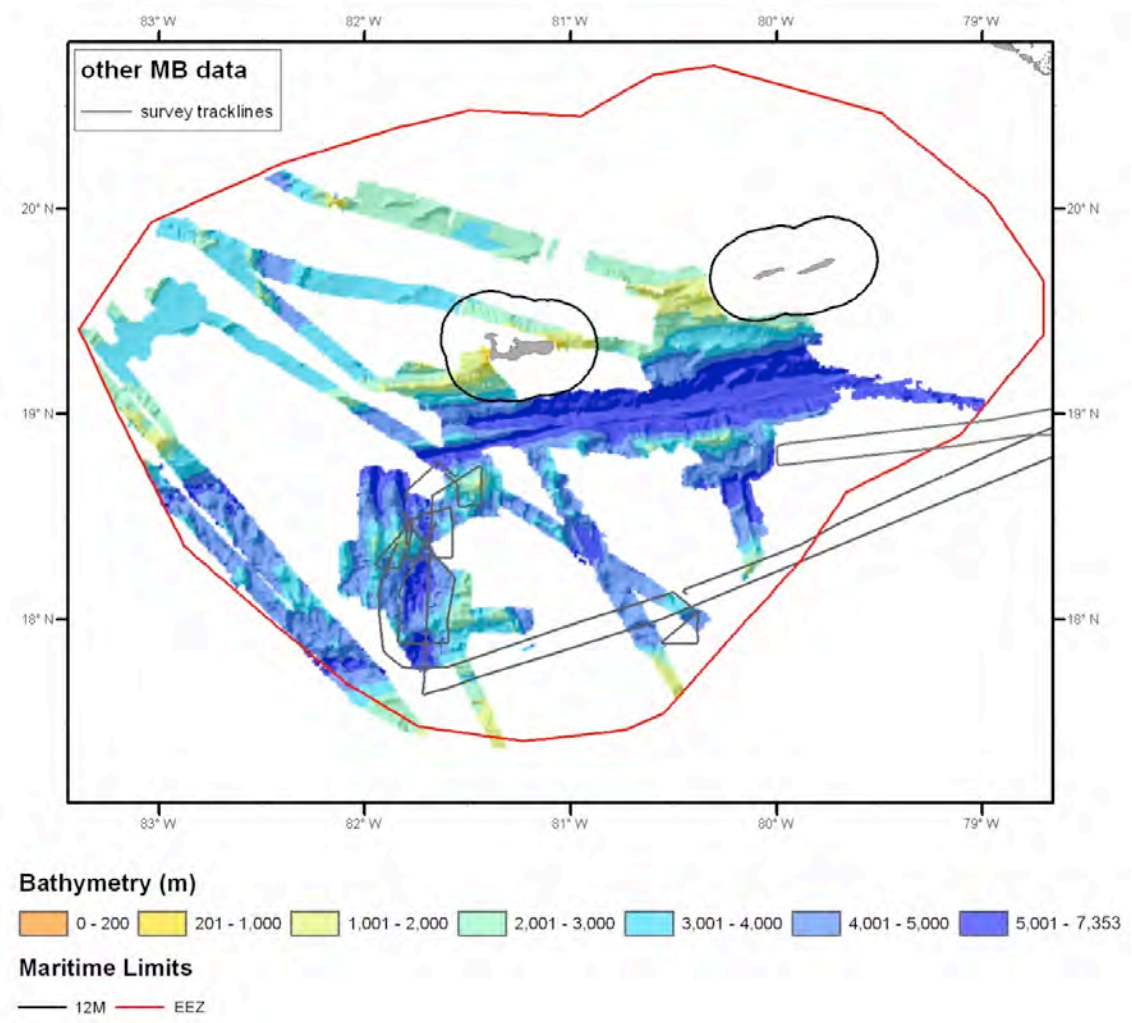

Figure 3.15: Map showing multibeam bathymetry coverage identified offshore Cayman. Land is shown in grey shading. Grey lines indicate survey lines where additional data are potentially available.

Multibeam coverage is 38,200 km^2 or 32.1% of EEZ

depth range (m)	0-200	201-1000	1001-2000	2001-3000	3001-4000	>4001
% of MB coverage	0.003	0.23	4.99	16.58	26.35	51.83
MB area (km^2)	1.15	87.86	1906.18	6333.56	10065.70	19799.06
% of EEZ	0.0010	0.0738	1.6018	5.3223	8.4586	16.6379

Table 3.14: Depth range analysis of the multibeam bathymetry data shown in Fig. 3.15. About a third of the offshore area has been surveyed, >95% of which is at water depths >2000 m.

There is potentially an additional 10,000 km^2 of other multibeam data that have been identified. This would result in a total of 48,200 km^2, equating to 40.47% of the EEZ.

Competent Institutions
Department of the Environment http://www.doe.ky/

MPA
Darwin Marine Parks. Significant interest in a chemosynthetic environment located within the EEZ of the Cayman Island, possibly a unique situation in UK territorial waters.

3.9. Cyprus Military Bases at Akrotiri and Dhekelia

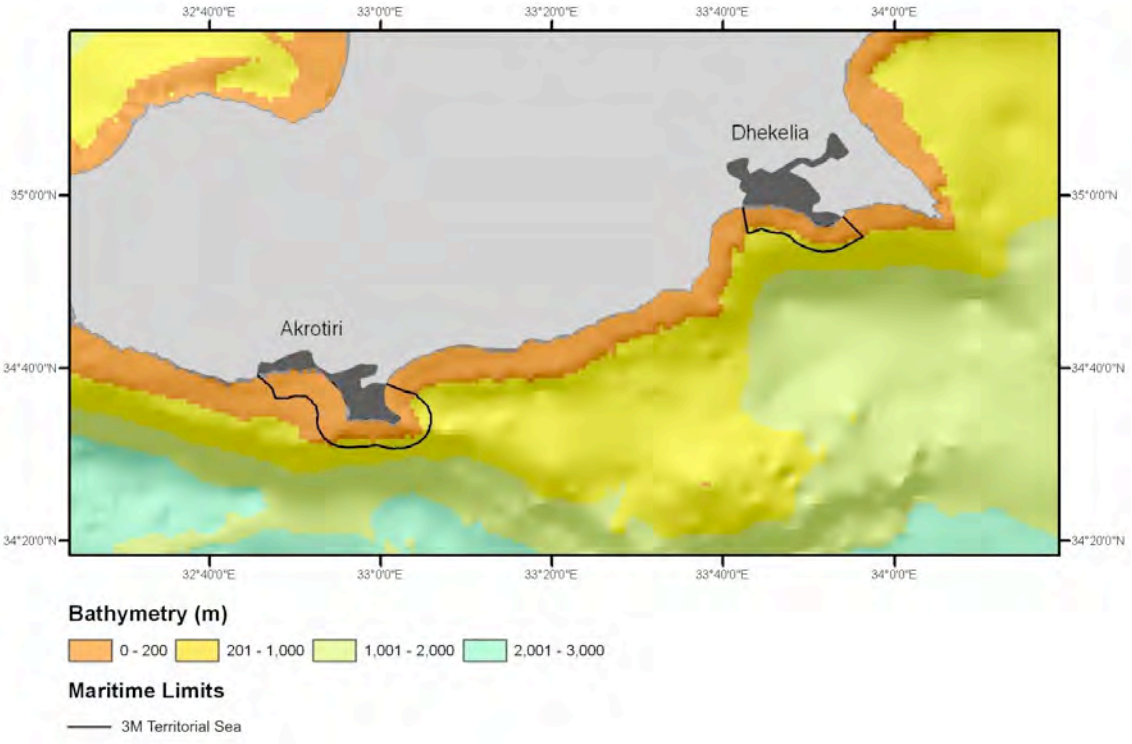

Figure 3.16: GEBCO bathymetry map of the Cyprus Military Bases. Land is shown in grey.

Land area 253 km^2; 3 Mile Territorial Sea (combined) 360 km^2

It is apparent that the majority of the marine area for these two territorial seas is predominantly in water depths of <200m.

For the area offshore Akrotiri the water depth ranges from 0 to 673m, where 80% of the area is shallower than 200m.

For the area offshore Dhekelia the water depth ranges from 0 to 470m, where 70% of the area is shallower than 200m.

3.10. Falkland Islands

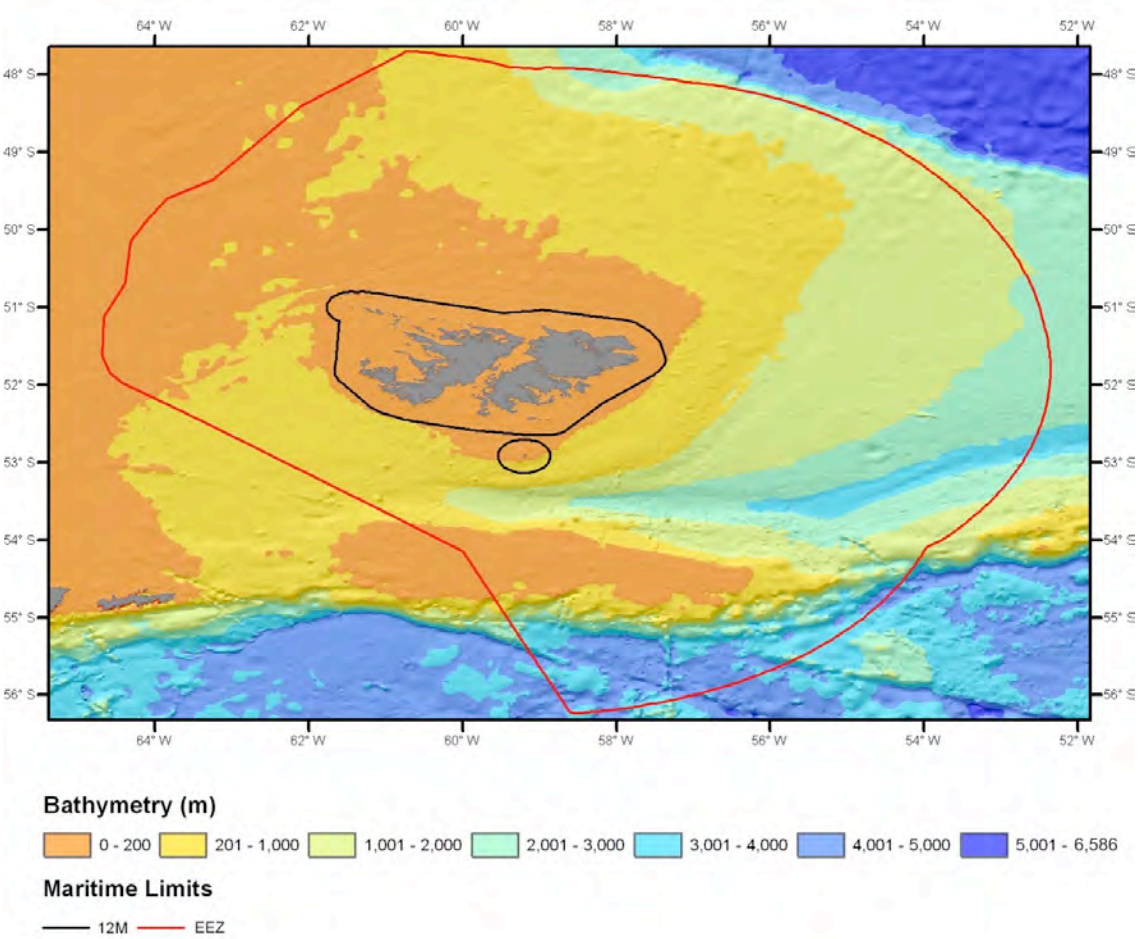

Figure 3.17: GEBCO bathymetry map of the Falkland Islands EEZ. Land is shown in grey.

Land area 12,173 km^2; EEZ 545,800 km^2

depth range (m)	**0-200**	**201-1000**	**1001-2000**	**2001-3000**	**3001-4000**	**>4001**
% of EEZ	29.122	32.707	22.05	9.631	3.947	2.541
depth range (m)	**0-200**	**0-1000**	**0-2000**	**0-3000**	**0-4000**	
cumulative %	29.122	61.829	83.879	93.51	97.457	

Table 3.15: Depth range analysis of the Falkland Islands EEZ shown in Fig. 3.17. Almost 30% is at water depths <200 m, with about 60% at water depths <1000 m.

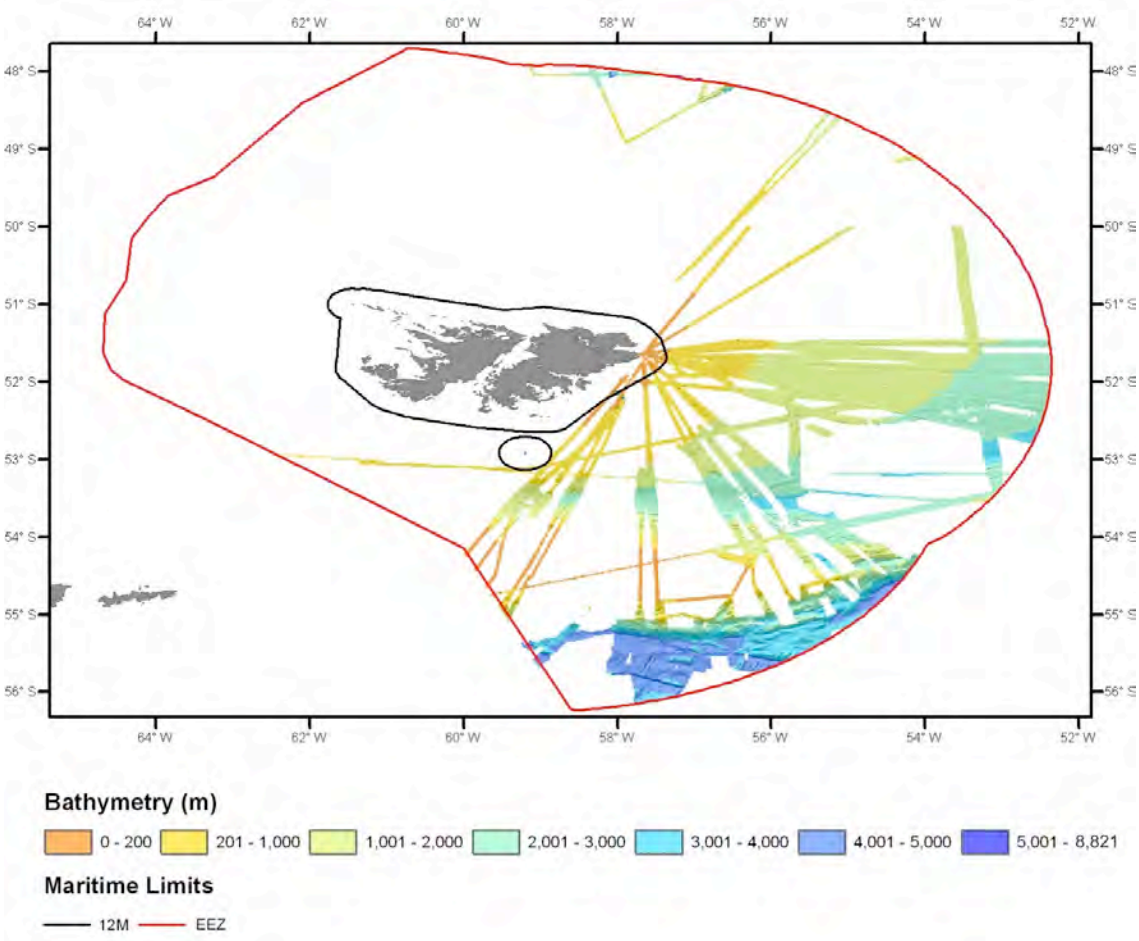

Figure 3.18: Map showing multibeam bathymetry coverage identified offshore Falkland Islands. Land is shown in grey shading.

Multibeam coverage is 135,000 km^2 or 24.7% of EEZ

depth range (m)	0-200	201-1000	1001-2000	2001-3000	3001-4000	>4001
% of MB coverage	4.6490	16.8370	33.4690	25.9840	10.0970	8.9610
MB area (km^2)	6276.15	22729.95	45183.15	35078.40	13630.95	12097.35
% of EEZ	1.1499	4.1645	8.2783	6.4270	2.4974	2.2164

Table 3.16: Depth range analysis of the multibeam bathymetry data shown in Fig. 3.18. About a quarter of the offshore area has been surveyed, only 5% of which is at water depths <200 m.

Competent Institutions
Falkland Islands government http://www.falklands.gov.fk/

MPA
Unknown

3.11. Gibraltar

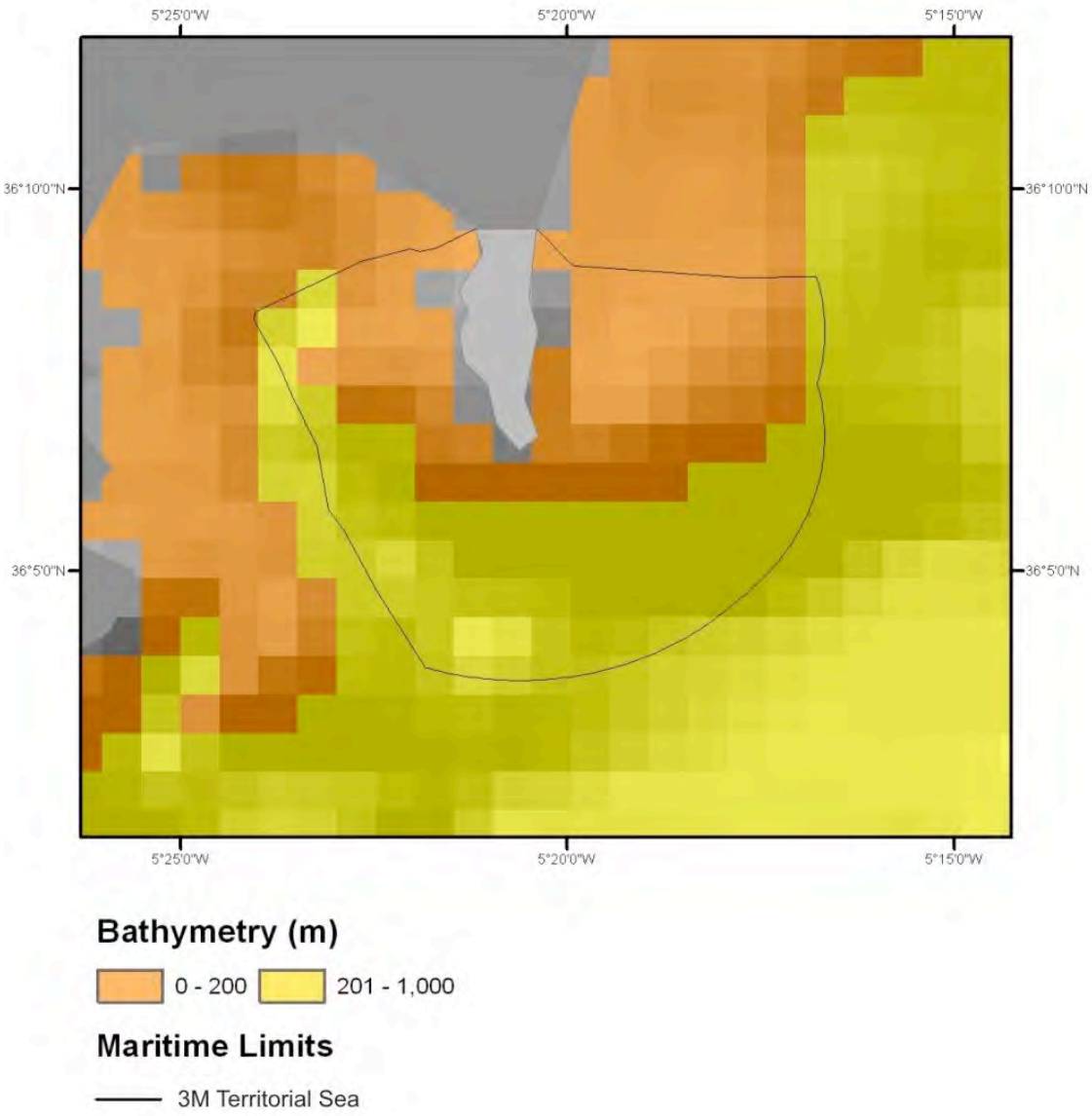

Figure 3.19: GEBCO bathymetry map of the Gibraltar Territorial Sea. Land is shown in grey.

Land area 6.5 km^2; 3 Mile Territorial Sea 82.5 km^2

It is apparent that the majority of the marine area offshore Gibraltar is in water depths of <1000m.

For the Gibraltar 3 Mile Territorial Sea area, the water depth ranges from 0 to 764m, where 42% of the area is shallower than 200m.

3.12. Montserrat

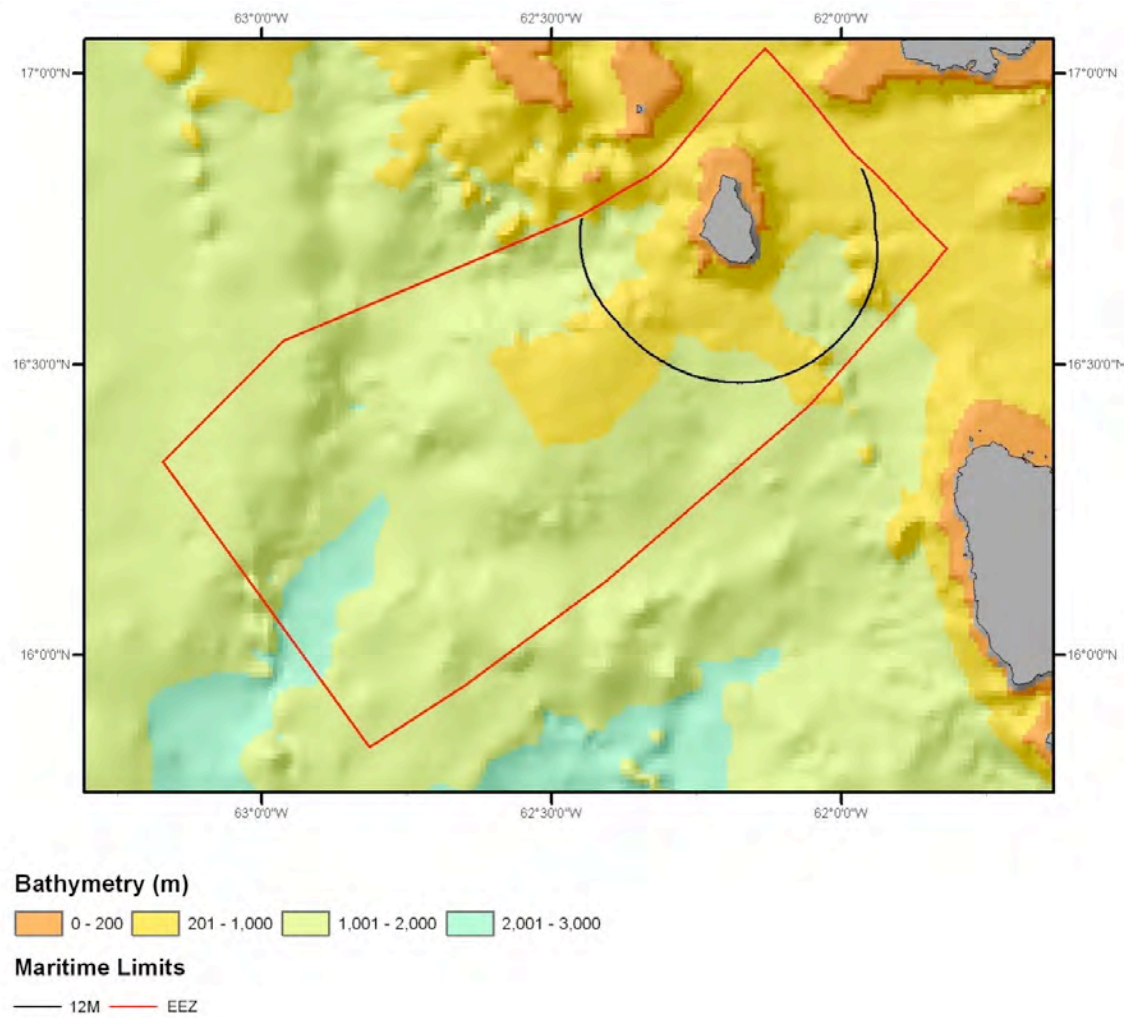

Figure 3.20: GEBCO bathymetry map of the Montserrat EEZ. Land is shown in grey.

Land area 100 km^2; EEZ 8500 km^2

depth range (m)	**0-200**	**201-1000**	**1001-2000**	**2001-3000**	**3001-4000**	**>4001**
% of EEZ	3.12	26	67.21	3.65	0	0
depth range (m)	**0-200**	**0-1000**	**0-2000**	**0-3000**	**0-4000**	
cumulative %	3.12	29.12	96.35	100		

Table 3.17: Depth range analysis of the Montserrat EEZ shown in Fig. 3.20. Only about 3% is at depths of <200 m, with 93% being between 200 and 2000 m.

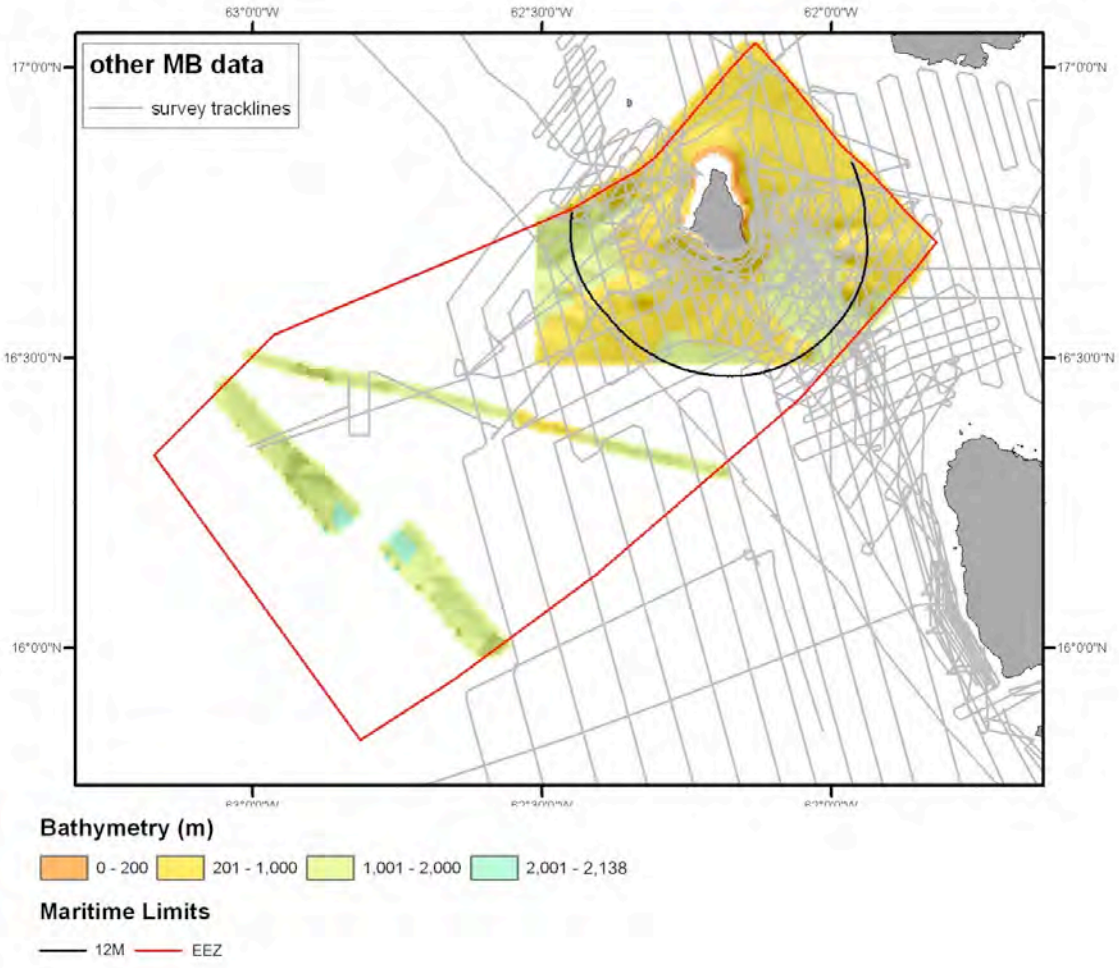

Figure 3.21: Map showing multibeam bathymetry coverage identified offshore Montserrat. Land is shown in grey shading. Grey lines indicate survey lines where additional data are potentially available.

Multibeam coverage is 3290 km^2 or 38.7% of EEZ

depth range (m)	0-200	201-1000	1001-2000	2001-3000	3001-4000	>4001
% of MB coverage	0.8400	48.8900	47.9300	2.3400		
MB area (km^2)	27.64	1608.48	1576.90	76.99		
% of EEZ	0.3251	18.9233	18.5517	0.9057		

Table 3.18: Depth range analysis of the multibeam bathymetry data shown in Fig. 3.21. Almost 40% of the offshore area has been surveyed, although <1% of this is at water depths <200 m.

There is potentially an additional 2,500 km^2 of other multibeam data that have been identified. This would result in a total of 5,790 km^2, equating to 68.11% multibeam coverage within the EEZ.

Competent Institutions
Unknown

MPA
None (but example of work done seen in http://sei.org/coral.html). There is ongoing research into the marine environment, especially relating to the impact of previous volcano eruptions.

3.13. Pitcairn Islands (incl. Oeno, Henderson and Ducie)

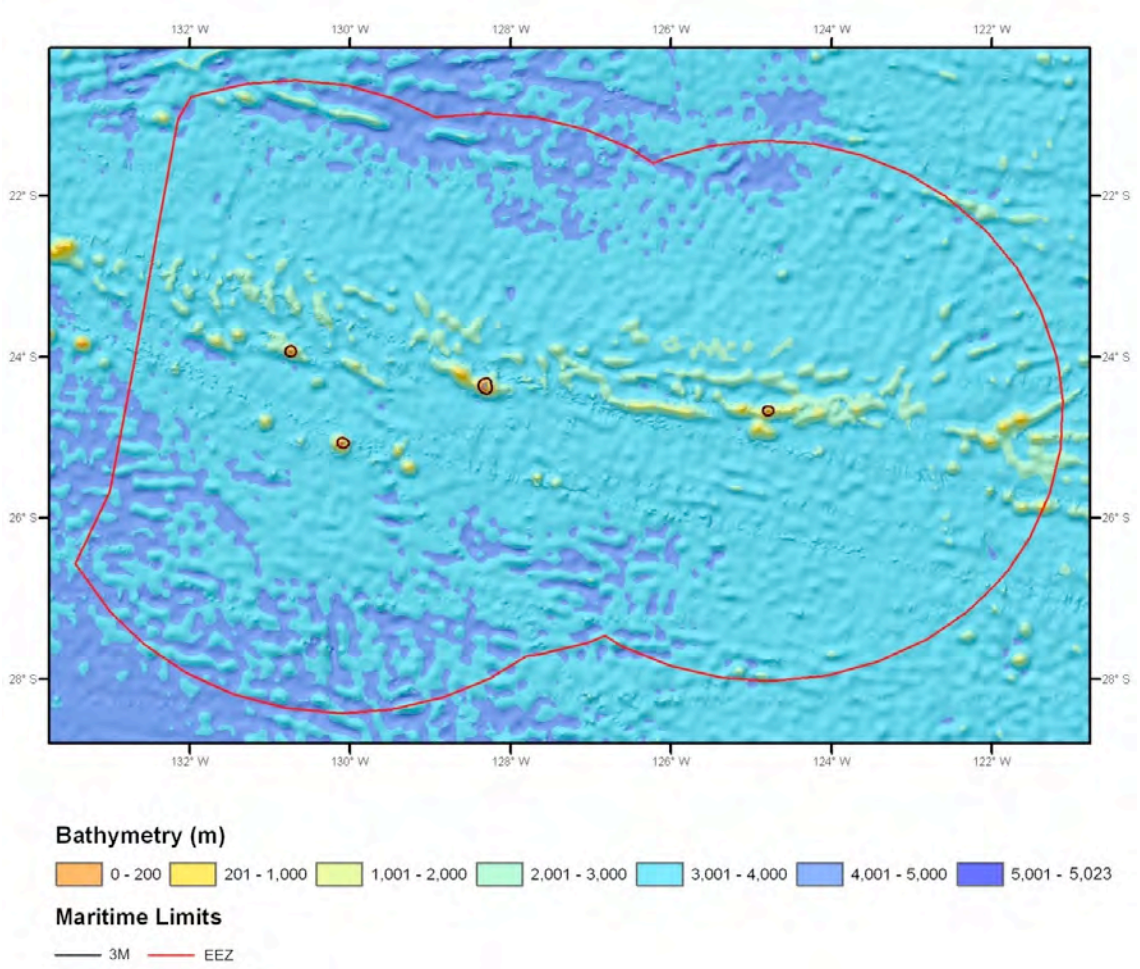

Figure 3.22: GEBCO bathymetry map of the Pitcairn Islands EEZ. Land is shown in grey.

Land area 45 km^2; EEZ 838,500 km^2

depth range (m)	**0-200**	**201-1000**	**1001-2000**	**2001-3000**	**3001-4000**	**>4001**
% of EEZ	0.01	0.01	0.52	5.07	80.94	13.35
depth range (m)	**0-200**	**0-1000**	**0-2000**	**0-3000**	**0-4000**	
cumulative %	0.01	0.02	0.54	5.61	86.55	

Table 3.19: Depth range analysis of the Pitcairn Islands EEZ shown in Fig. 3.22. Over 99% is at water depths >2000 m, with just 0.01% at depths <200 m.

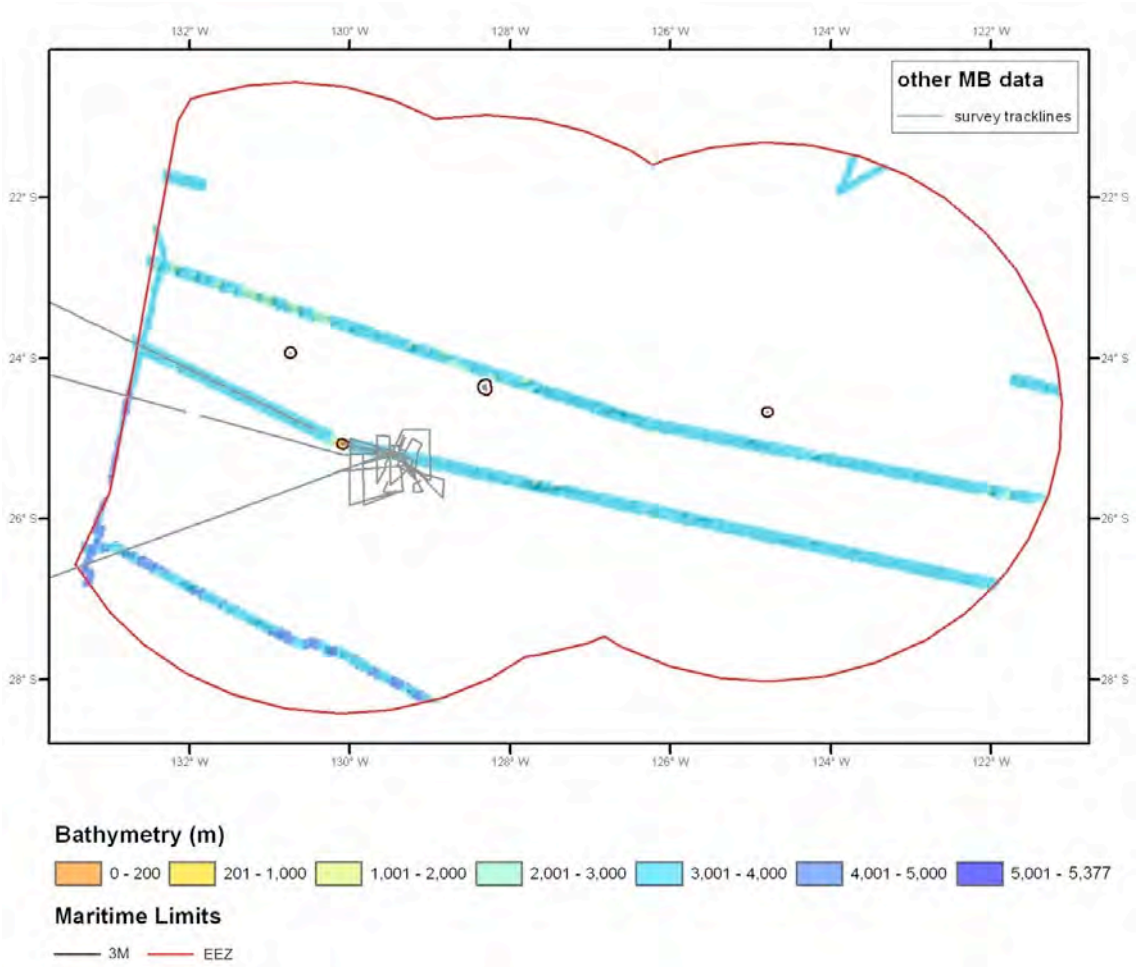

Figure 3.23: Map showing multibeam bathymetry coverage identified offshore Pitcairn Islands. Land is shown in grey shading. Grey lines indicate survey lines where additional data are potentially available.

Multibeam coverage is 51,447 km^2 or 6.14% of EEZ

depth range (m)	0-200	201-1000	1001-2000	2001-3000	3001-4000	>4001
% of MB coverage	0.0300	0.0700	0.2200	5.7500	87.0000	6.9300
MB area (km^2)	15.43	36.01	113.18	2958.20	44758.89	3565.28
% of EEZ	0.0018	0.0043	0.0135	0.3528	5.3380	0.4252

Table 3.20: Depth range analysis of the multibeam bathymetry data shown in Fig. 3.23. Only about 6% of the offshore area has been surveyed, almost all of which is at water depths >2000 m.

There is potentially an additional 22,350 km^2 of other multibeam data that have been identified. This would result in a total of 73,797 km^2, equating to 8.8% of the EEZ.

Competent Institutions
Unknown

MPA
Unknown

3.14. South Georgia and the South Sandwich Islands

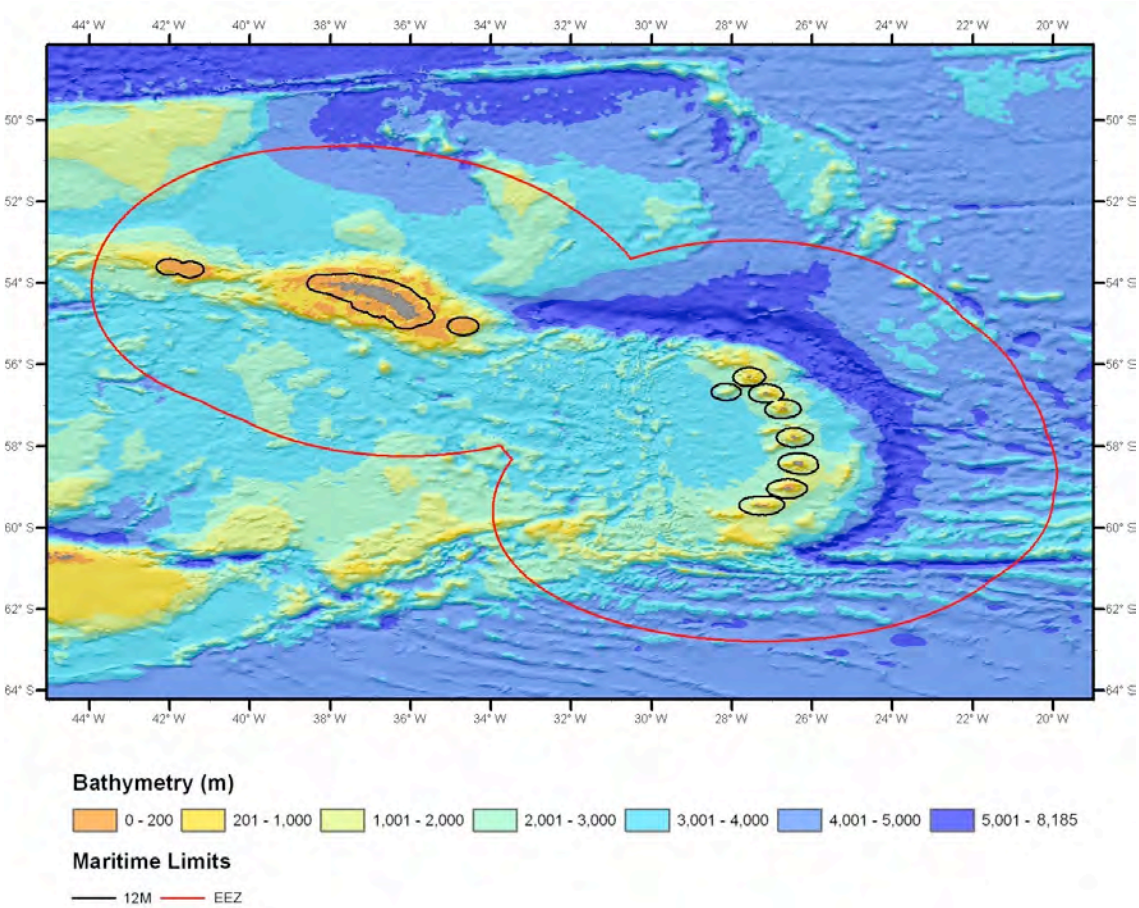

Figure 3.24: GEBCO bathymetry map of the South Georgia and South Sandwich Islands EEZ. Land is shown in grey.

Land area 3900 km^2; EEZ 1,240,500 km^2

depth range (m)	**0-200**	**201-1000**	**1001-2000**	**2001-3000**	**3001-4000**	**>4001**
% of EEZ	1.81	3.021	5.576	17.596	39.4	32.594
depth range (m)	**0-200**	**0-1000**	**0-2000**	**0-3000**	**0-4000**	
cumulative %	1.81	4.831	10.407	28.003	67.403	

Table 3.21: Depth range analysis of the South Georgia and South Sandwich Islands EEZ shown in Fig. 3.24. About 90% is at water depths >2000 m, with just 1.8% at depths <200 m.

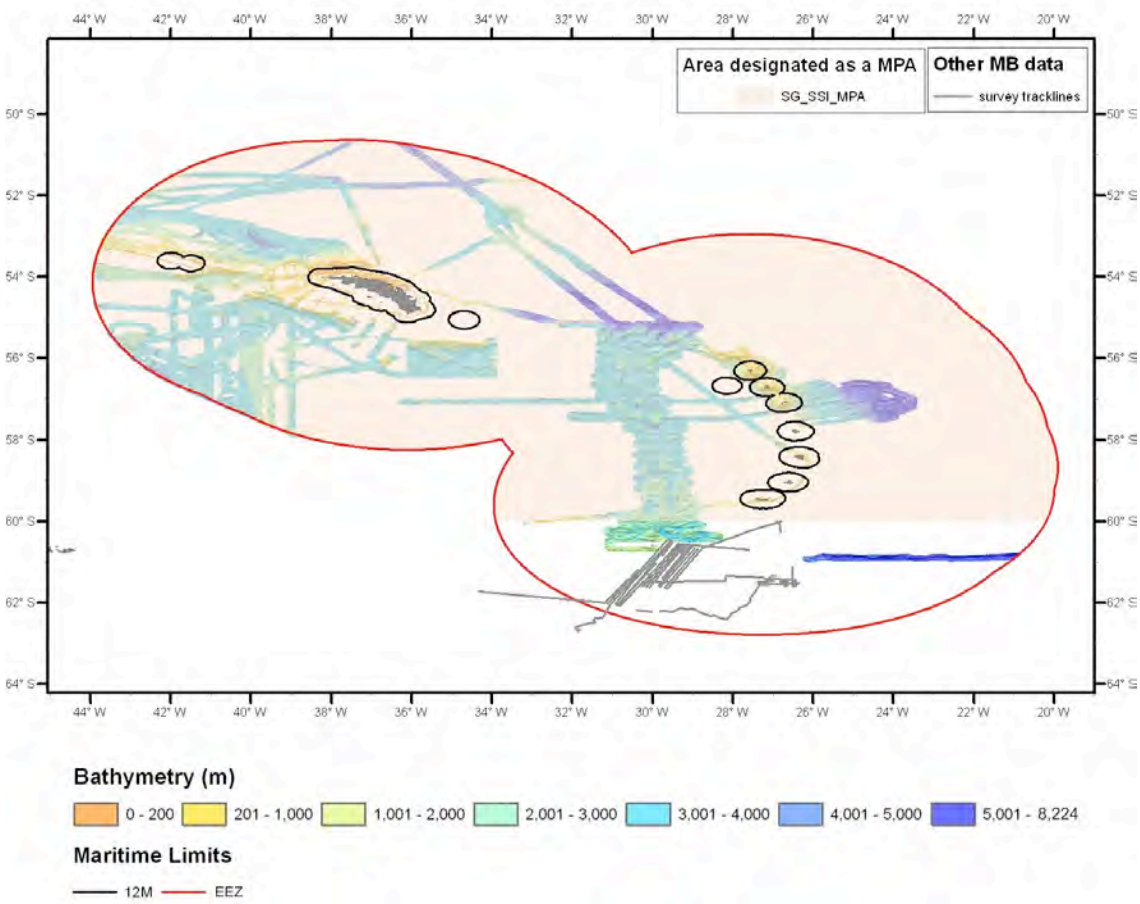

Figure 3.25: Map showing multibeam bathymetry coverage identified offshore South Georgia and South Sandwich Islands. Land is shown in grey shading. Grey lines indicate survey lines where additional data are potentially available.

Multibeam coverage is 350,000 km^2 or 28.2% of EEZ

depth range (m)	0-200	201-1000	1001-2000	2001-3000	3001-4000	>4001
% of MB coverage	1.2190	3.7650	6.8540	24.2280	51.5250	12.4060
MB area (km^2)	4266.50	13177.50	23989.00	84798.00	180337.50	43421.00
% of EEZ	0.3439	1.0623	1.9338	6.8358	14.5375	3.5003

Table 3.22: Depth range analysis of the multibeam bathymetry data shown in Fig. 3.25. Of the 28% multibeam coverage, 87% is in water depths >2000 m.

There is potentially an additional 10,500 km^2 of other multibeam data that have been identified. This would result in a total of 360,500 km^2, equating to 29% of the EEZ.

Competent Institutions
GSGSSI http://www.sgisland.gs/index.php/Main_Page
British Antarctic Survey http://www.antarctica.ac.uk/

MPA
On the 23rd February 2012 the entire area north of 60˚ south was designated as a MPA. The areas beyond the 12 Mile limits of South Georgia, Clerke Rocks and Shag and Black Rocks, and beyond 3 Miles of the South Sandwich Islands, are designated as IUCN Category VI; the areas within these limits are categorised as IUCN Category I.

3.15. St Helena

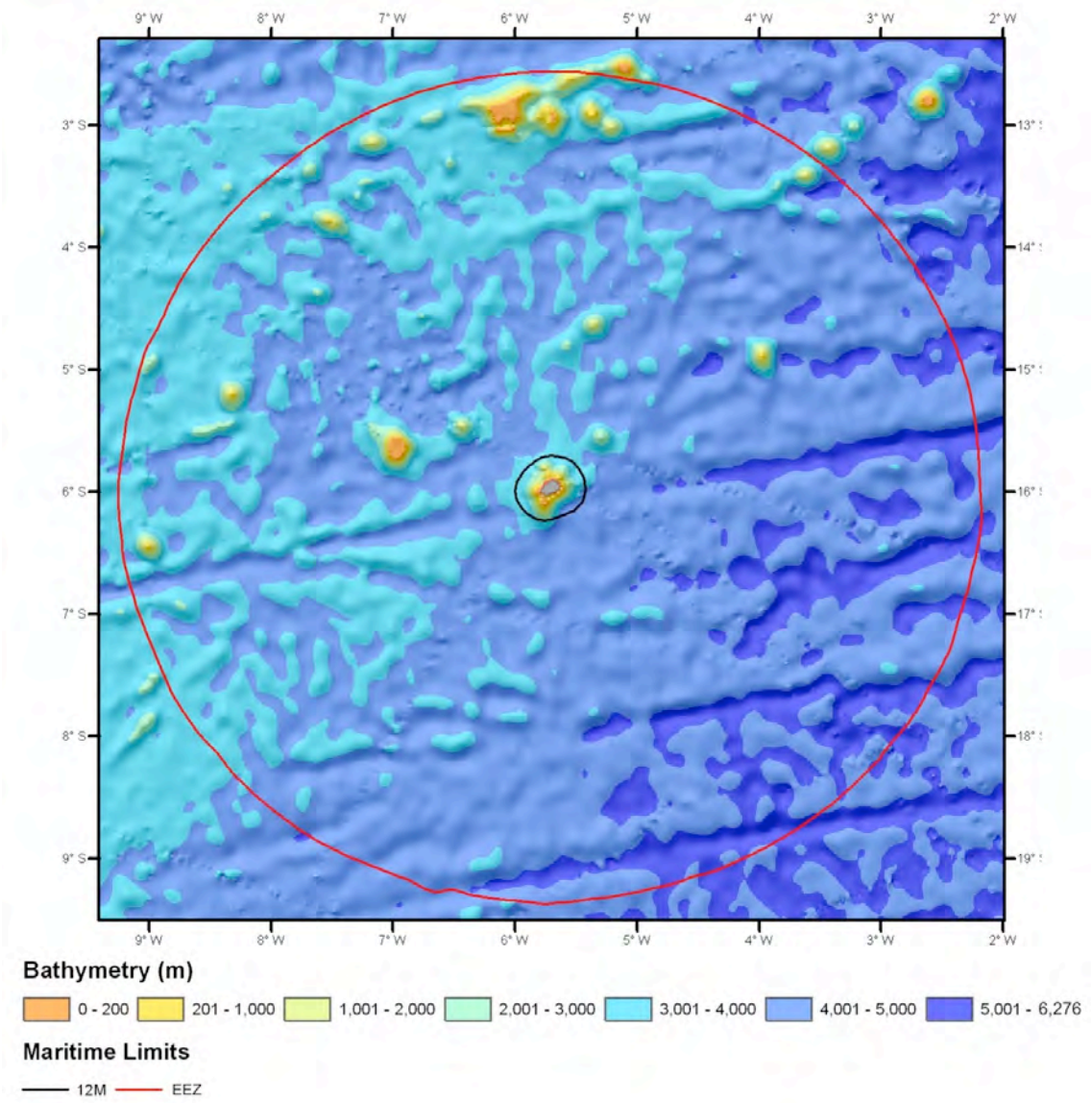

Figure 3.26: GEBCO bathymetry map of the St Helena EEZ. Land is shown in grey.

Land area 129 km^2; EEZ 446,000 km^2

depth range (m)	**0-200**	**201-1000**	**1001-2000**	**2001-3000**	**3001-4000**	**>4001**
% of EEZ	0.211	0.314	0.642	1.445	25.844	71.542
depth range (m)	**0-200**	**0-1000**	**0-2000**	**0-3000**	**0-4000**	
cumulative %	0.211	0.525	1.167	2.612	28.456	

Table 3.23: Depth range analysis of the St Helena EEZ shown in Fig. 3.26. About 99% is at water depths >2000 m, with just 0.2% at depths <200 m.

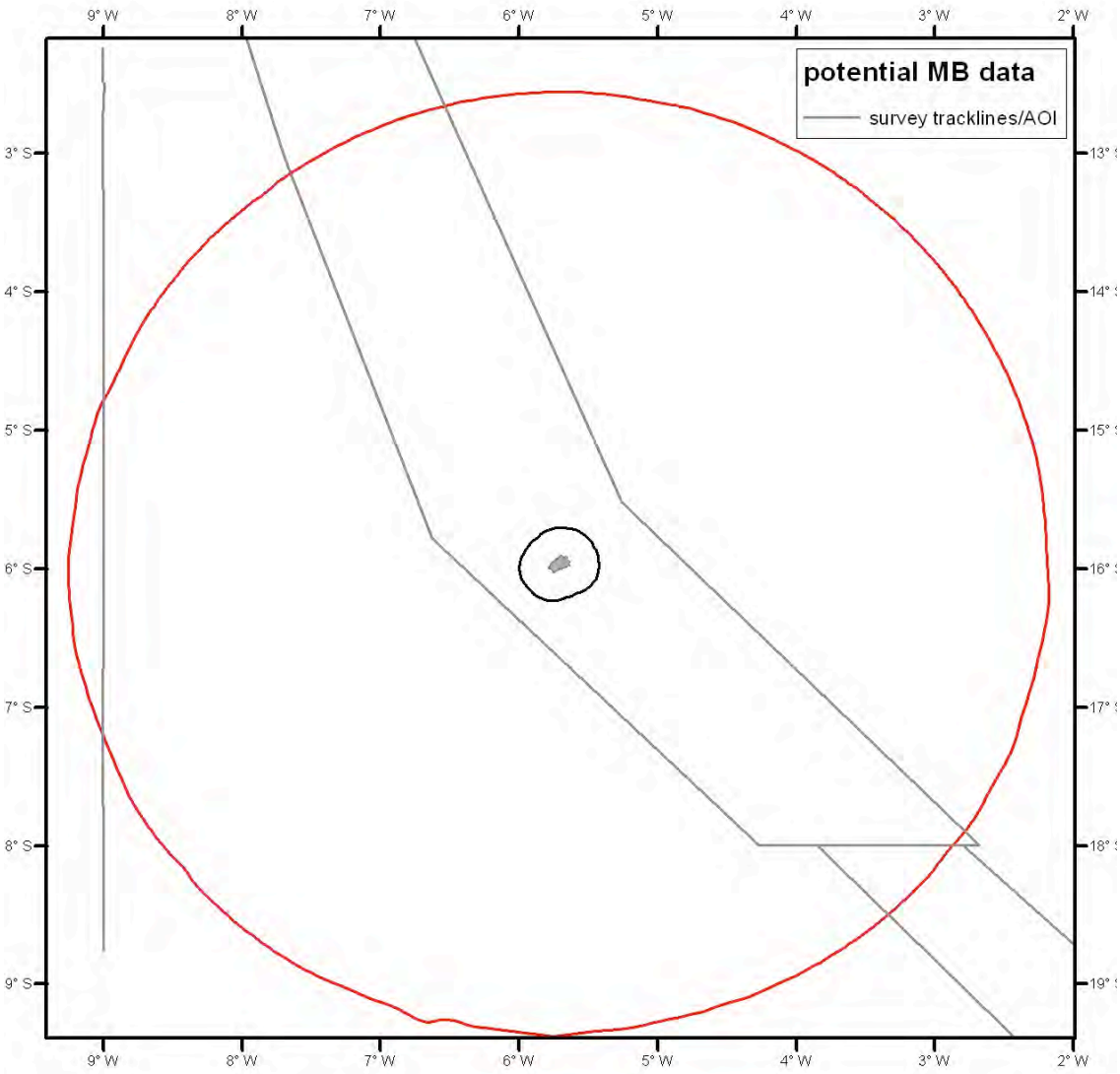

Figure 3.27: Map showing multibeam bathymetry coverage identified offshore St Helena. Land is shown in grey shading. Grey lines indicate survey lines where additional data are potentially available.

Multibeam coverage is 0 km^2 or 0% of EEZ

There is currently no accessible multibeam coverage in the St Helena EEZ, although there are a small number of tracklines that might indicate the presence of potential data.

Competent Institutions
Unknown

MPA
Unknown

3.16. Tristan da Cunha (incl. Nightingale, Inaccessible and Gough Island)

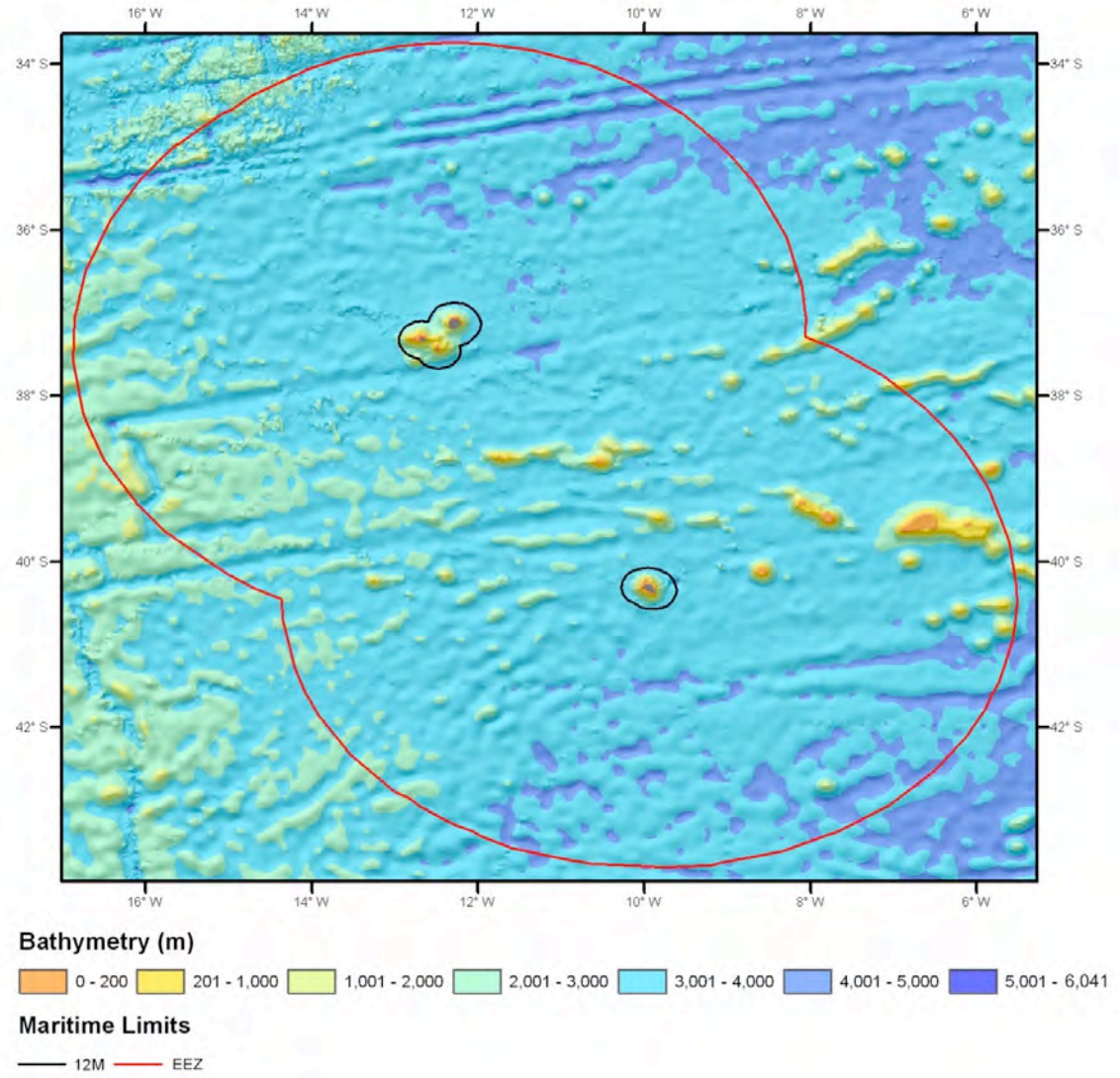

Figure 3.28: GEBCO bathymetry map of the Tristan da Cunha EEZ. Land is shown in grey.

Land area 203 km^2; EEZ 752,850 km^2

depth range (m)	**0-200**	**201-1000**	**1001-2000**	**2001-3000**	**3001-4000**	**>4001**
% of EEZ	0.188	0.512	1.142	12.166	79.666	6.323
depth range (m)	**0-200**	**0-1000**	**0-2000**	**0-3000**	**0-4000**	
cumulative %	0.188	0.7	1.842	14.008	93.674	

Table 3.24: Depth range analysis of the Tristan da Cunha EEZ shown in Fig. 3.28. About 98% is at water depths >2000 m, with just 2% at water depths at <200 m.

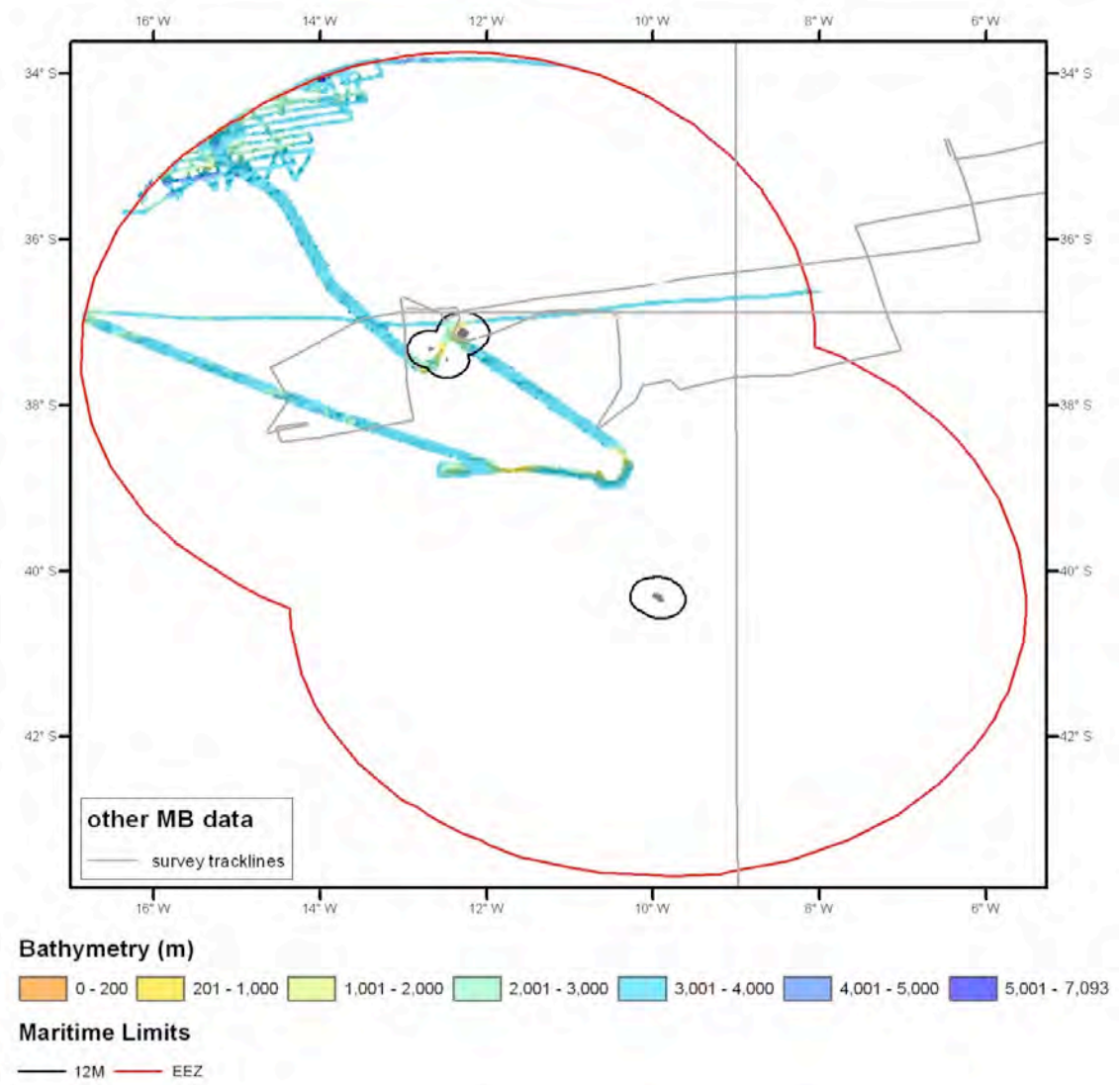

Figure 3.29: Map showing multibeam bathymetry coverage identified offshore South Georgia and South Sandwich Islands. Land is shown in grey shading. Grey lines indicate survey lines where additional data are potentially available.

Multibeam coverage is 45,500 km^2 or 6.0% of EEZ

depth range (m)	0-200	201-1000	1001-2000	2001-3000	3001-4000	>4001
% of MB coverage	0.0210	0.5390	2.5290	19.2970	75.0180	2.5940
MB area (km^2)	9.56	245.25	1150.70	8780.14	34133.19	1180.27
% of EEZ	0.0013	0.0326	0.1528	1.1663	4.5339	0.1568

Table 3.25: Depth range analysis of the multibeam bathymetry data shown in Fig. 3.29. 6% of the EEZ has multibeam coverage, with 97% of this at water depths >2000 m.

There is potentially an additional 35,000 km^2 of other multibeam data that have been identified. This would result in a total of 80,500 km^2, equating to 10.7% of the EEZ.

Competent Institutions
Unknown

MPA
Unknown

3.17. Turks and Caicos

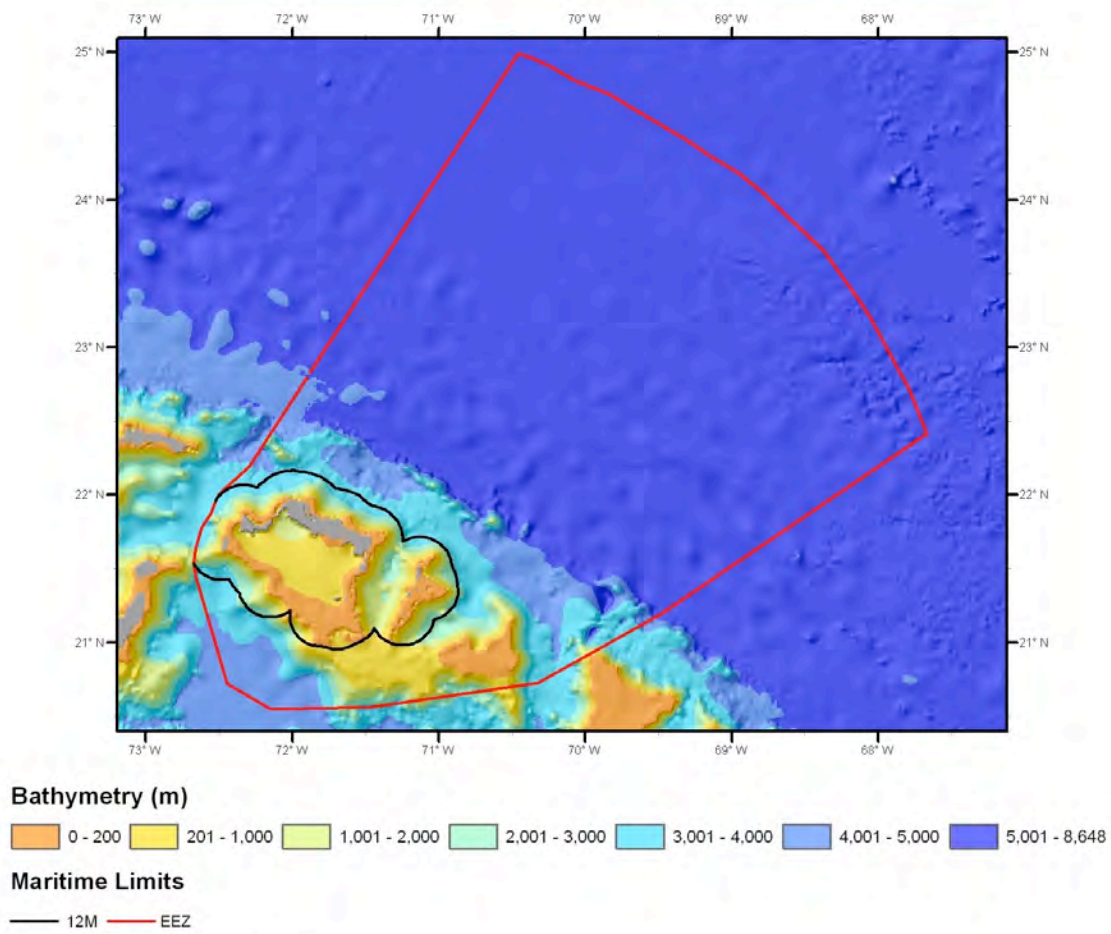

Figure 3.30: GEBCO bathymetry map of the Turks and Caicos EEZ. Land is shown in grey.

Land area 1000 km^2; EEZ 148,700 km^2

depth range (m)	**0-200**	**201-1000**	**1001-2000**	**2001-3000**	**3001-4000**	**>4001**
% of EEZ	3.46	5.6	3.22	2.92	7.45	77.32
depth range (m)	**0-200**	**0-1000**	**0-2000**	**0-3000**	**0-4000**	
cumulative %	3.46	9.06	12.28	15.2	22.65	

Table 3.26: Depth range analysis of the Turks and Caicos EEZ shown in Fig. 3.30. Over 77% is at water depths >4000 m, with 3.5% at depths <200 m.

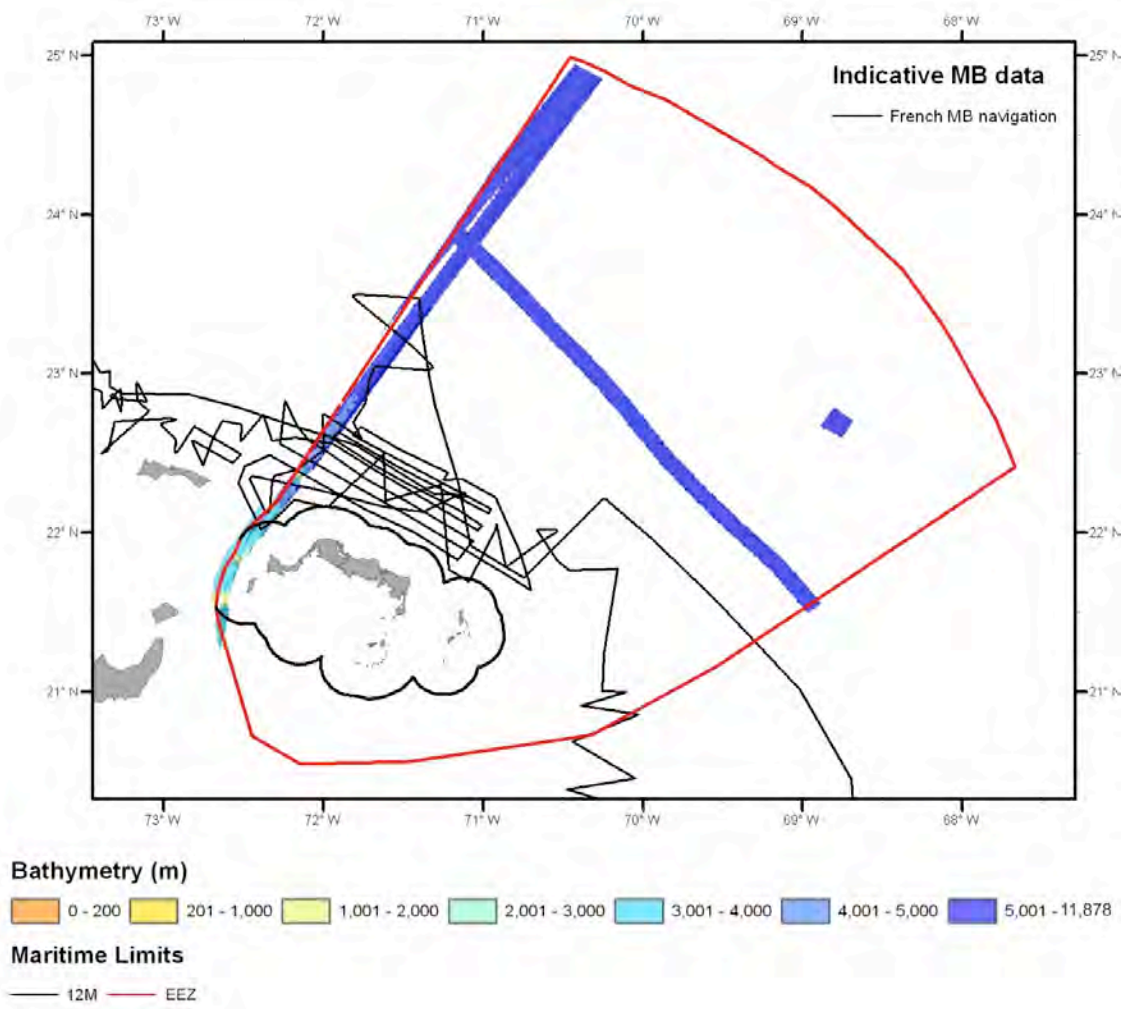

Figure 3.31: Map showing multibeam bathymetry coverage identified offshore Turks and Caicos. Land is shown in grey shading. Dark grey lines indicate survey lines where additional data are potentially available.

Multibeam coverage is 11,800 km^2 or 7.9% of EEZ

depth range (m)	0-200	201-1000	1001-2000	2001-3000	3001-4000	>4001
% of MB coverage	0.0000	0.0000	0.7700	1.0600	8.3300	89.7900
MB area (km^2)	0.00	0.00	90.86	125.08	982.94	10595.22
% of EEZ	0.0000	0.0000	0.0611	0.0841	0.6610	7.1252

Table 3.27: Depth range analysis of the multibeam bathymetry data shown in Fig. 3.31. 8% of the EEZ has multibeam coverage, with 98% of this at water depths >3000 m.

There is potentially an additional 18,600 km^2 of other multibeam data that have been identified. This would result in a total of 30,400 km^2, equating to 20.4% of the EEZ.

Competent Institutions
The Dept of Environment and Coastal Resources http://www.environment.tc/
Turks & Caicos National Trust http://www.tcimall.tc/nationaltrust/

MPA
Inshore waters and reefs
http://www.environment.tc/Protected-Areas-Division.html

3.18. Comparison with UK EEZ

The UK EEZ covers an area of 781,800 km^2, the majority of which (70%) is at water depths of <200 m (Fig. 3.32).

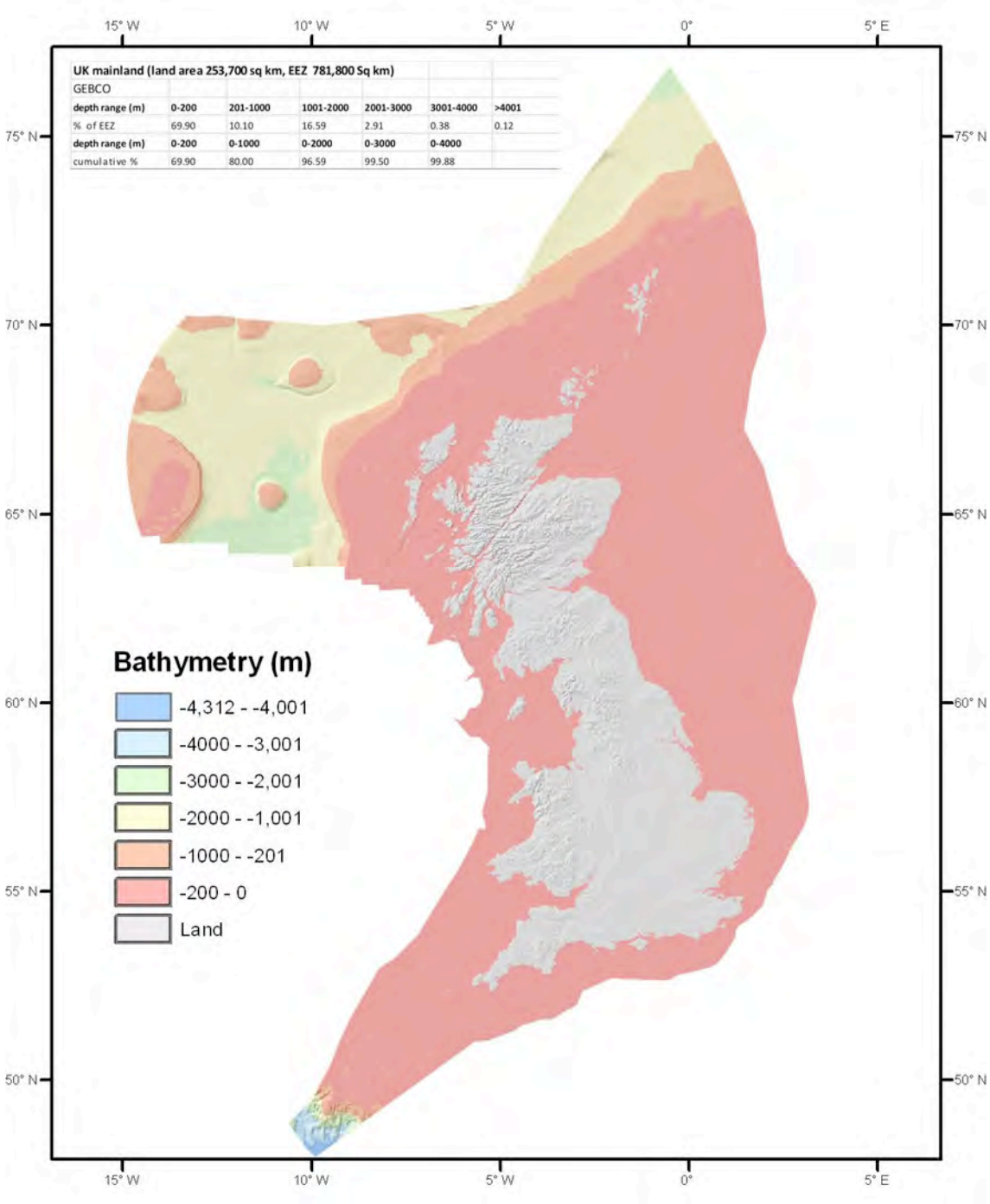

Figure 3.32: Map of the UK EEZ, based on GEBCO bathymetry. Note the dominance of shallow shelf waters, with depths <200 m.

About 205,000 km^2 (26%) of the UK EEZ has been mapped with multibeam bathymetry (Fig. 3.33), with an additional 23,400 km^2 planned as part of the MCA Civil Hydrography Programme (CHP). This would take the coverage total to about 30% in 2013/14.

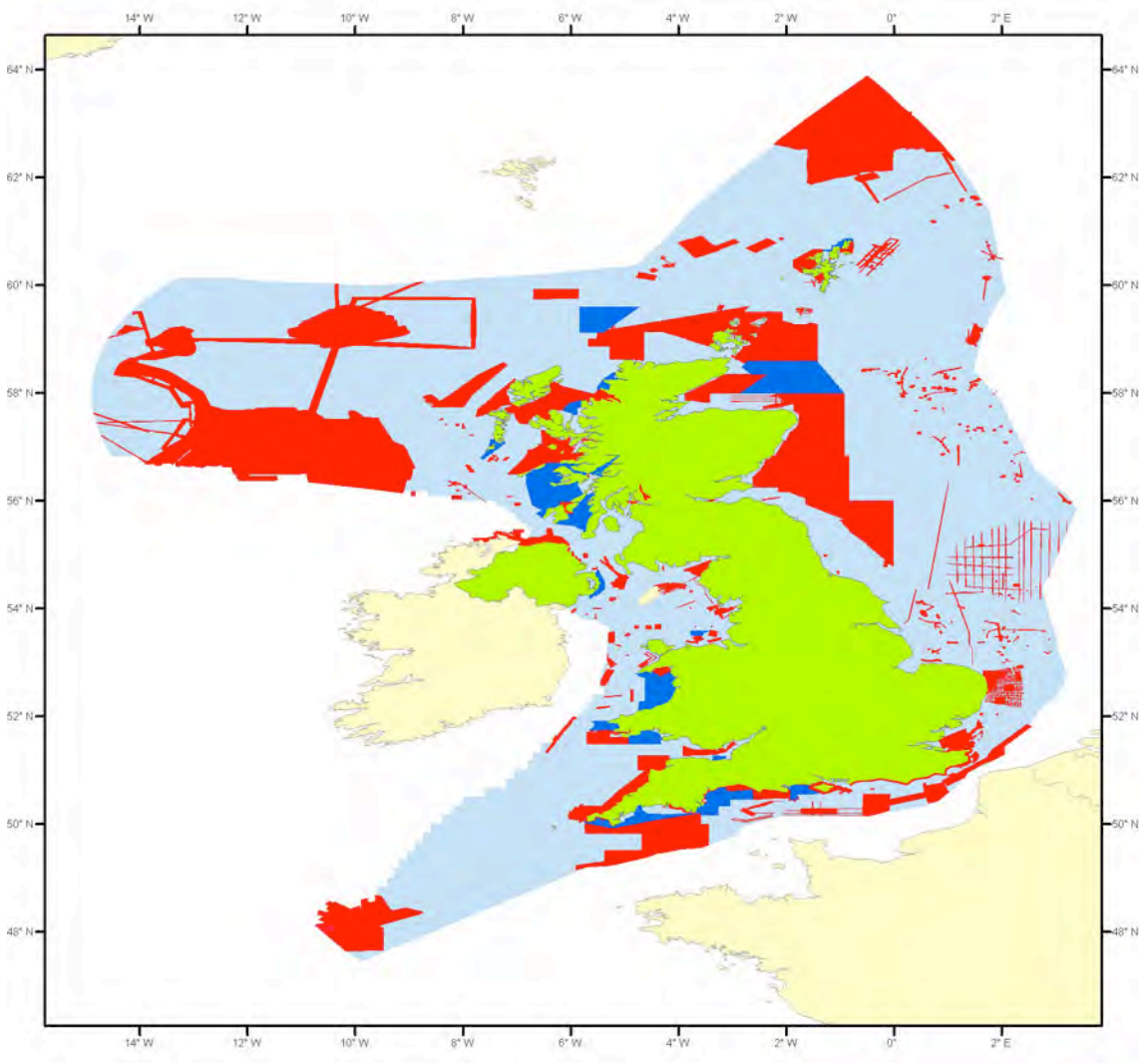

Figure 3.33: Map of the UK EEZ (shaded in light blue), showing existing multibeam bathymetry data (red) and planned surveys as part of the CHP (dark blue).

3.19. WP Summary

In total 911,714 km^2 of multibeam bathymetry data from the UK OT EEZs have been identified and accessed, with at least an additional 118,950 km^2 of potential data identified but that are not readily available. These values combined equate to 17.7% of all OT EEZ areas.

In order to assess the effort that would be required to address the data shortage within each OT, Table 3.28 below lists the area (in km^2) and % of each OT that remains to be mapped with multibeam. It should be noted that these values are based solely on data that have been identified and as such do not represent the true values.

	Anguilla	Ascension	Bermuda	BIOT	BVI	Cayman	Akrotiri	Dhekelia
EEZ Area	83500	443344	446560	636000	87650	119000	123	130
MB ID to survey (km^2)	32427	83250	146800	0	31000	48200	0	0
to survey (km^2)	51073	360094	299760	636000	56650	70800	123	130
to survey (% EEZ)	61.17	81.22	67.13	100.00	64.63	59.50	100.00	100.00

	Falkland	Gibraltar	Montserrat	Pitcairn	SG-SSI	St Helena	Tristan	Turks & Caicos
EEZ Area	545800	83	8500	838500	1240500	446400	752850	148700
MB ID to survey (km^2)	135000	0	5790	73797	360500	0	80500	30400
to survey (km^2)	410800	83	2710	764703	880000	446400	672350	118300
to survey (% EEZ)	75.27	100.00	31.88	91.20	70.94	100.00	89.31	79.56

Table 3.28: Summary of Sq Km and % areas that remain un-surveyed by Multibeam bathymetry data

The above values represent significant survey effort, far beyond the scope of current AUV capacity, but new surveys are already in progress in some regions, e.g. by the UK Navy for use in updating Admiralty Charts. An example of this is in the seas surrounding Montserrat, where, during May 2012, the HMS Protector surveyed the entire shallow water area (<200m) to the west and northwest of the Island. These data would significantly reduce the area of 31.88% that is still left to survey in this OT.

An ongoing project, led by the United Kingdom Hydrographic Office, is specifically attempting to address the data shortfall in the UK OTs. In the next few months a White Paper will be drafted, outlining the need to address this data shortfall. NOC and its MAREMAP partners will retain a watching brief on any developments from this project, and will provide updates to DEFRA as and when they materialise.

Work Package 4: Case Studies

WP Leader: Various NOC, BGS and SAMS staff

4.1. The WP4 task

As set out in the proposal this task's remit was as follows:

"*This WP will comprise seven case studies, with a focus on providing representative examples (maps and images) of the data collected. The aim will be to demonstrate the resolution, spatial extent, calibration/repeatability and quality of data collected with different survey methods. Note that new case study data due to be collected after 31 May (which is when we anticipate delivery of the main project report) will be added to the report as a series of appendices*."

Case Study 1: Deep-water AUV mapping off NW UK

CS Leader: Dr Veerle Huvenne (NOC)

CS1.1. The CS1 task

As set out in the proposal this task's remit was as follows:

"*This case study will focus on data collected during a £1M NERC-funded MAREMAP cruise to NW UK in summer 2011 on RRS James Cook. The cruise was undertaken in partnership with JNCC, and focused on benthic habitat mapping and human impacts on vulnerable habitats The main aim was to carry out habitat mapping work in selected areas of the Rockall Trough, Rockall Bank and Hatton Basin in order to assess the status of different benthic habitats in relation to human activities, especially deep-sea bottom trawling. The cruise included a revisit of the Darwin Mound cold-water coral reefs, discovered in 1998 and protected in 2003, and an assessment of the status of two fisheries closure areas on Rockall Bank. In addition, two pilot studies of a more geological nature were carried out: one was targeting a Polygonal Fault System in the Hatton Basin, potentially linked to fluid flow, while the other focused on the history of the Rockall Bank Mass Flow. The tools used to achieve these objectives included the Autosub6000 Autonomous Underwater Vehicle (AUV), newly equipped with an EdgeTech dual frequency high-resolution sidescan sonar plus chirp profiler and a monochrome stills camera, a commercial inspection class ROV, and more traditional equipment including piston-, mega- and boxcore, CTD and shipborne multibeam (EM120 and EM710). Although the unsettled weather hampered the operations to a certain extent (including a forced return to the shelter of the Minches, resulting in an ad hoc survey of the E Shiant Bank), the cruise was a success, with 88h of ROV footage & photography collected, 125km^2 of seabed mapped at high resolution (metre to centimetre-scale) by the Autosub6000, 400km^2 mapped with the EM710 on Rockall Bank, and 52 coring operations for geological and biological studies. The full cruise report can be found at: http://eprints.soton.ac.uk/193835/*

This Case Study will be compiled by NOC between 1 March and 31 May 2012."

CS1.2. Introduction

The main aim of expedition JC060 was to carry out habitat mapping for the assessment of human impacts on a variety of deep-sea environments west of Scotland. There was a particular focus on the effects of deep-sea trawling, and of potential conservation measures, on benthic ecosystems such as cold-water coral communities. We visited three areas that have received varying levels of protection under different fisheries closure schemes over the last 5 to 10 years (Fig. CS1.1).

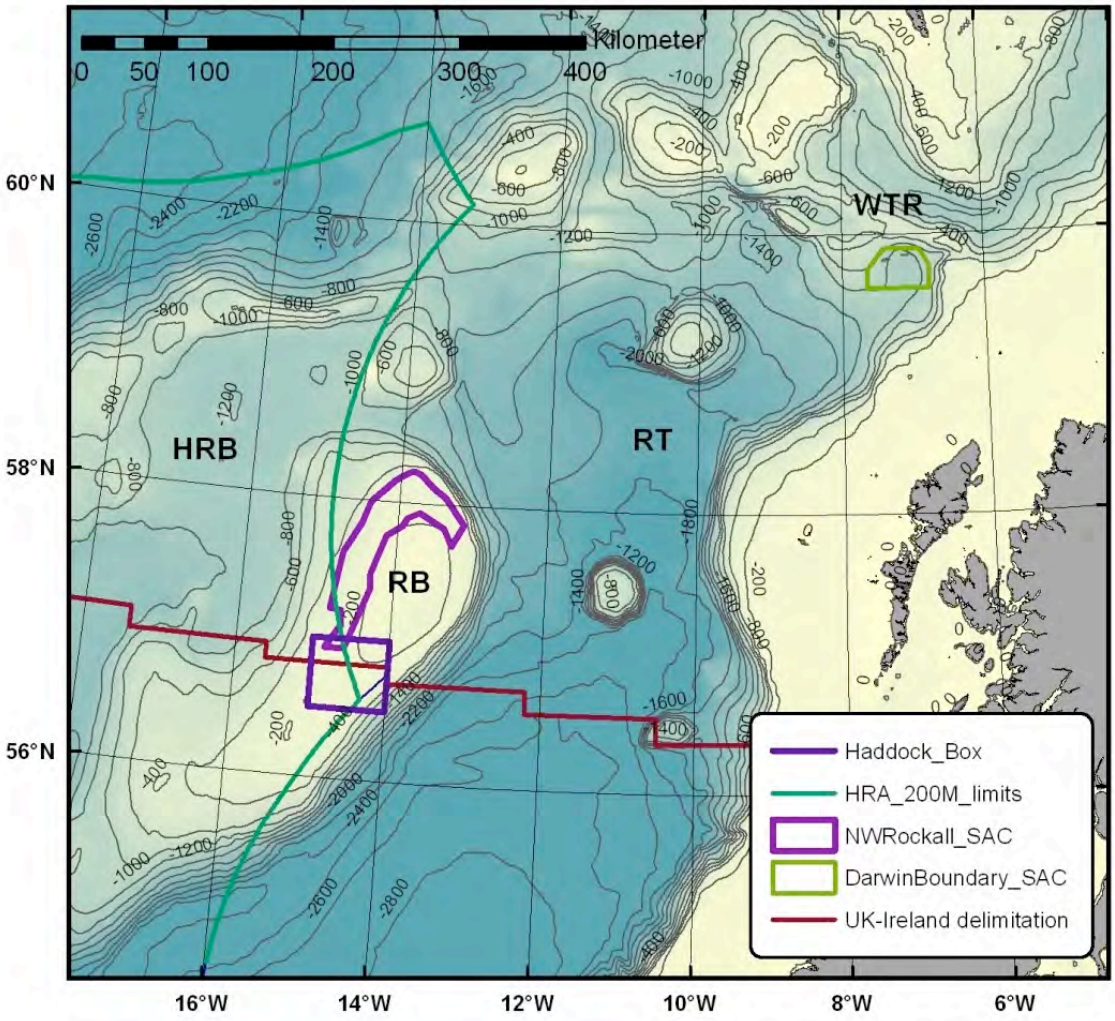

Figure CS1.1: Study areas for JC060. HRB: Hatton-Rockall Basin, RB: Rockall Bank, RT: Rockall Trough, WTR: Wyville-Thomson Ridge. Bathymetry from GEBCO (2003), 200 m depth contours.

CS1.2.1. Darwin Mounds

The Darwin Mounds (Fig. CS1.2) are small cold-water coral mound features, up to 5 m high and 75 m across, discovered in 1998 in the northern Rockall Trough (Masson et al., 2003). They were first identified on TOBI 30kHz sidescan sonar maps during the AFEN surveys (Atlantic Frontier Environmental Network; Bett, 2001), and were later investigated in more detail using high-resolution sidescan sonar and video datasets (Bett et al., 2001). This follow-on work revealed that the area has been heavily impacted by deep-water bottom trawling; several mounds were scarred by trawl doors and nets, and coral colonies were broken to pieces and scattered around (Wheeler et al., 2005). The information was passed on to policy-makers, which resulted in the emergency closure of the area under the EU Common Fisheries Policy in August 2003 (De Santo and Jones, 2007). The closure was made permanent in spring 2004, and meanwhile the area has also become the first UK deep-water Special Area of Conservation (SAC) under the EU Habitats Directive. However, since conservation measures were put in place, no further scientific surveys have been carried out in the area, and in May 2011 the status of the Darwin Mounds was unsure. A worrying observation was published by Davies et al. (2007), who reported, based on Vessel Monitoring System data (VMS), increased vessel activity in the area in August 2003, immediately before the closure.

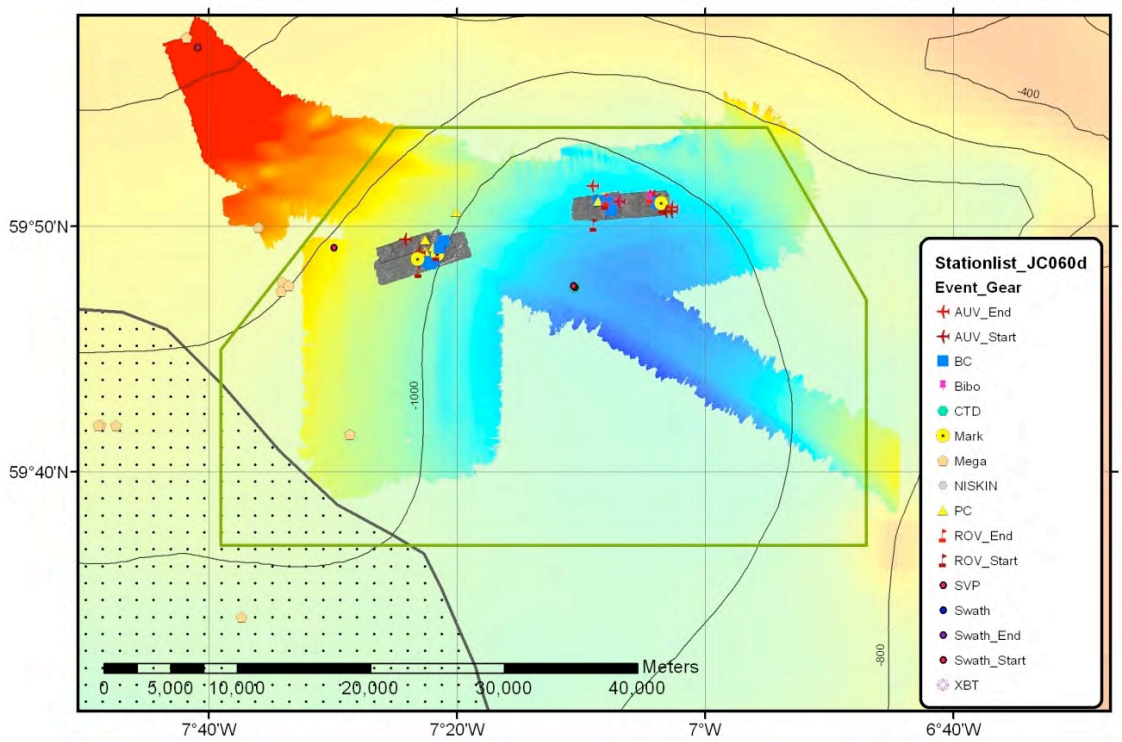

Figure CS1.2: Location map of the Darwin Mound SAC (green outline) and datasets gathered during JC060. Brightly coloured shades represent vessel-mounted multibeam bathymetry coverage. Grey shaded areas represent AUV data.

CS1.2.2. Haddock Box

Haddock fisheries on Rockall Bank first started more than 100 years ago, and peaked in the 1930's and 1970's. Currently there mainly is a Scottish and Russian haddock fleet working in the area. Based on observations collected over the last 25 years by the Fisheries Research Services in Aberdeen, Newton et al. (2008) suggested an age-related distribution of Haddock on Rockall Bank/Plateau. Young haddock seem to concentrate on the southwestern part of Rockall Bank; based on these results the North-East Atlantic Fisheries Council (NEAFC) and the EU decided to close the area now called the 'Haddock Box' (Fig. CS1.3). The closure was put in place in 2001(NEAFC)/2002(EU) and has been revised regularly by ICES and NEAFC, although a general lack of information and data is often cited as hampering the assessments. The restrictions are aimed towards bottom fisheries (including trawling), while longlining is currently allowed.

CS1.2.3. NW Rockall Bank

This area was closed to bottom fisheries much more recently, again to protect cold-water coral reefs. It was chosen based on a study of areas with cold-water coral occurrence (from bycatch reports, scientific papers etc) compared to areas with high fishing pressure (from VMS data; Hall-Spencer et al., 2009). The NW edge of Rockall Bank appeared to receive less fishing pressure, and contained several records of cold-water coral reefs; therefore was identified as an area that may still contain pristine reefs. The area was closed to all types of bottom fisheries in 2007 under NEAFC regulations, and was also proposed as a candidate SAC in 2010 by JNCC. However, the cSAC has a slightly different outline (Fig. CS1.3) compared to the original NEAFC closure. This suggested adaptation was based on additional records of coral occurrence that have recently become available. The habitat mapping work during JC060 was aimed at providing an increased evidence base to guide the discussion about the potential extension of the NEAFC fisheries closure area.

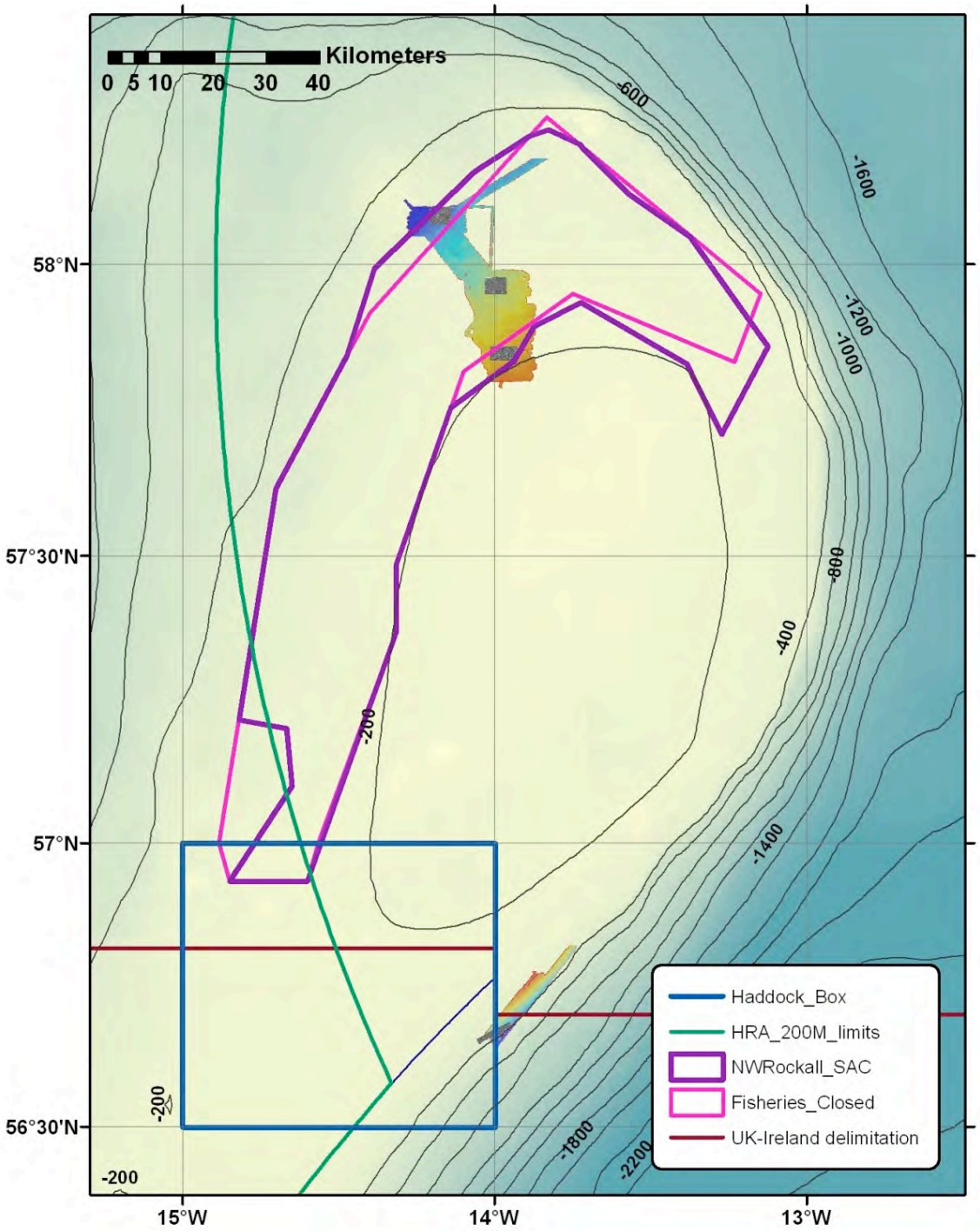

Figure CS1.3: Location map of Haddock Box (blue square) and NW Rockall Bank fisheries closure areas (purple polygons), indicating JC060 working areas (brightly coloured shaded areas).

In addition we also studied an area in the Hatton-Rockall Basin (Fig. CS1.1) where polygonal fault systems have been identified as outcropping at the seabed. Such systems have been reported from several sedimentary basins worldwide, and are often mentioned as potential sites for fluid flow as a result of sediment contraction, although the actual formation process is still under debate (e.g. through syneresis, residual shear strength faulting, density inversion or gravitational collapse – see Cartwright et al. (2003) and references therein). However, most known polygonal fault systems occur in the sub-seafloor, which makes the

polygonal faults in the Hatton-Rockall Basin a unique study site. The work in the area during JC060 was part of a reconnaissance study of these features, to assess their activity and the presence of absence of rare chemosynthetic biological communities.

CS1.3. The JC060 research cruise

The basic information about research cruise JC060 is summarised below (Table CS1.1):

Vessel	RRS James Cook
Start	9 May 2011
End	12 June 2011
Duration	35 days
Darwin Mound on site	12 days
Haddock Box on site	2.5 days
NW Rockall Bank on site	5.5 days
Hatton Basin on site	2 days
Weather downtime/transit	8.5 days/4.5 days
Partner organisations involved in JC060	6
Scientists on board	18
Technicians on board	11
Ship's officers and crew	22
Cost of shiptime (NERC)	xxx
Cost of 'superstructure', i.e. equipment, technicians, mob/demob etc (shared between NERC (55%), JNCC (28%), Lenfest Ocean Program (PEW, 16.5%), ERC-CODEMAP (0.5%))	£288,000
Cost of scientists (FEC), consumables, travel (paid from various sources, e.g. NERC-MAREMAP, ERC-CODEMAP, EC-HERMIONE, partner HEI funding)	Difficult to estimate due to different partner organisations and variable costs for consumables and personnel. Estimate: £180,000

Table CS1.1: Summary of information about research cruise JC060.

CS1.3.1. Equipment

To carry out the above-described research, we carried the following tools:

1) Shipboard acoustics

The RRS James cook is equipped with Kongsberg Simrad EM120 and EM710 multibeam bathymetry systems and a Kongsberg SBP120 parametric sub-bottom profiler.

2) Autosub6000 Autonomous Underwater Vehicle (AUV)

The full specification of the Autosub6000 AUV is given under WP1 of this report. For JC060, the vehicle was equipped with:

- EM2000 multibeam system,
- EdgeTech 2200-FS dual frequency sidescan sonar (120/410kHz) with chirp sub-bottom profiler,
- Prosilica GE1380 monochrome digital camera with Canon 580 flash,
- Digiquartz depth sensor,
- Set of Seabird CTD units, including oxygen sensor,
- Eh Sensor,
- Magnetometer,
- a Sea Point LSS sensor,

- and an RDI Teledyne 300kHz ADCP.

3) Commercial, inspection class ROV (model SeaEye Lynx), hired from Hallin Marine UK Ltd. The ROV carried:

- a Kongsberg OE14-208 stills camera,
- a Kongsberg)E14-366 colour zoom video camera,
- a Tritech SK700 bathymetric and altimeter unit,
- and a 4-function manipulator arm

4) Sampling equipment including a Seabird CTD with 24 Niskin bottle rosette, Piston core, Mega core and Boxcore.

Full details of these instruments, their setup and operation are providedn in the cruise report (Huvenne et al., 2011).

CS1.3.2. Autosub6000 missions

In total, 12 Autosub missions were carried out during JC060. They are summarised in Appendix 3. Most missions were aimed at mapping various parts of the study areas, either using the EM2000 multibeam system or the EdgeTech sidescan sonar. For reasons of acoustic interference, both systems could not operate simultaneously. Mission M46 however was specifically planned to acquire a more technical dataset for the ERC project CODEMAP, in order to evaluate the repeatability of AUV-based mapping and monitoring. Instead of the typical pattern of parallel survey lines, the AUV was programmed to pass repeatedly over the same two points, albeit with varying configurations (time-lapse, changes in heading, different equipment or frequency, etc.).

CS1.3.3. Autosub6000 data processing

Processing of the Autosub6000 data was carried out in a variety of software packages. For the EM2000 bathymetry data we used the commercial package CARIS Hips & Sips, but the backscatter information, together with the low-res and high-res sidescan sonar data were processed with our NOC in-house software PRISM (Le Bas and Huvenne, 2009). Table CS1.2 gives an overview of the different resolutions and data qualities we obtained throughout the cruise.

In general, the EM2000 bathymetry was recorded from an altitude of 100m, which results in bathymetry with pixel sizes in the order of 1 to 2 m. The backscatter data often obtained a better resolution because the PRISM software can sub-sample backscatter ‘snippets’. The 120kHz sidescan sonar data was recorded at a similar altitude (100m), providing imagery with a pixel resolution of 50 cm. The 410kHz data was recorded at 15m altitude, and was processed to 50 or 20cm resolution (the latter taking much longer and hence not carried out during the cruise). Specific subsets of the data were processed close to the fullest resolution available in the across-track sidescan data (although this means oversampling in the along-track direction due to the AUV velocity and sidescan ping-rate).

Area	EM2000 Bathy	EM2000 Backs	Edge Low	Edge High
M37	✓ (1m)	✓ (1m)	×	
M38	✓ (2m)	✓ (1m)	×	
M39	✓ (2m)	✓ (50cm)	✓ (50cm)	
M40				✓ (20cm)
M41	✓ (2m)	✓ (50cm)		✓ (50cm) (2cm)
M42				✓ (20cm)
M43				✓ (50cm)
M44				✓ (50cm)
M45				✓ (50cm)
M46 (repeatability)			✓	✓
M48				✓ (50cm) (5cm)

Table CS1.2: Overview of processing results of the Autosub6000 bathymetry, backscatter and sidescan sonar data.

The EdgeTech chirp data were less accessible during the cruise itself, as this was the first time the profiler had been used and no processing protocol had been set up for this data format. However, post-cruise, PhD student Melis Cevatoglu (University of Southampton, Ocean and Earth Sciences) developed a conversion routine which allows transfer of data into the much more common .segy format. Further data processing and visualisation will now take place using the Promax software.

Raw images from the monochrome camera were processed in Matlab to apply, amongst others, an adaptive histogram equalisation and a noise reduction filter.

CS1.4. Results

CS1.4.1. Bathymetry

Accurate knowledge of seabed morphology is essential for the understanding of seafloor processes and the determination of seafloor habitats. The Autosub6000 EM2000 bathymetry provides seabed morphology information at a resolution that cannot be achieved with shipborne systems, especially in deep water (>1000 m). Data examples from cruise JC060 are given in Figs. CS1.4-1.7. When navigated at 100m altitude, the system can easily resolve features such as the Darwin Mounds (ca. 50m across, a few metres high) or a suite of pockmarks in the Hatton-Rockall Basin (ca. 8m across and less than a metre deep), features that could not be identified from shipboard multibeam data, but are of vital importance for understanding faunal distributions.

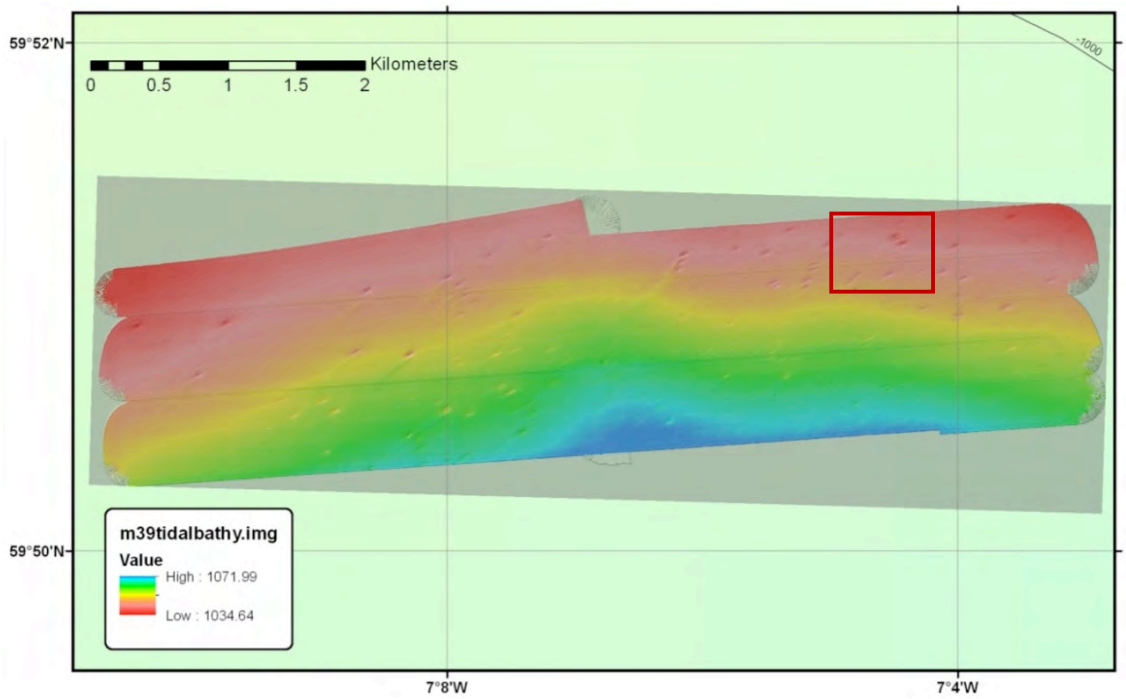

Figure CS1.4: Autosub6000 EM2000 bathymetry of the Eastern Darwin Mound area. For location see Fig. CS1.2. Red box indicates the approximate location of Fig. CS1.5.

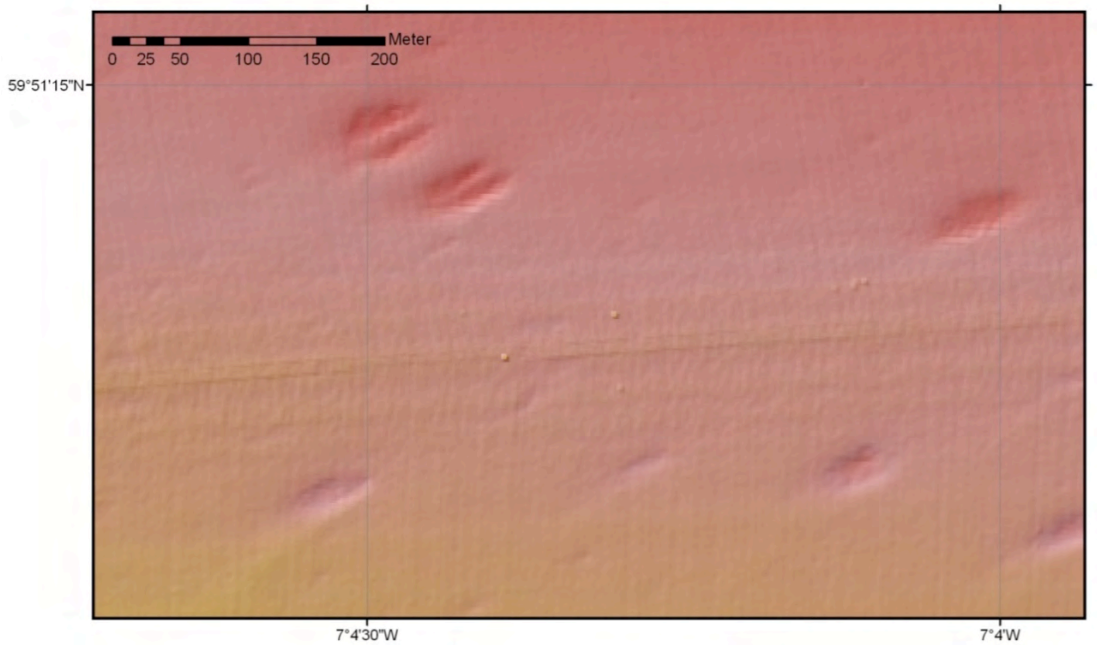

Figure CS1.5: Detail of the East Darwin Mounds Autosub6000 bathymetry; for location see Fig. CS1.4.

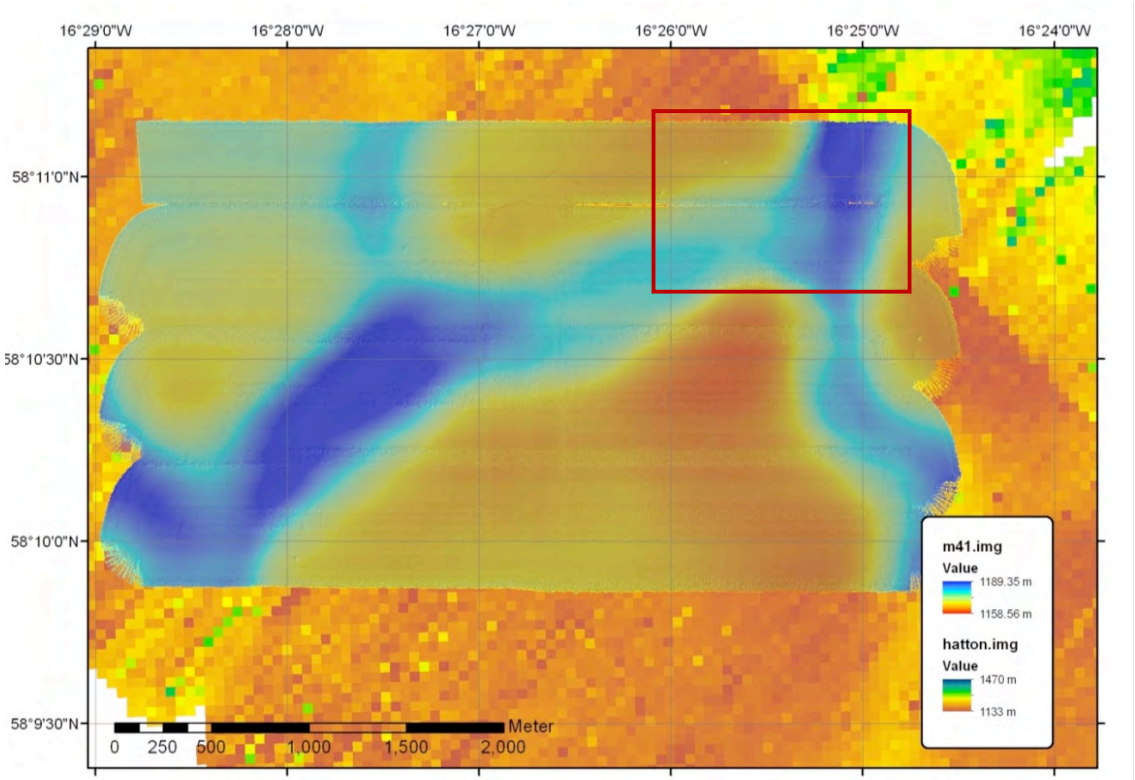

Figure CS1.6: Autosub6000 EM2000 bathymetry over a set of polygonal faults in the Hatton-Rockall Basin. For location see Fig. CS1.1. Background illustrates the resolution of shipboard bathymetry over the same area. Red box indicates the approximate location of Fig. CS1.7.

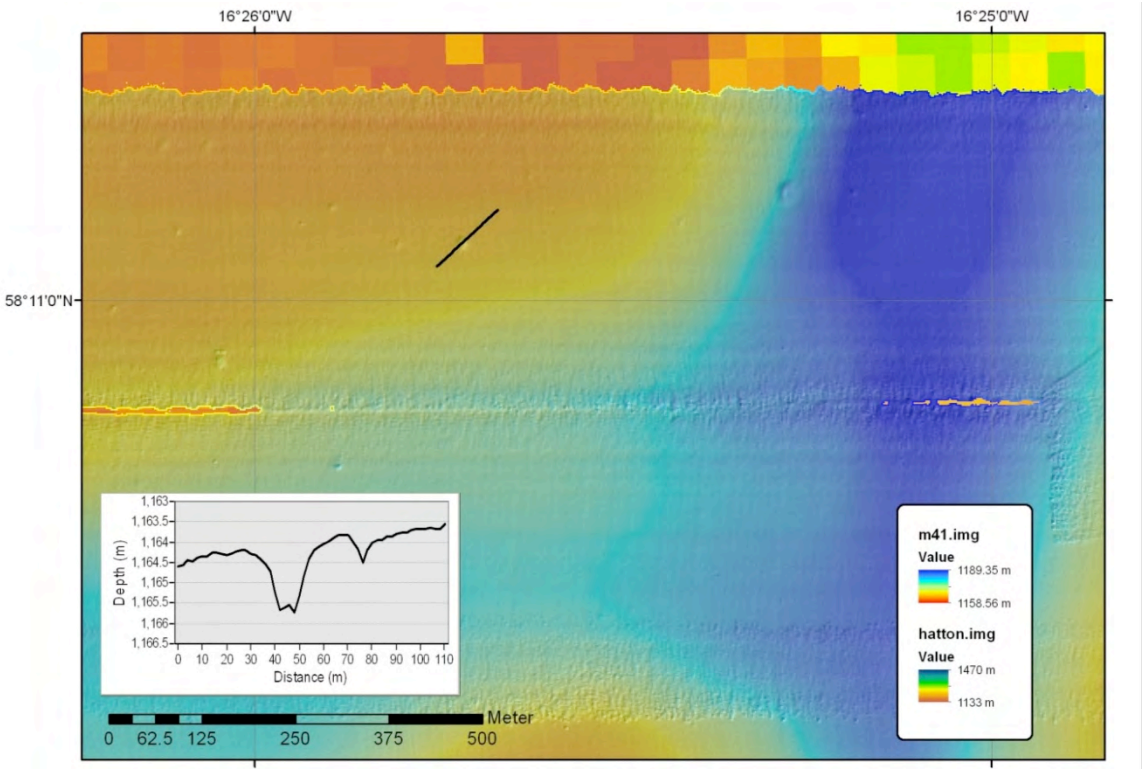

Figure CS1.7: Detail of Autosub6000 bathymetry data over the Hatton-Rockall Basin Polygonal Fault system. Profile across two pockmarks (black line and inset image) shows the resolution and resolving power of this system. For location see Fig. CS1.6.

CS1.4.2. Multibeam backscatter and sidescan sonar imagery

With regard to imaging seafloor characteristics and substrate type, Autosub offers several options. In addition to depth information, the EM2000 system also provides backscatter data, which gives an initial indication of seabed character. Figs. CS1.8-1.11 show examples of backscatter data from the Eastern Darwin Mounds and Hatton-Rockall Basin.

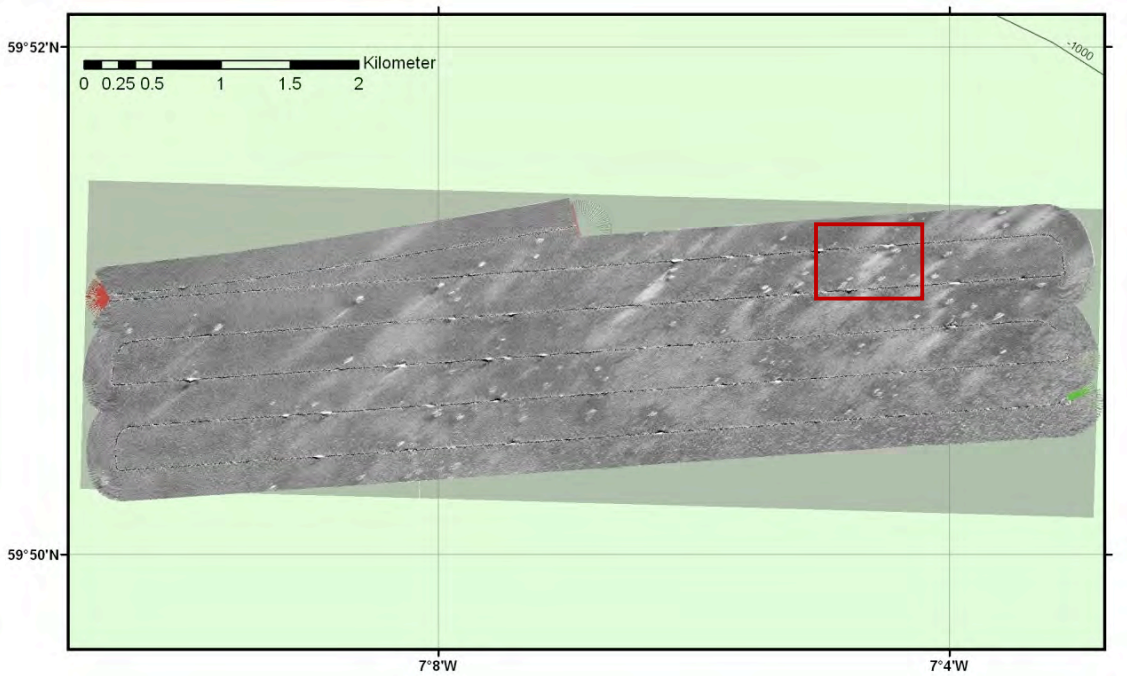

Figure CS1.8: Autosub6000 EM2000 backscatter map of the Eastern Darwin Mounds. For location see Fig. CS1.2. Darker tones = low backscatter; lighter tones = high backscatter. Note the presence of the mounds and erosional tails, which contain sediments with slightly coarser grain sizes. Towards the southeast of the area, more gravel is encountered on the seabed. Red box indicates the approximate position of Fig. CS1.9.

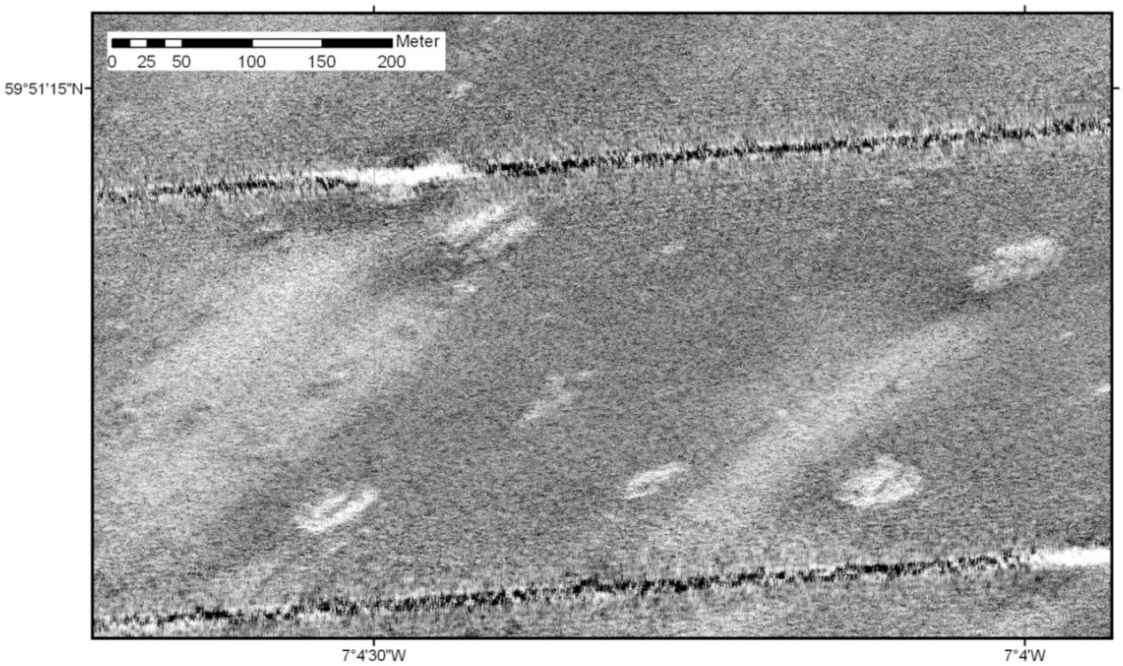

Figure CS1.9: Detail of Autosub6000 EM2000 backscatter data in the Eastern Darwin Mounds, showing erosional tails and small coral patches in addition to the main coral mounds. For location see Fig. CS1.8.

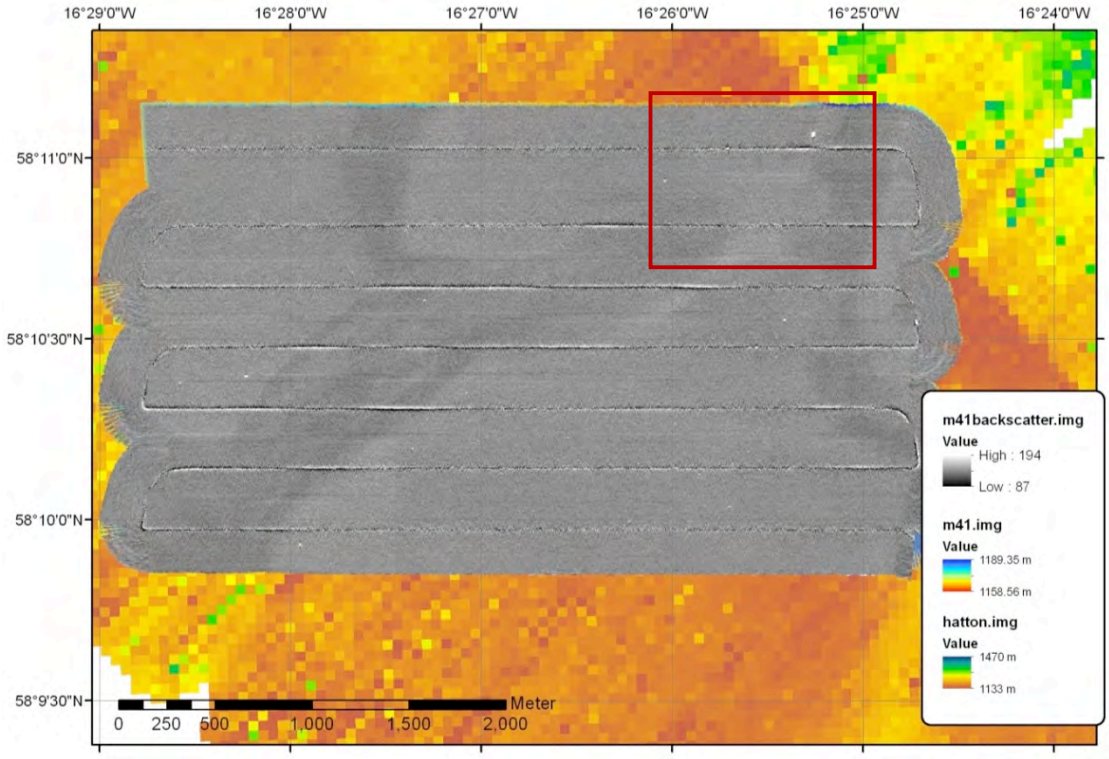

Figure CS.1.10: Autosu6000 EM2000 backscatter data from the Polygonal Fault Area in Hatton-Rockall Basin. As the entire area is draped with hemipelagic sediments, the backscatter variations are minimal. Red box indicates the approximate location of Fig. CS1.11.

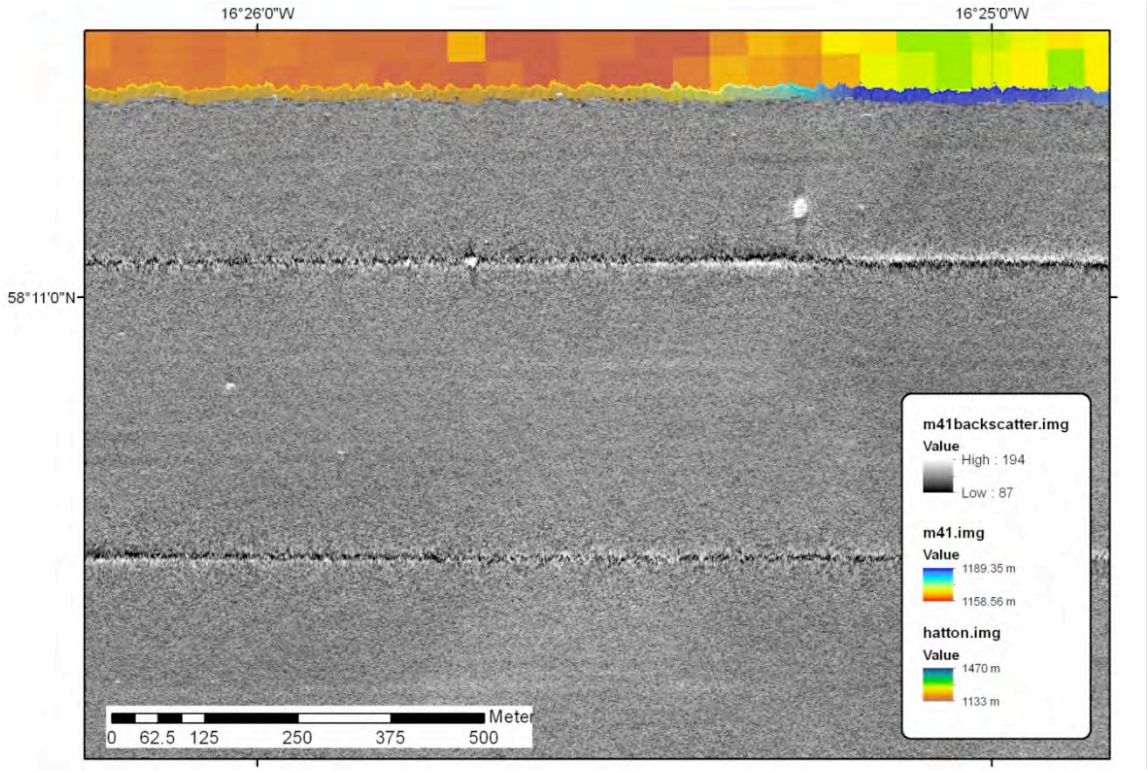

Figure CS1.11: Detail of the Autosub6000 EM2000 backscatter recorded in Hatton Basin. For location see Fig. CS1.10. The sediment type of the area is very homogeneous, as is reflected by the uniform backscatter data. Only the larger pockmarks provide a high backscatter signal in the backscatter map.

The overall distribution of sediments can be interpreted from these maps. Low backscatter, in darker tones, corresponds to finer grained or better-sorted sediments, while higher backscatter identifies coarser and/or more poorly sorted sediments, e.g. in the erosional tails behind the Darwin Mounds (Fig. CS1.8-1.9). Note that these mound tails cannot always be identified from the bathymetry alone (compare Figs CS1.5 and 1.9).

In addition to the multibeam system, Autosub6000 is equipped with a dual-frequency sidescan sonar. Unfortunately, due to acoustic interference, both systems cannot operate simultaneously, which means that the acquisition of sidescan sonar data requires an extra time investment. However, depending on the circumstances, the results can certainly justify this extra cost. During JC060, a block of 120kHz data was collected at the Eastern Darwin Mounds, flying the system at 100 m above the seabed (similar to the multibeam). The imagery could be processed to the same, or even a finer pixel size as the multibeam backscatter, and provides better maps due to the larger dynamic range and the better signal/noise ratio (Figs CS1.12-1.13). In addition, the range of the sidescan is twice that of the multibeam, so it only took half the time to cover the same ground and there are only half as many nadir artefacts in the final mosaic. The longer range also means a lower grazing angle of the outgoing acoustic pulse, especially towards the outer ranges, which helps to resolve small features that have a very limited vertical expression and similar backscatter intensity compared to the surrounding sediment.

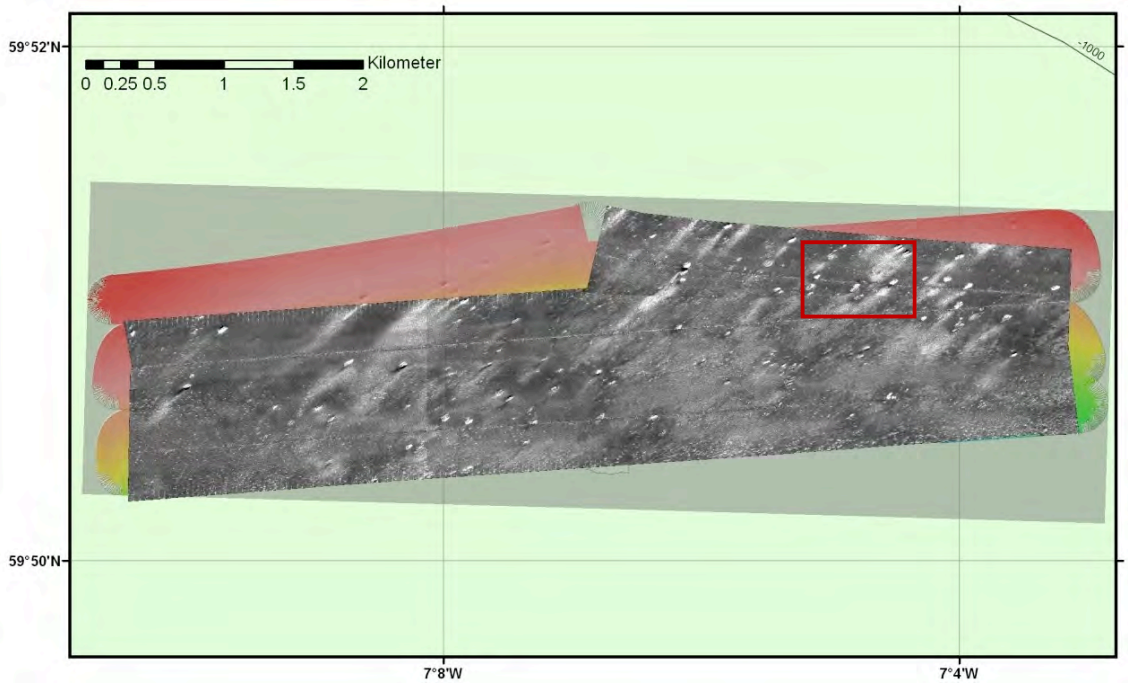

Figure CS1.12: Autosub6000 EdgeTech 120kHz sidescan sonar imagery collected over the Eastern Darwin Mounds. For location see Fig. CS1.2. High backscatter (mounds, coarser sediments) is indicated in lighter tones, low backscatter in darker tones. The red box indicates the approximate location of Fig. CS1.13.

However, in the framework of the cold-water coral research carried out during JC060, the biggest asset of the Autosub6000 was the high-frequency function (410kHz) of the EdgeTech sidescan sonar. The resulting images with pixel resolution of 20cm (or less) clearly show the locations of cold-water colonies, and even allow the interpreter to distinguish between live and dead coral (e.g. Figs CS1.14-1.18). The system was typically used at an altitude of 15 m above the seabed, which could have provided a range of about 150 m either side of the vehicle. In practice, data quality reduced beyond about 90-110 m, hence the ping rate was increased to obtain a better along-track resolution, reducing the

range to 125 m. As a conservative measure, track spacing was chosen at 150-180 m, i.e. about half the spacing of the multibeam tracks, resulting in about double the data acquisition time.

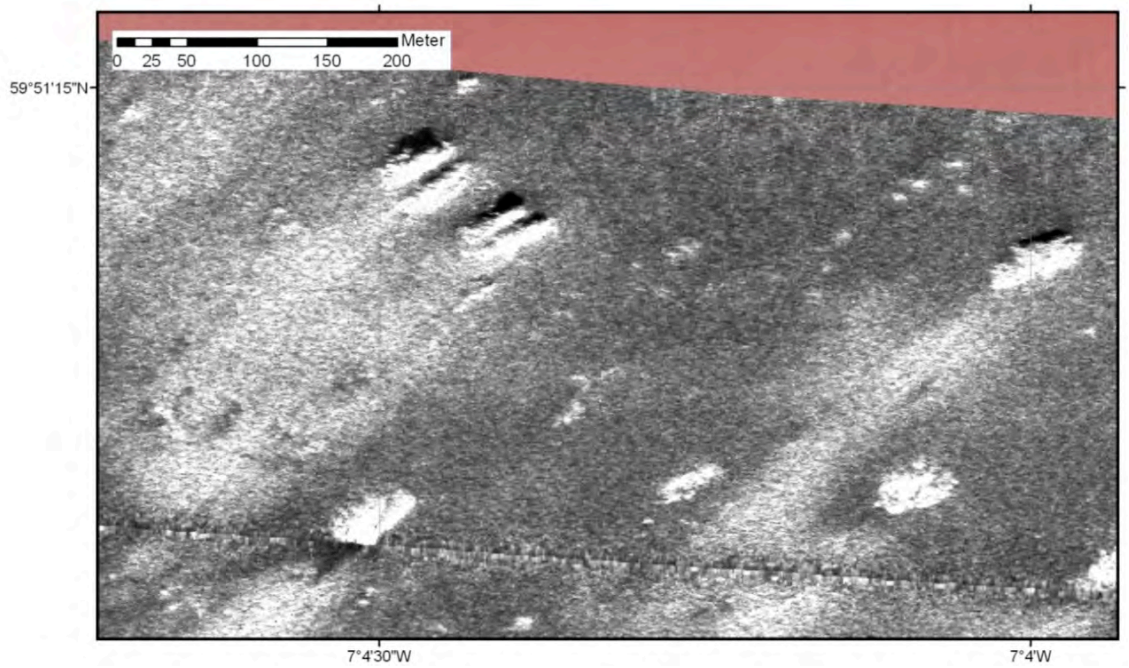

Figure CS1.13: Detail of Autosub6000 EdgeTech 120kHz sidescan sonar mosaic of the Eastern Darwin Mounds. For location see Fig. CS1.12.

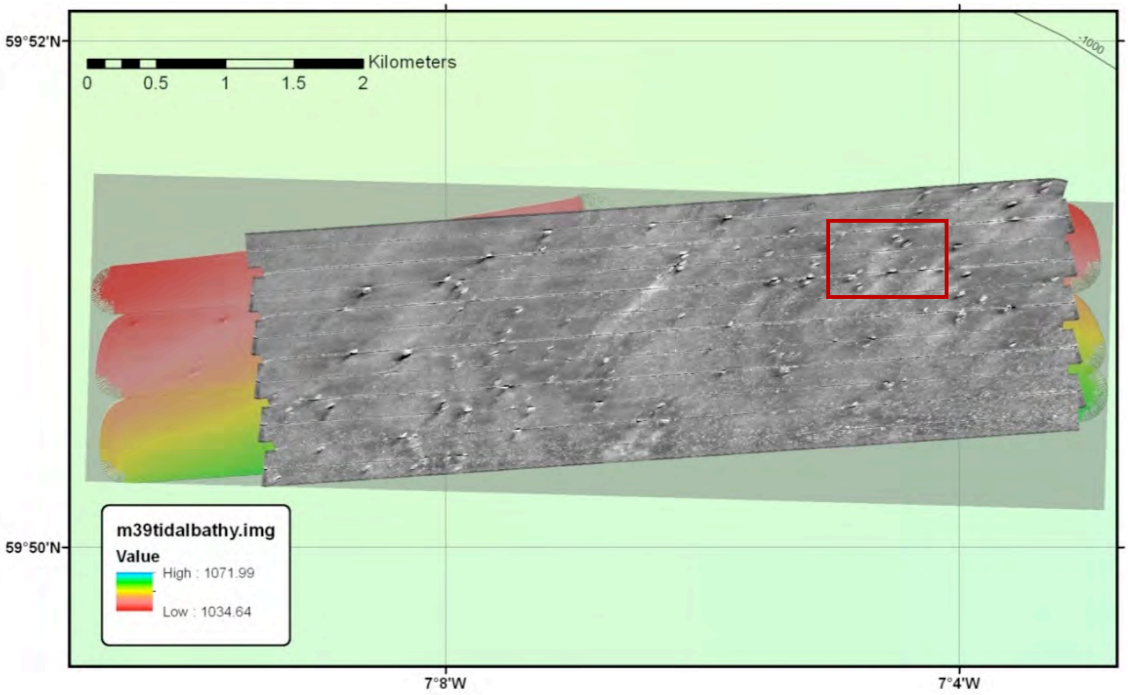

Figure CS1.14: Autosub6000 EdgeTech 410kHz sidescan sonar mosaic of the Eastern Darwin Mounds. For location see Fig. CS1.2. High backscatter (mounds, coarser sediments in the tails) indicated in light tones, low backscatter (shadows, finer sediments) in darker tones. Red box indicates the approximate position of Fig. CS1.15.

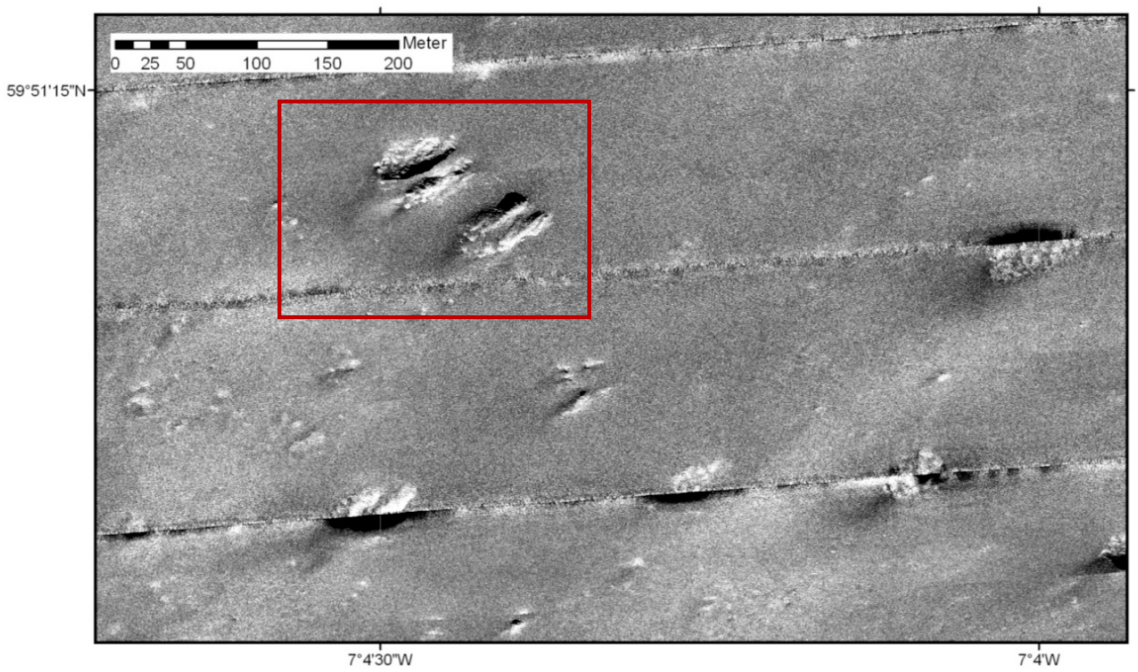

Figure CS1.15: Detail of the Autosub6000 high-resolution sidescan sonar data from the Eastern Darwin Mounds. For location see Fig. CS1.14. Data processed to 20 cm pixel size, showing the morphology of individual coral mounds. Note the increase in detail compared to the 120kHz sidescan sonar data (Fig. CS1.13) and multibeam backscatter (Fig. CS1.9). Red box indicates approximate position of Fig. CS1.16.

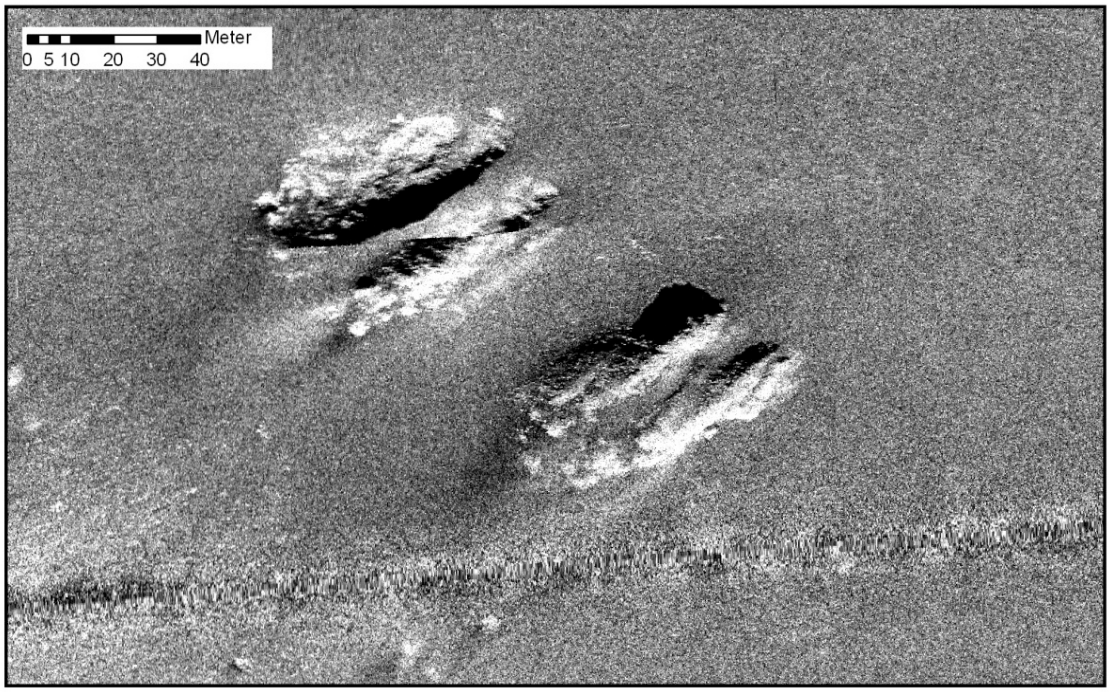

Figure CS1.16: Further zoom onto the Autosub6000 high-resolution sidescan sonar imagery of the Eastern Darwin Mounds. For location see Fig. CS1.15. The mounds shown here are mainly covered with dead coral.

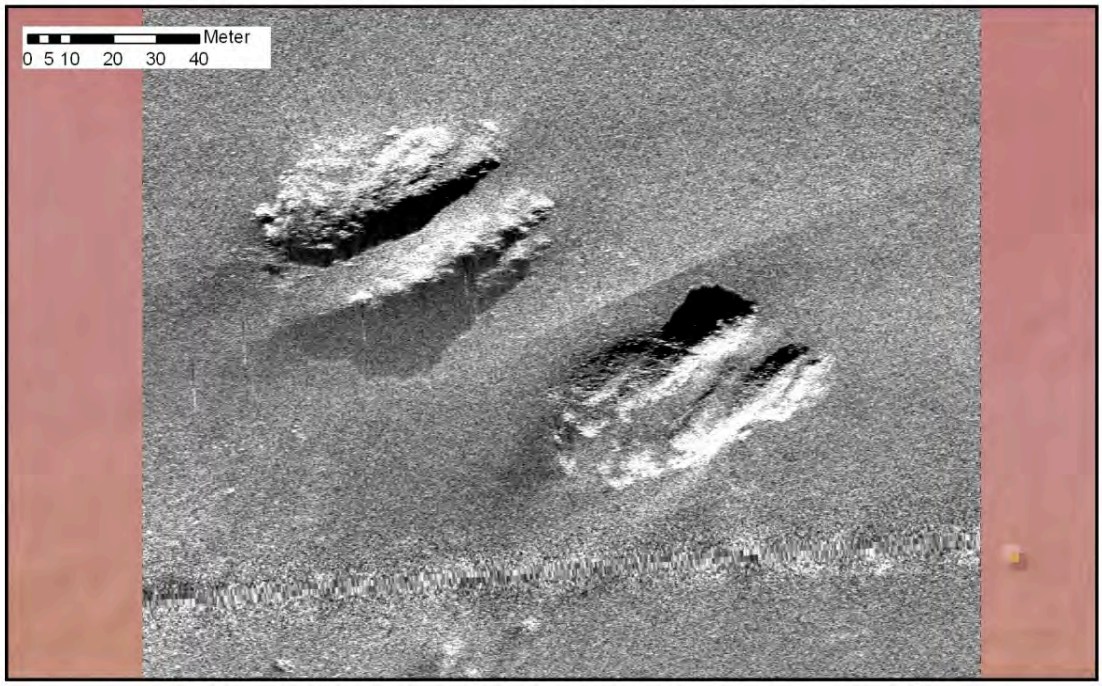

Figure CS1.17: Same data as previous figure (Fig. CS1.16), however this time processed at 5 cm resolution to illustrate the power of the sidescan sonar data. Working at such fine resolution is currently only useful for specific features and details, as it results in very large file sizes that become unpractical (long loading times in GIS etc).

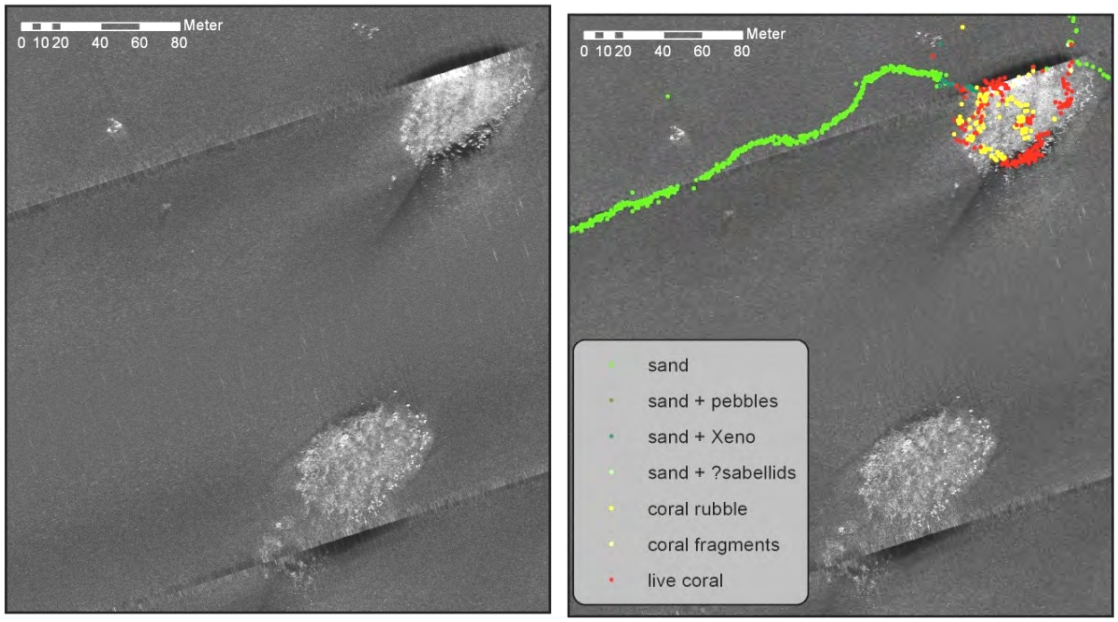

Figure CS1.18: Autosub6000 high-resolution EdgeTech sidescan sonar example from the Western Darwin Mounds, including initial seabed interpretation from ROV video (right-hand panel). It appears that the live coral colonies are mainly located on the outer edges of the mound, where they can be recognised based on their specific acoustic character (more contrast between high backscatter of the clean, upright coral branches and shadows they create).

Ultimately, the choice of backscatter type to be used in any habitat mapping or monitoring project will depend on the type of terrain and the information that needs to be extracted. For cold-water coral research, the high frequency, fine resolution sidescan sonar data clearly is essential, and the additional time-investment to collect it is certainly justified. In other cases,

where the acoustic signature of the habitats under study is less pronounced at this fine pixel scale, the use of multibeam backscatter may be sufficient, and extra time could be used to map a larger area instead. At the Hatton-Rockall Basin site, for example, the high-resolution sidescan sonar mosaic provides a little more detail than the backscatter map (stronger contrast between polygon and trough sediments, illustration of all pockmarks and dropstones, compare Figs CS1.19-1.20 with Figs CS1.10-1.11), but most of this information could already be derived from the multibeam bathymetry and backscatter maps.

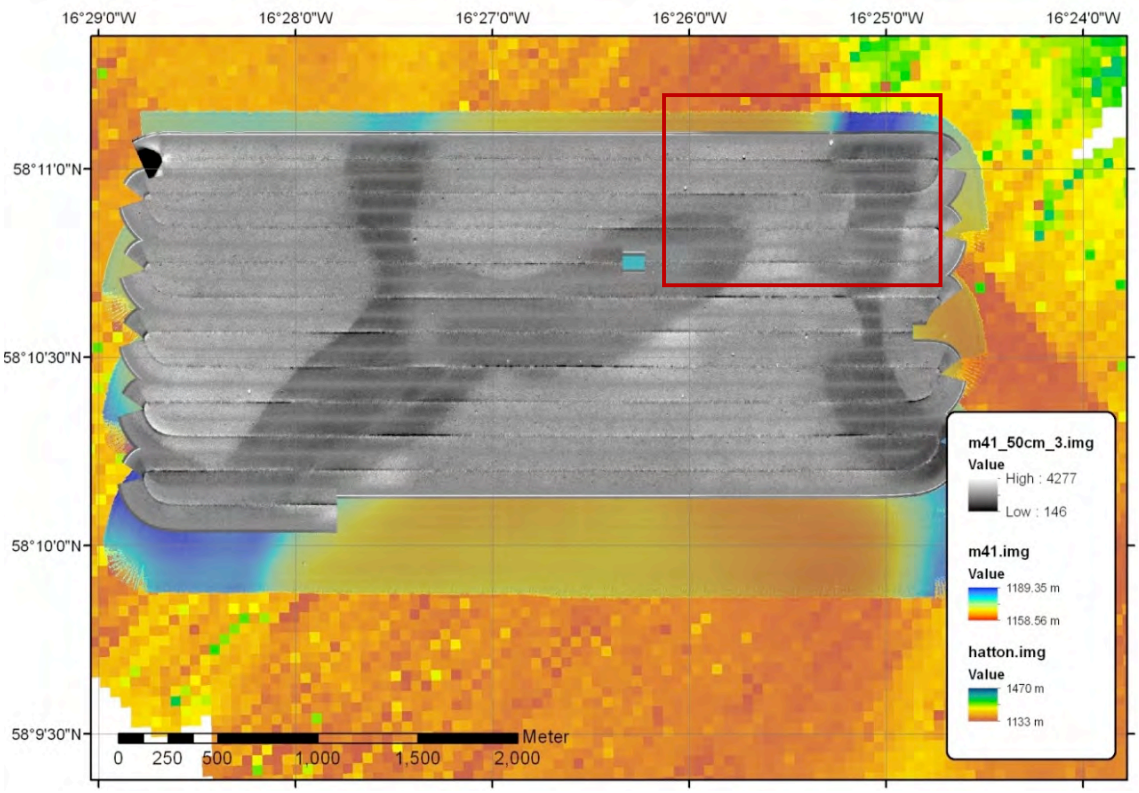

Figure CS1.19: Autosub6000 EdgeTech 410kHz sidescan sonar mosaic of the Polygonal Fault Area in Hatton-Rockall Basin. For location see Fig. CS1.1. Note the better signal/noise ratio of the data compared to the multibeam backscatter data in Fig. CS1.10, which allows better identification of the sediment characteristics of polygons vs. troughs due to better contrast. Red box indicates approximate location of Fig. CS1.20.

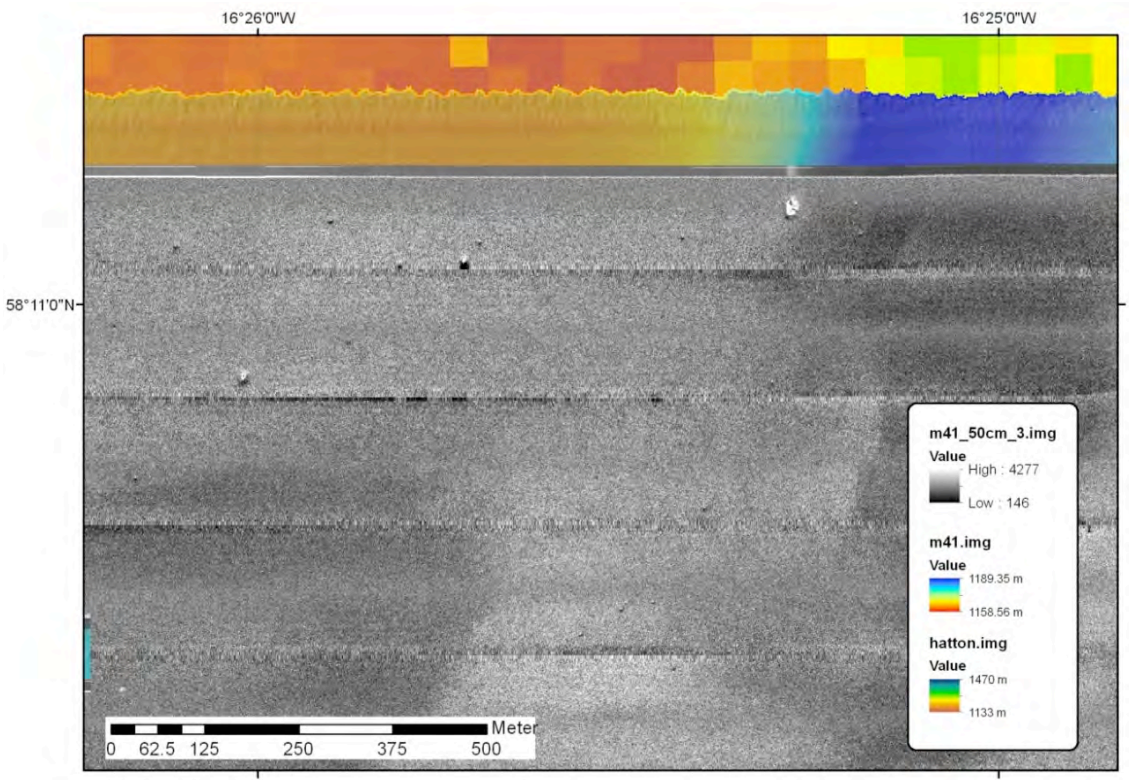

Figure CS1.20: Detail of the Autosub6000 high-resolution sidescan sonar mosaic over the Polygonal Fault Area in Hatton-Rockall Basin. For location see Fig. CS1.19. The data resolution allows identification of the smallest pockmarks and dropstones in the area, some of which were not visible on the backscatter (Fig. CS1.11), but were identifiable from the bathymetry (Fig. CS1.7).

CS1.4.3. Chirp sub-bottom profiler

JC060 was the first cruise during which the EdgeTech chirp system was used on Autosub6000, and some initial problems with the installation and parameter settings had to be overcome (see cruise report for more details). However, the hardware problems were solved halfway through the trip, and post-processing efforts have resulted in some promising initial results in terms of seismic profiles (Figs CS1.21-1.22). The Darwin Mounds can be identified, and the system resolved a number of subbottom reflectors and high reflection targets in the sections outside the mounds. Further work to improve the seismic processing will take place in the coming year as part of the PhD thesis of Melis Cevatoglu under the supervision of Prof. J. Bull (OES - University of Southampton).

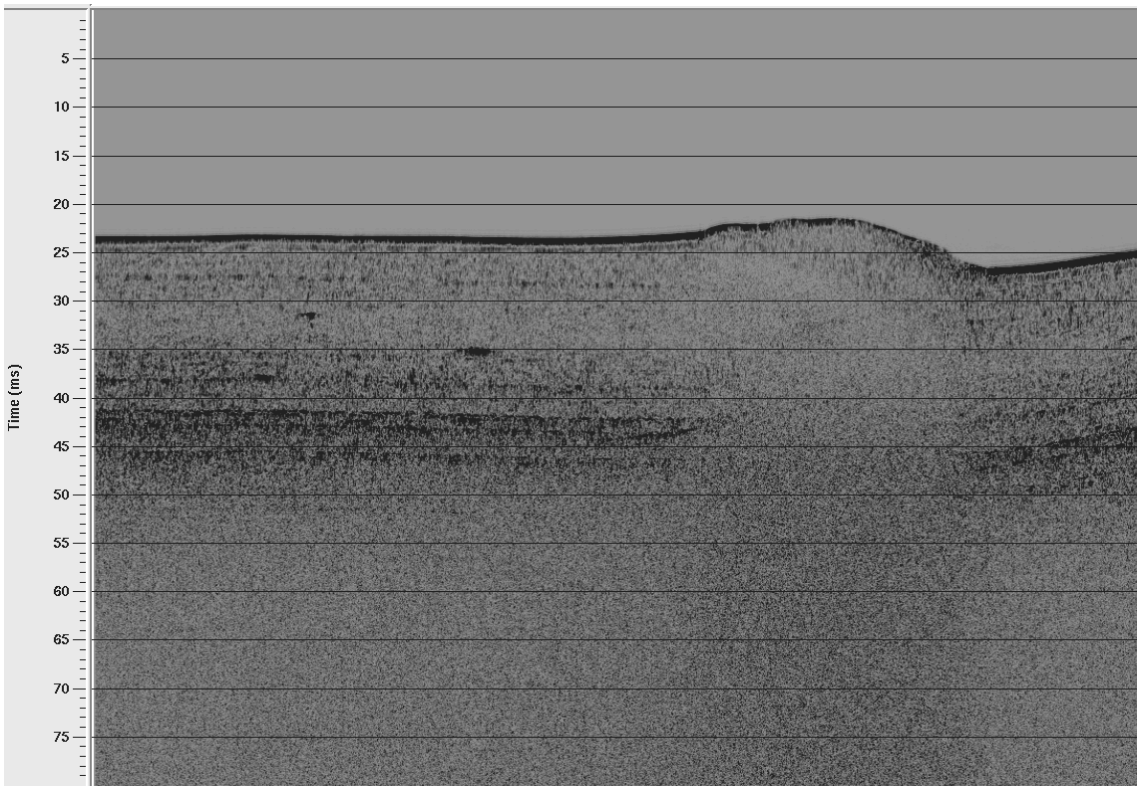

Figure CS1.21: Autosub6000 EdgeTech chirp subbottom profile across one of the Eastern Darwin Mounds.

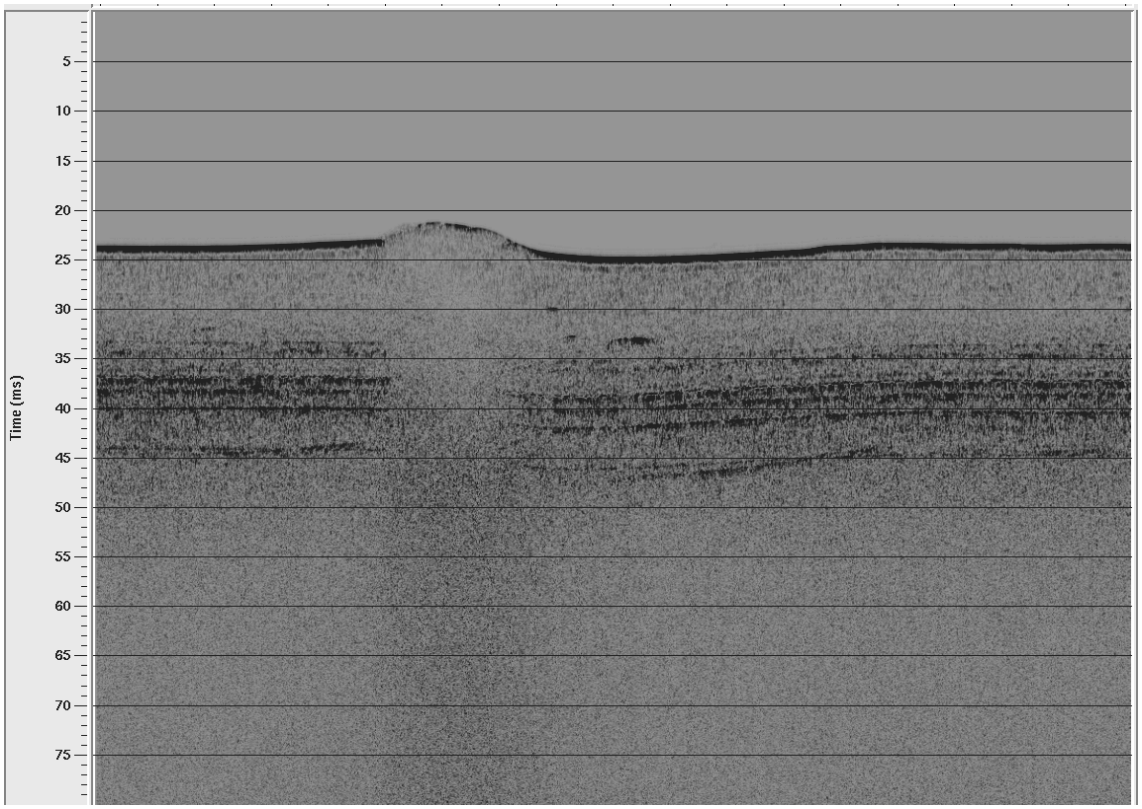

Figure CS1.22: Further example of the Autosub6000 chirp profiler first results across the Eastern Darwin Mounds.

CS1.4.4. Autosub6000 monochrome photographs

In order to further increase the time-efficiency of the Autosub surveys, the Prosilica monochrome camera and lens system were set for an optimal altitude of 15m, which meant that digital stills could be taken simultaneously with the high-resolution sidescan sonar surveys. This results in perfectly co-located acoustic and visual data, a real asset to habitat mapping (Fig. CS1.23). When working in deep water, navigational accuracy (both absolute and relative) of repeated surveys or different instruments is always a challenge, especially when looking at metre-scale processes. Having data collected simultaneously from the same vehicle avoids this problem. The only drawbacks of the camera system during JC060 were (1) the charging time of the flash, resulting in a frame rate of 1/20s or one picture per ca. 30 m of AUV track; (2) that the camera was pointing directly onto the trackline of the vehicle, which meant that pictures correspond to areas with nadir artefacts on the sidescan sonar imagery; (3) that in areas with a high amount of particulate material in the water column, image quality was severely impaired (Fig. CS1.24). However, in areas where visibility was good, the Autosub images provided a unique ground-truthing dataset, allowing the extrapolation of insights into seabed habitat distribution (obtained from localised ROV video surveys) over the entire area of the high-resolution sidescan sonar mosaic. Although not all megafauna can be identified from the Autosub pictures, the larger species are identifiable (e.g. holothurians, squat lobsters) and the images provide sufficient detail to classify seabed substrate (soft sediment, cobbles, boulders, hardrock, coral framework, etc). Issues with image frame rate will be partly resolved in the near future (summer 2012), when Autosub will be equipped with new cameras and flash guns that allow much faster charging. The turbidity problem can be avoided when the Autosub is navigated closer to the seabed, although this would require an extra mission (too low for the sidescan) and needs the terrain to be sufficiently smooth and safe for such operations.

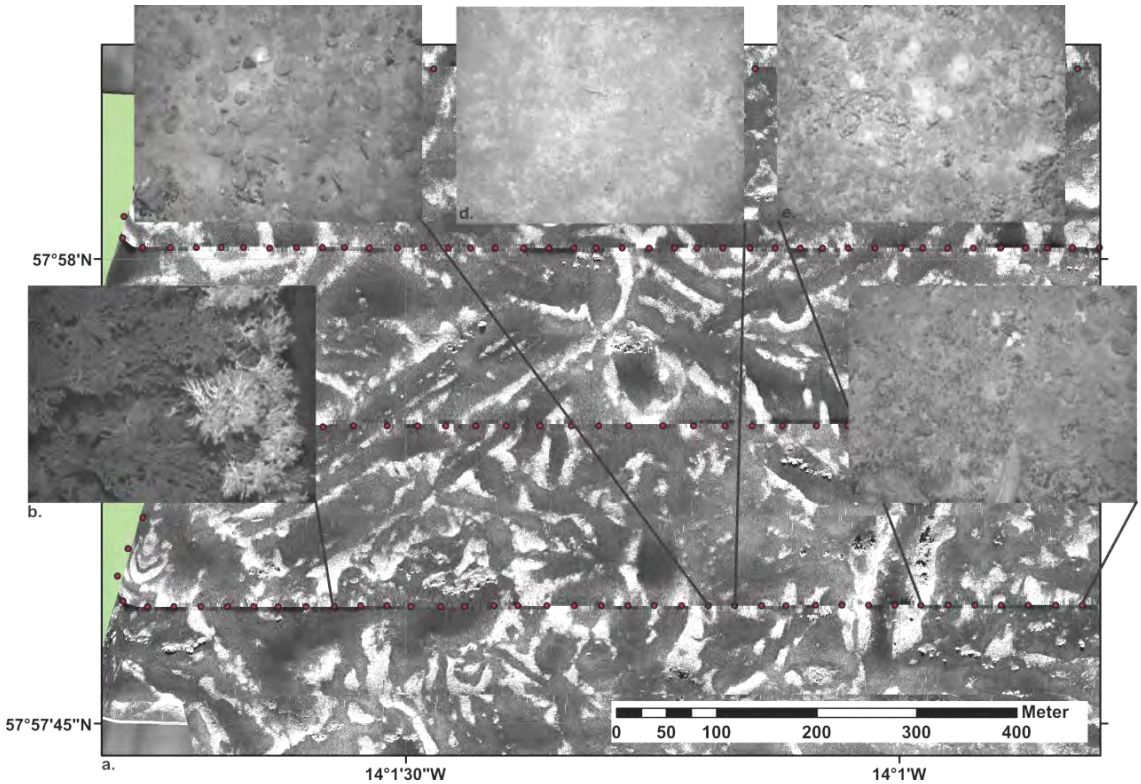

Figure CS1.23: Examples of Autosub6000 monochrome photographs and simultaneously collected high-resolution sidescan sonar data from the central study area on NW Rockall Bank. For survey location see Fig. CS1.3. (a) 410kHz sidescan sonar mosaic illustrating the type of terrain, heavily scarred by iceberg ploughmarks. High backscatter from boulders, rock and coral colonies is shown in light colours, low backscatter from fine-grained sediment in dark colours. Red dots indicate the locations of Autosub6000 photographs, unfortunately

coincident with the sidescan nadir line; (b) Lophelia pertusa cold-water coral colony, with live coral on the right-hand side; (c) coarse seabed consisting of cobbles and boulders pushed aside by the iceberg keels; (d) fine-grained seabed with squat lobster; (e) dead coral framework on gravel ridge; (f) cobble & gravel field with fish.

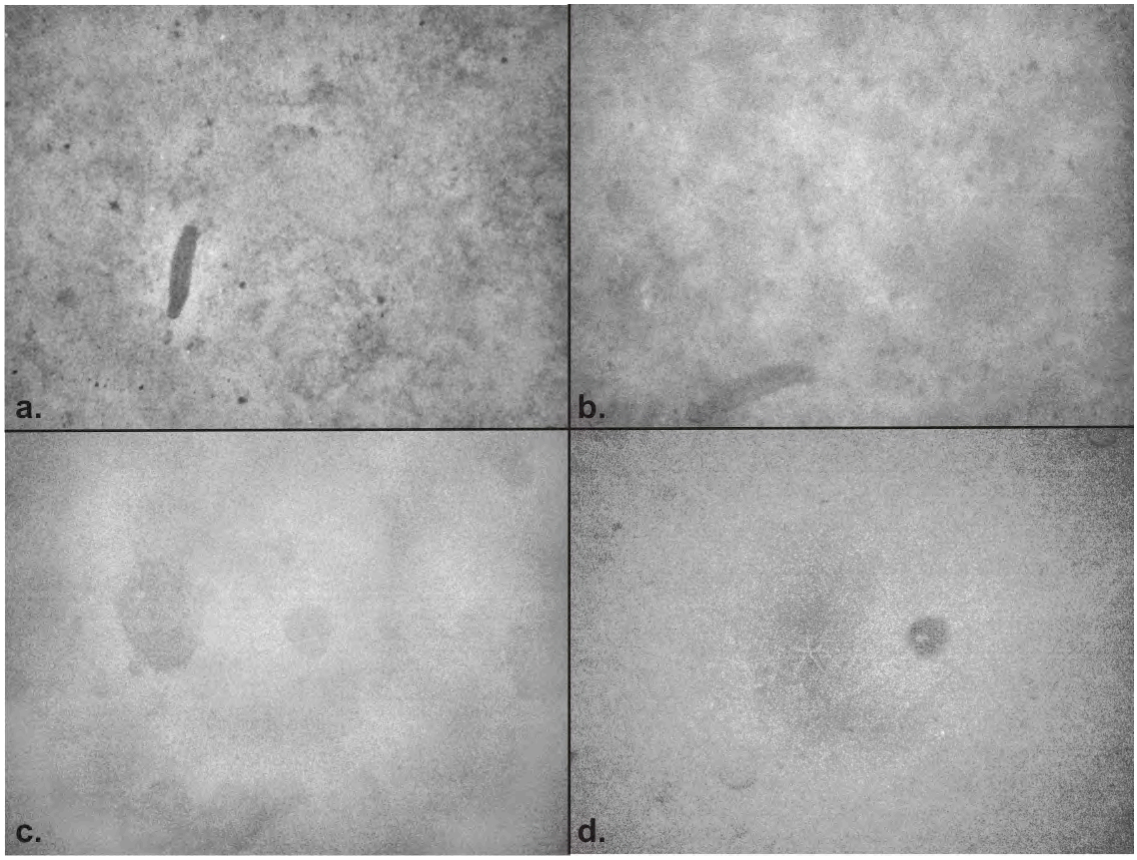

Figure CS1.24: Examples of the effect of water column turbidity on Autosub6000 monochrome photographs. (a) Holothurian from NW Rockall Bank, photographed in clear water conditions (Mission 43); (b) Holothurian in similar setting, photographed in waters with higher particle content (Mission 44); (c) example of coarse seabed (boulders) on NW Rockall Bank, photographed in turbid conditions (Mission 44). Compare with Fig. CS1.23c; (d) Xenophyophore and seastar photographed in the turbid waters of the Eastern Darwin Mounds.

CS1.5. Implications

CS1.5.1. Automated image analysis and repeated monitoring

Due to the stability of the AUV and the resulting high-quality acoustic data, the JC060 multibeam and sidescan sonar maps are ideally suited as input for automated image classification approaches to habitat mapping. Initial tests on the high-resolution sidescan sonar mosaics from NW Rockall Bank have provided promising results (Fig. CS1.25), and further analyses with this respect will be carried out within the ERC Project CODEMAP.

In order to test the repeatability of the automated classification techniques (with the aim of facilitating future monitoring surveys in the most efficient way), repeated survey lines with varying configurations (heading) were run over two small areas on NW Rockall bank, using both multibeam and high resolution sidescan sonar (Fig. CS1.26). Once the optimal automated habitat classification method is developed, the variation in habitat assignment between the different datasets will be quantified as a measure of the error on the method.

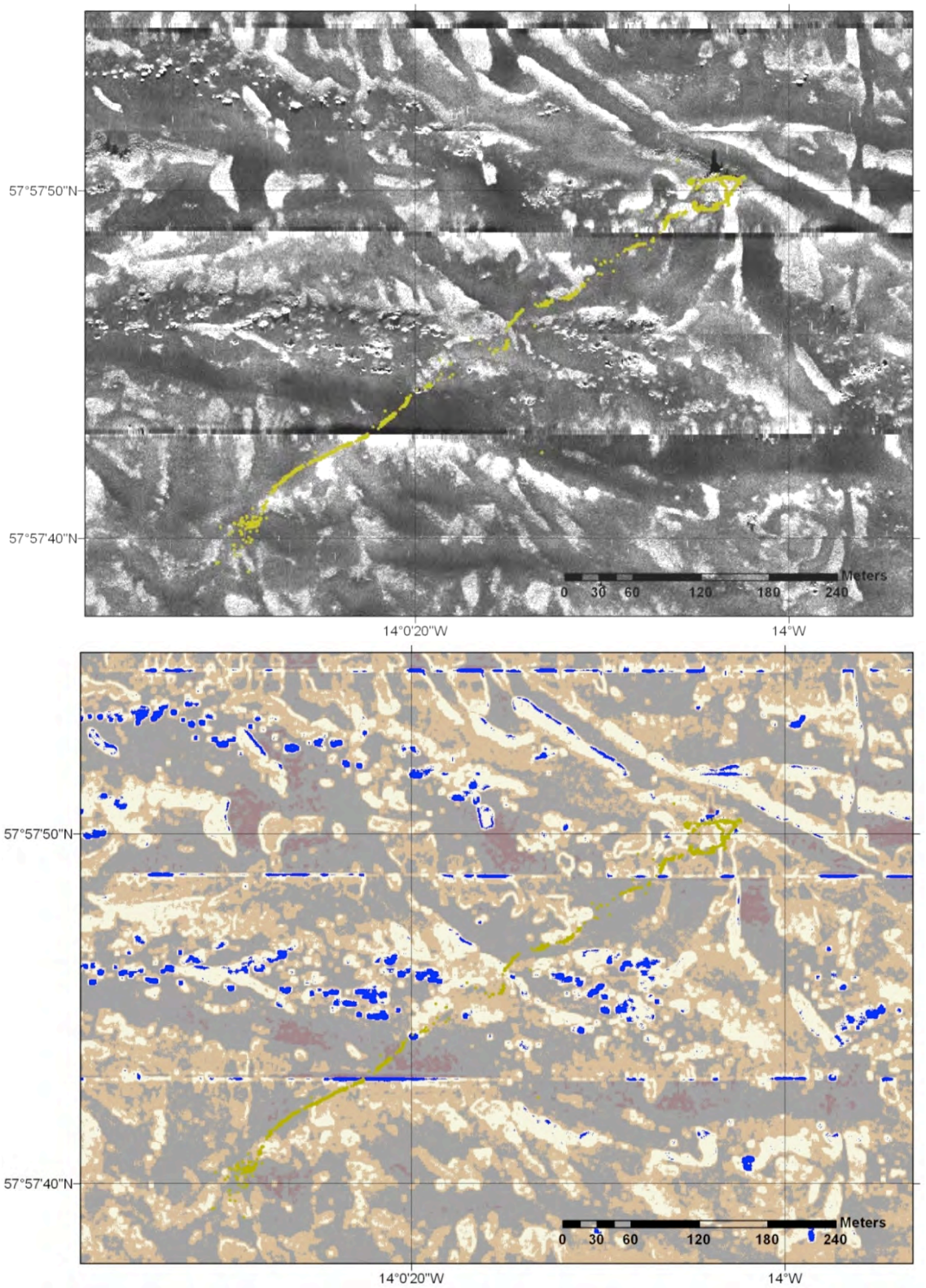

Figure CS1.25: Initial results from automated image classification of the high-resolution sidescan sonar mosaic from the central survey area on NW Rockall Bank (Mission 43), based on unsupervised classification of image texture parameters calculated on 9x9 pixel moving windows. For survey location see Fig. CS1.3. Blue = coral colonies; beige = cobbles and gravels; tan = gravelly sand; grey and maroon = sand & fine sediments; yellow = ROV ground-truthing track.

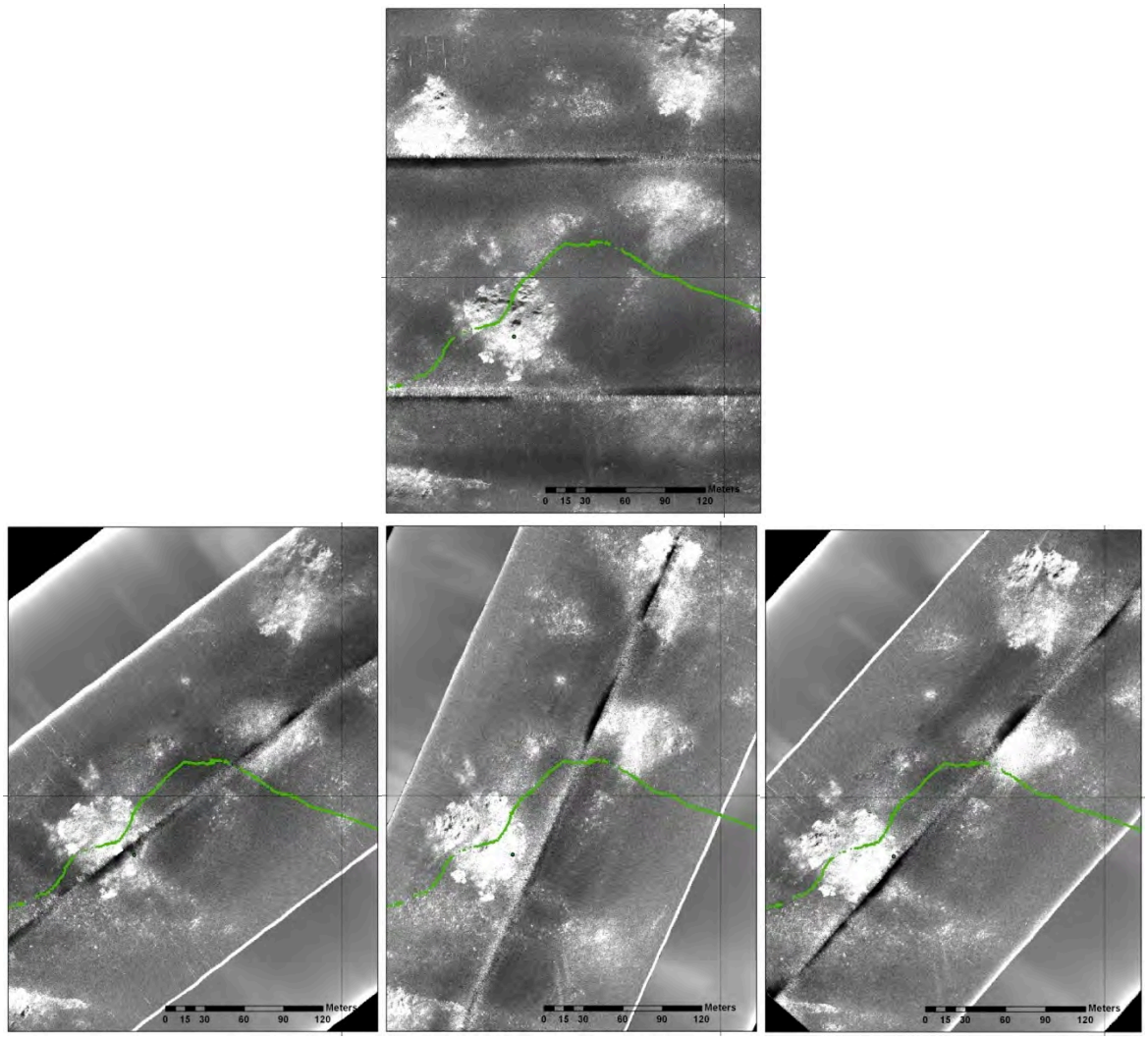

Figure CS1.26: Repeatability tests: original high-resolution sidescan sonar mosaic from NW Rockall Bank (top, from Mission 44), re-visited three times under slightly different headings (lower panels, from Mission 46) to provide input data as test for the robustness of automated habitat classification methods.

CS1.5.2. Back to the Darwin Mounds

Thanks to the large number of clearly identifiable features on sidescan sonar maps of the Darwin Mounds, historical 410kHz sidescan sonar data collected in 2000 using a towed vehicle (Wheeler et al., 2005), could be georectified to the position of the new data. This allows a first approach to monitoring of the area, and to an assessment of the impact of the fisheries closure on the level of deep-sea trawling in this cSAC (Figs CS1.27-1.28). Trawling intensity has clearly reduced, especially in the Eastern Darwin Mounds. None of the historical trawl marks can be recognised in the new data, which illustrates that (the off-mound part of) the seabed in this area is completely reworked on at least a 10-year timescale. The mounds themselves, however, do not appear to have changed much over the last decade (Fig. CS1.29). The results of this study, together with species assemblage evaluations from towed/ROV video data, will be passed on to JNCC for further management of the Darwin Mounds, and will be prepared for publication in the scientific literature.

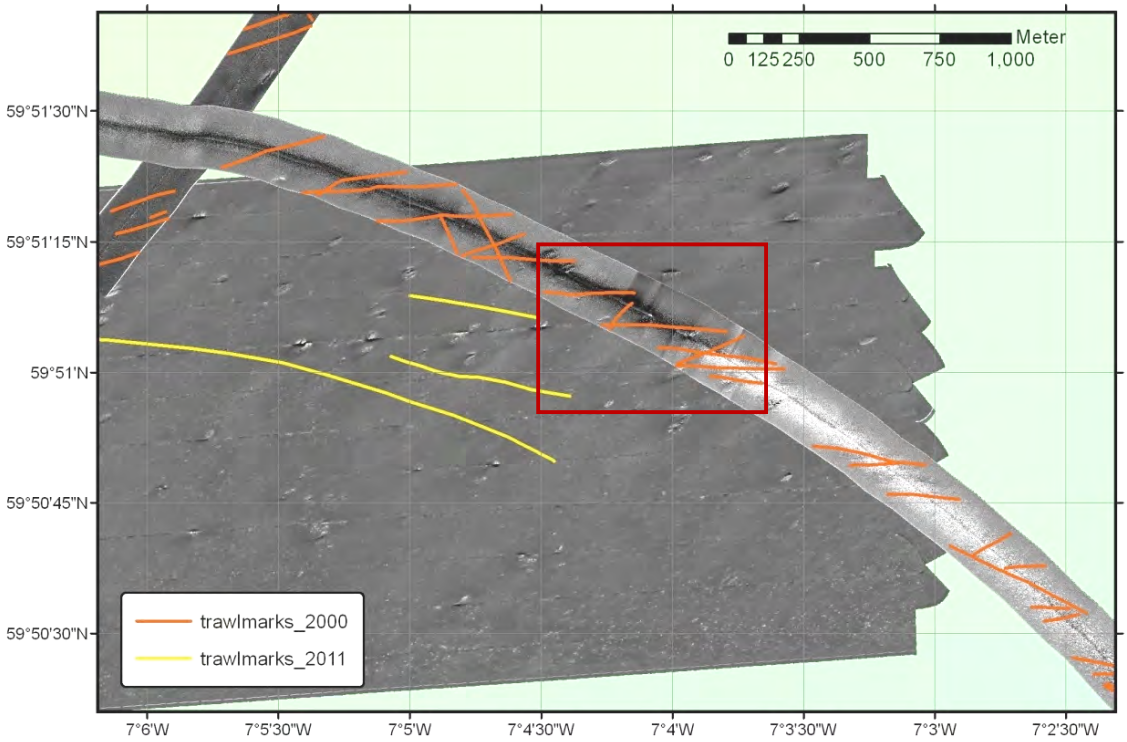

Figure CS1.27: Spatial distribution of potential trawl door marks identified on 410kHz sidescan sonar data from a towed Geo-Acoustics system in 2000 (orange) and from the JC060 AUV-based mosaic (yellow) in the Eastern Darwin Mounds. For survey location see Fig. CS1.2. Trawling intensity has clearly decreased since the fisheries closure was put in place in 2003. Red box shows location of Fig. CS1.28.

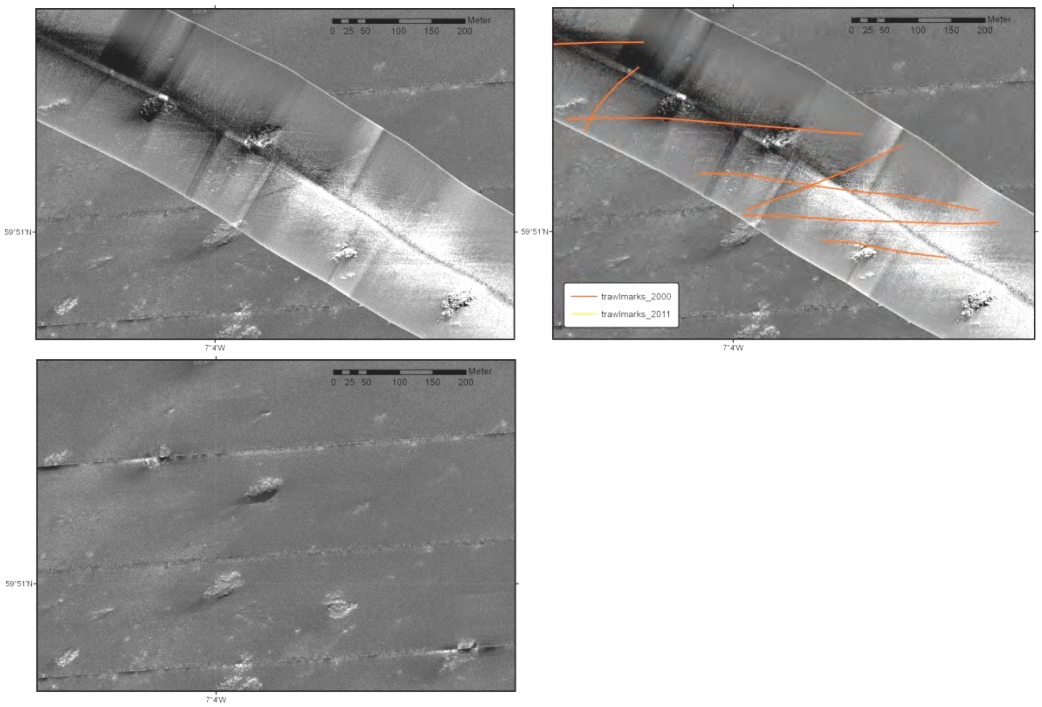

Figure CS1.28: Detail of the high-resolution sidescan sonar data from 2000 (top) and JC060 (below), illustrating the large number of trawl marks in 2000, and how these have disappeared over the past 10 years. For location see Fig. CS1.27.

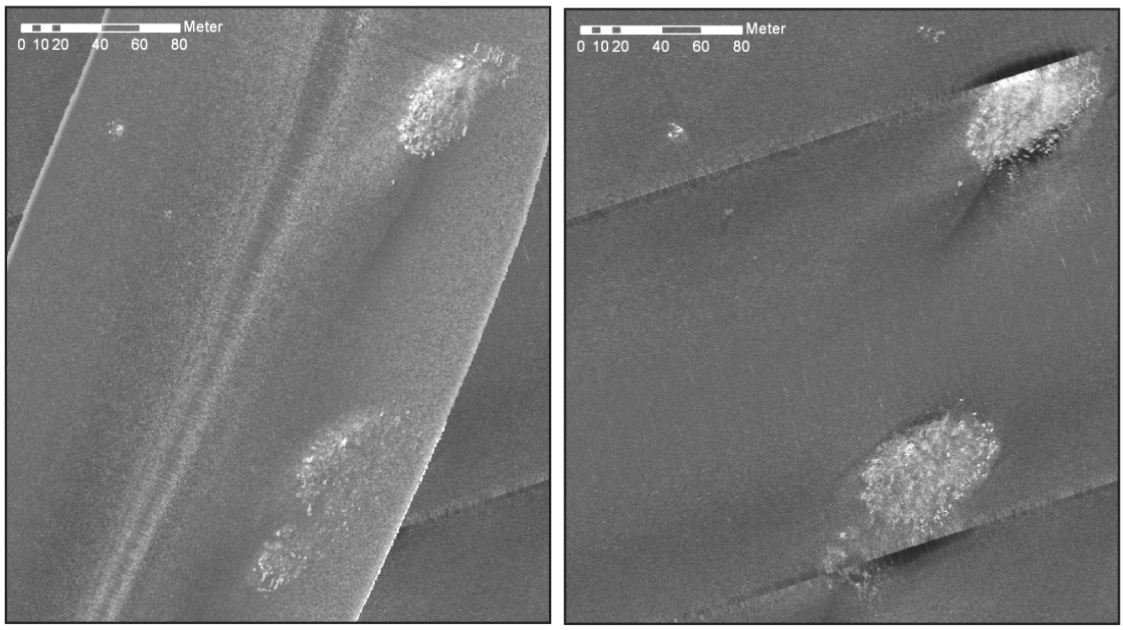

Figure CS1.29: Towed Geo-Acoustics 410kHz sidescan sonar data from 2000 (left), and Autosub6000 EdgeTech 410kHz sidescan sonar data from JC060 (right), Western Darwin Mounds. Note the small coral colonies in the top left part of the maps, or the tiny speck just SW of the mound in the top right: the mounds themselves have apparently not changed very much over the last decade.

CS1.5.3. Delineation of fisheries closure and SAC on NW Rockall Bank

The mapping results obtained on NW Rockall bank, in addition to the ROV video footage, provided clear evidence that live cold-water coral colonies are present within the boundaries of the current fisheries closure (Fig. CS1.25). Also, outside of that area, along the SE boundary, rich coral communities were encountered, hosting large schools of fish (Fig. CS1.30). However, the situation in the study area along the NW boundary appeared less positive: ample evidence of intense bottom trawling was found on sidescan sonar maps (Fig. CS1.31) and video data, together with large areas containing sediment-clogged cold-water coral rubble (Fig. CS1.32). No sizeable colonies of live coral seem to be left in that area.

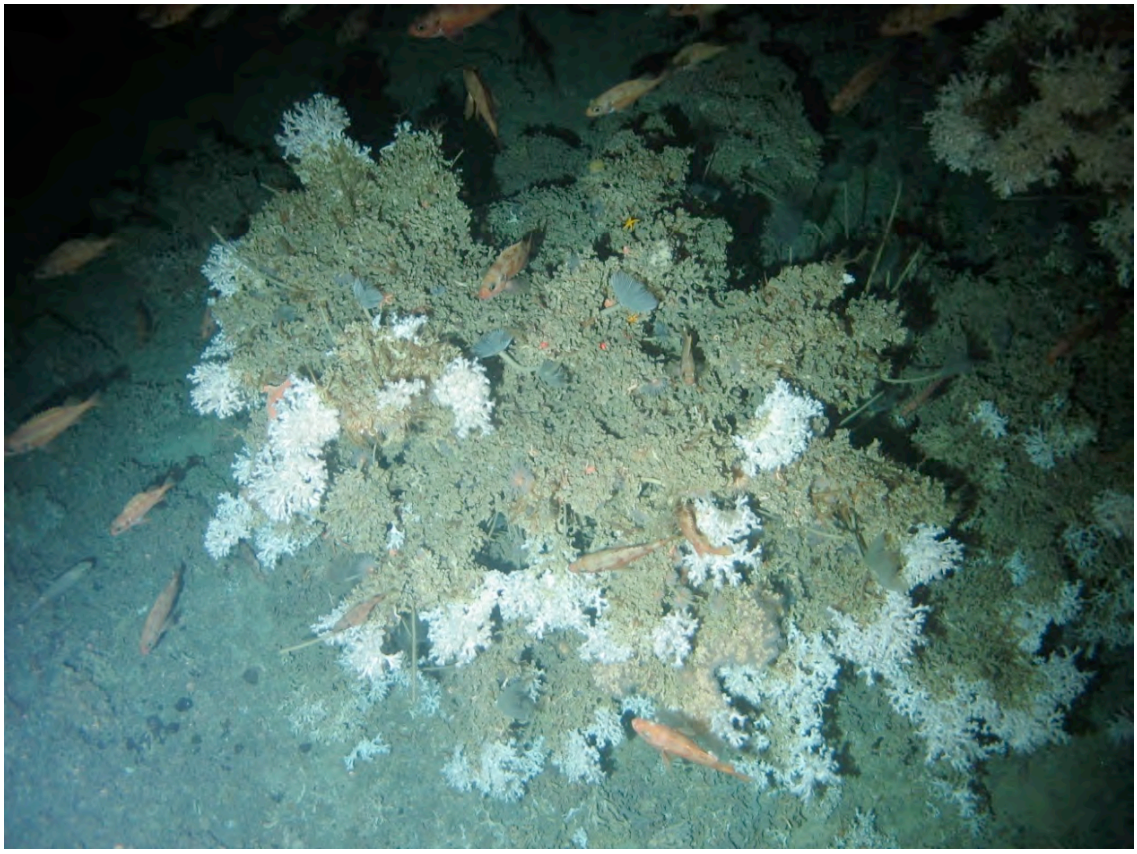

Figure CS1.30: ROV stills image from the NW Rockall Bank, SE boundary of the current fisheries closure. For survey location see Fig. CS1.3. Large cold-water coral colonies are used as habitat for a variety of fish and other associated fauna. Laser dots are 10 cm apart.

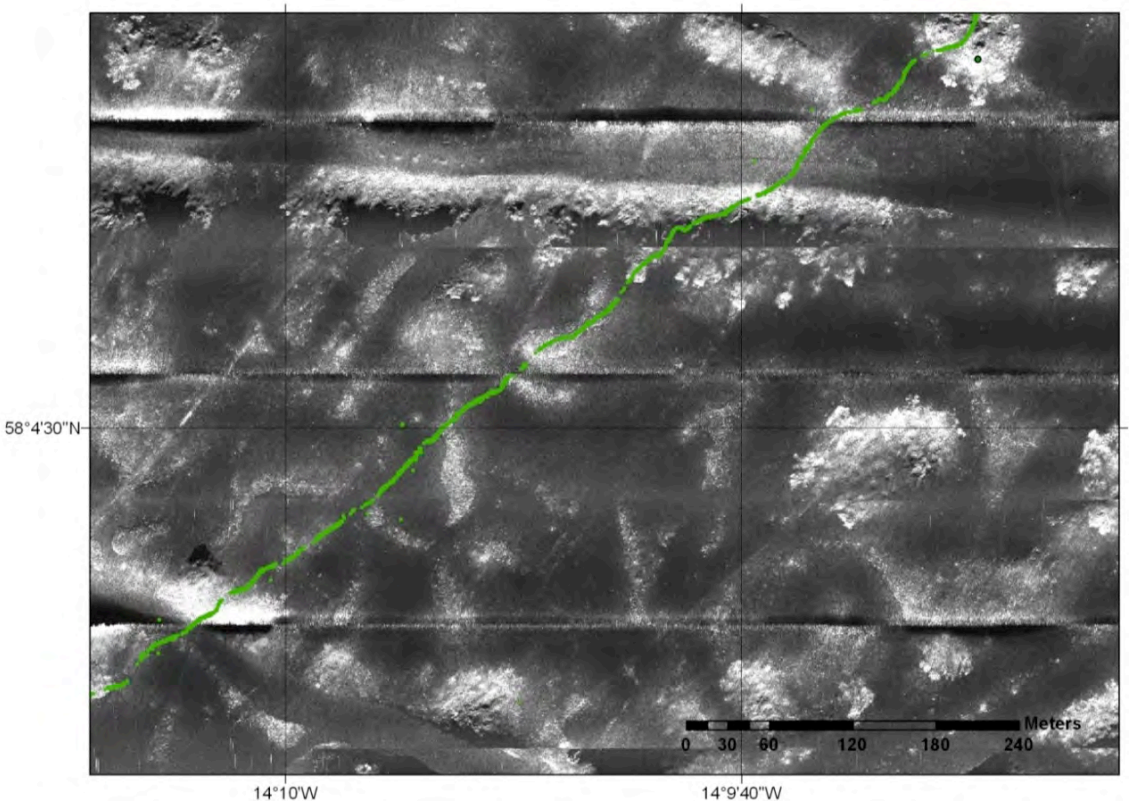

Figure CS1.31: Detail of Autosub6000 high-resolution sidescan sonar mosaic on NW Rockall Bank, NW boundary of the current fisheries closure. For survey location see Fig. CS1.3. Note the extensive scarring of the seabed by trawlmarks. High-backscatter patches related to iceberg ploughmark ridges still provide a signature of cold-water coral presence, but its reduced crispness (compared with Fig. CS1.25) suggests that there is no live coral. This was confirmed with the ROV video and stills imagery (e.g. Fig. CS1.32). ROV track is indicated in green

Figure CS1.32: Trawling impact along the boundary of the NW Rockall Bank fisheries closure (NW edge): marks of a trawl net, broken coral pieces.

Based on the results summarised above, the JNCC decided to indeed extend the boundary of the cSAC, as suggested before. In addition, they presented the results at the ICES Working Group on Deep Water Ecology meeting in spring 2012, with the suggestion to adapt the boundary of the fisheries closure as well. This suggestion has been taken up by ICES, and will now be presented to NEAFC.

CS1.6. References

Bett BJ (2001) UK Atlantic margin environmental survey: introduction and overview of bathyal benthic ecology. Continental Shelf Research 21: 917-956.

Bett BJ, Billet DSM, Masson DG, Tyler PA (2001) RRS Discovery cruise 248 - A multidisciplinary study of the environment and ecology of deep-water coral ecosystems and associated seabed facies and features (The Darwin Mounds, Porcupine Bank and Porcupine Seabigth). Southampton Oceanography Centre, cruise report 36, 52 p.

Cartwright JA, James D, Bolton A (2003) The genesis of polygonal fault systems. In: Van Rensbergen P, Hillis RR, Maltman A, Morley CK, editors. Subsurface sediment mobilisation. London: Geological Society pp. 223-243.

Davies AJ, Roberts JM, Hall-Spencer J (2007) Preserving deep-sea natural heritage: emerging issues in offshore conservation and management. Biol Conserv 138: 299-312.

De Santo E, Jones PJS (2007) Offshore marine conservation policies in the North East Atlantic:emerging tensions and opportunities. Marine Policy 31: 336-347.

GEBCO (2003) GEBCO Digital Atlas : Centenary edition of the IOC/IHO General Bathymetric Chart of the Oceans. Liverpool: British Oceanographic Data Centre.

Hall-Spencer JM, Tasker M, Soffker M, Christiansen S, Rogers S et al. (2009) Design of marine protected areas on high seas and territorial waters of Rockall Bank. Marine Ecology Progress Series 397: 305-308.

Huvenne VAI (2011) RRS James Cook Cruise 60, 09 May-12 June 2011. Benthic habitats and the impact of human activities in Rockall Trough, on Rockall Bank and in Hatton Basin. Southampton: National Oceanography Centre, Southampton. Cruise Report 04. 133 p.

Le Bas TP, Huvenne VAI (2009) Acquisition and processing of backscatter data for habitat mapping - Comparison of multibeam and sidescan systems. Appl Acoust 70(10): 1248-1257.

Masson DG, Bett BJ, Billett DSM, Jacobs CL, Wheeler AJ et al. (2003) The origin of deep-water, coral-topped mounds in the northern Rockall Trough, Northeast Atlantic. Marine Geology 194: 159-180.

Newton AW, Peach KJ, Coull KA, Gault M, Needle CL (2008) Rockall and the Scottish haddock fishery. Fisheries Research 94(2): 133-140.

Wheeler AJ, Bett BJ, Billet DSM, Masson DG, Mayor D (2005) The impact of demersal trawling on NE Atlantic deep-water coral habitats: the case of the Darwin Mounds, UK. In: Barnes PW, Thomas JP, editors. Benthic habitats and the effects of fishing. Bethesda, Maryland: America Fisheries Society. pp. 807-817.

Case Study 2: Shallow-water AUV mapping off SW UK

CS Leader: Dr Brian Bett (NOC), with input from Tim Le Bas (NOC) and Roger Coggan (Cefas)

CS2.1. The CS2 task

As set out in the proposal this task's remit was as follows:

"*In July 2012 NOC will lead a cruise on RRS Discovery to the Porcupine Abyssal Plain as part of the NERC-funded Autonomous Ecological Surveying of the Abyss (AESA) project. The cruise will include benthic mapping and monitoring using Autosub6000. This case study will involve an additional one-day Autosub6000 deployment on the outer shelf off SW UK during the return passage to Southampton. The aim will be to undertake high-resolution mapping and colour photography over an rMCZ, in order to highlight the capability of AUV technology for high-resolution shallow-water mapping and benthic species identification. It is hoped that the data will also contribute to ongoing efforts to increase the evidence base from selected rMCZs. The precise survey area will be identified following consultation with JNCC and Cefas.*

This Case Study will be compiled by NOC between 27 July (the approximate time of deployment) and 31 August 2012."

CS2.2 Introduction

Deep-water Autosub6000 missions during RRS *James Cook* cruise 060 (see Case Study 1 above) demonstrated the potential value of high altitude (15m) monochrome photography in seabed habitat mapping. Subsequent to that cruise, seabed survey photography from Autosub6000 was further developed through the NERC-funded Autonomous Ecological Surveying of the Abyss (AESA) project. The AESA project added colour digital cameras to the vehicle with an intended operating altitude of 3 m, hard disk storage for mass image collection, and flashgun recharge rates to enable photography at a 1Hz operating frequency. This case study examines the use of Autosub6000 as a habitat mapping tool on the outer shelf off SW UK, focussing particularly on the potential value of the AESA camera system.

CS2.2.1. AESA project

The AESA field programme was undertaken from RRS *Discovery* cruise 377 (5-27 July 2012). The work was sited at the Porcupine Abyssal Plain Sustained Observatory, 48º 50' N 016º 30' W, at 4850m water depth. Several Autosub6000 missions were successfully completed, providing an unprecedented level of photographic coverage of abyssal hill topography[54]. *En route* back to Southampton, Defra funding enabled an additional Autosub6000 mission to be undertaken on the outer UK shelf in an area of particular marine conservation interest.

CS2.2.2. Haig Fras

Following discussions with Defra, JNCC and Cefas, the Greater Haig Fras area (Fig. CS2.1) was selected for the Autosub6000 Case Study 2 mission. Haig Fras itself is an isolated, bedrock outcrop some 90 km northwest of the Isles of Scilly. It is thought to be the only substantial area of rocky reef in the Celtic Sea beyond the coastal margin. The rock outcrop is the focus of both a Special Area of Conservation[55] and a recommended Marine

[54] http://www.bbc.co.uk/news/science-environment-19080305
[55] http://jncc.Defra.gov.uk/PDF/HaigFras_SelectionAssessment_4.0.pdf

Conservation Zone[56]. The specific location of the Autosub6000 mission was chosen to correspond with an area of ship-based seabed survey co-ordinated by Cefas (Fig. CS2.2) just prior to the arrival of RRS *Discovery.* This would enable direct comparison of vessel- and AUV-based data.

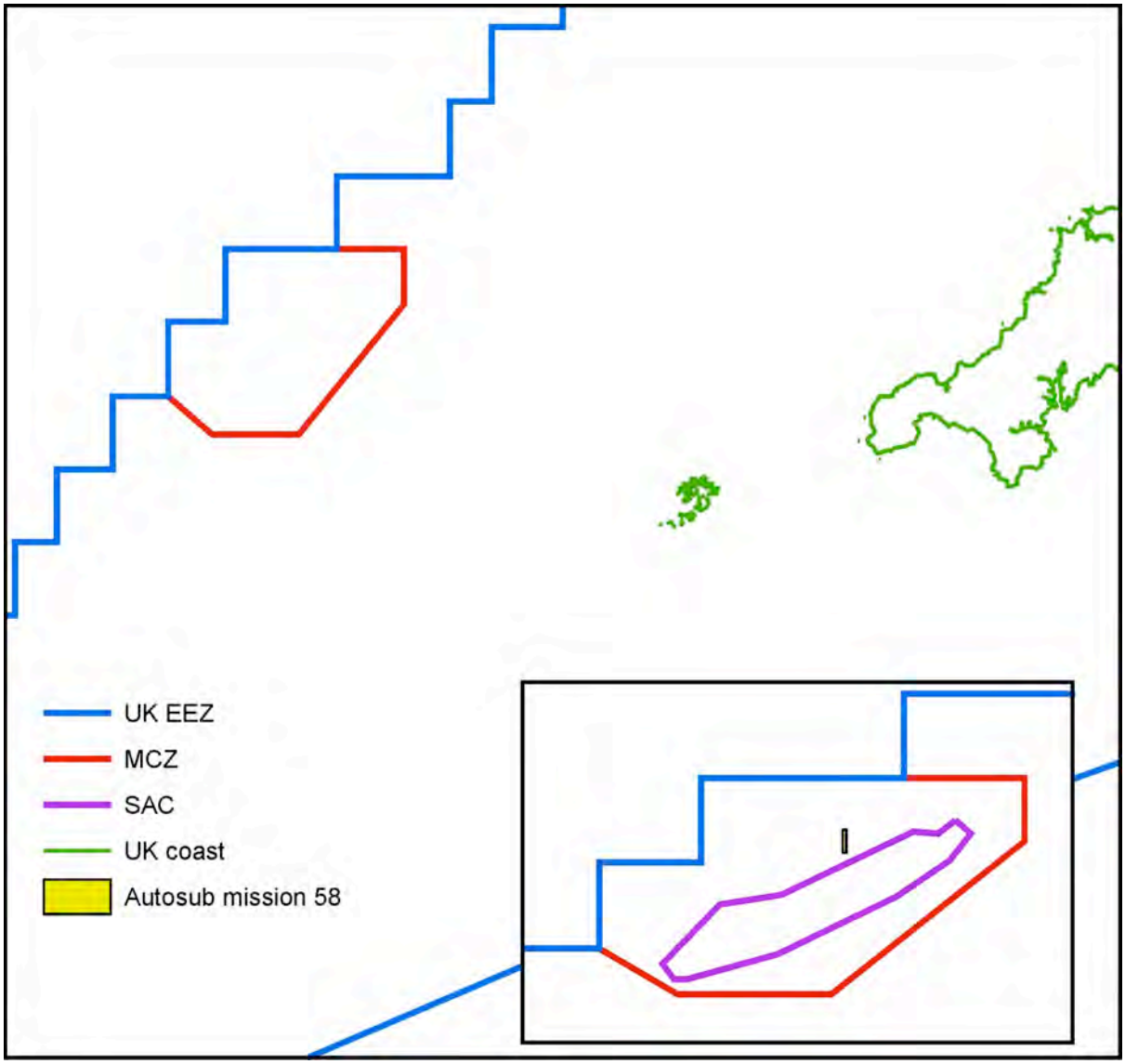

Figure CS2.1: General location map for Autosub6000 mission 58 (Case Study 2) within the Greater Haig Fras recommended Marine Conservation Zone (MCZ) adjacent to the Haig Fras Special Area of Conservation (SAC). Inset map (bottom right) shows the location of the Autosub track just north of the SAC boundary.

[56] http://www.wildlifetrusts.org/MCZ/greater-haig-fras

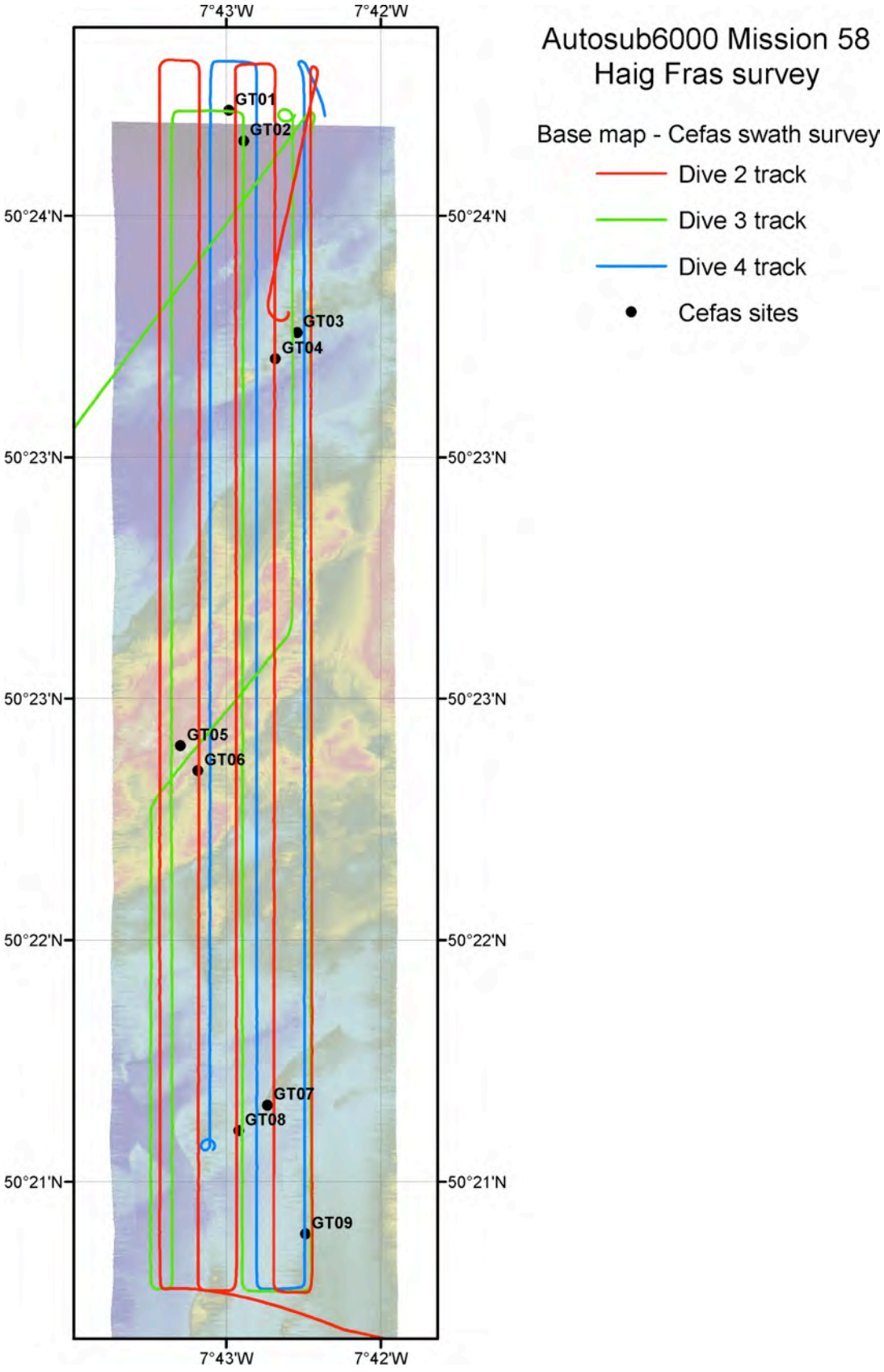

Figure CS2.2: Track chart for Autosub6000 mission 58 within the Greater Haig Fras rMCZ. For location see Fig. CS2.1. The underlying base map is taken from a CEFAS swath survey of the study area, and CEFAS sampling sites are also indicated.

CS2.3 Autosub6000 mission 58 – Greater Haig Fras

Our time at Haig Fras was somewhat curtailed as a result of having to divert to Penzance for a Medivac. The assistance of the local Lifeboat (coming well out to meet us) and Coastguard (allowing us to route through the Scillies) helped to minimise the time lost.

We carried out one Autosub6000 deployment (Mission 58; 25-26 July 2012; NOC station number D377-062) in the Haig Fras test area. The mission comprised of four separate dives:

Dive 1 – Vehicle sensor test (including camera trial)
Dive 2 – Swath bathymetry survey (including camera trial), survey altitude 50m
Dive 3 – Photographic survey, survey altitude 3m
Dive 4 – Sidescan sonar survey, survey altitude 15m

This multi-dive operation allowed us to (a) check the correct operation of the vehicle, particularly that useful photographic images were being obtained, and (b) initiate each phase of the survey (dives 2-4) with a new GPS fix at the surface.

Dive profiles (vehicle altitude above seafloor with time) and tracks are shown in Figs CS2.2 and CS2.3.

The full specifications of the Autosub6000 AUV are given in WP1 of this report. For mission 58 the key sensors were:

- EM2000 multibeam system
- EdgeTech 2200-FS dual frequency sidescan sonar (120/410kHz)
- Point Grey Research Grasshopper 2 digital camera with 10J flashgun
- Seabird CTDs (Conductivity, Temperature, Depth instrument)
- Sea Point LSS (light scattering sensor)
- RDI Teledyne 300kHz ADCP

Details of photographic set-up:

- Frame interval: 850mS
- Camera down-angle: 90°
- Lens type: Navitar
- Lens focal length: 12mm
- Lens f number: c. 2
- Focus in air: 2.5m
- Flash energy: 10J
- Shutter speed: 1mS
- Camera model: Point Grey Research, Grasshopper2, GS2-GE-50S5C
- Imaging sensor: Sony ICX625AQ (2/3" 2448x2048 CCD)
- Resolution: 2448x2048 pixels
- Image recording format: raw 8-bit, Bayer tile format: GBRG

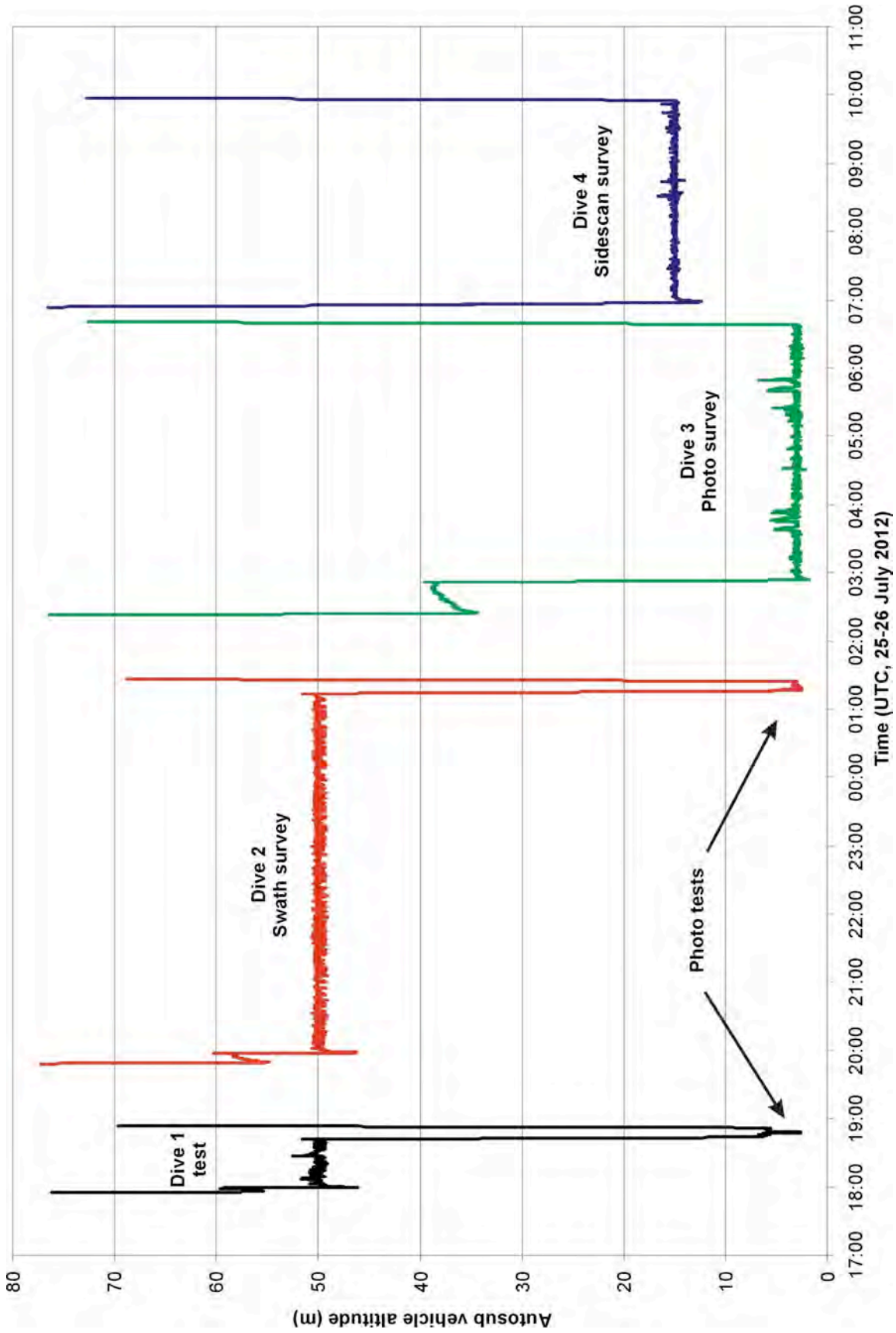

Figure CS2.3: Autosub6000 mission 58, dives 1-4, showing dive profiles as vehicle altitude against time. For dive locations see Fig. CS2.2.

CS2.4 Survey results

CS2.4.1. CTD and LSS

Although undertaken as a seabed survey, mission 58 also generated useful data on the environment of the over-lying water column. Fig. CS2.4 illustrates the water column profiles of Conductivity, Temperature, Depth (CTD) and Light Scattering Spectroscopy (LSS) instrument data. A strong thermocline is evident between 30 and 50m water depth, with some 10m variance in its location that may be attributed to both temporal and spatial variations. Salinity profiles exhibit similar variation. Turbidity, as determined from the light scattering sensor, shows a marked increase below the thermocline, generally increasing with proximity to the seafloor.

Figs CS2.5-2.7 illustrate along-track (i.e. spatial) variation in CTD and LSS instrument data during the seabed survey phases of mission 58. As the vehicle was operating in fixed altitude mode they do not entirely represent mapping on a constant depth surface; however, they do provide some indication of the scope for systematic spatial variation in the water column environment. Overall, the northern part of the survey area appears slightly cooler, more saline, and more turbid than the southern part.

CS2.4.2. Multibeam bathymetry and sidescan sonar

Fig. CS2.8 illustrates the multibeam bathymetry (dive 2) and sidescan sonar backscatter (dive 4) obtained during Autosub6000 mission 58. The bathymetry indicates a ridge-like central high trending SW to NE, with minor ridge-like highs of the same trend located both north and south of the central high.

In general terms the sidescan data has alternating bands of higher and lower backscatter, having a broadly similar SW to NE trend. In simple terms these may be interpreted as changes from coarser mixed sediments (high backscatter) to finer more homogeneous sediments (low backscatter) (see example in Fig. CS2.9). Many other finer-scale details are apparent on close inspection of these data. Of particular interest are areas of sinusoidal striations on the central high region that may be interpreted as outcropping rock strata (see example in Fig. CS2.9).

CS2.4.3. Preliminary comparison of vessel-based and Autosub6000 geophysical data

Fig. CS2.10 provides an initial comparison of vessel-based and Autosub6000 multibeam swath bathymetry. In terms of both topographic interpretation and spatial geo-referencing, the two datasets are highly consistent. Similarly Figs CS2.11-2.12 provide an initial comparison of vessel-based multibeam backscatter and Autosub6000 sidescan sonar backscatter. Again in terms of both seabed fabric interpretation and spatial geo-referencing, the two datasets are highly consistent.

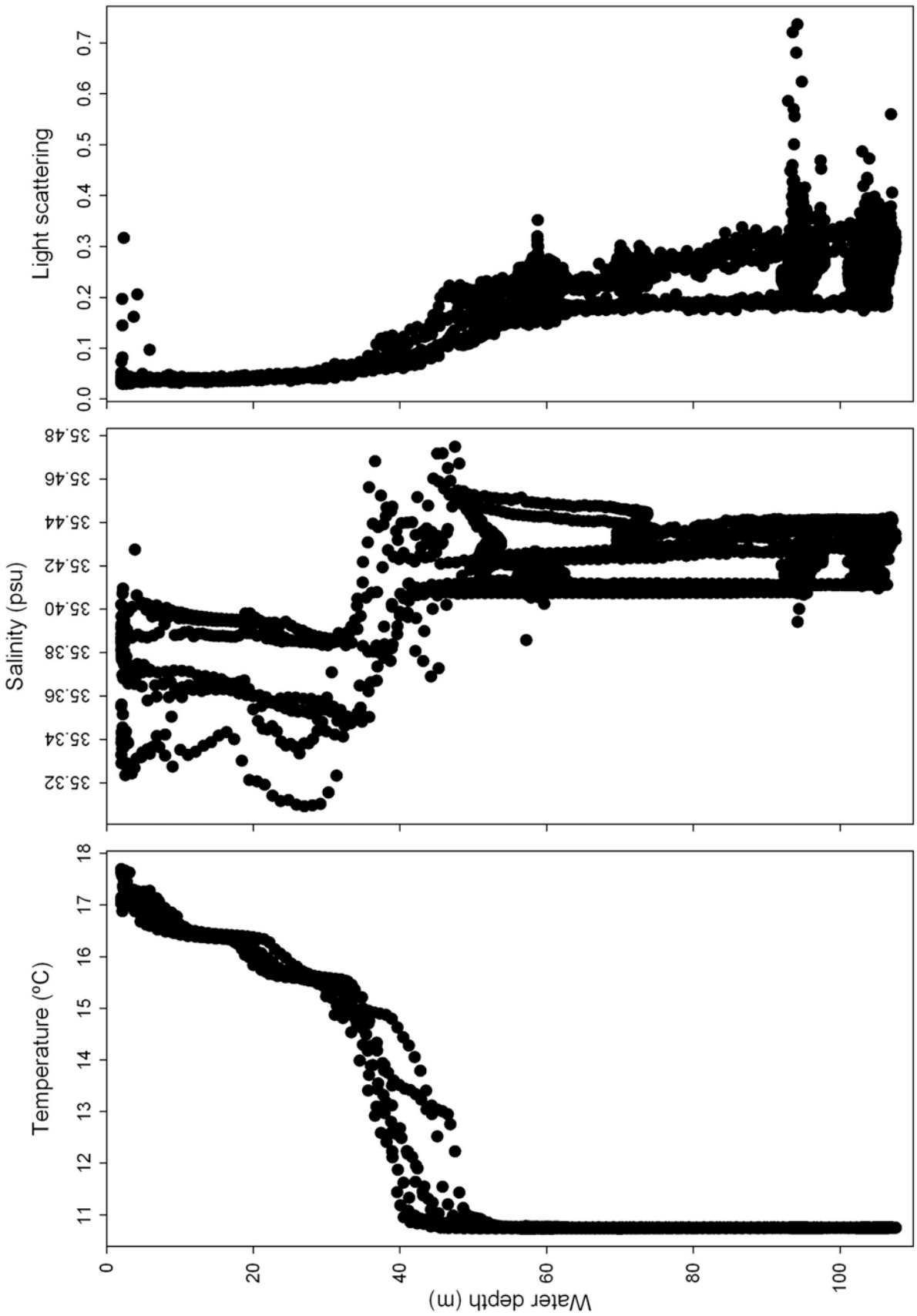

Figure CS2.4: Autosub6000 mission 58, dives 1-4, water column profiles of CTD and LSS instrument data.

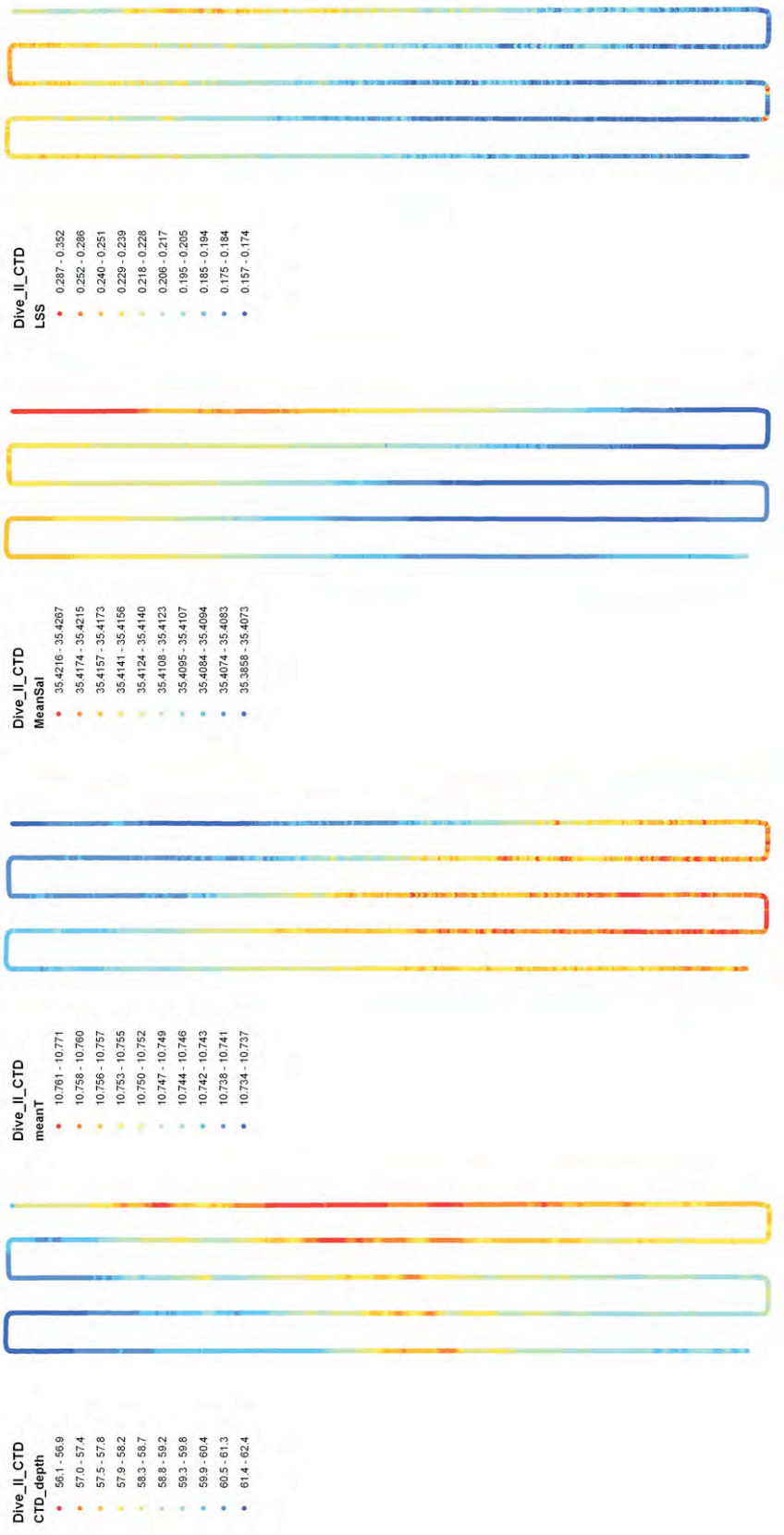

Figure CS2.5: Autosub6000 mission 58, dive 2 (multibeam survey), along-track variation in CTD and LSS instrument data (vehicle altitude c. 50m). CTD_depth = water depth of vehicle; MeanT = mean temperature from pair of sensors; MeanSal = mean salinity from pair of sensors; LSS = light scattering sensor.

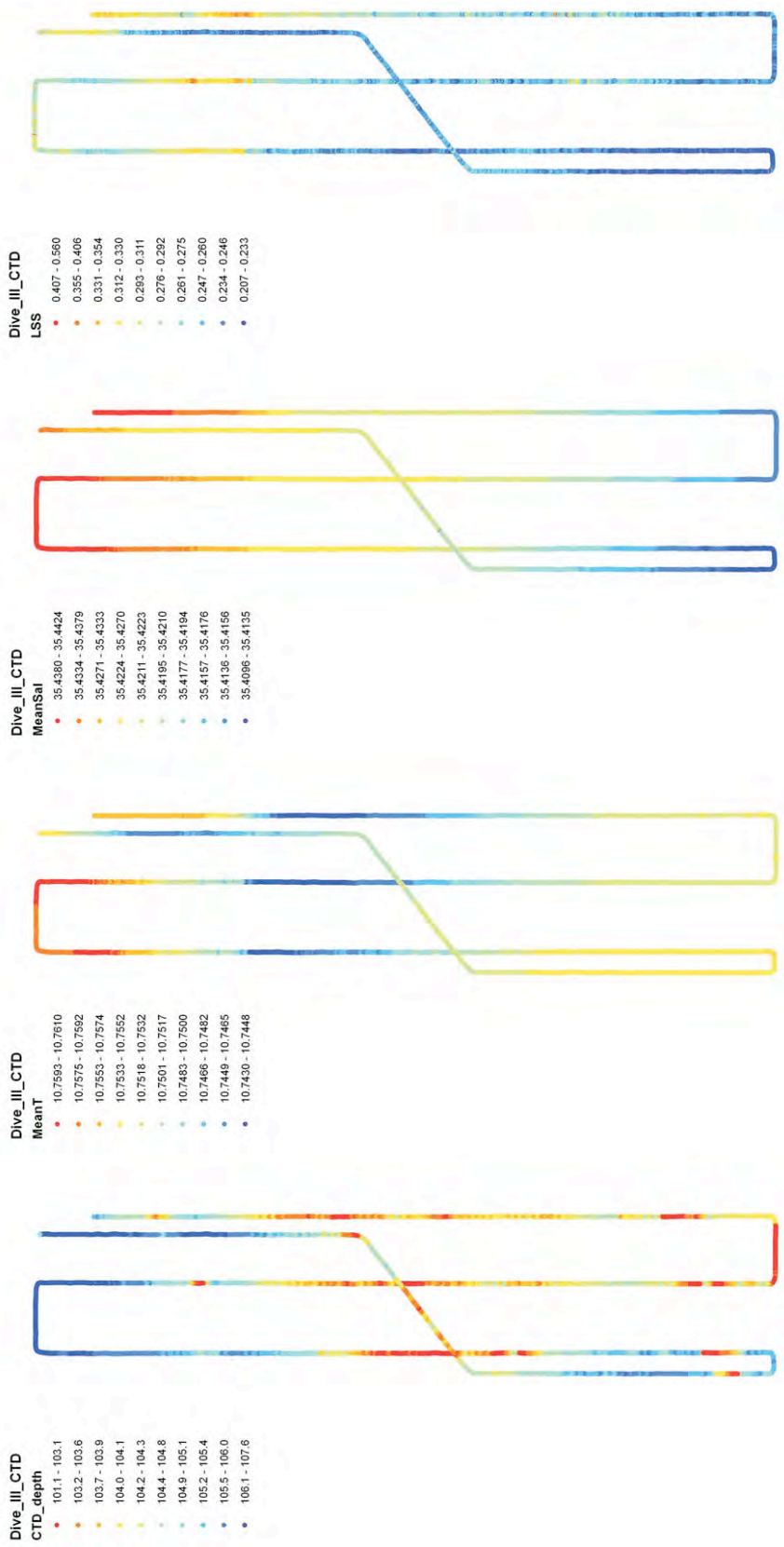

Figure CS2.6: Autosub6000 mission 58, dive 3 (photographic survey), along-track variation in CTD and LSS instrument data (vehicle altitude c. 3m). CTD_depth = water depth of vehicle; MeanT = mean temperature from pair of sensors; MeanSal = mean salinity from pair of sensors; LSS = light scattering sensor.

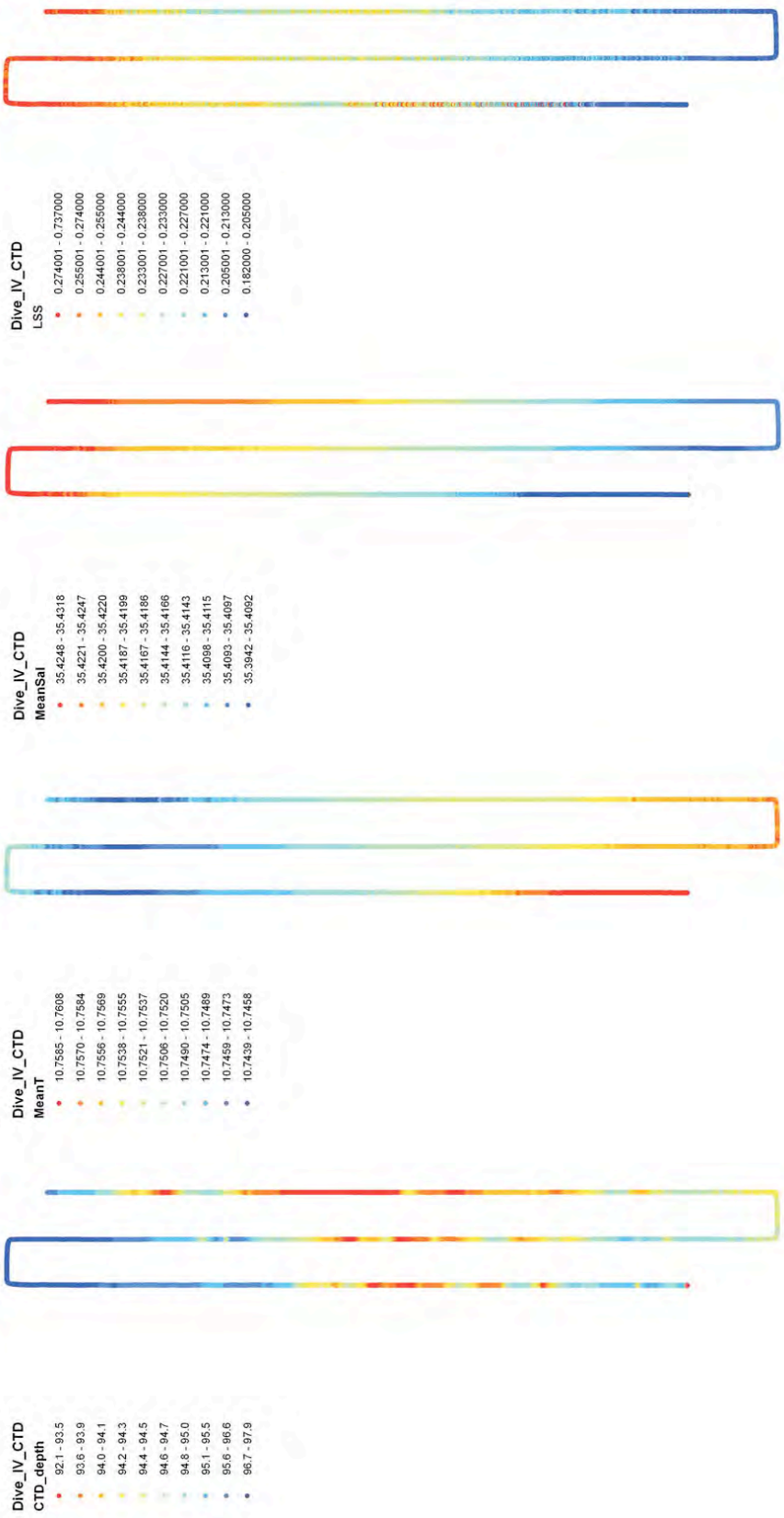

Figure CS2.7: Autosub6000 mission 58, dive 4 (sidescan survey), along-track variation in CTD and LSS instrument data (vehicle altitude c. 15m). CTD_depth = water depth of vehicle; MeanT = mean temperature from pair of sensors; MeanSal = mean salinity from pair of sensors; LSS = light scattering sensor.

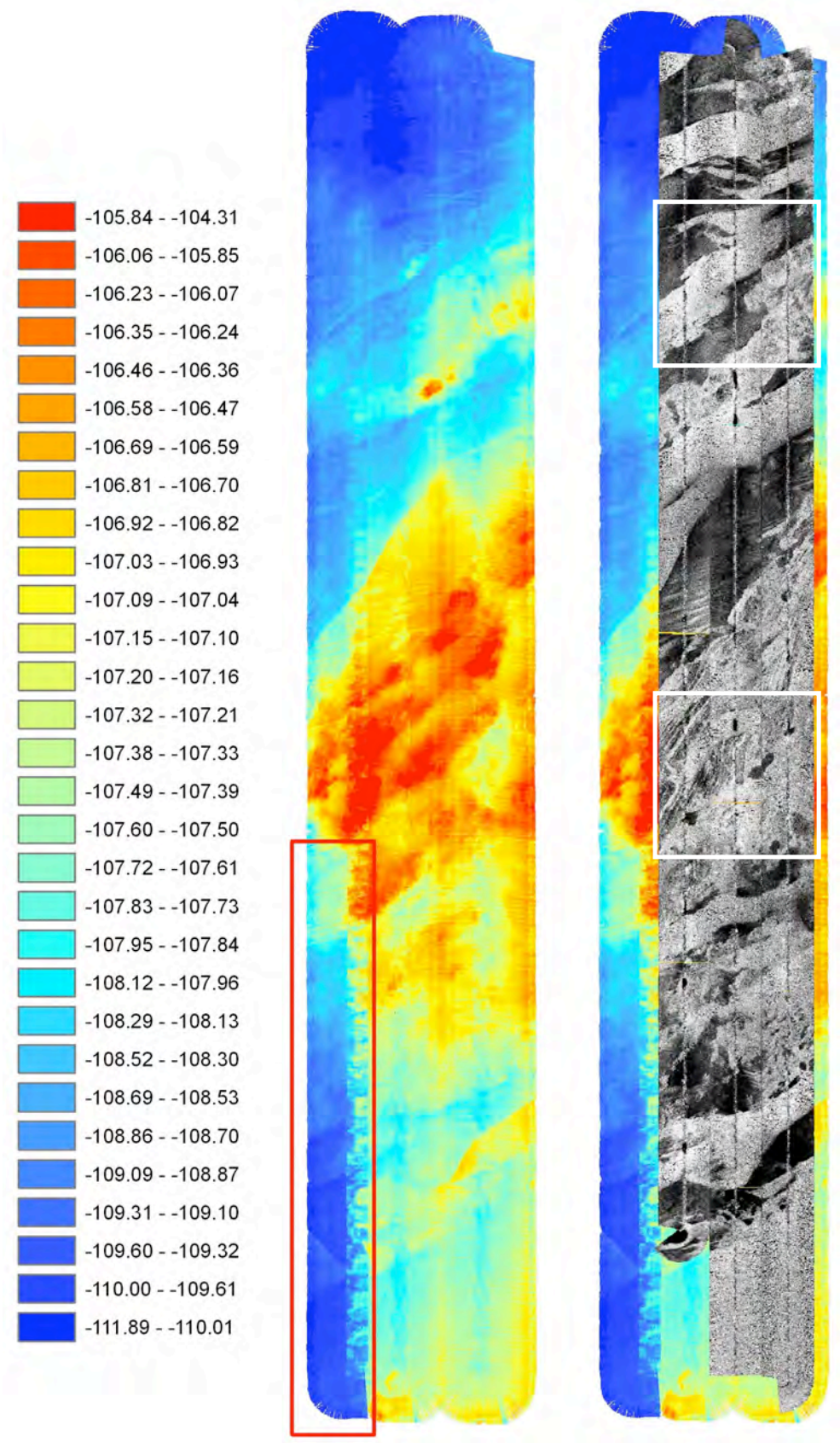

Figure CS2.8: Autosub6000 mission 58, multibeam swath bathymetry (left, dive 2) and sidescan sonar backscatter (right, dive4). High backscatter = light tones; low backscatter = dark tones. Red box indicates area of biased data from erroneous vehicle depth record. White boxes show approximate locations of sidescan images in Fig. CS2.9.

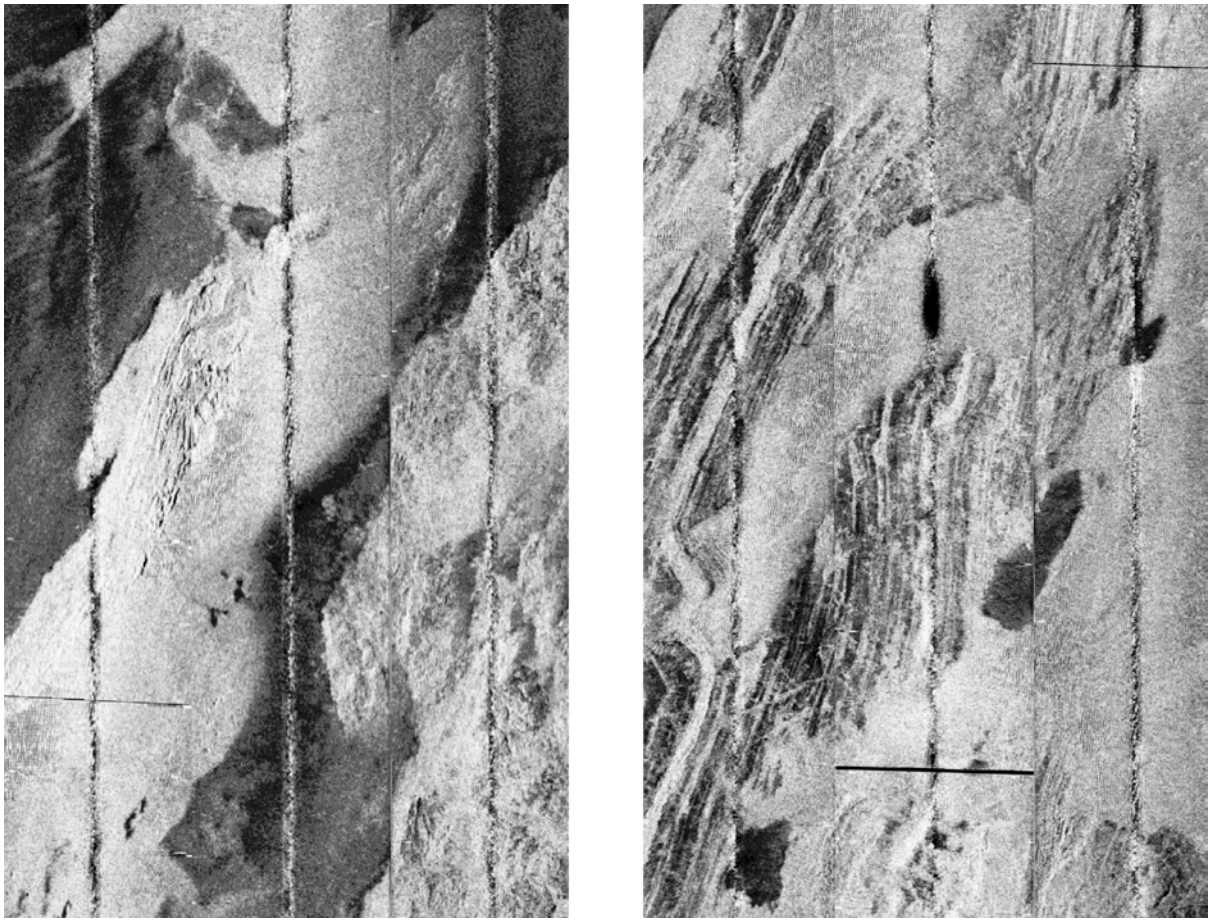

Figure CS2.9: Autosub6000 mission 58 sidescan sonar backscatter (dive4) examples: left, high-low backscatter transitions presumed to reflect changes in sediment grade; right, fine sinusoidal patterning presumed to be outcropping rock strata. High backscatter = light tones; low backscatter = dark tones. For locations see Fig. CS2.8.

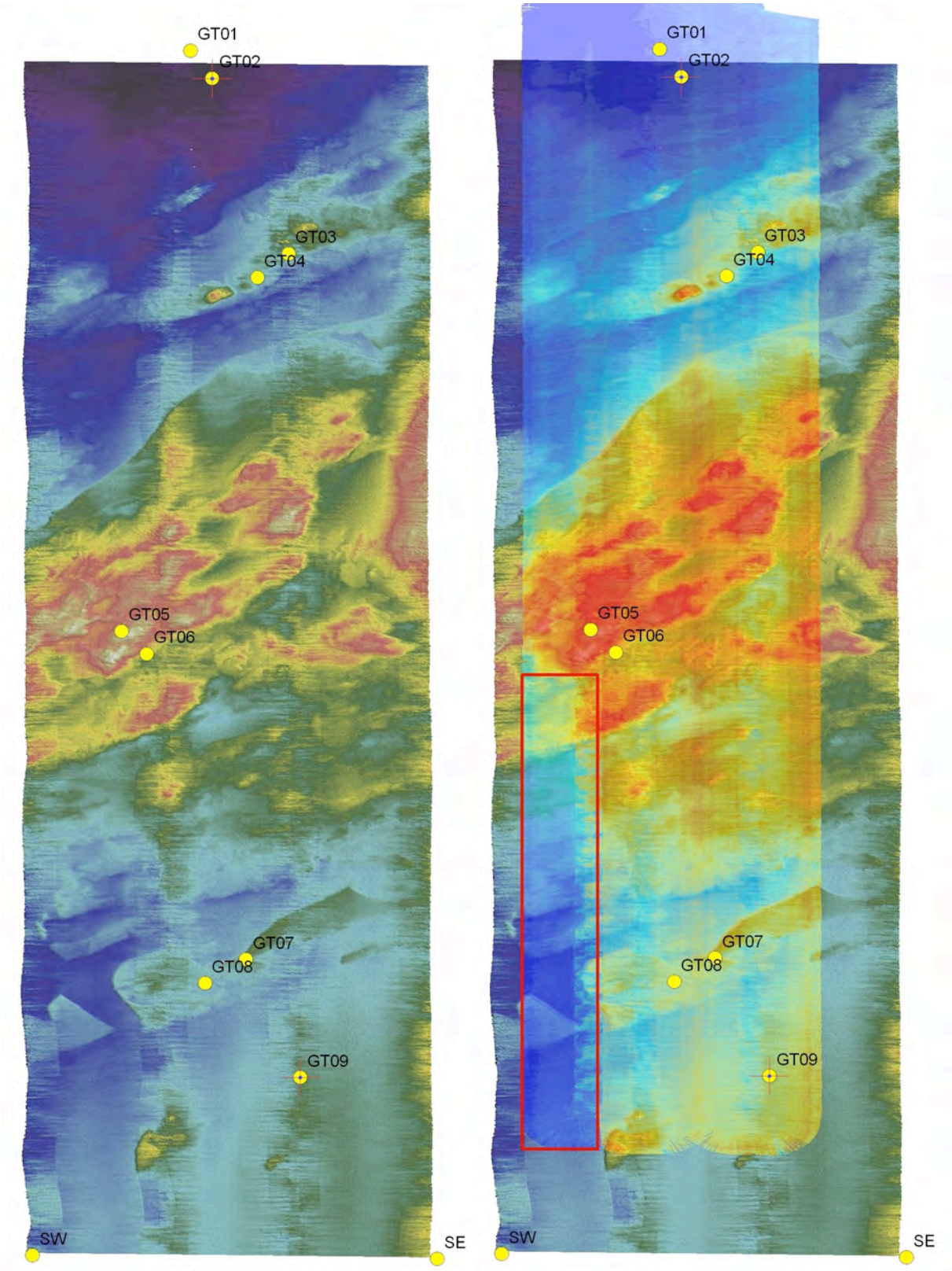

Figure CS2.10: Preliminary comparison of vessel-based (left) and Autosub6000 mission 58 (overlain, right) multibeam swath bathymetry. Red box indicates area of biased data from erroneous vehicle depth record. Sites indicated are Cefas ground truth stations, GT, and general extent of survey area.

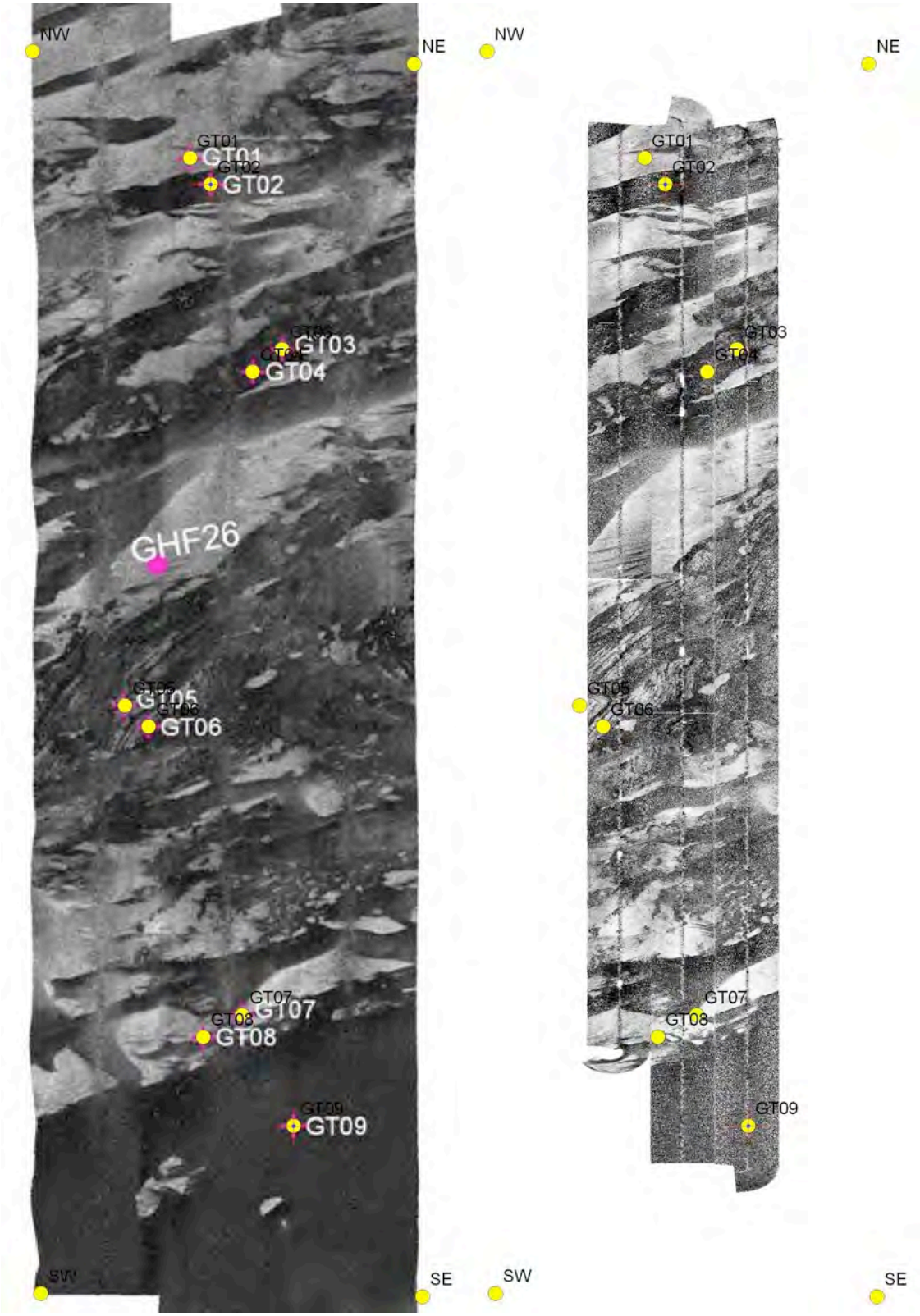

Figure CS2.11: Preliminary comparison of vessel-based multibeam backscatter (left) and Autosub6000 mission 58 sidescan sonar backscatter (right). High backscatter = dark tones; low backscatter = light tones). Sites indicated are Cefas ground truth stations, GT, and general extent of survey area.

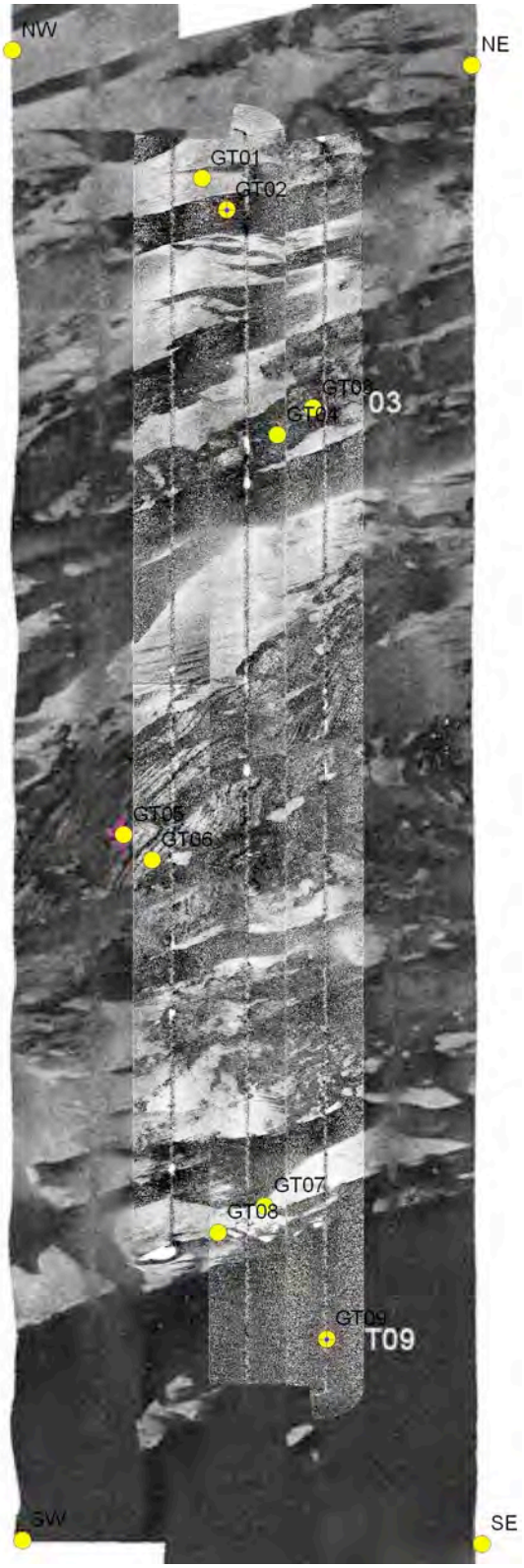

Figure CS2.12: Overlay of Autosub6000 mission 58 sidescan sonar backscatter on vessel-based multibeam backscatter. High backscatter = dark tones; low backscatter = light tones. Sites indicated are Cefas ground truth stations, GT, and general extent of survey area.

CS2.4.4. Photographic survey

The AESA camera systems were run continuously during Autosub6000 mission 58. Only those images recorded from the downward facing camera during dive 3 have been examined for the purposes of this report. In total some 16,000 images were recorded during dive 3, around 15,000 of those during the near-seabed phase of the dive. For this report the raw format images recorded were batch converted to jpeg images at 80% image quality and with automatic colour correction using the freely available IrfanView (V 4.33) software.

The images are somewhat degraded by particle backscatter in the near-bottom water; however, they are of sufficient quality for seabed characterisation. We are currently developing an average backscatter removal algorithm that should significantly improve image quality for later analyses.

All of the batch-converted images were (very) briefly reviewed to provide a general sense of the seabed environments and fauna present and to select example images for this report. These include some mid-water images that recorded garfish and jellyfish (Fig. CS2.13), and some seabed images showing human artefacts (Fig. CS2.14). Human artefacts observed included lost / discarded trawl gear, cables and plastic material. The larger diameter cable encountered appeared to cross the width of the survey area (Fig. CS2.15).

Selected examples of the benthic invertebrates and demersal fish encountered during Autosub6000 mission 58 dive 3 are shown in Fig. CS2.16. A photograph contact sheet is also provided (Fig. CS2.17) as reference to a larger set of images of the benthic invertebrates and demersal fish to be supplied with this report (and for future use by JNCC and Cefas).

Underwater photography often generates serendipitous observations of natural history; the Haig Fras survey was no exception. It included multiple observations of an apparent association between stone crabs (*Lithodes*) and large anemones (*Bolocera*) (Fig. CS2.18).

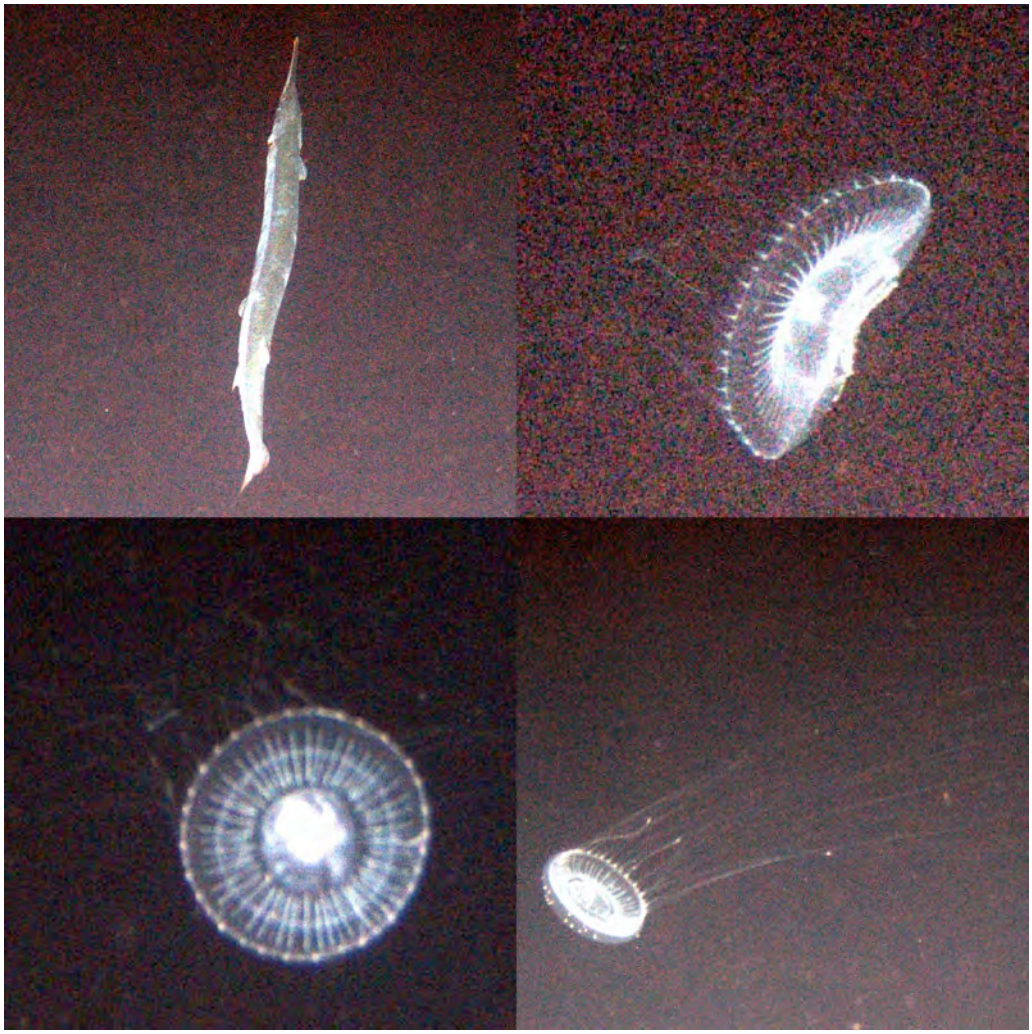

Figure CS2.13: Example images from the mid-water phase of Autosub6000 mission 58 dive 3. Top left – garfish; others – medusae (jellyfish).

Figure CS2.14: Example images of human artefacts at the seabed from Autosub6000 mission 58 dive 3. Top row – section of demersal trawl ground line (overlapping images); middle rows – cables; bottom row - plastics.

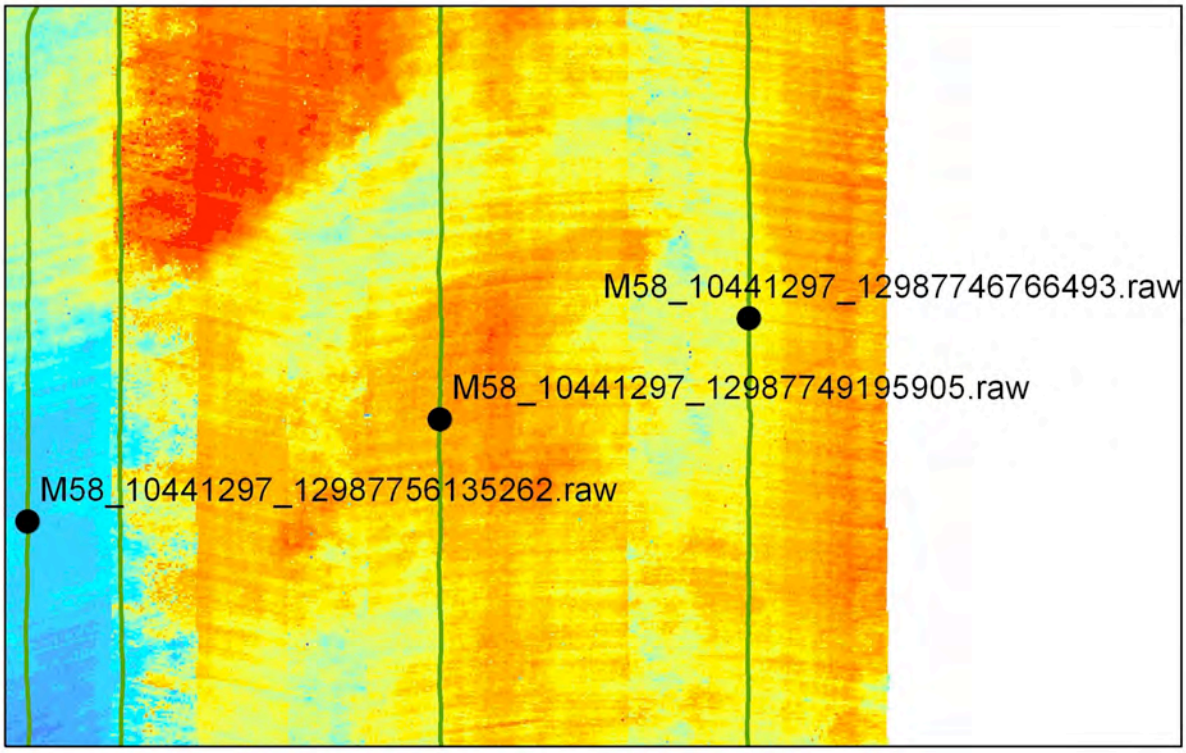

Figure CS2.15: Photograph locations for the three instances of large diameter cable noted at the seabed during Autosub6000 mission 58 dive 3, indicating presence of a continuous cable.

Figure CS2.16: Selected examples of benthic invertebrates and demersal fish encountered during Autosub6000 mission 58 dive 3 (images 1-30, reading left to right, top to bottom). The invertebrate megafauna included several species of sponge (images 1-4); anthozoans (anemones: Actinaria; Zoanthidea; Ceriantharia; images 5-10); 'Ross coral' the bryozoan Pentapora fascialis (images 11-12); the 'coral or filigree worm' Filograna implexa (images 13-14); several species of starfish and brittle stars (images 15-20); octopus and cuttlefish (images 21-22); stone crabs and squat lobsters (images 23-24). The demersal fish fauna included smoothhound, bull huss, skate, cuckoo ray, rockling and megrim (images 25-30).

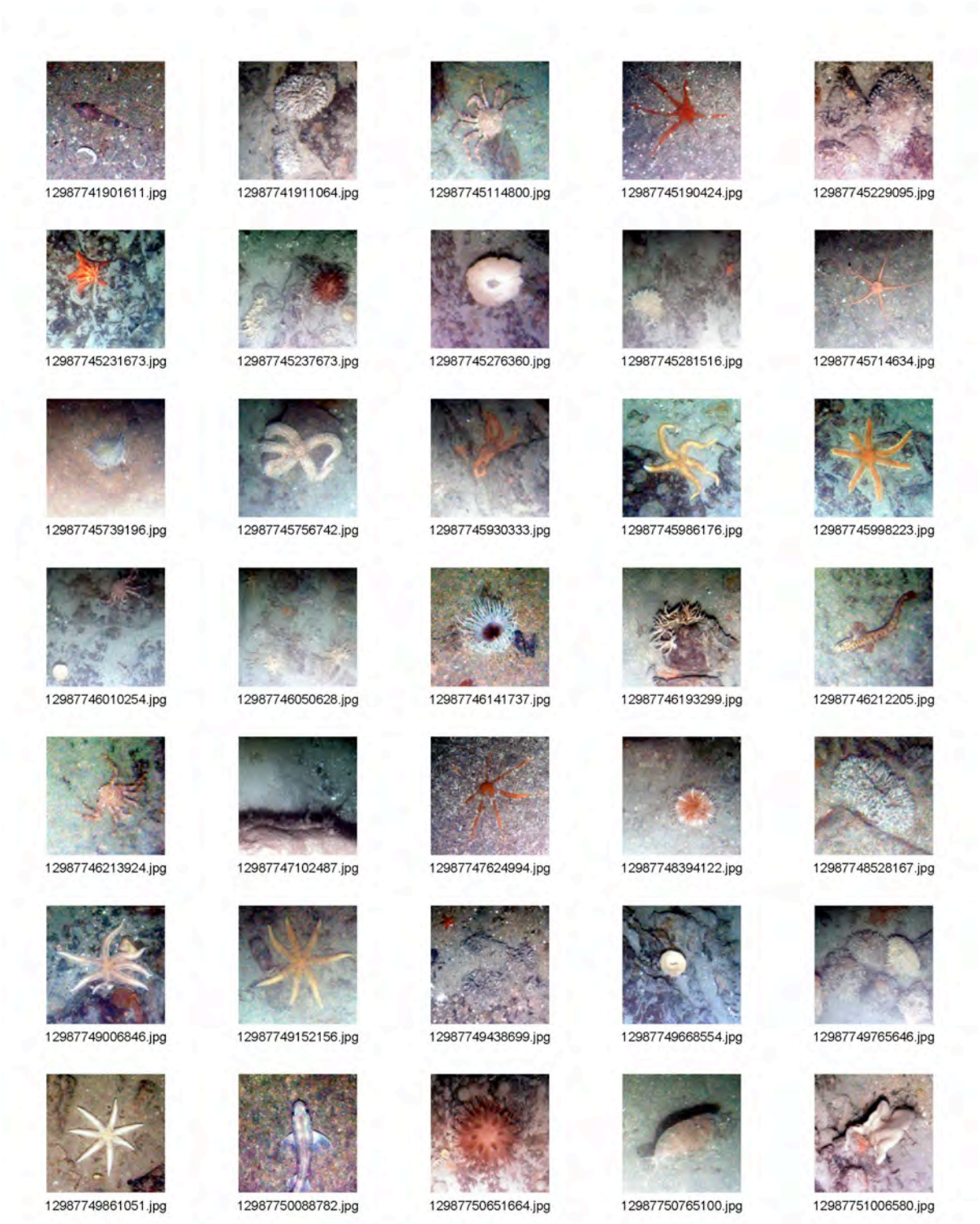

Figure CS2.17: Contact sheet for supplied images of selected examples of the benthic invertebrates and demersal fish encountered during Autosub6000 mission 58 dive 3.

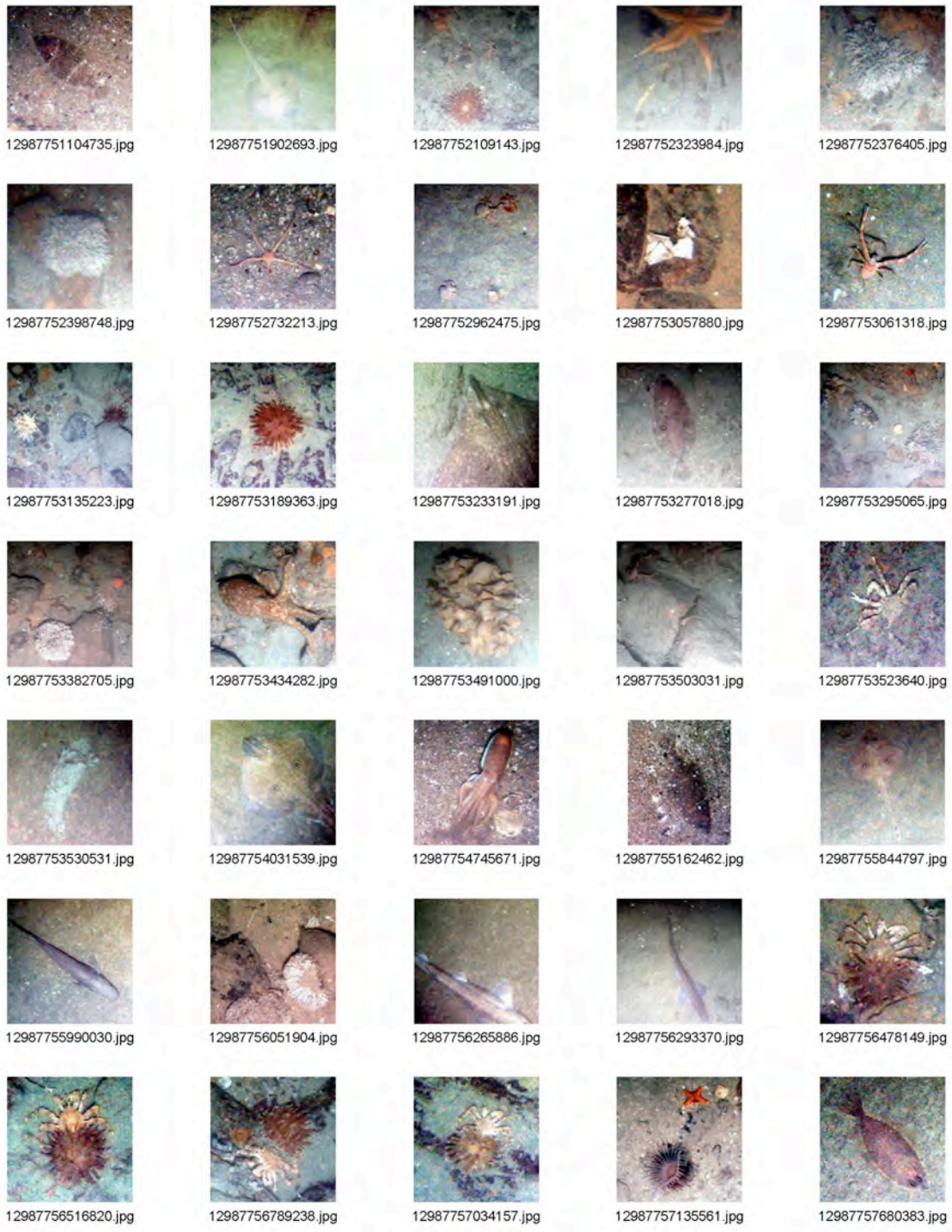

Figure CS2.17-continued: Contact sheet for supplied images of selected examples of the benthic invertebrates and demersal fish encountered during Autosub6000 mission 58 dive 3.

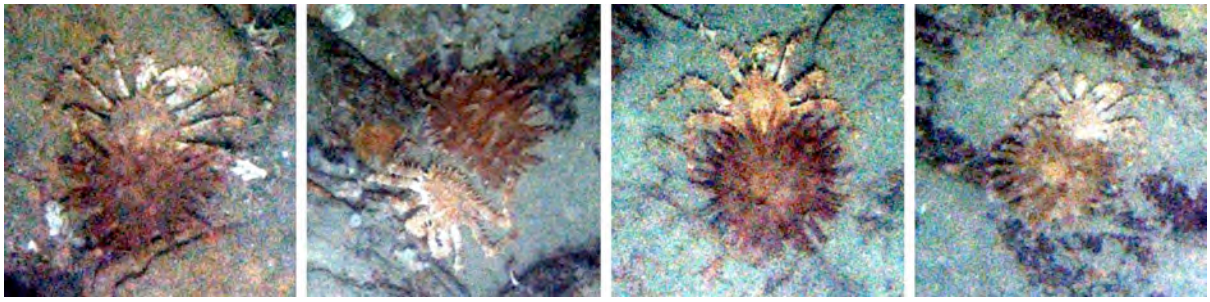

*Figure CS2.18: Multiple observations of an apparent association between stone crabs (*Lithodes*) and large anemones (*Bolocera*) encountered during Autosub6000 mission 58 dive 3.*

CS2.4.4 Seabed classification / habitat mapping

The c.15,000 seabed images collected during the near-seabed phase of dive 3 were reduced to every 30th image for analysis of seabed type (i.e. 518 photographs; 3.3% of the available data). Of those images 36 (7%) were unsuitable for analysis, having been recorded while the vehicle was out of photographic range of the seabed. Each useful image was assigned to a seafloor type category, representing the predominant nature of the seabed within the image; the categories employed were: bed rock; boulder; coarse (mixed sediment); 'mega-ripples' (sediment ripples/waves of metre-scale wavelength and decimetre amplitude, typically with shelly debris in the troughs); and fine rippled (sands and muddy sands). A detailed assessment of seabed fauna was not included in this analysis; however, the occurrence of abundant Zoanthidea (colonial anemones) was recorded as a biological marker for 'good reef habitat'.

Figs CS2.19-2.21 provide example photographs from the three main seafloor types recognised: Bed rock and boulder; mega-ripples; and fine rippled. Fig. CS2.22 shows an overlay of the photographic seabed classification on the sidescan sonar backscatter image. There appears to be a good and close match between the photographic classification and variations in acoustic fabric. Note, for example, the higher to lower backscatter band transitions in the northern half of the survey and the matching transitions between 'mega-ripples' and 'fine rippled' categories. Note also the correspondence of the 'bed rock and boulder' category with the striated sidescan fabric of the central high area, and also on the lesser northern high. These two areas are also marked by the occurrence of abundant Zoanthidea (Fig. CS2.23).

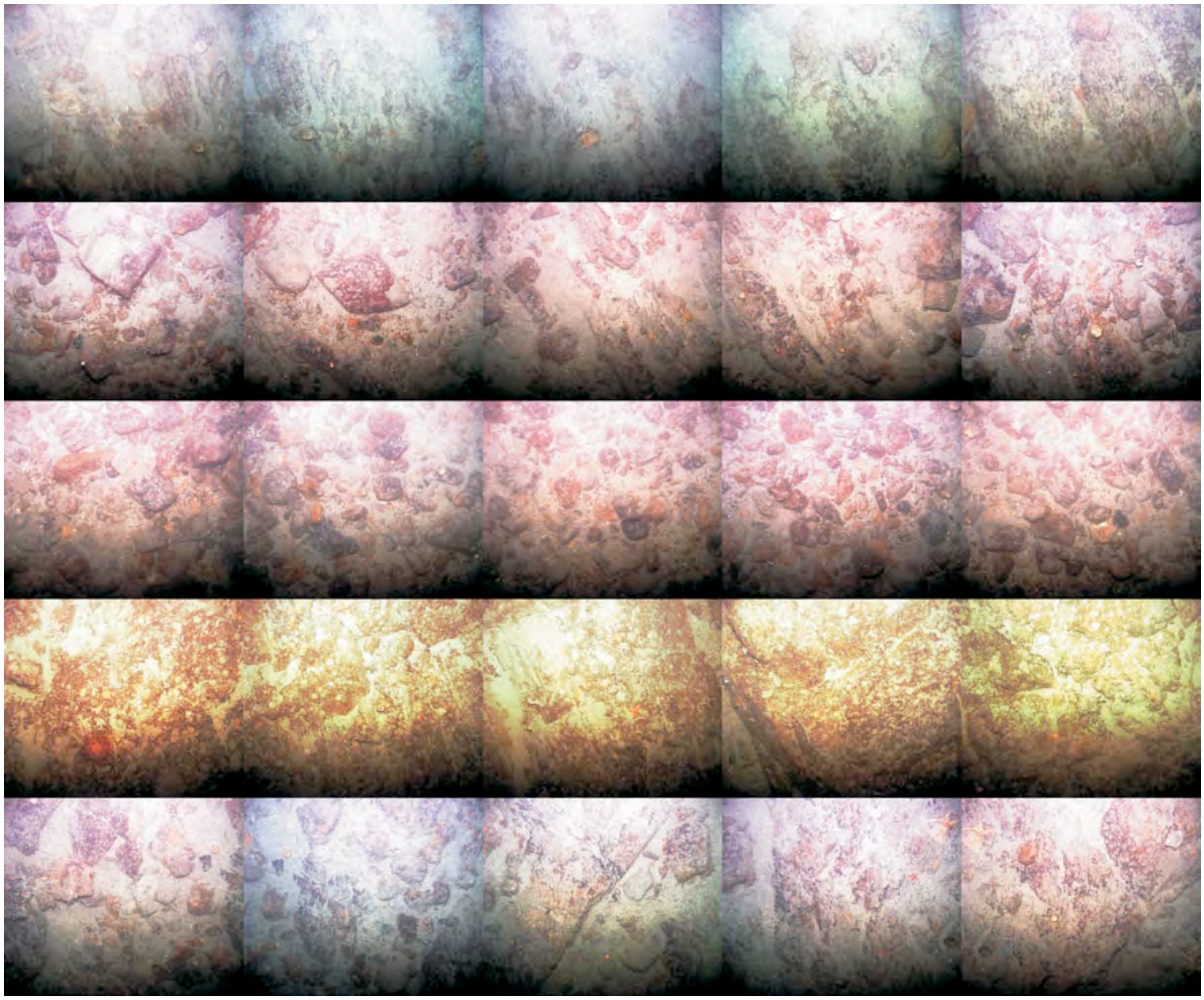

Figure CS2.19: Autosub6000 mission 58 dive 3; examples of bedrock and boulder terrain. Each strip of images is sequential and overlapping.

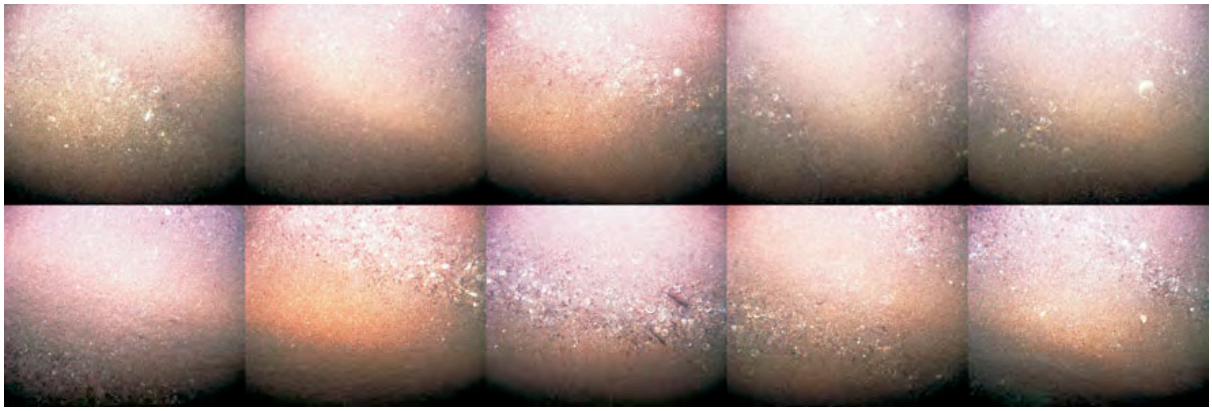

Figure CS2.20: Autosub6000 mission 58 dive 3; examples of 'mega-ripple' terrain. Each strip of images is sequential and overlapping.

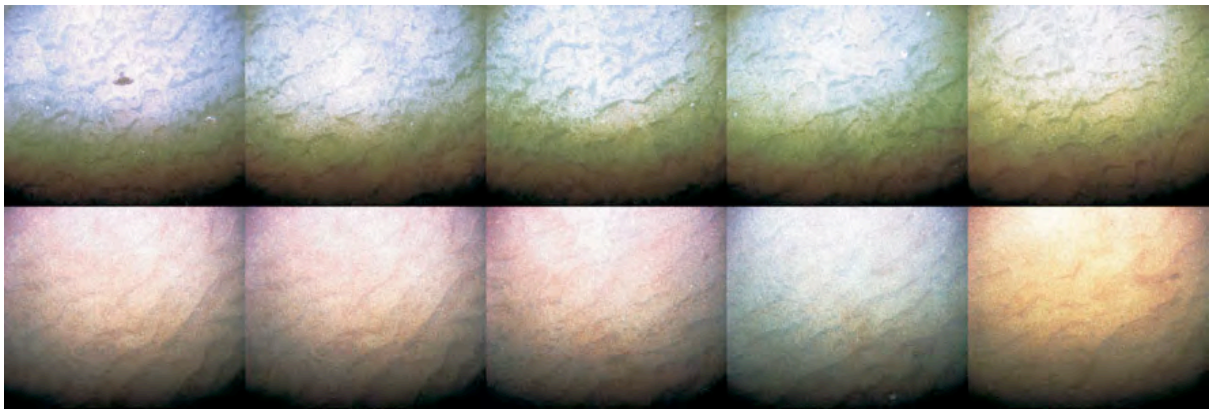

Figure CS2.21: Autosub6000 mission 58 dive 3; examples of fine rippled terrain. Each strip of images is sequential and overlapping.

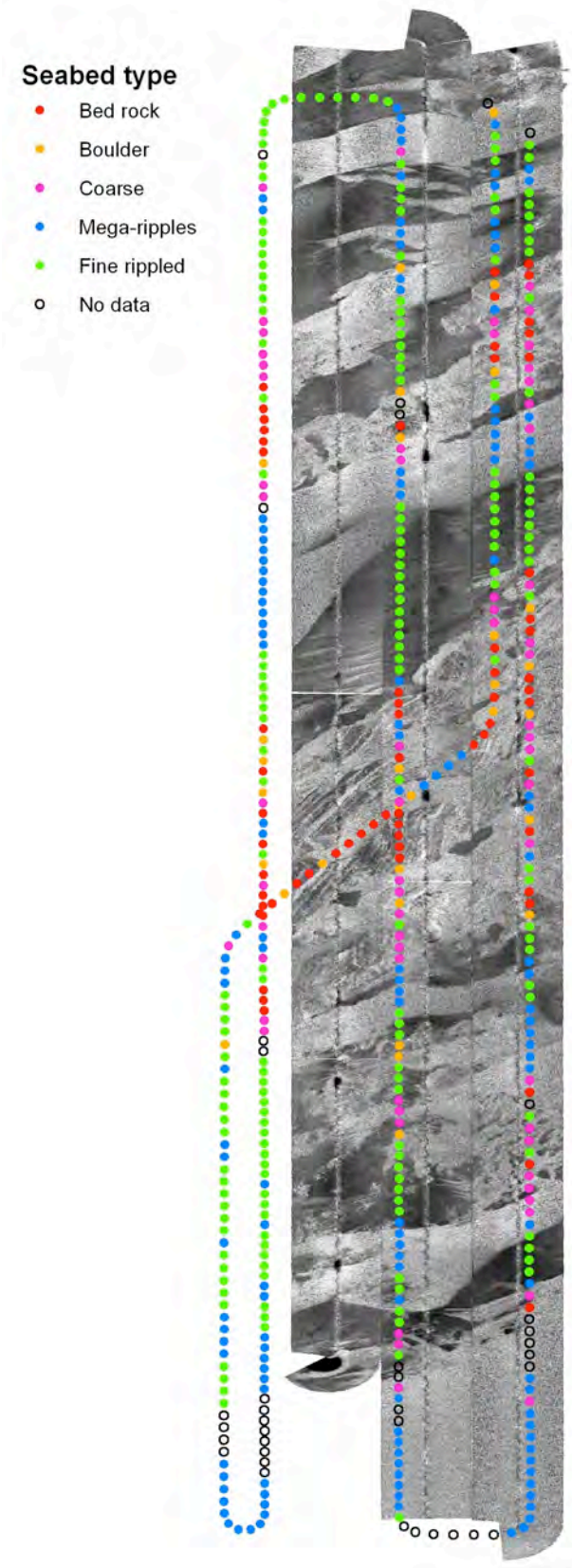

Figure CS2.22: Overlay of photographic seabed classification on sidescan sonar backscatter from Autosub6000 mission 58 (dives 3 and 4).

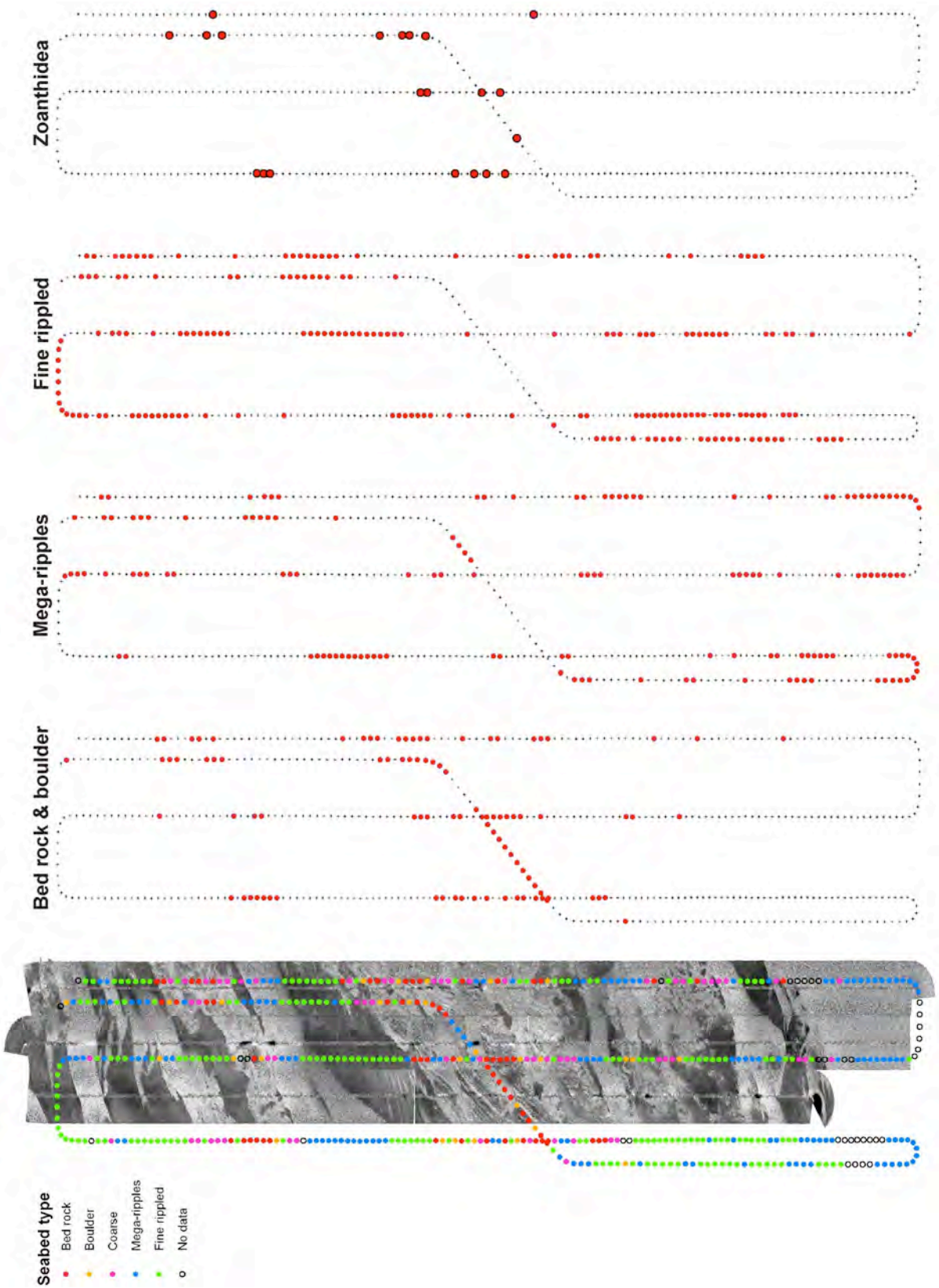

Figure CS2.23: Photographic seabed classification and sidescan sonar backscatter from Autosub6000 mission 58 (dives 3 and 4). The occurrence of abundant Zoanthidea (colonial anemones) is also indicated.

CS2.5 Summary and conclusions

The AESA camera systems were successfully integrated with the Autosub6000 vehicle. Several successful missions were carried out in abyssal hill topography on the Porcupine Abyssal Plain during RRS *Discovery* cruise 377. These have yielded an unprecedented detailed view of this deep-sea environment. A similarly successful Autosub6000 mission was carried out in the Greater Haig Fras rMCZ area. Useful data were obtained from all of the survey sensors employed (CTD; light scattering sensor; multibeam bathymetry; sidescan sonar; seabed cameras). Initial comparisons indicate that the Autosub6000 geophysical data (multibeam and sidescan) is a close match in terms of seabed topography, acoustic fabric and geo-referencing to the multibeam data acquired in the same area from a research vessel. Although somewhat degraded by near-bottom water turbidity, the photographs obtained with the AESA camera are effective in both censusing the seabed fauna and classifying seabed types for habitat mapping purposes. There is a close match between the photographic seabed classification and the variations in seabed acoustic fabric detected by Autosub6000's high frequency sidescan sonar. Joint use of the camera and sidescan systems may be particularly effective in providing ground-truthed habitat maps.

Case Study 3: Deep-water Glider mapping off NW UK

CS Leader: Dr Tim Boyd with input from Toby Sherwin, Mark Inall, Estelle Dumont (SAMS)

CS3.1. The CS3 task

As set out in the proposal this task's remit was as follows:

"*In spring 2010, the SAMS Glider 'Talisker' traversed west from the Sea of Hebrides to the northern Rockall Trough, where it undertook four (roughly E-W oriented) round trips of ~500 km at a speed of 0.5 knots, covering a total distance of ~2000 km. During this deployment, Talisker completed 789 dives. During each dive the Glider collected vertical profiles of ocean temperature, salinity, dissolved oxygen, chlorophyll-a fluorescence and optical backscatter. This case study will therefore provide an excellent example of Glider capability in mapping and monitoring of offshore water column features, such as fronts, eddies and upwelling zones.*

This Case Study will be compiled by SAMS between 1 March and 31 May 2012."

CS3.2. Introduction and overview

In autumn/winter 2009-2010 and again in spring/summer 2011, the SAMS buoyancy-driven Seaglider 'Talisker' traversed the Rockall Trough, a deep basin between the Sea of Hebrides in the east and Rockall Bank in the west, conducting measurements of water properties from the surface to a maximum depth of 1000 m.

During mission 1 (autumn/winter 2009-10), Talisker undertook four roughly E-W oriented round trips of ~500 km at a speed of 0.5 knots, covering a cumulative transect distance of ~2000 km. During this deployment, Talisker completed 789 dives, on each of which the glider collected two vertical profiles of ocean temperature, salinity, dissolved oxygen, chlorophyll-a fluorescence, and optical backscatter. Mission 1 demonstrates the capability of the Seaglider to repeatedly sample an ocean region at high spatial resolution while navigating through the oceanic eddy field and capturing the seasonal evolution of the upper ocean during harsh winter conditions.

During mission 2 (spring/summer 2011), Talisker again sampled through the Rockall Trough, in a deployment that demonstrates the capability of the Seaglider to replicate some aspects of a conventional hydrographic expedition. In this case, the glider replicated CTD sampling along the Extended Ellett Line, which extends W from the Sea of Hebrides to Rockall Bank, NW from Rockall to the Iceland Basin, and then N to Iceland. During the first segment of this hydrographic line, from the Sea of Hebrides (8.78°W) to Rockall Bank (13.63°W), the glider conducted 157 dives (314 profiles) over a period of 21 days, in comparison to the ship-based Ellett Line hydrographic survey, which conducted 19 profiles over a period of 2 days.

The objectives of this case study are to provide representative data from glider deployments in this environment in different seasons, and to demonstrate the spatial resolution and quality of the data collected, while underscoring the capability of the platform for a persistent sampling presence during harsh environmental conditions. Additionally, we outline the advantages, limitations, and operational constraints of the glider as an oceanic sampling platform, and quantify the operational costs.

CS3.3. Background: Monitoring the NE Atlantic

CS3.3.1. Oceanographic context

A significant fraction of the relatively warm and salty North Atlantic water flowing northward across the Greenland-Scotland Ridge (GSR) into the Nordic Seas passes through the Rockall Trough (RT), an approximately 200 km wide basin bounded on the east by the Sea of the Hebrides and on the west by Rockall Bank (Inall and Sherwin, 2006). The upper 500-700 m of water in RT is characterized as eastern North Atlantic water (ENAW, Fig. CS3.1), which flows northward primarily along the Hebridean shelf at the eastern boundary of the basin (Sherwin et al., 2012). Emanating from the Norwegian Sea and flowing southward at intermediate depth (to about 1000 m) in the RT, and primarily on the western side of the basin, is Wyville Thompson Overflow Water (WTOW). At depths greater than 1000 m, deep waters originating in the Labrador Sea (LSW in Fig. CS3.1) and the Southern Ocean (AABW in Fig. CS3.1) are constrained from moving north of the RT by the Wyville Thompson Ridge. The broader significance of the region derives from the controlling influence of surrounding bathymetry on the thermohaline circulation, including the climatically significant exchanges across the GSR. For more information on the water mass distribution in the RT and temporal variability in the waters to the west of Scotland, see Johnson et al. (2010) and Inall et al. (2009), respectively.

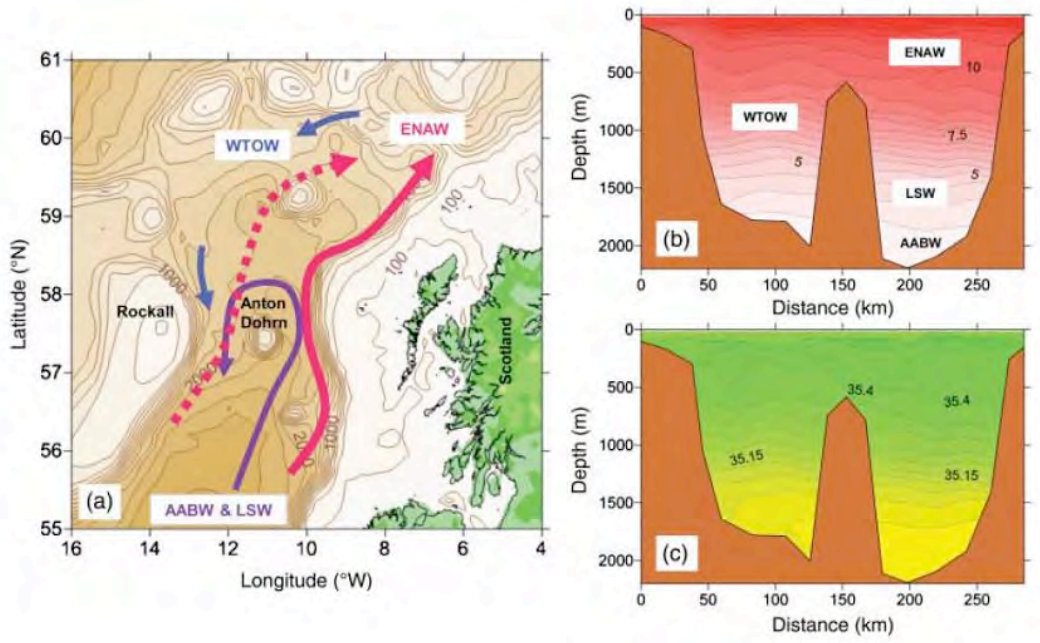

Figure CS3.1: Bathymetry of the Rockall Trough (RT, left), and temperature (top right) and salinity (bottom right) on sections along ~57.5°N from October 2006, including identification of the major water masses and transport pathways: northward flowing Eastern North Atlantic Water (ENAW), southward flowing Wyville Thompson Overflow Water (WTOW), and deeper Labrador Sea Bottom Water (LSBW) and Antarctic Bottow Water (AABW). From Sherwin et al. (2012). Note that AABW and LSW are bathymetrically constrained at the northern end of the RT. Note also that AABW and LSW are below the Seaglider maximum sampling depth (1000 m).

CS3.3.2. Monitoring the NE Atlantic

Beginning in 1975, full-depth hydrographic sections were conducted on a regular basis across the RT at 57.5 °N. Initially, this section, which came later to be known as the 'Ellett Line' in memory of physical oceanographer David Ellett, was conducted quarterly, however the frequency of the section was reduced to annual and the length extended in 1996 beyond Rockall Bank to the Iceland Basin and north to Iceland (see Fig. CS3.2). The overall objectives of the repeat section are to monitor the characteristics of the northward relatively warm inflow to the Nordic seas and the southward colder Iceland-Scotland ridge and Wyville Thompson ridge overflows, and to provide a platform for targeted studies. These data now form a 36-year long record of oceanic variability in the North Atlantic to the west of the UK. Over this time frame, only 70% of the attempted occupations of the section have been successful, due to the potential for harsh oceanic conditions (Read, 2011). In 2009, SAMS acquired a buoyancy-driven autonomous ocean glider and deployed it in 2010 to conduct hydrographic sampling along the Ellett Line in the RT; the deployment was in autumn-through-winter conditions that would have ranged from challenging to impossible for ship-based hydrographic observations. A further deployment in 2011 was conducted along the full and extended Ellett Line to Iceland (Fig. CS3.2).

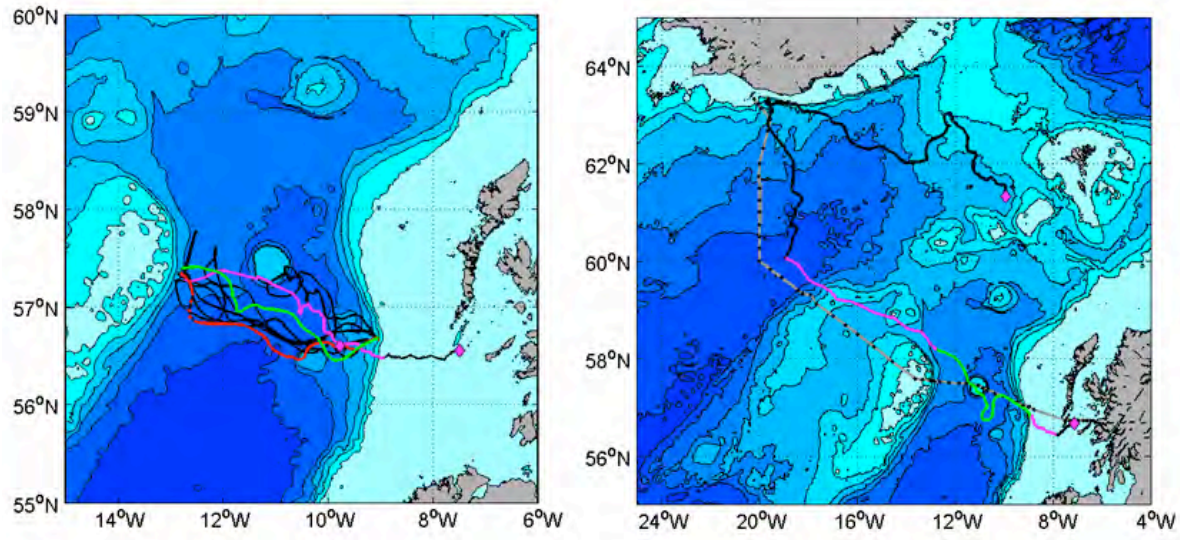

Figure CS3.2: Tracks of SAMS Seaglider 156 ('Talisker') on repeated crossings of the Rockall Trough during mission 1 (left, autumn-winter 2009-10) and from the Sea of the Hebrides to the Faroes via Rockall Bank, the Iceland Basin, and Iceland during mission 2 (right, spring-summer 2011). The missions began at the locations of the magenta diamonds in the Sea of the Hebrides. The location of the last dive for each mission is also marked with a magenta diamond. Bathymetric contours shown are 200 m, 500 m, and at 500 m intervals thereafter. For mission 1 (left), the entire track of Talisker is shown in black; transect 1 (conducted east to west) is shown overlaid in magenta; transect 2 (west to east) is overlaid in red (with dots at the locations of dives omitted from Figs CS3.4 and 3.6-3.8); and transect 4 (west to east) is overlaid in green. For mission 2 (right), the entire Seaglider track is shown in black; the transect extending northwest from Scotland (Fig. CS3.11) is shown overlaid magenta; the subset of that transect extending through the Rockall Trough (Fig. CS3.10) is overlaid in green. The track of the Extended Ellet Line 2011 cruise (RRS Discovery Cruise D365), 11 May – 02 June, is shown in grey with CTD station locations overlaid in black (right panel).

CS3.4. Seaglider: a persistent ocean observing presence in harsh conditions

CS3.4.1.Objectives of the Case Study

In this Case Study we provide representative data from glider deployments in the NE Atlantic to the west of Scotland in different seasons to demonstrate the spatial resolution and quality of hydrographic data collected by gliders, while underscoring the capability of the platform for a persistent sampling presence during harsh environmental conditions. Through presentation of data from two missions with different objectives, we illustrate advantages, limitations, and operational constraints of the glider as an oceanic sampling platform, and we quantify the operational costs. During mission 1 (autumn/winter 2009-10), SAMS Seaglider Talisker undertook four roughly E-W oriented round trips of the Rockall Trough of ~500 km at a speed of 0.5 knots, covering a cumulative transect distance of ~2000 km over the traditional Ellett Line hydrographic section (Fig. CS3.2, left). During mission 2 (spring/summer 2011), Talisker again sampled through the RT, in a deployment which replicated CTD sampling along the Extended Ellett Line, which extends westward beyond Rockall Bank into the Iceland Basin and then north to Iceland, prior to traversing eastward along the Iceland-Faroe Ridge towards the Faroes (Fig. CS3.2, right).

CS3.4.2. Seaglider methodology

The Seaglider is a buoyancy driven Unmanned Underwater Vehicle (UUV), that rises or falls through the ocean by adjusting its volume to be either slightly larger or smaller than an equal mass of seawater, with wings to provide the hydrodynamic lift that drives the vehicle forward as it rises or falls (Eriksen et al., 2001). The vehicle has no active external control surfaces. Attitude (pitch and roll) is controlled by shifting the centre of mass relative to the centre buoyancy, primarily through moving a mass (the battery pack) fore/aft to alter pitch (thus glide slope) and laterally to alter roll (thus rate of turn). The vehicle is about 1.8 m in length, 1 m in wingspan, and 52 kg in dry weight. With a lithium battery pack of 10 MJ, it has sufficient energy to nominally cover a path length of order 4600 km (or 650 dives to 1 km depth) in a single deployment, at a typical speed of 0.5 knots (0.25 m/s). The Seaglider navigates by dead reckoning between surface GPS position fixes. The difference between the dead reckoned and GPS fixes at the end of a dive cycle can be used to infer the depth-averaged horizontal ocean velocity (Frajka-Williams et al., 2009), and a vehicle flight model can be combined with onboard pressure measurements to form estimates of ocean vertical velocity (Frajka-Williams et al., 2011).

CS3.4.3. Data pathways

At the end of each dive, the Seaglider comes to the surface, shifting the ballast in order to orient the antenna free of the ocean surface, as shown in Fig. CS3.3. After obtaining a position fix from the constellation of GPS satellites, the Seaglider establishes a communication link to the computer base station in the laboratory via the Iridium satellite network and gateway ground station. Time between surfacings is dependent on the depths of the dives, with separations of 5-6 hours typical for a dive to the maximum depth of 1000 m.

Data arrives at the lab from the Iridium gateway via one of two pathways. At present, the primary pathway is from the gateway via RUDICS (Router-Based Unrestricted Digital Internetworking Connectivity Solutions, see www.iridium.com/products/RUDICS.aspx) to the base station ('velocity.sams.ac.uk') at SAMS using TCP/IP. A secondary pathway is from the gateway to the backup base station ('speed.sams.ac.uk') at SAMS using PSTN (Public Service Telephone Network) services through the base station modem. During mission 1, the RUDICS pathway was not operable due to a technical problem. A third (failsafe) pathway involves only the gateway and Seaglider in real-time, should communication with the laboratory base stations not be possible.

The Iridium connection supports two-way real-time communication between the base station and surfaced Seaglider, providing data telemetry from the Seaglider to the base station and command updates to the Seaglider. In practise, because the Seaglider is only at the surface for a short period, the commands uploaded are usually based on the pilot's analysis of Seaglider performance through the previous dive.

Seaglider metadata and raw dive data are downloaded to the base station, after which a metadata database is automatically updated, and dive sensor data is processed automatically with Matlab scripts to generate a new set of plots for display on the SAMS Seaglider website: 'velocity.sams.ac.uk'. The raw data and processed ascii files (split into upward and downward profiles for each dive) are made available to BODC (British Oceanographic Data Centre), which pulls the data and makes the raw data available to the GTS (Global Telecommunication System) of the WMO (World Meteorological Organization) for incorporation into operational weather prediction systems. Processed data are made available to BODC in near-real time, and to the general community through BODC.

Figure CS3.3: Image of SAMS Seaglider 156 'Talisker' (top left), schematic of a Seaglider dive (top right), photograph of Talisker enroute to mission 1 deployment in the Sea of Hebrides on 12 October, 2009 (bottom left), and recovery by the Northern Lighthouse Board 'NLV Pole Star' on 9 March, 2010 (bottom right). The Talisker image shows the Seabird Electronics CT and dissolved oxygen sensors (top forward and aft, respectively), and Wetlabs triplet puck (barely visible bottom aft). Deployment was conducted from an 11 m RHIB operated by Coastal Connection, of Oban, Scotland. The Seaglider schematic, illustrating glider attitude during GPS fixes and Iridium satellite communications, is from www.apl.washington.edu/projects/seaglider/summary.html. Talisker image is from the SAMS

Seaglider basestation webpage, velocity.sams.ac.uk; Talisker deployment and recovery photos are from Sherwin and Dumont (2012a).

CS3.5. Seaglider 156 Mission 1: Repeat transects of the Rockall Trough in winter

CS3.5.1. Operational information

For its first operational deployment, SAMS Seaglider Talisker was tasked with repeatedly sampling across the Rockall Trough (RT), in a mission that was designed to not only return useful data on the evolution of the North Atlantic in winter, but also resolve otherwise unanswerable questions regarding the level of effort and expense, as well as reliability and practicality, of running glider operations from the west coast of Scotland. Talisker was deployed on 12 October 2009 about 15 nm west of the island of Tiree, in the Sea of the Hebrides, from a commercially operated 11 m RHIB operating out of Oban (see Fig. CS3.3). After first traversing westward to the shelf edge, Talisker made 789 dives, while conducting four complete transects of the RT, until failure of the roll motor on 8 March 2010 prevented further navigation control, by which time it had used 63% of the total battery energy available. Recovery was completed on 9 March 2010 by the Northern Lighthouse Board vessel *NLV Pole Star*. Highlights from the mission are contained in the abbreviated mission diary in Appendix 4. A more complete description of mission 1 events can be found in Sherwin and Dumont (2012a).

During mission 1, Talisker was outfitted with a Sea-Bird Electronics (SBE) CT sail, measuring temperature and conductivity, an SBE 43F dissolved oxygen sensor, and a WET Labs BB2FL sensor, measuring chlorophyll-a fluorescence and optical backscatter at blue (470 nm) and red (700 nm) wavelengths (see Fig. CS3.3). Review of conductivity and temperature data from the un-pumped CT sensor (Sherwin and Dumont, 2012a), confirmed that conductivity cell thermal mass effects on derived salinity are minimal. Review of dissolved oxygen (DO) data revealed that the un-pumped configuration used on the Seaglider is problematic. Values of DO observed in the upper ocean during mission 1 were on the order of 1 ml l^{-1} lower than expected: in the range 83%-88% of saturation when wintertime values of about 97% were expected (Sherwin and Dumont, 2012a). Post deployment calibration by the manufacturer revealed little drift in the sensor, suggesting that positioning on the Seaglider is problematic with respect to flow through the sensor. The sensor is located aft of the maximum diameter of the vehicle (see Fig. CS3.3), in the region identified in wind tunnel tests as between the points of separation and reattachment of the linear flow (Eriksen et al., 2001).

CS3.5.2. Observational results: large-scale hydrographic structure and temporal variability

Comparison of the Seaglider temperature and salinity from transect 2 of mission 1 in November 2009 (Fig. CS3.4) to a CTD transect from October 2005 (Fig. CS3.1, Sherwin et al., 2012) reveals gross features that compare well between the Seaglider transect and 'climatology' data. In particular, there is general tilt (upward to the west) of isotherms, isohalines, and isopycnals (left column of Fig. CS3.4) although this is concentrated in the western half of the basin in the Seaglider data. There is also a higher concentration of dissolved oxygen within the low-density gradient region above about 800 m (right column of Fig. CS3.4 and right panel of Fig. CS3.5) and a near-surface chlorophyll maximum. The highest salinities are found at 200-300 m depth in the centre of the RT (Figs CS3.4-3.5).

A sequence of three Seaglider transects across the RT illustrates the evolution of the upper ocean in response to strong forcing in winter storms (Figs CS3.6-3.9). The three transects take 14, 13, and 15 days to complete, beginning October 17 (transect 1, east to west), October 31 (transect 2, west to east), and December 29 (transect 4, west to east). The upper ocean remains stratified into November (i.e. through the first two transects) then, during the long third transect (not shown) rapidly gets mixed from the surface to 400 m depth. Isopycnal slopes are considerably steeper in the western half of the RT during transect 2,

after which the DO concentration drops below 400 m, and the chlorophyll-a signal in the upper 100 m drops off. Both deep (400-1000 m) temperature and salinity appear to have increased during the fourth transect (Fig. CS3.9), consistent with both a general shift in the T/S properties in the RT over the course of mission and the presence of mesoscale eddies (Sherwin and Dumont, 2012a). Some oceanic features may be aliased or Doppler smeared, due to the slow speed of the Seaglider. See Rudnick and Cole (2011) for a discussion of the projection of high frequency variability onto spatial structure for features of length scales less than about 30 km.

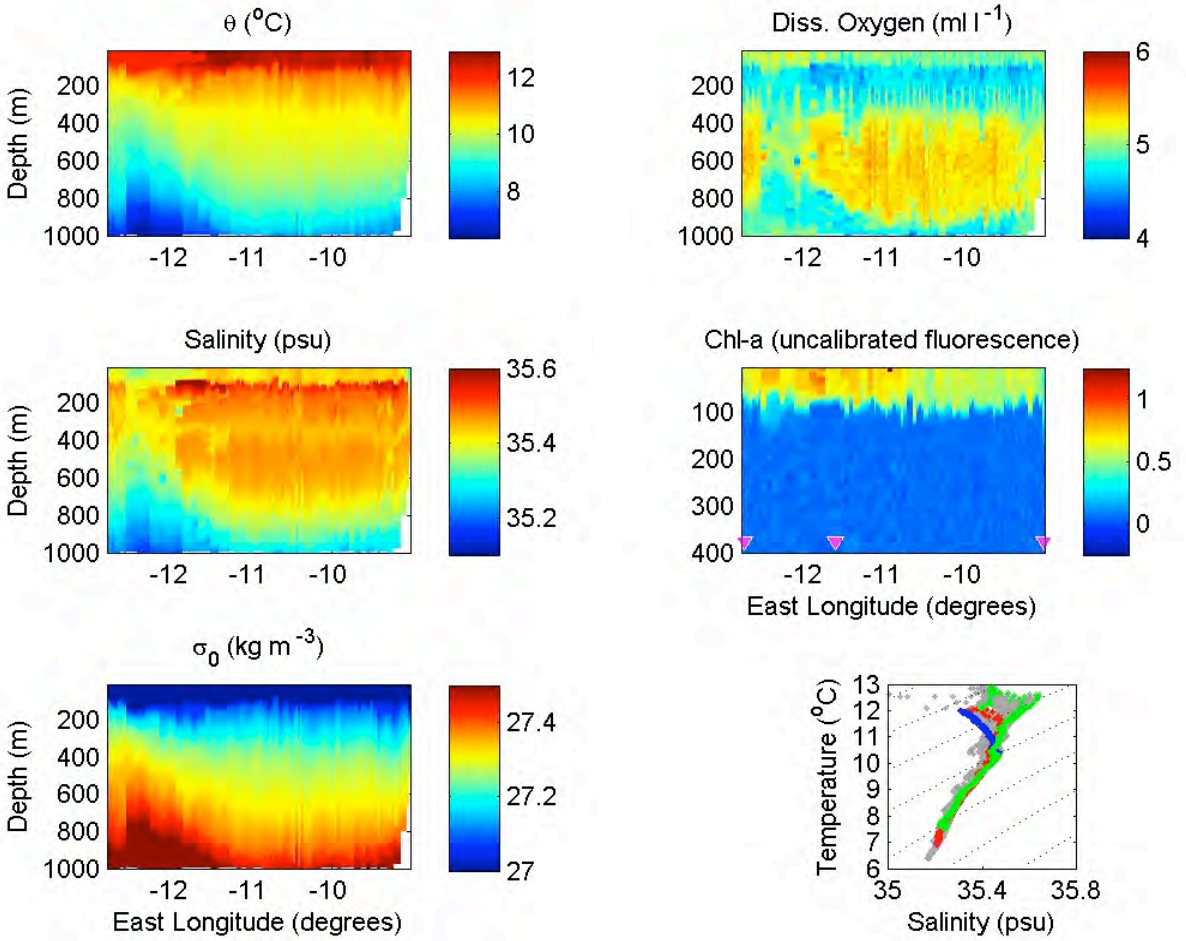

Figure CS3.4: Hydrographic section conducted across the Rockall Trough during Talisker mission 1, transect 2 from 10 October 2009 to 12 November 2009, extending from the eastern slope of Rockall Bank (left) to the Hebridean shelf (right) along the path shown in magenta in Fig. CS3.2 (left panel). Potential temperature (θ, top left), salinity (centre left), potential density (σ, bottom left), dissolved oxygen (top right), and chlorophyll-a fluorescence (centre right), are shown together with the temperature/salinity relationship within the section (bottom right). Potential temperature and potential density are referenced to the surface. All variables have been low-pass filtered in the vertical with a Gaussian scale-width of 10 m and window half-width of 10 m then output on a 5m vertical grid. Upward and downward profiles are plotted separately at the up/down profile-mean positions, as determined from dive start and end GPS fixes. Transect slices are shown as projections onto a line of constant latitude. θ/S curves are shown for all transect dives (grey), and for dives 305 (red, 12.78 °W), 318 (green, 11.63 °W), and 353 (blue, 9.03 °W). Further dive details are shown in Table CS3.1; dive locations are indicated by magenta triangles on the Chlorophyll-a panel.

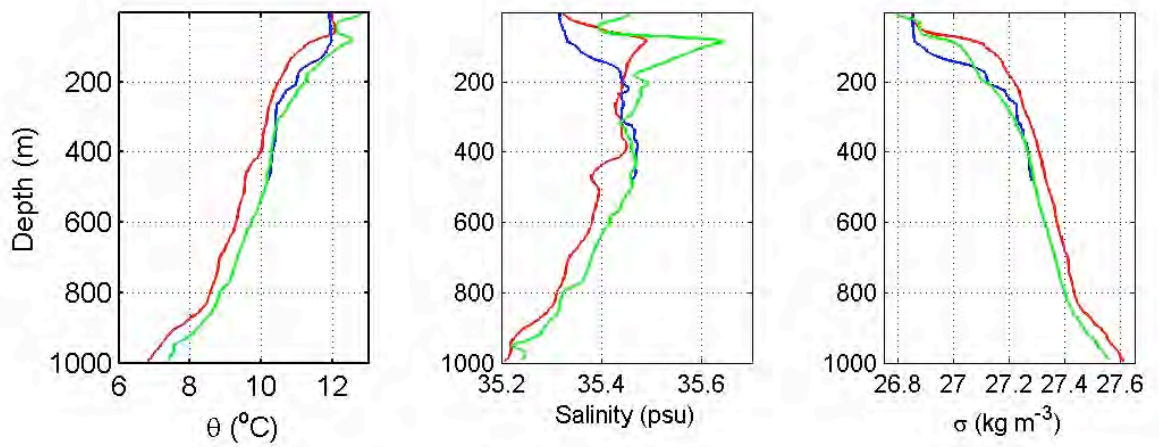

Figure CS3.5: Vertical profiles of potential temperature (θ, left), salinity (centre), and potential density (σ, right) for the downward segments of the dives shown on the T/S curves of Fig. CS3.4: 305 (red, 12.78 °W), 318 (green, 11.63 °W), and 353 (blue, 9.03 °W). Potential temperature and potential density are referenced to the surface. Locations of the dives are indicated by magenta triangles on the Chlorophyll-a panel of Fig. CS3.4.

SAMS Seaglider 'Talisker' mission 1, transect 2			
Dive number	Date	Latitude	Longitude
305	31/10/2009	57.34 °N	12.78 °W
318	03/11/2009	56.82 °N	11.63 °W
353	12/11/2009	56.67 °N	9.03 °W

Table CS3.1: Details of Seaglider dives during mission 1, transect 2, which are shown in the T/S plot of Fig. CS 3.4 and as vertical profiles in Fig. CS 3.5.

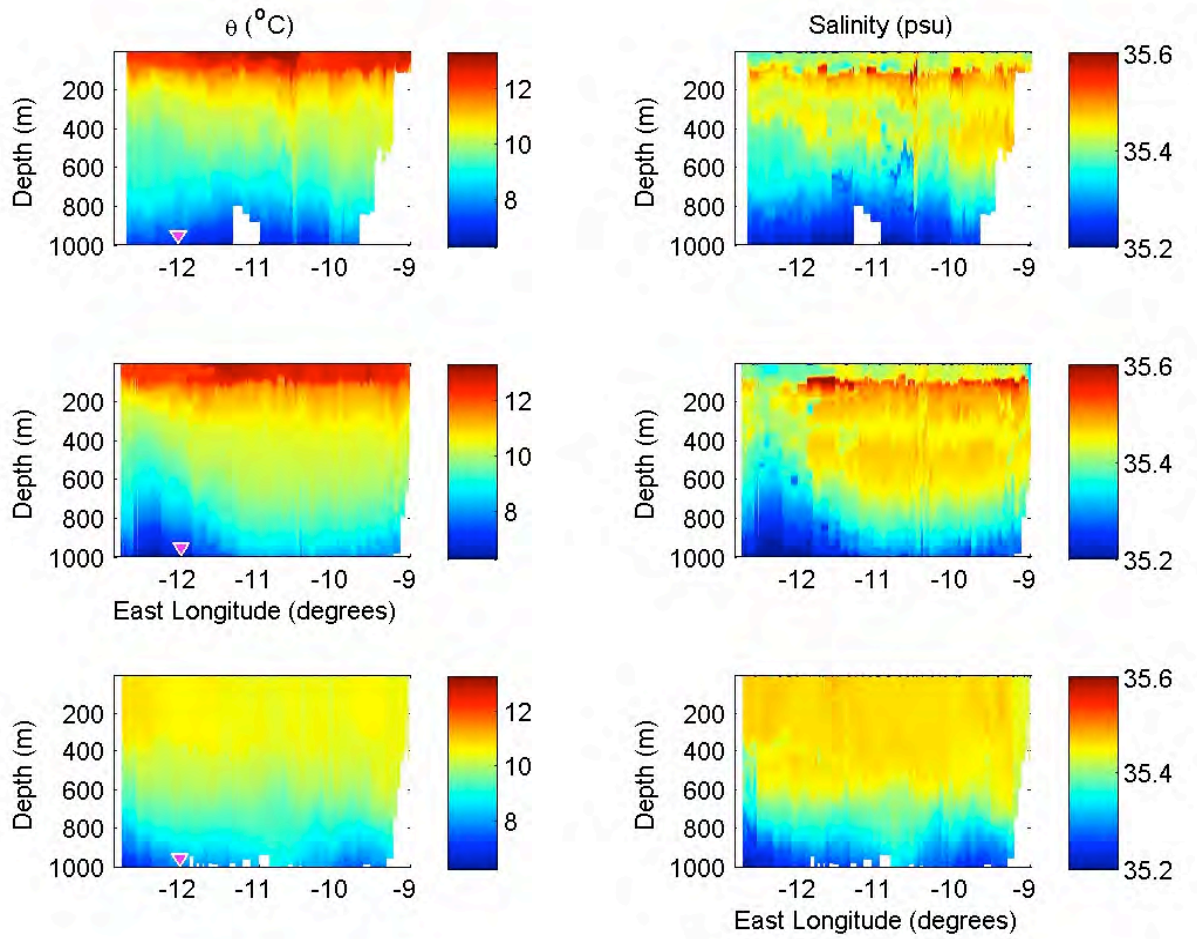

Figure CS3.6: Potential temperature (θ, left column) and salinity (right column) are shown for repeated sections across the Rockall Trough during Talisker mission 1, for transects 1 (top, westward), 2 (centre, eastward), and 4 (bottom, eastward). These transect paths are shown in magenta, red, and green, respectively, in Fig. CS3.2. Processing and plotting is as described for Fig. CS3.4. Eastern and western dive endpoints are shown in Table CS3.2. The locations of dives 294 (transect 1), 316 (transect 2), and 540 (transect 4), for which vertical profiles of θ, S, and σ are shown in Fig. CS3.9, are indicated by the magenta triangles in the θ sections (left panel).

Transect		Transect Western End Point		Transect Eastern End Point	
Number	Direction	Dive Number	Date	Dive Number	Date
1	Westward	299	30/10/2009	194	17/10/2009
2	Eastward	304	31/10/2009	353	12/11/2009
4	Westward	532	12/01/2010	592	29/12/2009

Table CS3.2: Details of the endpoints of Seaglider mission 1 transects 1, 2, and 4, data from which are shown in Figs CS3.6-3.9.

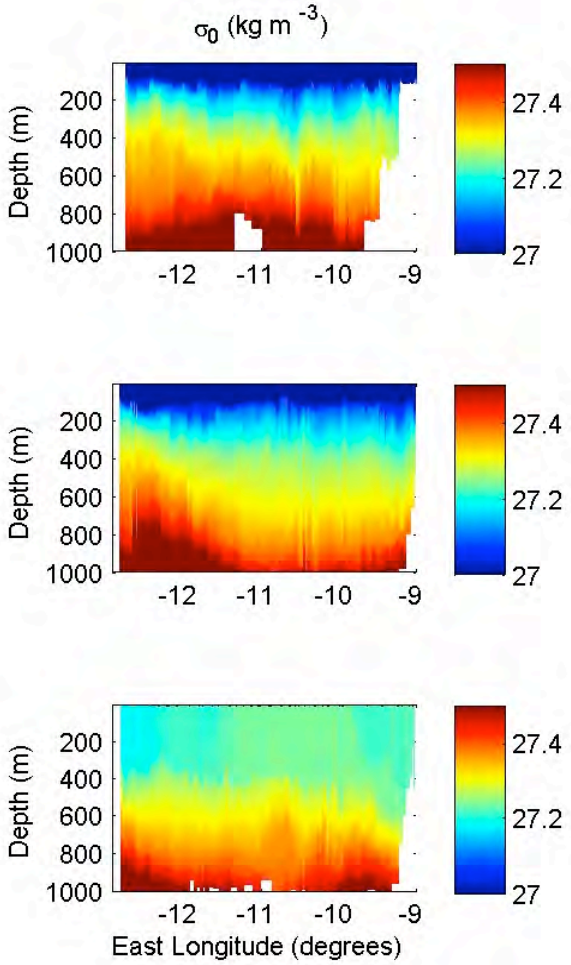

Figure CS3.7: Potential density (σ_0) is shown for repeated sections across the Rockall Trough during Talisker mission 1 for transects 1 (top, westward), 2 (centre, eastward), and 4 (bottom, eastward). Transect dive content as described for Fig. CS3.6.

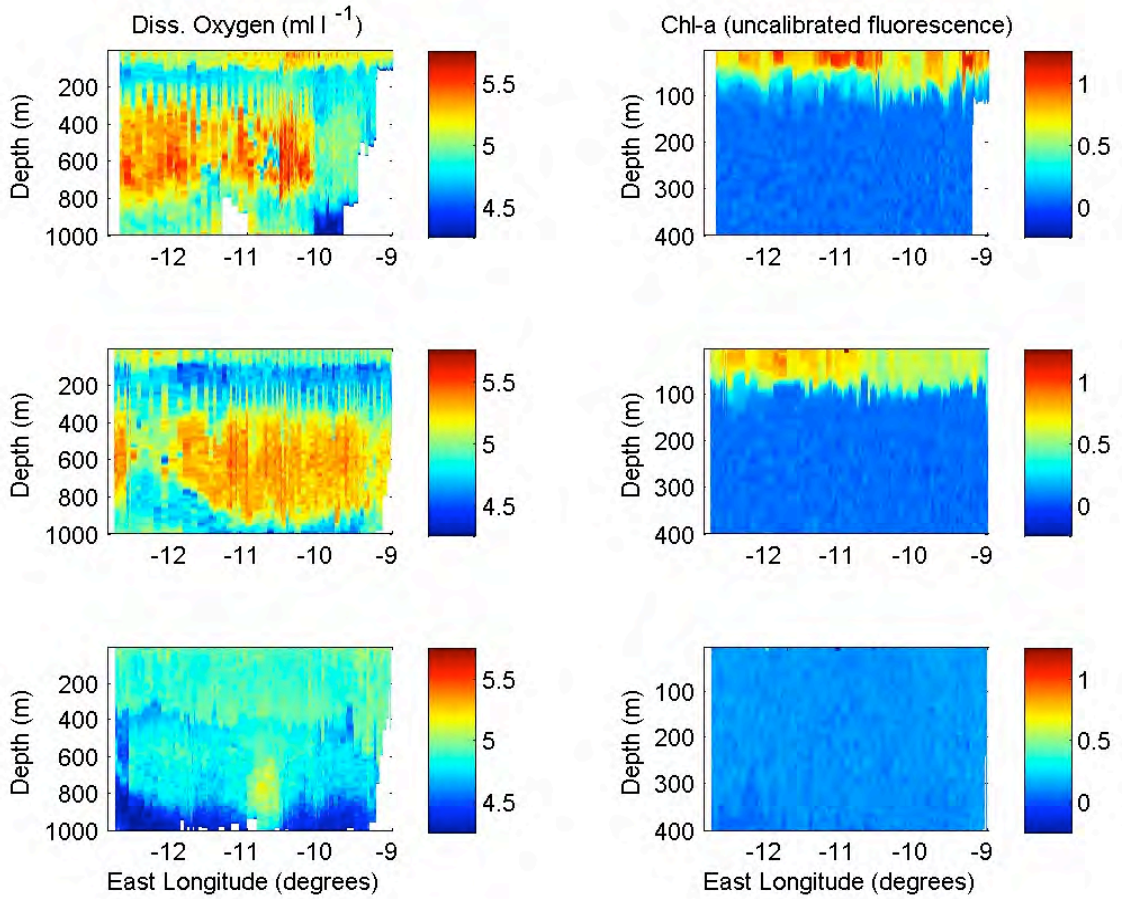

Figure CS3.8: Dissolved oxygen (left) and chlorophyll-a fluorescence (right) are shown for repeated sections across the Rockall Trough during Talisker mission 1 for transects 1 (top, westward), 2 (centre, eastward), and 4 (bottom, eastward). Transect dive content as described for Fig. CS3.6.

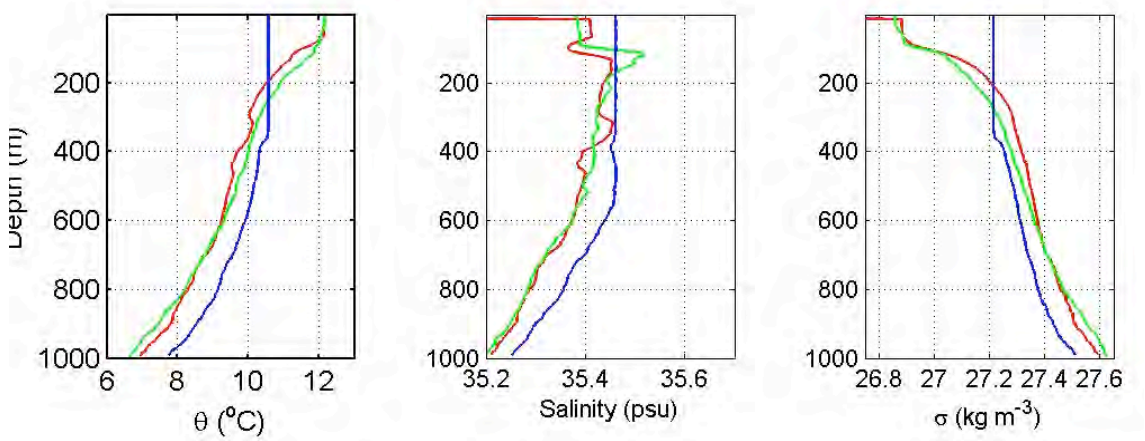

Figure CS3.9: Vertical profiles of potential temperature (θ, left), salinity (centre), and potential density (σ, right) for the downward segments of the dives closest to 12°W in Figs CS3.6-3.8, during Talisker mission 1: transect 1, dive 294 (red); transect 2, dive 316 (green); and transect 4, dive 540 (blue). Potential temperature and potential density are referenced to the surface. The locations of these dives are indicated by the magenta triangles in the potential temperature panel of Fig. CS3.6. Further dive details are shown in Table CS3.3.

SAMS Seaglider 'Talisker' mission 1				
Transect number	Dive number	Date	Latitude	Longitude
1	294	28/10/2009	57.38°N	12.05°W
2	316	03/11/2009	56.83°N	12.01°W
4	540	31/12/2009	57.34°N	12.03°W

Table CS3.3: Details of Seaglider dives closest to 12°W during mission 1, transects 1, 2, 4, which are shown as vertical profiles in Fig. CS3.9.

CS3.6. Seaglider 156 Mission 2: Scotland to Faroe via Rockall and Iceland

CS3.6.1. Operational information

The primary objective for Talisker's second mission was to conduct a survey of the Rockall Trough and Iceland Basin along the route of the Extended Ellet Line (Fig. CS3.2). A secondary objective was to then conduct repeated transects across the southern end of the Faroe-Shetland channel in support of measurements being made there by the Faroe Marine Research Institute (FAMRI), Marine Scotland, and SAMS. A third objective was to conduct a validation exercise through simultaneous Seaglider and ship-based CTD casts along the Ellett Line. Talisker was deployed west of Tiree on 3 May 2001, again using Oban-based RHIB operators Coastal Connection. The first few weeks of mission 2 coincided with the annual Extended Ellett Line survey conducted by the *RRS Discovery*, however, the planned validation rendezvous was not possible due to cruise delays and bad weather. Talisker successfully completed the primary objective and was transiting along the southern flank of the Iceland-Faroe Ridge when a battery pack failure forced premature termination of the mission on 24 August. Highlights from the mission are shown in the abbreviated diary in Appendix 4, and a more complete description of the mission can be found in Sherwin and Dumont (2012b).

CS3.6.2. Extended Ellett Line: Discovery Cruise D365

The 2011 Extended Ellett Line cruise of the *RRS Discovery* was delayed due to mechanical issues and then hampered by bad weather, allowing only 32% of the allocated cruise time (22 days) for sampling. Nevertheless, D365 successfully covered the Ellett Line, extending the time series of hydrographic sampling to 36 years. Working back along the survey line from Iceland, *Discovery* began the southward 20°W segment on 24 May and finished on 29 May, arrived at Rockall Bank on 29 May and reached the Hebridean shelf on 31 May. In comparison, the Seaglider was in the Rockall Trough from 10 May through 28 May.

CS3.6.3. Observational results: Seaglider mission

Figs CS3.11 and 3.12 show the large-scale hydrographic structure from the Sea of the Hebrides across the Rockall Trough and into the Iceland Basin as measured by the Seaglider between 6 May and 19 June, with the Rockall Trough subsection shown in greater detail in Fig. CS3.10. There is a clear distinction between water masses to the east and west of Rockall Bank, with colder, fresher water found in the Iceland Basin. Smaller scale variability is seen in the chlorophyll-a signal, while the dissolved oxygen signal also shows significant variability within the Rockall Trough. Some of the higher frequency variability in the temperature and salinity signals within the Rockall Trough (Fig. CS3.10) are related to capture within the mesoscale eddy apparent in the cruise track of Fig. CS3.2 (see also Appendix 4).

CS3.6.4. Observational results: Comparison to D365 CTD data

Having concluded that the consistently low measured values of dissolved oxygen during mission 1 were due to use of the SBE 43F sensor in an unpumped mode on the Seaglider (as discussed above), an Aanderaa 4330 Optode dissolved oxygen sensor was installed for

simultaneous measurement and comparison to the SBE 43 during mission 2. Whereas the SBE 43F dissolved oxygen sensor consistently provided lower values than expected, the Aanderaa Optode returned values that were consistently higher than expected. In a comparison between six Seaglider dives and six nearby D365 CTD casts, the Optode yielded DO values that were 0.72 mg l^{-1} higher. Detailed comparison shows that the bias is a function of depth, a correction algorithm for which is pending (Sherwin and Dumont, 2012b). Talisker Optode DO values are plotted uncorrected in Figs CS3.10 and 3.11, and offset by -1 ml l^{-1} in Fig. CS3.14, where Seaglider profiles are compared to D365 CTD profiles. Data from the WET Labs BB2FL triplet puck began to show signs of biofouling on 15 July and the sensor was consequently shut off on 30 July.

Comparison between the D365 and Seaglider transects from the Hebridean shelf to the Iceland Basin (Figs CS3.11 and 3.13) shows very good agreement with respect to the large scale temperature, salinity, and density structure throughout the upper 1000 m, although the Seaglider data reveals much more variability because these fields are more highly resolved (albeit with noise due to aliasing). Chlorophyll-a fluorescence shows the same vertical dependence, and similar horizontal features in the upper 100 m, notably a large patch of high fluorescence between 14°W and 16°W. Although the magnitudes of the dissolved oxygen signals differ by about 1 ml l^{-1}, similar vertical and horizontal structures are sampled by both sensors, subject to the same caveat regarding horizontal resolution. Comparison between specific vertical profiles from similar longitudes, though temporally and latitudinally separated, reveal the high level of correlation in the vertical and distinction between water masses on either side of Rockall Bank (Fig. CS3.14).

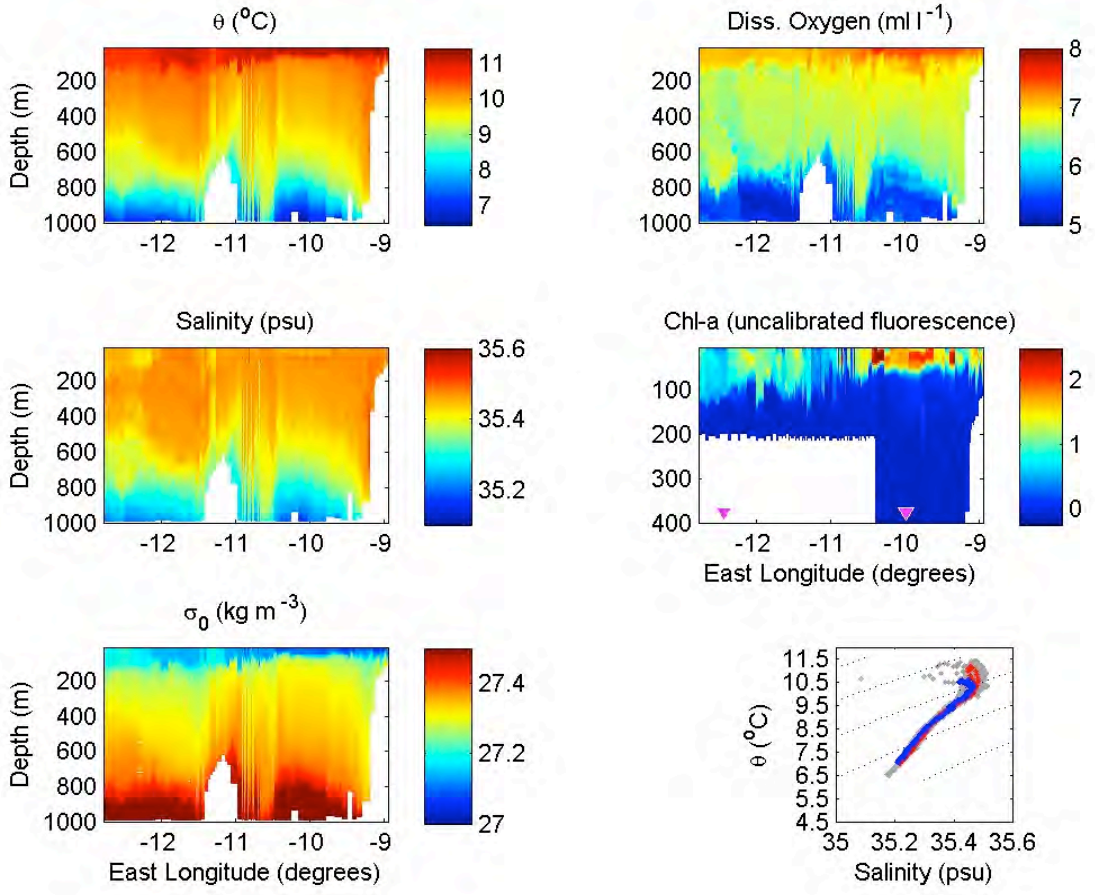

Figure CS3.10: Hydrographic section conducted across the Rockall Trough during Talisker mission 2 from 10 May to 28 May 2011, extending from the western slope of the Hebridean shelf (right) to the eastern slope of Rockall Bank (left) along the path shown in green in Fig.

CS3.2 (right). Potential temperature (θ, top left), salinity (centre left), potential density (σ, bottom left), dissolved oxygen (top right), and chlorophyll-a fluorescence (centre right), are shown together with the temperature/salinity relationship within the section (bottom right). Processing and plotting is as described for Fig. CS3.4. θ/S curves are shown for all transect dives (grey), and for dives 310 (red, Hebridean continental slope), and 376 (blue, Rockall Trough). Locations of these dives are indicated by magenta triangles on the Chlorophyll-a panel.

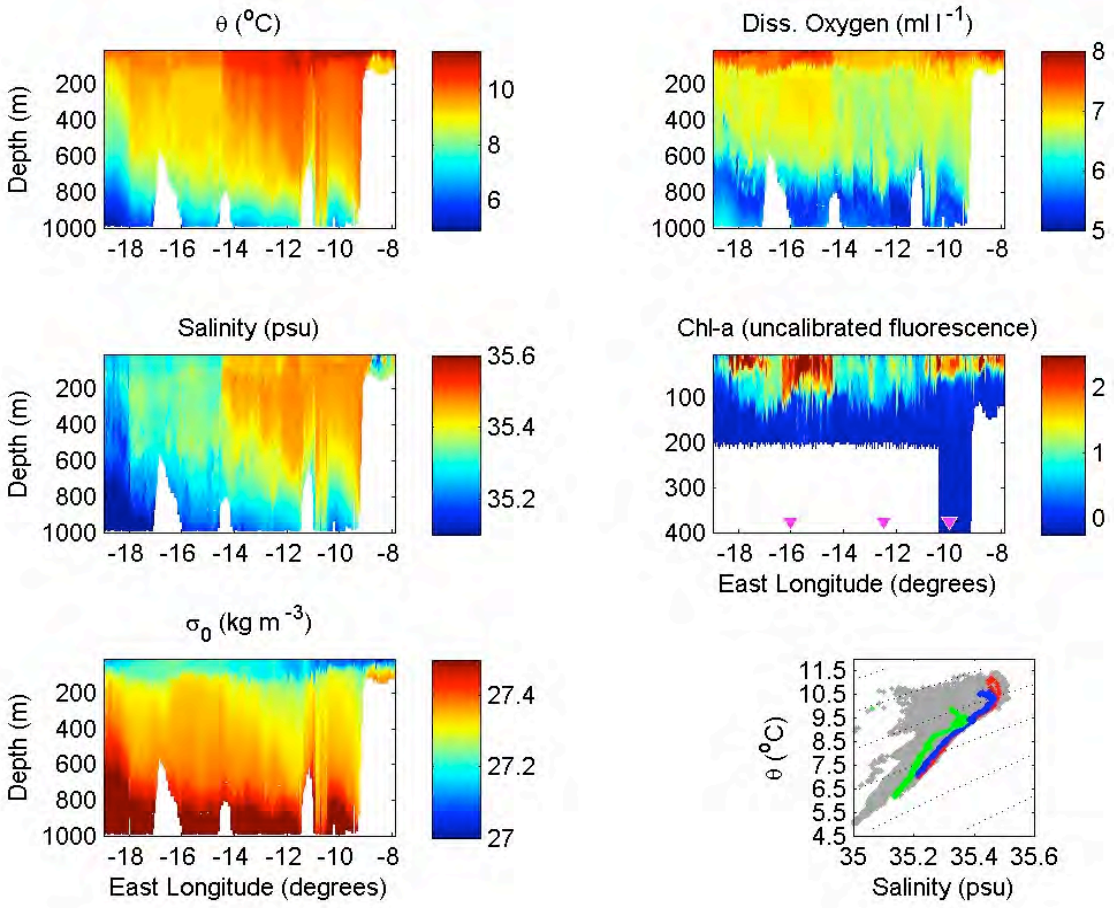

Figure CS3.11: Hydrographic section conducted along the Ellett Line from 06 May to 19 June 2011, during Talisker mission 2, encompassing the sub-section shown in Fig. CS3.10 and extending from the Hebridean shelf (right) through the Rockall Trough and over Rockall Bank to the Iceland Basin (left) along the path extended in magenta in Fig. CS3.2 (right). Potential temperature (θ, top left), salinity (centre left), potential density (σ, bottom left), dissolved oxygen (top right), and chlorophyll-a fluorescence (centre right), are shown together with the temperature/salinity relationship within the section (bottom right). Processing and plotting is as described for Fig. CS3.4. θ/S curves are shown for all transect dives (grey), and for dives 310 (red, Hebridean continental slope), 376 (blue, Rockall Trough), and 422 (green, Iceland Basin). Locations of these dives are indicated by magenta triangles on the Chlorophyll-a panel.

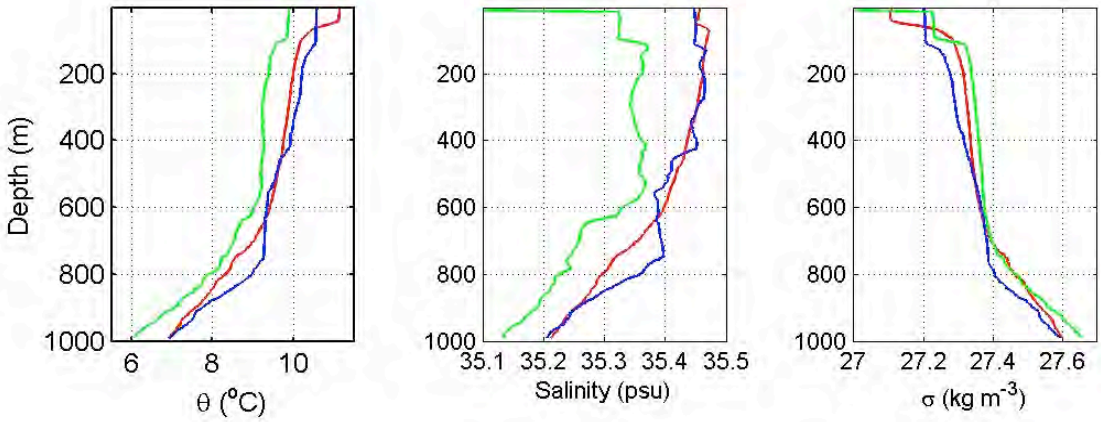

Figure CS3.12: Vertical profiles of potential temperature (θ, left), salinity (centre), and potential density (σ, right) for downward segments of dives 310 (red, Hebridean continental slope), 376 (blue, Rockall Trough), and 422 (green, Iceland Basin). Potential temperature and potential density are referenced to the surface. Locations of these dives are indicated by magenta triangles on the Chlorophyll-a panel of Fig. CS3.11.

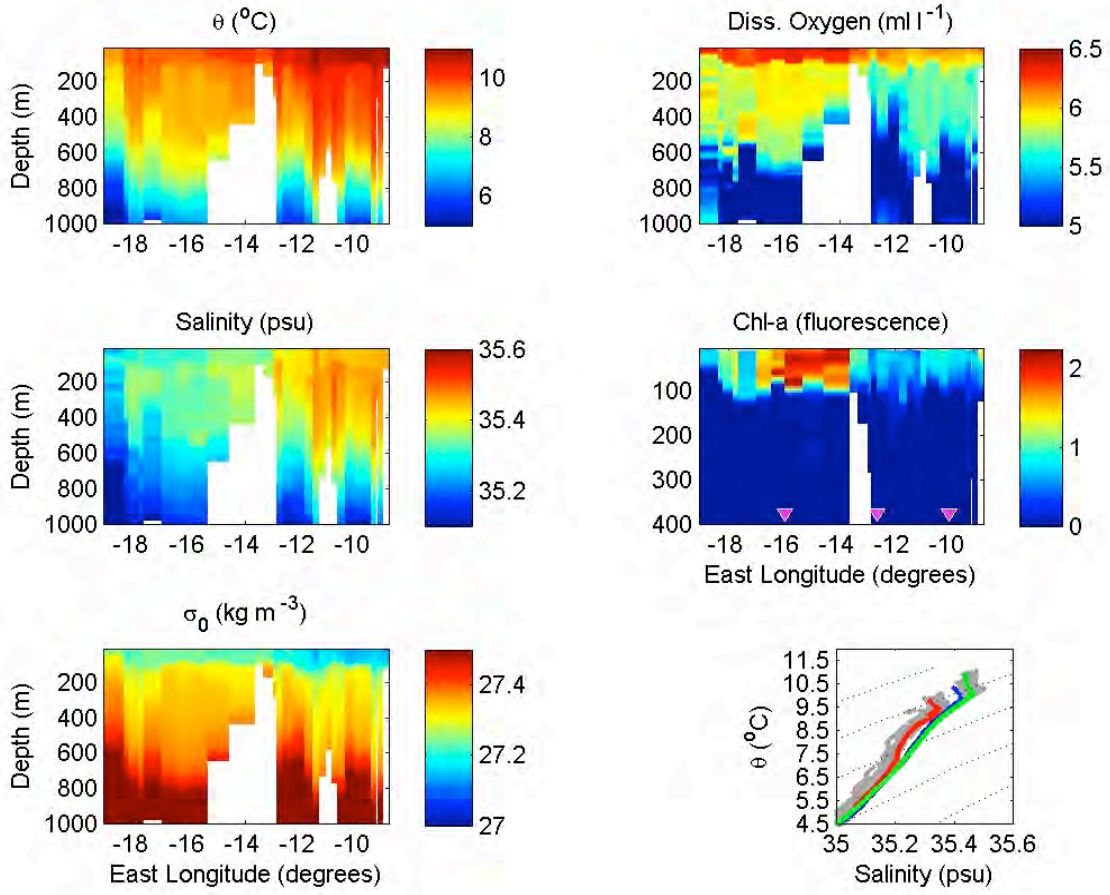

Figure CS3.13: CTD hydrographic section conducted by RRS Discovery as cruise D365 along the Ellett Line from 27 May to 31 May 2011, extending from to the Iceland Basin (left) over Rockall Bank and through the Rockall Trough to the Hebridean shelf (right), along the grey path in Fig. CS3.2 (right). Potential temperature (θ, top left), salinity (centre left), potential density (σ, bottom left), dissolved oxygen (top right), and chlorophyll-a fluorescence (centre right), are shown together with the temperature/salinity relationship within the section (bottom right). θ/S curves are shown for all transect CTD casts (grey), and for casts 34 (red, Iceland Basin), 41 (blue, Rockall Trough), and 50 (green, base of Hebridean continental

slope). Locations of these dives are indicated by magenta triangles on the Chlorophyll-a panel.

Location	SAMS Seaglider 'Talisker' mission 2				RRS Discovery Ellett Line cruise D365			
	Dive number	Date	Latitude	Longitude	CTD cast number	Date	Latitude	Longitude
Hebridean Slope	310	12/05/11	57.235°N	9.978 °W	50	31/05/11	57.241°N	10.042 °W
Rockall Trough	376	28/05/11	58.131°N	12.445 °W	41	30/05/11	57.528°N	12.641 °W
Iceland Basin	422	08/06/11	59.118°N	15.988 °W	34	29/05/11	58.499°N	16.000 °W

Table CS3.4: Details of selected Seaglider mission 2 dives and closest D365 CTD casts, as shown in the T/S plots of Figs CS3.11 and 3.13, and as profiles in Figs CS3.12 and 3.14.

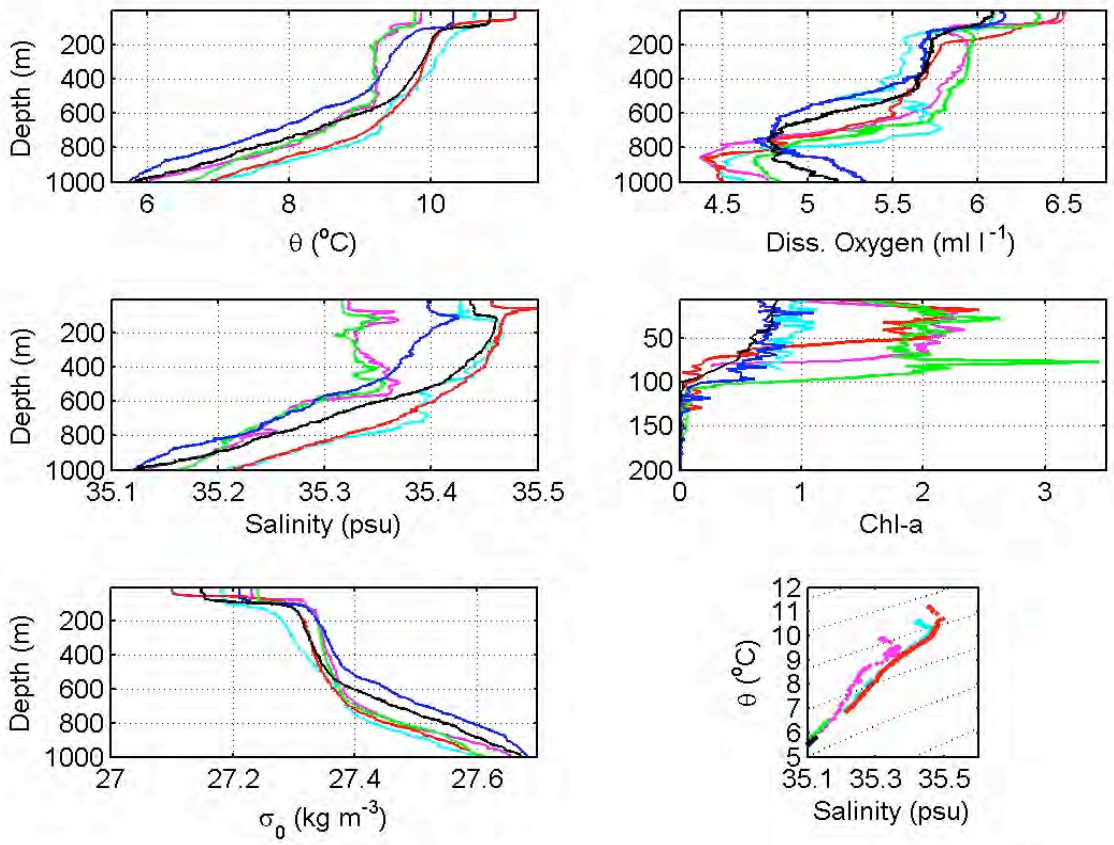

Figure CS3.14: Vertical profiles of potential temperature (θ, top left), salinity (centre left), potential density (σ, bottom left), dissolved oxygen (top right), dissolved oxygen (top right), and chlorophyll-a fluorescence (centre right), are shown together with the temperature/salinity relationship for selected locations from cruise D365 and Talisker mission 2, details of which are shown in Table CS3.4, and locations shown in Figs CS3.11 and 3.13. Talisker dives 422, 376, and 310 are shown as magenta, cyan, and red, respectively, and D365 CTD casts 34, 41, and 50 are shown as green, blue, and black, respectively

CS3.7. Seaglider performance

CS3.7.1. Mission 1 endurance

The energy supply in the Seaglider is split between low voltage (10 VDC) and high voltage (24 VDC) battery packs of nominally 112 Ah and 147 Ah, respectively. During the 5.1-day westward traverse to the shelf edge after deployment in the shallow Sea of the Hebrides, Talisker used 12% of the 24V battery and 3.6% of the 10V battery, at rates of 2.4% per day and 0.7% per day, respectively. Once in deep water, making dives to the full range of 1000 m, the Seaglider rate of energy consumption dropped considerably. The average consumption over the next 141.6 days, until mission termination due to roll motor failure, was 0.4% per day for both battery packs. From the point of beginning the RT transects with the first deep dive (>300 m, dive 232) on 18 October 2009 to completing the fourth round trip (eighth transect) 140 days later on 5 March 2010 (dive 780), Talisker covered 3759 km over the ground in sampling over a nominal path length of about 8*242 km = 1936 km.

CS3.7.2. Mission 2 endurance

During mission 2, Talisker covered a total of 2987 km over the ground while completing 841 dives over 123 days (compared to 789 dives over 148 days during mission 1). During the Extended Ellett Line segment of the mission, from 9 May 2011 (dive 232) to the farthest north point (dive 566 at 63.31°N) near the Icelandic shelf on 13 July, Talisker completed 335 dives and covered 1691 km over the ground in nominally sampling the 1126 km path covered by the *Discovery* between CTD stations 14 (Icelandic shelf edge) and 55 (Sea of the Hebrides shelf edge at 8.78°W).

Mission 2 was terminated after the voltage in the 24 V battery pack dropped precipitously from 20.6 to 19.6 VDC between dives 744 and 755. Such rapid drops in voltage are characteristic of the end stage of discharge of lithium batteries. This occurred after use of significantly less energy than was expected from the battery pack. This battery also exhibited an uncharacteristic continuous decrease in voltage over the course of the mission, and an indeterminate battery fault is suspected as the cause of the shortened mission.

CS3.8. Conclusions and future work

CS3.8.1. Operations and sensors

The first two missions of SAMS Seaglider 156 ‘Talisker’ demonstrated the capability of gliders to maintain a persistent sampling presence and replicate some aspects of a conventional hydrographic cruise in the North Atlantic. Following these two successful, long missions, SAMS has opened the North Atlantic Glider Base (NAGB) as a facility to support deep water testing, as well as deployment and recovery of gliders on North Atlantic missions. Building on the experience described here, the NAGB offers access to laboratory space, coastal vessels for testing, deployment, and recovery, as well as advice and assistance with glider operations.

Over the past decade, the oceanographic community has demonstrated the capability of gliders to measure fundamental ocean properties autonomously for long durations in a cost effective manner, and in particular to do so in harsh oceanic conditions whilst removing people from harm’s way. The potential for gliders to replace some aspects of conventional hydrographic cruises has been demonstrated through these early deployments. In the near future, the development of gliders as sampling platforms is expected to focus on the implementation of a variety of low-power, miniaturized sensors, in order to make gliders more effective for conducting a broader spectrum of measurements. For example, the implementation of field-tested microfluidic, reagent-based lab-on-a-chip sensors for measuring several key nutrients on UUVs is currently underway through a NERC-funded research project, with field deployments in the 2013-2015 timeframe.

CS3.8.2. Platforms and autonomy

Low speed is a design trade-off that follows from the specification for long duration at low power usage. The limiting consequence of this for gliders is that navigation through mesoscale eddies and boundary currents, where water velocities are comparable to or greater than the glider speed, can be problematic. At the other end of the UUV spectrum are propeller-driven vehicles that operate at higher speed, but with much shorter deployment durations. One approach being used to expand the functionality of gliders is the development of hybrid vehicles, which behave like traditional gliders most of the time, but use a propeller for short periods to push through adverse boundary currents or eddies.

Finally, while unmanned underwater vehicles (UUVs), such as the gliders described here, are sometimes also referred to as autonomous underwater vehicles (AUVs), they in fact operate as pre-programmed vehicles, with low degrees of autonomy. Another key future development for gliders, as well as propeller-driven UUVs, will be towards increased autonomy, with particular applications to mapping and identification of accidental spills, point sources of pollution, and harmful algal blooms, all of which have potential value in sensitive or economically important coastal regions.

CS 3.9. References

Eriksen, C. C., T. J. Osse, R. D. Light, T. Wen, T. W. Lehman, P. L. Sabin, J. W. Ballard, and A. M. Chiodi (2001), Seaglider: A Long-Range Autonomous Underwater Vehicle for Oceanographic Research, IEEE J. Oceanic Eng., 26, 424-436.

Frajka-Williams, E., P. B. Rhines, and C. C. Eriksen (2009), Physical controls and mesoscale variability in the Labrador Sea spring phytoplankton bloom observed by Seaglider, Deep Sea Research I, 56, 2144-2161. doi:10.1016/j.dsr.2009.07.008

Frajka-Williams, E., C. C. Eriksen, P. B. Rhines, and R. R. Harcourt (2011), Determining Vertical Water Velocities from Seaglider. J. Atmos. Oceanic Technol., 28, 1641–1656.

Inall, M., P. Gillibrand, C. Griffiths, N. MacDougal, and K. Blackwell (2009), On the oceanographic variability of the North-West European Shelf to the West of Scotland, J. Mar. Sys., 77, 210-226.

Inall, M. E., and T. J. Sherwin (2006), SEA7 Technical Report – Hydrography, SAMS Report No. 251, 69pp.

Johnson, C., T. Sherwin, D. Smythe-Wright, T. Shimmield, andW. Turrell (2010), Wyville Thompson Overflow Water: spatial and temporal distribution in the Rockall Trough, Deep Sea Res., 57, 1153-1162, doi:10.1016/j.dsr.2010.07.006.

Nicholson, D., S. Emerson, and C. C. Eriksen (2008), Net community production in the deep euphotic zone of the subtropical North Pacific gyre from glider surveys, Limnol. Oceanogr., 53 (5), 2226-2236.

Perry, M. J., B. S. Sackmann, C. C. Eriksen. and C. M. Lee (2008), Seaglider observations of blooms and subsurface chlorophyll maxima off the Washington coast, Limnol. Oceanogr., 53 (5), 2169-2179.

Read, J. F., (2011), Cruise Report No. 06, RRS Discovery Cruise 365, 11 May – 02 Jun 2011, The Extended Ellett Line 2011, National Oceanography Centre, Southampton, 90pp.

Rudnick, D. L., and S. T. Cole (2011), On sampling the ocean using underwater gliders, J. Geophys. Res., 116, C08010, doi:10.1029/2010JC006849.

Sherwin, T., and E. Dumont (2012a), Talisker (Seaglider 156) Mission 001, Rockall Trough 12 October 2009 to 09 March 2010: A winter survey of the Ellett Line, SAMS Report No. 272.

Sherwin, T., and E. Dumont (2012b), Talisker (Seaglider 156) Mission 002, Scotland to Faroe, 03 May 2011 to 03 September 2011: A survey of the NE Atlantic, SAMS Report, in preparation.

Sherwin, T.J., J. F. Read, N. P. Holliday, and C. Johnson (2012), The impact of changes in North Atlantic Gyre distribution on water mass characteristics in the Rockall Trough, ICES J. Mar. Sci., doi:10.1093/icesjms/fsr185, in press.

Case Study 4: Shallow-water Glider mapping in the Irish Sea

CS Leader: Dr Matthew Palmer (NOC) with contributions from Dr. Chris Balfour, Phil Knight (NOC) and Carl Spingys (Univesity of Liverpool)

CS4.1. The CS4 task

As set out in the proposal this task's remit was as follows:

"*In spring 2012, a MARS Glider will be deployed from a boat offshore north Wales with the intention of monitoring development of spring stratification of the water column in an area of the Western Irish Sea. This will also allow study of tidal mixing front development in this region (frontogenesis), which is partly covered by a rMCZ. Measured parameters will include temperature, salinity and biomass (via chlorophyll-a fluorescence). Traditionally, measurements in such regions have depended on short-lived shipborne surveys and single-point measurements from moorings. This two-month Glider deployment offers sufficient longevity and resolution to capture important processes in these spatially and temporally dynamic regions. Importantly, Glider data will be calibrated with in situ boat-based measurements obtained during deployment, mid-mission and recovery, and also with NEODAAS satellite remote-sensing data. The data will also be used to validate and test larger-scale hydrodynamic-ecosystem models being developed at NOC. Additional Glider data collected from a rMCZ in Liverpool Bay in February 2011 will also contribute to this case study.*

This Case Study will be compiled by NOC between 1 March and 31 August 2012."

CS4.2. Introduction and overview

The two glider deployments contained within this case study cover significantly different regions of the Irish Sea, one in the deeper western regions off the coast of Ireland and the other in the shallow Liverpool Bay region in the east.

CS4.2.1. Western Irish Sea (WIS)
The Western Irish Sea (WIS) is a region that has attracted extensive scientific focus due to its isolated seasonal cycle of stratification and circulation (e.g. Sherwin, 1987; Hill et al, 1994) and for its associated ecological importance as a spawning and nursery ground for many commercially exploited fish e.g. Dickey-Collas, 1997).

A NOC shallow water (200m rated) Slocum glider (unit 117) was deployed between 2nd April and 17th May 2012 with the intention of performing multiple transects between two waypoints in the WIS, which have been identified from previous years' surveys and remote sensing data to be located to the east and west of the seasonal front that typically develops in the region during spring months (Fig. CS4.1). The scientific objectives of the deployment were to 1) study the physical development of the WIS front and stratified gyre, 2) develop greater understanding of the competition between stratifying and mixing forces within such features, 3) observe the biological consequences of the developing physical structure, and 4) produce a high-quality dataset for testing and validation of state-of-the-art coupled physical-ecosystem models being developed and run at NOC. Alongside this primary mission, NOC was also testing the Slocum glider capability for extended duration missions in shelf sea environments following upgrades to the glider power supply. Prior to this deployment the longest duration mission achieved by NOC was three weeks. To exploit the extended duration capability of unit 117 the decision was made to 'fly' the glider into position from a more easily accessible location in Liverpool Bay (see Fig. CS4.1), close to the NOC-L laboratory, and within range of the University of Liverpool research vessel RV *Marisa*. This

provided a cost effective deployment option and a novel dataset from the across-Irish Sea transit. Prior to the early April 2012 deployment, the UK and Ireland experienced unseasonably fine weather and high temperatures (Fig. CS4.2) during the last week of March; this led to early stratification of the WIS region and subsequently triggered an early '*spring plankton bloom*'. Unfortunately, therefore, the development of such features was not observed as planned, however, the subsequent evolution of physical and biological structure was achieved and is reported here.

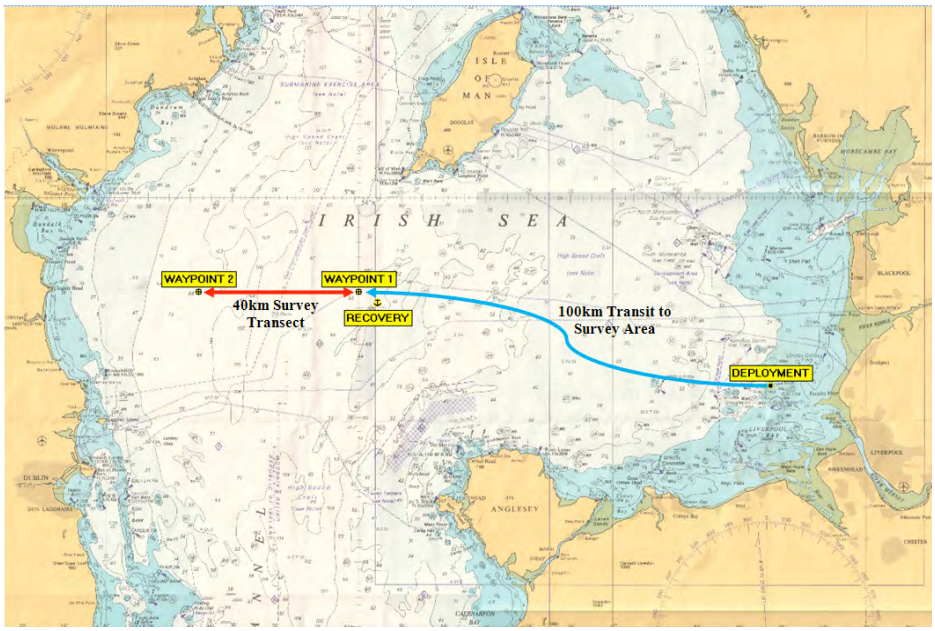

Figure CS4.1. Overview of the Unit 117 Western Irish Sea deployment and survey transect

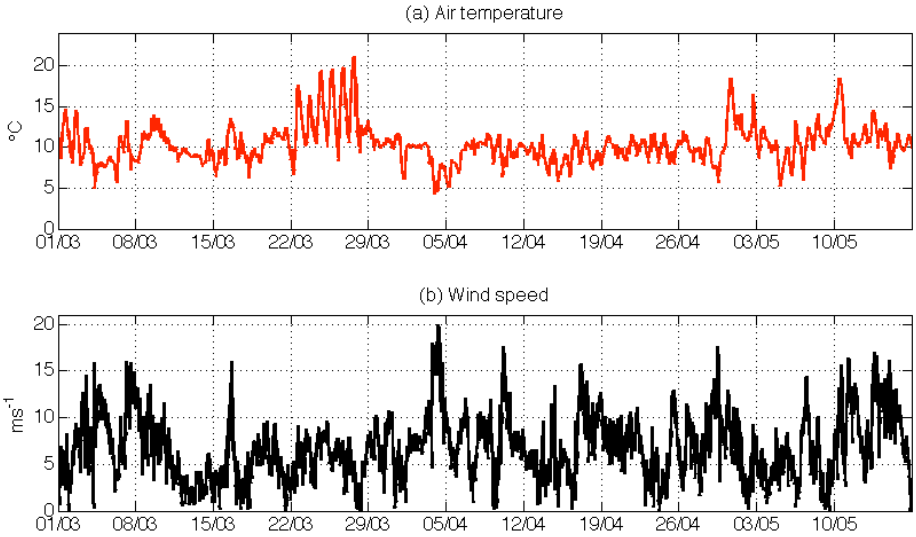

Figure CS4.2: (a) Air temperature and (b) wind speed from a land based Irish Sea meteorological station from 1st March 2012 to the end of the glider deployment period in mid-May.

CS4.2.2. The Mersey Plume region of the Eastern Irish Sea

The Mersey Plume region is a Region Of Freshwater Influence (ROFI, Simpson et al, 1993) where high river flow, shallow water, and strong tidal currents interact to control the local dynamics (Palmer, 2010; Palmer and Polton, 2011) and impact on the freshwater and

biogeochemical pathways of major English and Welsh rivers (Greenwood et al, 2011). Initial investigations of the Mersey Plume were first carried out in 2011, as outlined below.

A NOC shallow water Slocum glider (unit 194) was deployed for a period of 19 days between 10th February and 1st March 2011 with the intention of performing multiple transects between two waypoints in Liverpool Bay that had been identified from remote sensing measurements to regularly intersect the coastal current produced by freshwater inputs from the Rivers Mersey, Ribble and Dee (Fig. CS4.3). The scientific driver for this study was to develop greater understanding of the freshwater and biogeochemical pathways in Liverpool Bay, the largest influence on which is the River Mersey, and to provide high resolution, near-shore data for testing and validation of NOC coastal ocean models, something identified as lacking from the decade-long sustained observations of the Liverpool Bay Coastal Observatory (Howarth and Palmer, 2011). Additionally, the mission aimed to test the capability of such platforms in the highly dynamic environment of Liverpool Bay, where 10 m tides drive regular 1 m/s flows and complex shallow water dynamics result in strongly sheared tidal currents (Palmer, 2010). The shallow water of the bay provided a further test for the gliders; since vertical motion is required to generate propulsion, gliders are traditionally considered inefficient in shallow water. This study showed, for the first time, that correctly tuned gliders provide a suitable platform for monitoring coastal environments.

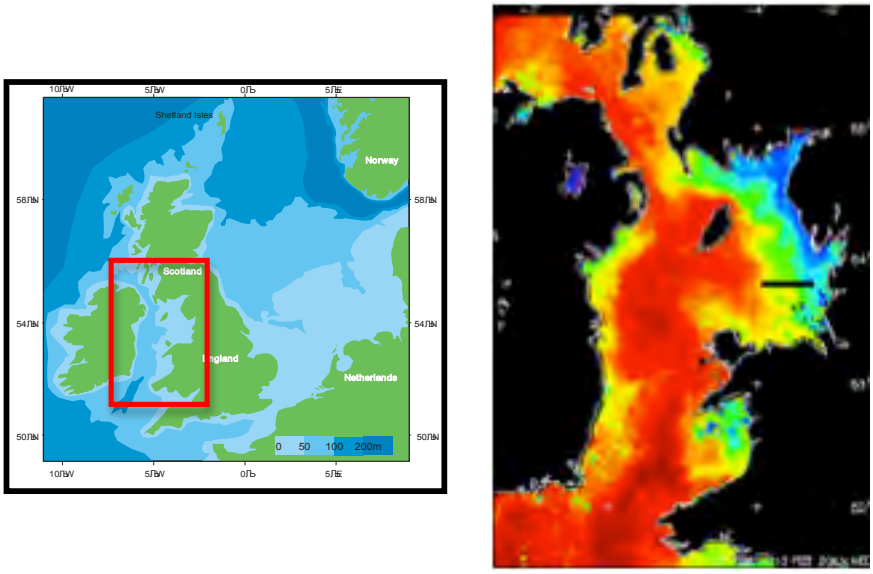

Figure CS4.3: The right panel shows the approximate location of the glider transect relative to the freshwater inflow to Liverpool Bay and the Irish Sea in late winter 2011. The sea surface temperature (NEODAAS) identifies freshwater land run-off as cooler (blues and greens) than the warmer (reds and yellows) pelagic waters of the Irish Sea. The approximate position of the glider transect is shown as a black line in the right panel.

CS4.3 Mission details

CS4.3.1. Western Irish Sea

Technical details: Glider 117 was configured to internally record data from its science sensors at two-second intervals. In addition to the internal sensors required for navigation and flight management, the glider sensors comprised a Seabird CTD (conductivity/salinity, temperature and depth), a WetLabs Triplet sensor and an Aanderaa Optode dissolved oxygen sensor. The triplet sensor measures fluorescence and optical backscatter (OBS), from which Chlorophyll-a concentration, CDOM and OBS turbidity can be estimated. The glider was programmed to surface at three-hourly intervals to report its GPS-derived position. After each surfacing an attempt was then made to transfer a portion of the latest

glider operational and science data in near-real-time to the NOC-Liverpool laboratory (NOC-L). This was achieved using the Iridium satellite network.

Deployment: Glider 117 was deployed in Liverpool Bay on 2nd April 2012 using the RV *Marisa*, which is a small charter vessel operated by University of Liverpool. The RV *Marisa* has an onboard, sheltered laboratory area with mains power. This provided suitable facilities for calibration samples to be collected, and configuration of the glider to be undertaken during the early phases of the deployment in Liverpool Bay (Fig. CS4.4).

The RV *Marisa*

The RV *Marisa* internal, sheltered wet laboratory work area

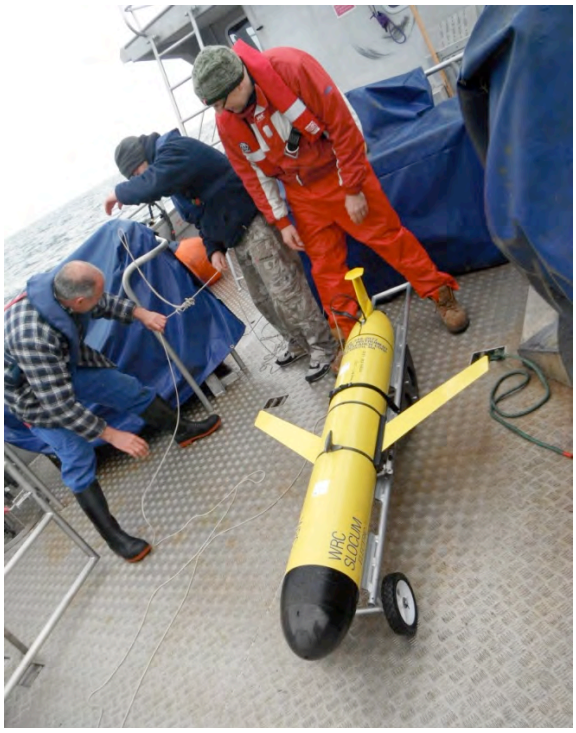

Aft deck preparations for the unit 117 glider deployment on 2nd April 2012

Initial Testing of the deployed glider with a tether and float

Onboard collection and processing of sensor calibration water samples during the cruise

Figure CS4.4: Glider deployment operations aboard the RV Marisa

Flight details: Approximately five days were required for the glider to navigate a distance of just over 100 km to the eastern waypoint of the 40 km-long east-to-west survey transect in the WIS (Fig. CS4.1). When the glider arrived at the required location an east-to-west survey transect was then started between Waypoints 1 and 2 (Table CS4.1).

	Latitude (N)	Longitude (W)
Waypoint 1	53°47.0’	5°00.0’
Waypoint 2	53°47.0’	5°38.0’

Table CS4.1: Transect waypoints for WIS mission

The maximum dive depth of the glider was programmed to 150 m. The glider altimeter was used to initiate a glider climb; if the altimeter reported a seabed range of less than 5 m before the required depth of 150 metres was attained then a climb was initiated, thus allowing maximum safe coverage of the water column to be achieved (Fig. CS4.5).

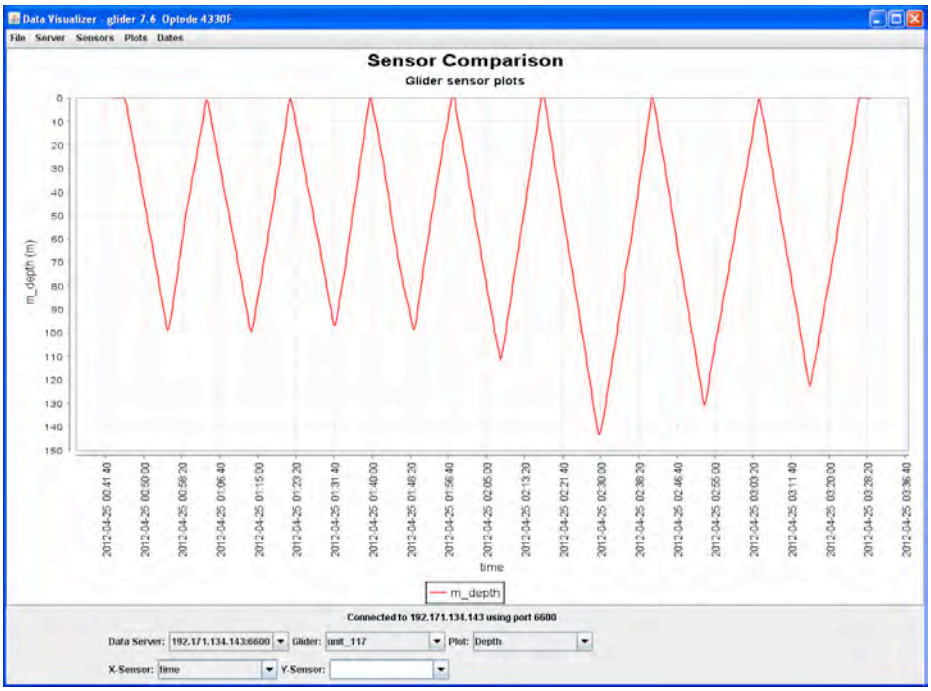

Figure CS4.5: Screengrab showing an example of a glider depth profile

The effect of the altimeter can be seen in Fig. CS4.5 as the glider surveys over what is likely to be uneven seabed, with the peak dive depth occurring at approximately 145 m. The glider was also programmed to inflect when a depth of 5 m was attained during a climb and the sea surface was approached. Vehicle momentum resulted in the glider subsequently turning close to the sea surface after the 5 m inflection threshold had been achieved. The result of this was for scientific measurements to be recorded along almost the full water column during dives and climbs, as required. The resultant effect of tidal currents was to either oppose the glider motion or provide assistance in the required general direction of travel. This depended on the phase of the tidal current relative to the intended glider direction of travel. The result of this interaction with tidal currents was to cause the glider to typically follow a ‘zig-zag’ pattern along the desired survey transect. In general, the glider would provide the required repeated survey around the desired locations as illustrated in Figure CS4.6. As shown in Fig. CS4.5, this provided scientific measurements in a ‘saw-tooth’ pattern diagonally along the water column, with a nominal glider dive and climb angle of 26°. The graphical glider positional plot in Figure CS4.6 demonstrates that sustained scientific measurements with a good spatial and temporal resolution were achieved during the deployment.

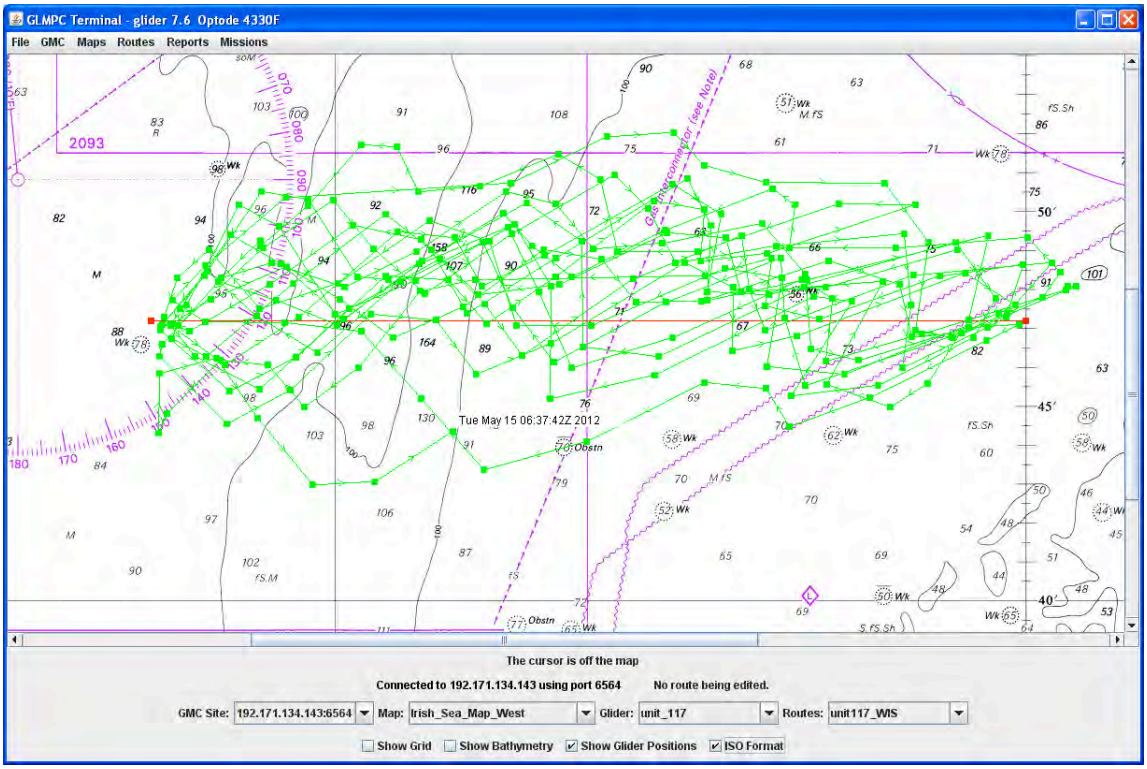

Figure CS4.6: Screengrab showing typical GLMPC Glider Plotting Software Output, indicating actual glider surface positions (green dots) and interpolated tracks (green lines). The two target waypoints (~40 km apart) are shown with red squares, with the straight-line transect indicated by a red line. For precise locations see Table CS4.1.

A rota of 'glider pilots' was used during the glider deployment. Phil Knight and Chris Balfour from NOC-L monitored glider communications during days, evenings and weekends. This ensured that any technical problems that arose during the glider deployment were dealt with in a timely manner. This involved such tasks as monitoring the glider internal memory and battery usage, managing any near real time data transfer issues, and providing updated vehicle endurance estimates. This helped with the scheduling of sensor calibration operations and determining when the glider should be recovered.

Mid-cruise Glider sensor calibration using RV Corystes: Within close proximity to the western WIS waypoint used by the glider during its survey transect is the 'Site 38A' moorings that are maintained by the Belfast-based Agri-Food and Biosciences Institute (AFBI). These moorings are regularly exchanged and sensor calibration reference measurements are taken. This is achieved using the AFBI survey vessel RV *Corystes*. The sensors used in these moorings can then be used to provide calibration cross-referencing measurements when the glider is close to its western survey waypoint. In addition, RV *Corystes* was chartered approximately mid-way through the glider deployment to provide additional glider sensor calibration readings. A one-day cruise aboard RV *Corystes* was required to undertake this work on 27th April 2012. The AFBI mooring is at a nominal GPS location of 53° 47.000N, 5° 37.903W. A diagram of the typical AFBI mooring arrangement is shown in Figure CS4.7.

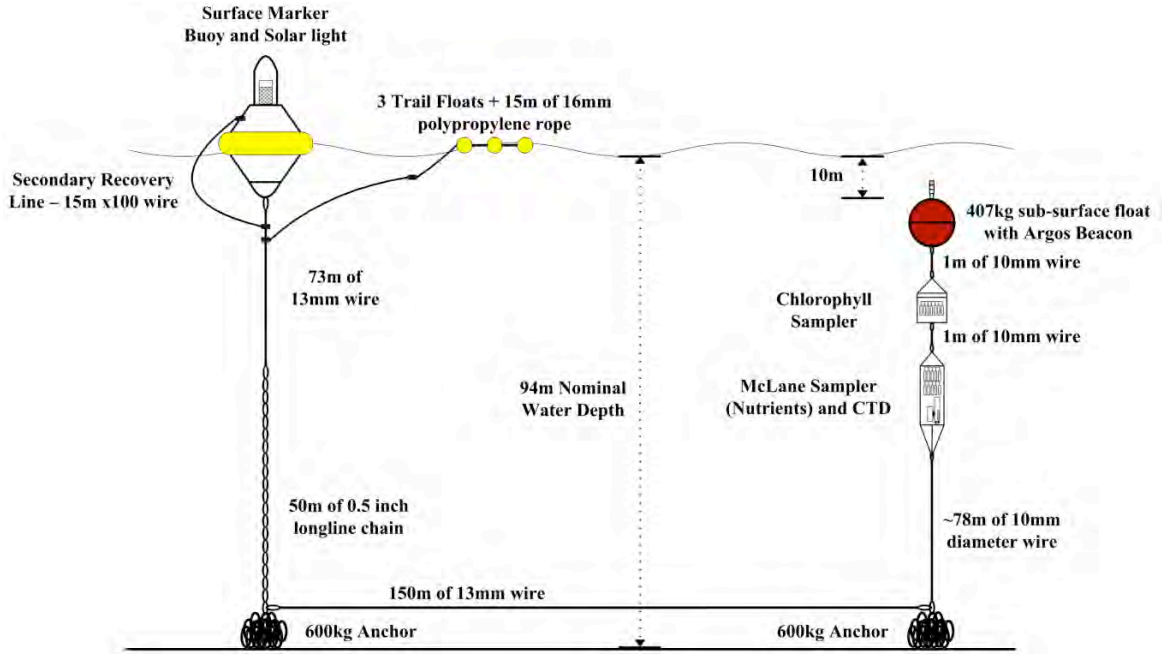

Figure CS4.7: Typical AFBI Site 38A mooring arrangement

The site 38A mooring has a CTD and automated water sampling instruments to help to determine physical water properties, chlorophyll concentration and dissolved nutrients concentration. During AFBI cruises, ship-based calibration measurements of CTD, chlorophyll-a, CDOM, nutrients and dissolved oxygen are made or samples are collected for land based laboratory analysis. This information is used to calibrate the deployed sensors and compensate for any measurement drift in the sensors when the instrumentation is recovered for servicing, data recovery and subsequent data processing. The additional RV *Corystes* cruise on 27th April 2012 first collected some calibration measurements at site 38A for the deployed moorings. Phil Knight at NOC-L provided back-up piloting of the glider when it was out of short-range wireless data range. After glider GPS positional updates were provided by satellite phone to the ship, and the ship was positioned close to the glider, Chris Balfour then controlled the glider from the ship to allow calibration measurements to be taken by the onboard AFBI team in close proximity to the glider. The requirement was to collect the ship-based reference samples while the glider is undertaking its routine survey measurements. This provided essential reference measurements in parallel with the glider sampling that will allow the degree of drift off-calibration, if any, in the glider sensor measurements to be determined.

Emergency recovery and initial recovered Glider evaluation: At just over six weeks into the glider deployment the glider was reconfigured to head towards the Liverpool Bay, past its normal eastern survey waypoint. The general intention was to navigate the glider into shallower and more sheltered coastal waters. A sufficient contingency of approximately two weeks endurance in the internal batteries was allowed. This was in order for a recovery to be scheduled using a small coastal charter vessel when suitable weather and a suitable sea state existed to allow this. Shortly after the return of the glider was initiated a problem with the glider occurred. The glider did not surface to report its position as and when expected late on 16th May 2012. When the glider did eventually surface after midnight BST, it was reported that the rear emergency jettison weight had been released. At this stage the glider had lost the ability to dive and an emergency recovery was rapidly scheduled. A deep sea fishing charter vessel, Tuskar, which is based at Birkenhead, was used to recover the glider. A subsequent analysis of the internally recorded glider measurements, and the condition of the glider when it was recovered, indicates that some form of entanglement of the glider had

probably occurred close to the seabed. What seems to have happened is that the glider dived and, as it approached the seabed and began to inflect or turn in the normal manner, the glider has become entangled with the nose of the vehicle pointing upwards. The buoyancy pump and pitch control actuators operated correctly to initiate a climb at the required angle. Subsequent and severe movements of the glider pitch and roll sensors can also be seen in the recorded data after the initial suspected entanglement. This would seem to suggest that the entangled glider was being dragged along close to the seabed, possibly by tidal currents. After a period of time the criteria for the emergency jettison weight release from the tail section of the glider was satisfied after the ability of the vehicle to climb was lost. After the expulsion of the rear tail jettison weight of approximately 0.5 kg the added positive buoyancy of the glider tail section seems to have been sufficient to free the glider and allow it to surface. At this stage the glider reported its position and that the jettison weight had been released. The near real-time data transferred by the glider at the time did not provide sufficient detail to determine the root cause of the problem. It was the detailed analysis of the recovered glider data that allowed the most likely cause of the glider problem to be determined.

General observations regarding the operation of coastal Gliders: For shallow-water-based coastal gliders with 200 m depth rating that are operated in challenging coastal regions, sensor fouling is likely to be a problem for extended deployments. The ship- and mooring-based sensor cross-calibration effort during the Defra-funded deployment has helped to address this problem. Shortly after the final glider recovery the optical sensor and CTD measurement cell were inspected and were clean and generally free of contamination.

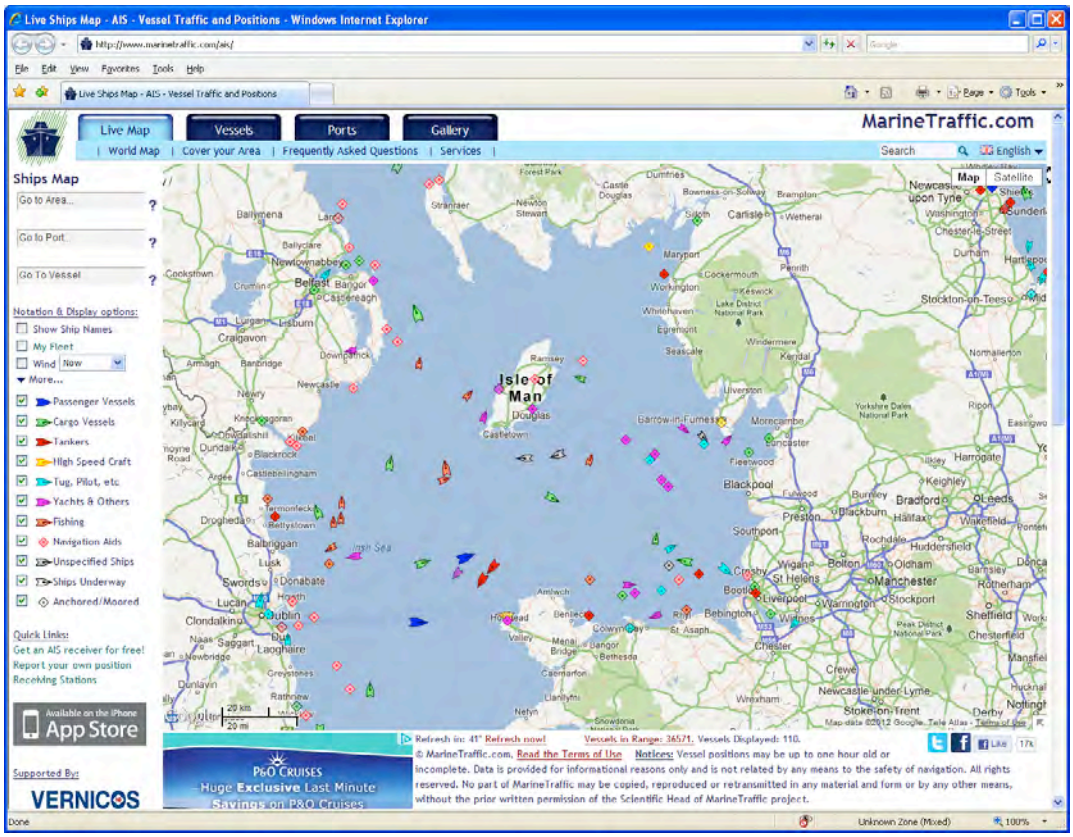

Figure CS4.8. Screengrab showing AIS Shipping Plot. Note that only ships larger than 300GT are required to have an AIS Transmitter installed. Captured at 17:05 GMT on 21st April 2012. This illustrates some of the larger shipping vessel hazards associated with Irish Sea glider deployments

Local shipping activity (as shown in Figure CS4.8) and reduced glider control due to tidal currents represent some of the other key risk factors with coastal glider deployments. Careful planning and subsequent monitoring or piloting of the glider deployment is required to maximise the probability of a successful deployment.

CS4.3.2. Mersey Plume

Technical details: A shallow water Slocum glider (unit 194) was deployed for a period of 19 days between 10th February and 1st March 2011. The glider performed longitudinal transects between 3.3°W and 4°W close to a near constant latitude around 53.4°N. Glider 194 was instrumented with a Seabird CTD, (recording conductivity/salinity, temperature and pressure), as well as a Wetlabs ECO Puck, (recording fluorescence and turbidity), and an Anderra Oxygen Optode, (recording oxygen concentration and saturation). Quality control of the glider output was undertaken using 1) independently collected salinity samples, analysed on an AutoSal salinometer, 2) temperature from a separate Seabird MicroCat and 3) chlorophyll samples analysed using standard laboratory flourometer techniques, from both the start and end of the mission. These samples were compared with the appropriate glider data points to ensure accuracy of the sensors and observe the level of sensor drift.

Accounting for strong tidal currents: Glider 194 was configured to achieve maximum forward propulsion in an attempt to minimise the effects of tidal advection. Horizontal velocity was estimated to be approximately 0.3-0.35 m/s, far slower than typical spring tide currents of Liverpool Bay that regularly approach 1 m/s. We were therefore presented with extra challenges when firstly attempting to pilot the gliders in shallow, highly dynamic environments, but also when attempting to process and interpret the glider data. This is demonstrated by the glider track in Figure CS4.9. In an attempt to reduce the impact of tidal advection on our data an adjustment was made to the apparent position of the glider relative to a set phase of the tidal cycle. A number of attempts were made to correct the glider position data (two of which are displayed in Figure CS4.9), in order to understand which technique best corrected the positions without producing spurious results. It was decided the correction using the POLPRED model to the low slack phase of the tide was most reliable, based on the assumption that the glider moved continuously relative to the local water and thus there should be no 'stall' points or inversions. POLPRED is a barotropic tidal prediction model that is based on the harmonic constituent components of the POLCOMS hydrodynamic shelf sea model (Holt and James, 2001).

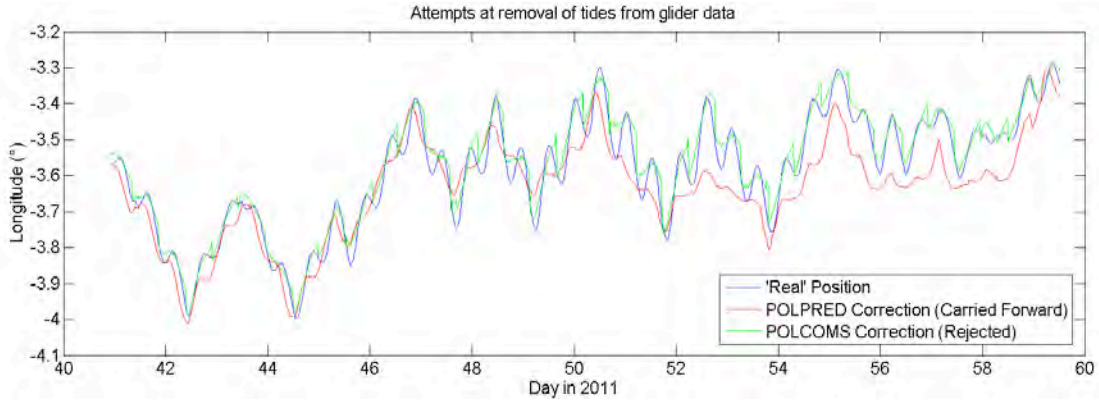

Figure CS4.9: Glider longitude position, including the position relative to land, and two attempts at correcting the position to remove tides.

Mission details: Glider 194 was deployed from the University of Liverpool research vessel RV *Marisa* at 1228 hrs (GMT) on 10th February at 53°43.992'N, 3°28.368' W in a water depth of 34.2 m. Pre-mission tests were undertaken with the glider tethered to a buoyant float for security until 1311 hrs. Untethered pre-mission tests were undertaken until 1718 hrs, when the glider mission commenced. Nearby CTD profiles were undertaken to provide *in*

situ calibration data. In addition, surface water samples were taken for salinity, CDOM, chlorophyll and suspended sediment calibration.

During the first five days of the mission the glider was kept within a water depth greater than 35 m to avoid seabed collision or grounding, should piloting in such a dynamic environment prove difficult. On successful completion of this tentative first phase the waypoints were moved closer to the coast into shallower water, in an attempt to intersect the coastal current (Fig. CS4.9).

The glider was successfully recovered at 1250 hrs (GMT) on 1st March 2012 at 53°40.418'N, 3°21.035' W. Prior to recovery, surface water samples were collected for onboard and laboratory analysis to provide final calibration data for the glider sensors.

CS4.4. Results

CS4.4.1. Western Irish Sea

Following transit from Liverpool Bay, Glider 117 successfully reached the WIS study area on the evening of 6th April 2012. Following arrival the glider proceeded to perform 'saw-tooth' transects between the two waypoints until 16th May 2012, providing 40 days of continuous measurement from all available sensors.

Throughout the mission the glider was advected by tidal currents, such that attempts to maintain a straight-line trajectory between the two waypoints was never achieved (see the glider track in Fig. CS4.6). Despite this somewhat meandering transect pathway, northerly excursion from the East-West survey line was minimised by the automatic piloting of the glider, such that 94% of glider measurements were confined within 5 km north or south of the desired transect line. Since this distance is small compared to the E-W excursion (47 km maximum) we may consider the survey as a near longitudinal transect between the two waypoints.

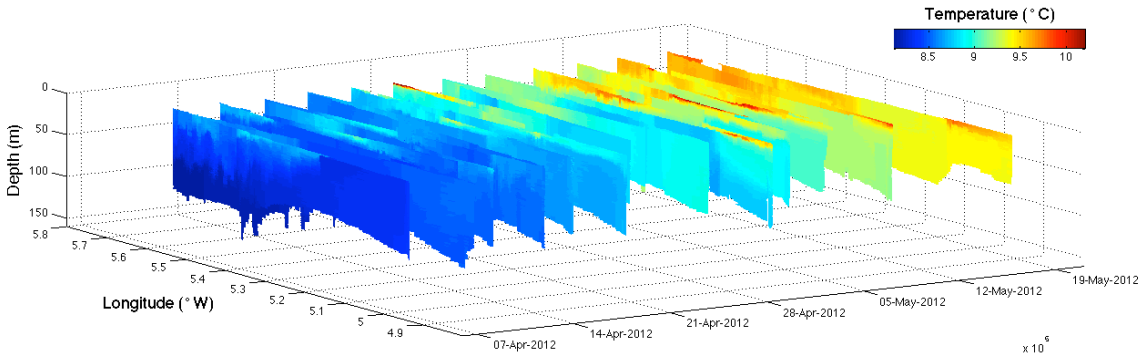

Figure CS4.10: Temperature data collected from glider 117 between 6th April and 16th May 2012.

Temperature data (Fig. CS4.10) reveal a clear and steady increase in sea temperature during the 40-day deployment. Intuitively, this increase is most evident in sea surface temperature (SST) as solar heating of the surface layer occurring as part of the seasonal cycle. However, evident from the beginning of the mission is the change in temperature with depth. This is more clearly observed in Fig. CS4.11b, which displays up to 0.5°C temperature difference between water at the near surface and near bed. This vertical stratification of the water column is strongest in the deeper, westernmost region of the survey area. More easterly regions of the survey transect are more vertically well mixed, displaying only small differences in temperature with depth. Despite clear changes in temperature at all depths throughout the deployment period, this pattern of stratification is

repeated throughout; stratification is strongest in the western regions. This is consistent with the recognised seasonal stratification of the Western Irish Sea.

Despite this persistent feature the vertical temperature and density structure displays considerable variability. Figure CS4.12 shows the vertical distribution of temperature at the boundaries of our transect (i.e. close to Waypoints 1 and 2), and displays the temporal evolution of this structure. Despite deployment in early April, thermal stratification has already occurred in the western section of the study area due to the unseasonably high temperatures and relatively calm weather experienced during late March. Three distinct layers are observed in the west during the first two transects, however, a deeper, single surface mixed layer is observed by mid-April when there is also some evidence of surface warming at the eastern waypoint. The extent of stratification weakens significantly during the last week of April, despite a continued increase in water column temperature in the west. This gradual rise in temperature is replicated in the east, where weak vertical structure is observed during the later stages of the study period.

Chlorophyll data (Fig. CS4.11c) reveal a clear maximum of phytoplankton biomass within the identified stratified region to the west of our survey area during the first two weeks of the deployment. This early 'spring bloom' is maintained as a discrete mass clearly divided from the unproductive, vertical mixed region to the east of our survey area. The tidal-mixing front (Simpson et al, 1978), which separates the mixed and stratified regions of the gyre, is clearly identified by the chlorophyll signature. Plots of chlorophyll close to the waypoints (Fig. CS4.13) indicate that the temporal and spatial evolution of biomass is strongly related to changes in temperature structure. The deepening of the surface mixed layer (Fig. CS4.12; 13 April) produces a similar redistribution of near surface phytoplankton to deeper depths of up to 60 m, although it is evident that primary production is occurring beneath the shallow mixed layer prior to mid-April.

Towards the end of April, the tight relationship between stratification and biomass appears to break down as chlorophyll concentration reduces rapidly, despite continued strong stratification. The breakdown of stratification in the western regions further reduces chlorophyll abundance until only background levels are observed, similar to those measured in the eastern, well-mixed region where little evidence of phytoplankton growth is observed. During May there is evidence of a secondary bloom occurring as stratification again re-establishes in the west.

Throughout the study period, phytoplankton abundance produces identifiable increases in oxygen concentration (Fig. CS4.12d); stratified, productive areas displaying near 100% saturation clearly distinguishable during the first half of the deployment from an oxygen minimum in the bottom waters of the western region which are typically around 80%. Following a reduction in stratification, vertical mixing of the water column produces a predictable ventilation of deeper water when saturation remains fairly steady for approximately one week at 86-89% for much of the water column with a weak horizontal gradient, increasing easterly. With the onset of stratification at the beginning of May, and an associated second, weaker phytoplankton 'bloom', we observe a similarly weak increase in near surface oxygen levels to 90-95% in the stratified western regions and a subtle decrease in levels in the lower mixed layer.

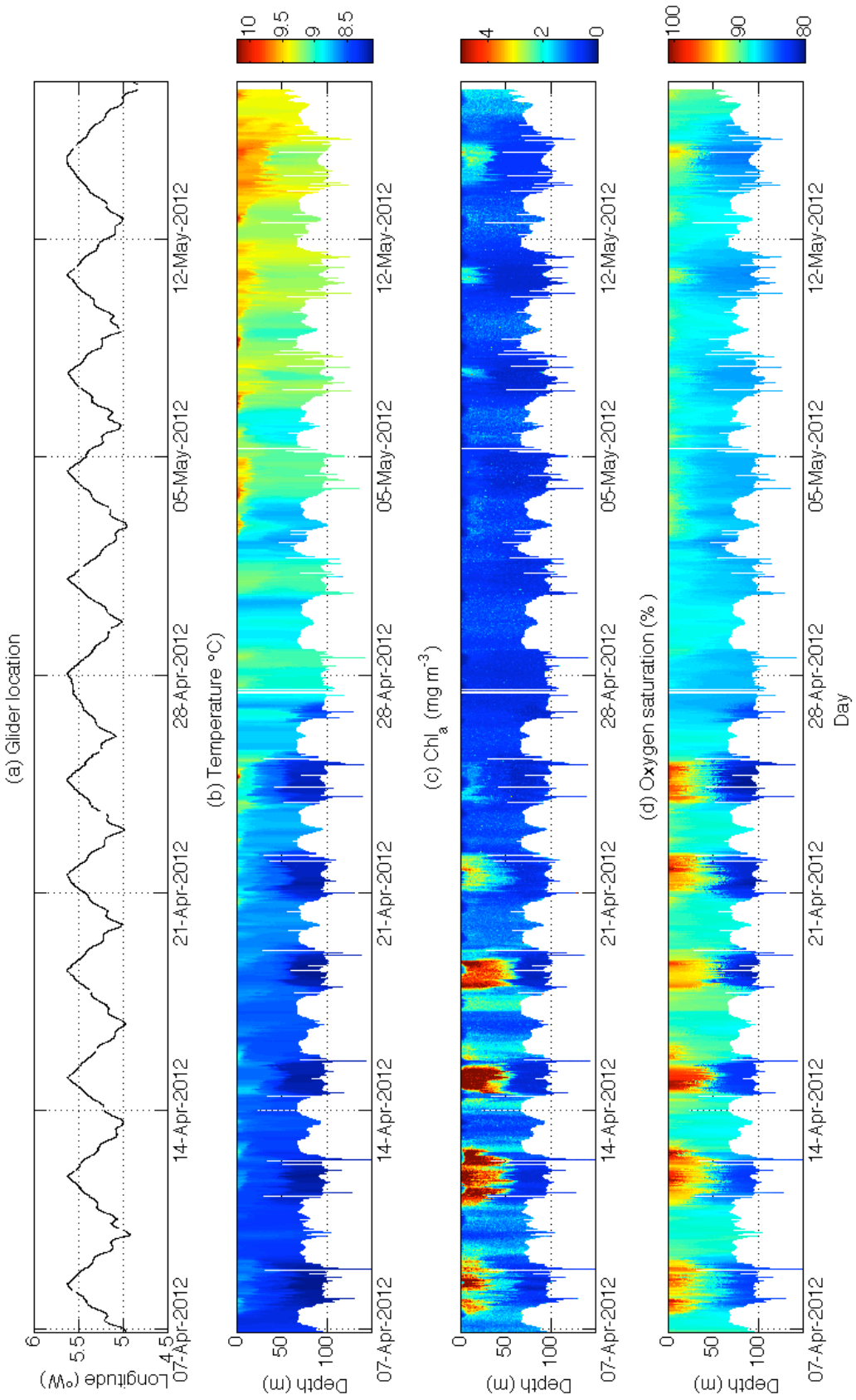

Figure CS4.11: Glider data collected between waypoints 1 and 2 during the WIS deployment. In total, 24 longitudinal transects were achieved over a duration of 40 days.

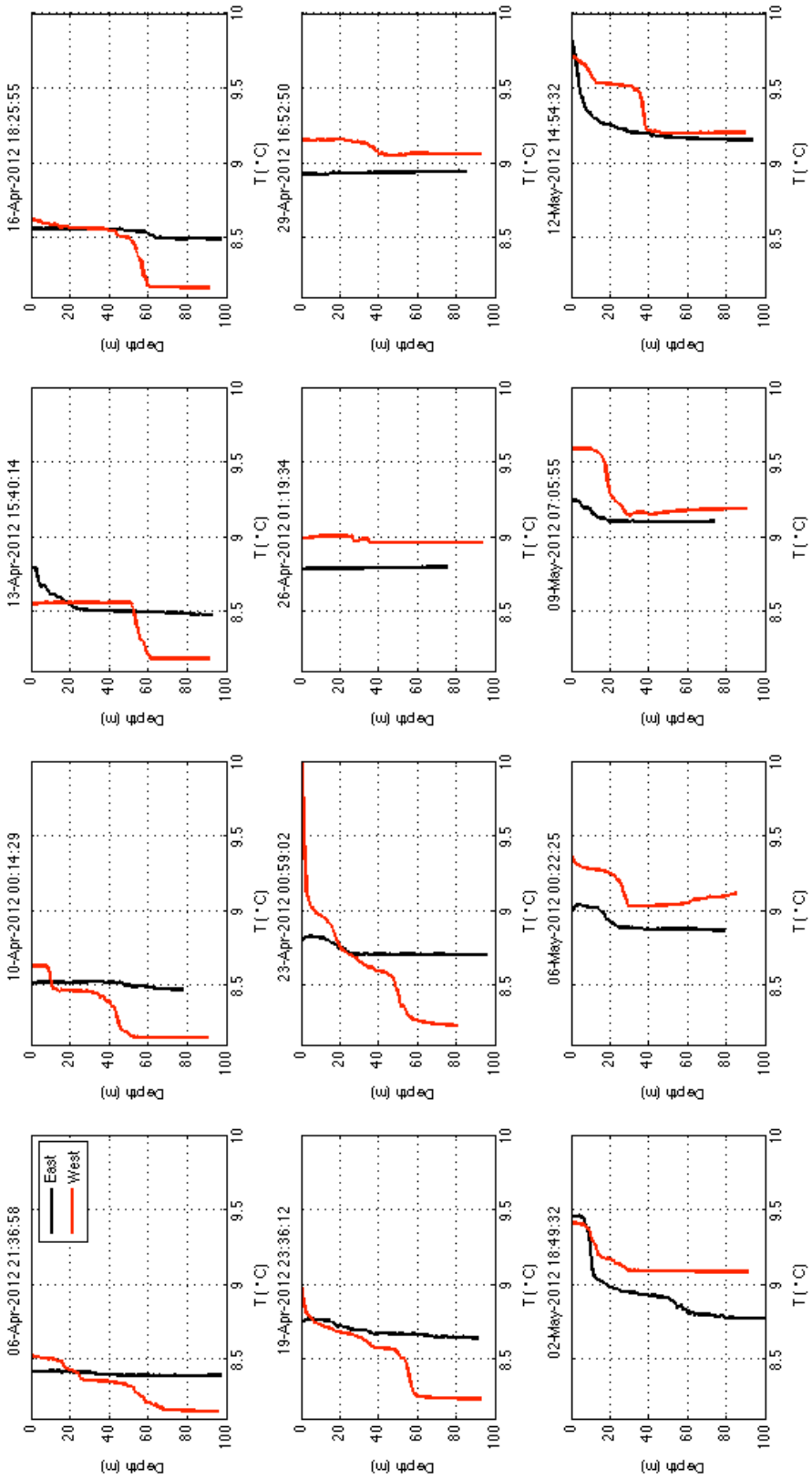

Figure CS4.12: Vertical profiles of temperature throughout the glider deployment, at the easternmost (black) and westernmost (red) extent of the glider survey track.

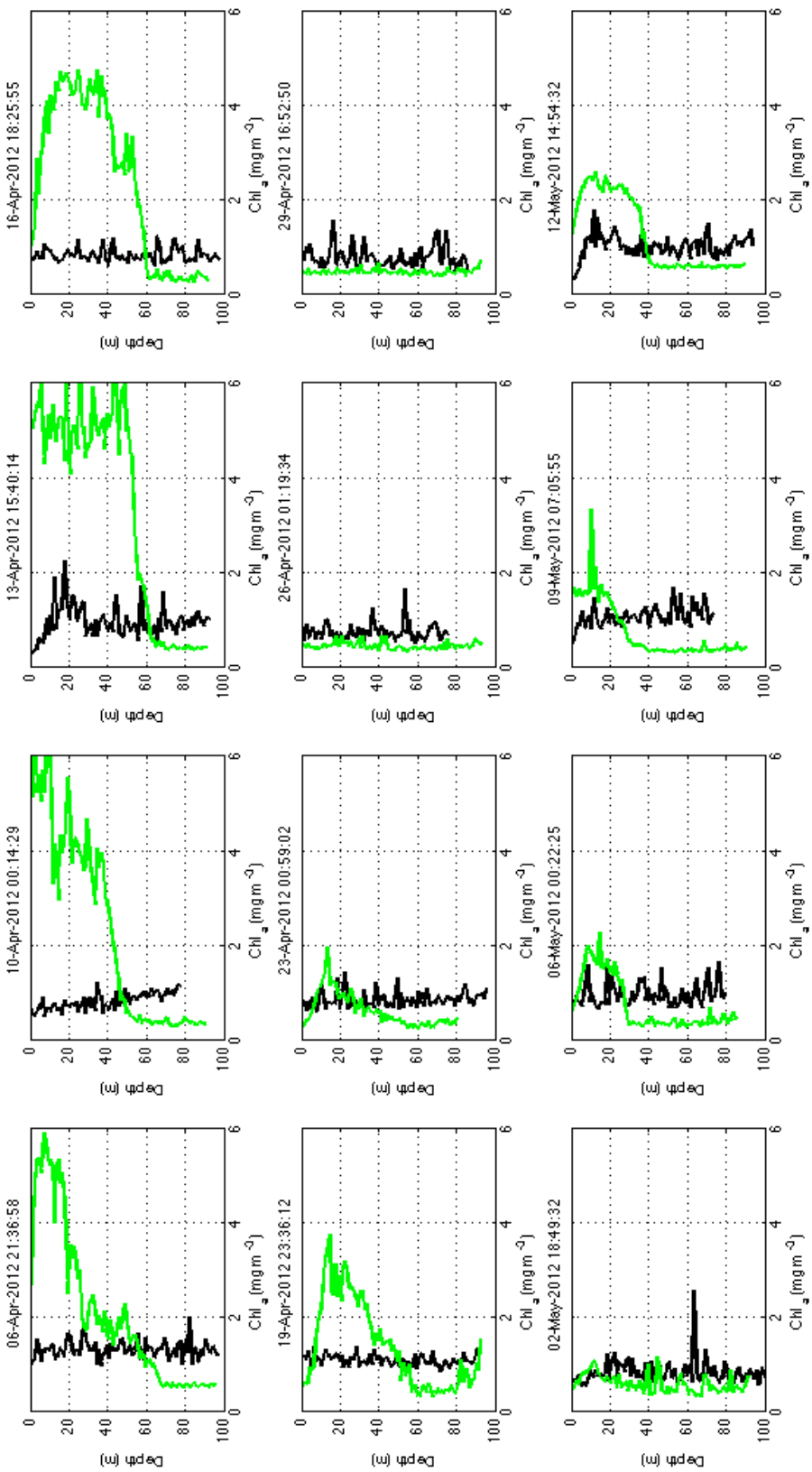

Figure CS4.13: Vertical profiles of Chlorophyll-a concentration throughout the glider deployment, at the easternmost (black) and westernmost (red) extent of the glider survey track.

CS4.4.2. Mersey Plume

The early stages of this mission were given over to testing of the glider capability in shallow, dynamic environments. As such, little evidence of the freshened coastal current identifiable in satellite SST measurements was observed (Fig. CS4.14). Once the glider pilots were confident in the capability of the glider to be navigable within the strong tidal flows of Liverpool Bay the glider was directed closer to the coast where horizontal and vertical salinity gradients were observed. Salinity ranges remained quite small, however, until a plume event was observed around the 25th February (decimal day 55; Fig. CS4.14).

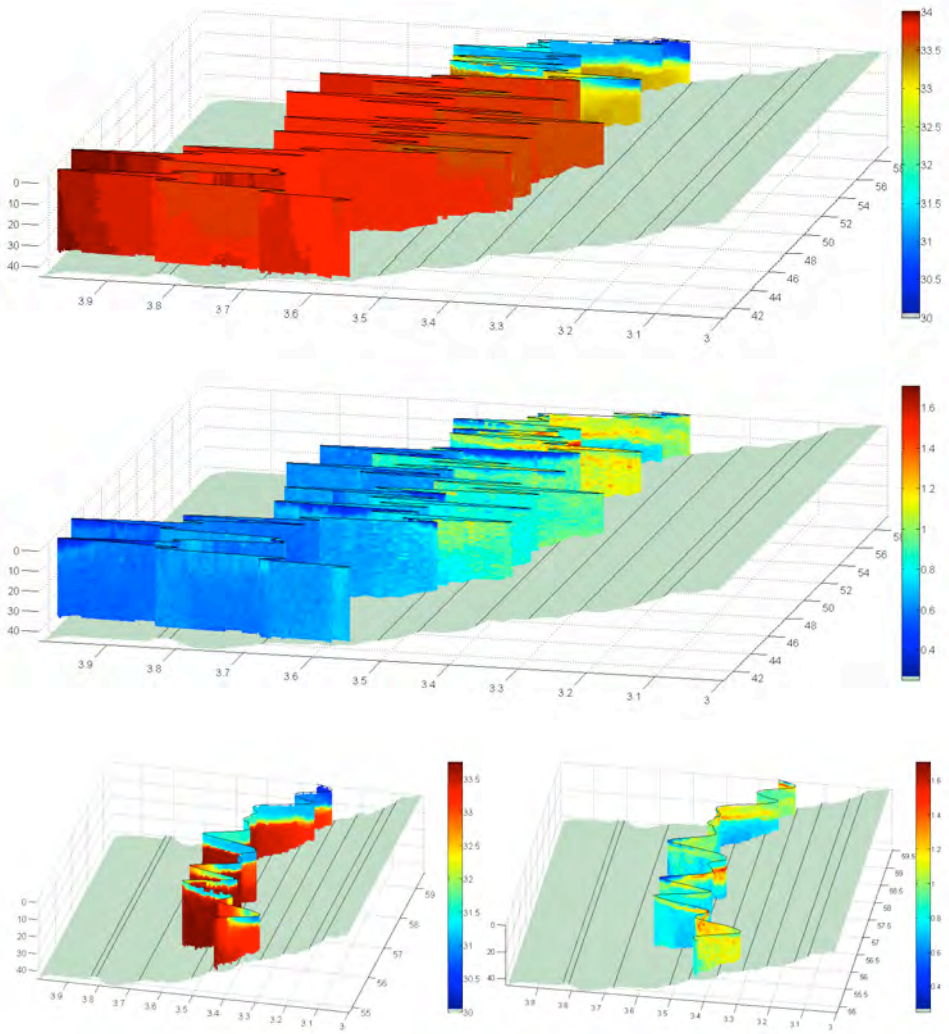

Figure CS4.14: Upper panel shows measured salinity as a function of time (decimal day 2011, right axis), longitude (°W, bottom axis) and depth (m, left axis). The middle panel shows a similar representation of Chlorophyll-a concentration derived from glider fluorescence data. The plume event identifiable in salinity data during the final stages of the mission is focused on in the lower two panels for salinity (left) and Chl-a (right).

The strong plume event had a clear and dramatic effect on the horizontal and vertical structure of the coastal waters. As can be seen in the subsection plots in Figure CS4.14, vertical salinity stratification increased significantly, from the otherwise weak variations of around 0.5 salinity units to as much as 3.5 salinity units of vertical stratification. The plume was maintained up to 45 km offshore, beyond the westernmost extent of the glider transect.

Similar to the temporal evolution of salinity, the chlorophyll data show a clear transition between pre and post-plume periods. Prior to the plume we do see a gradual increase in chlorophyll concentration towards the coast, coincident with a slight freshening of

surrounding waters; however, it is during the plume event that we see a dramatic increase in chlorophyll concentration.

If we examine the glider data in terms of time and depth alone (Fig. CS4.15) we may better observe the temporal evolution of the coastal waters and the biological response to the freshwater delivery to the bay.

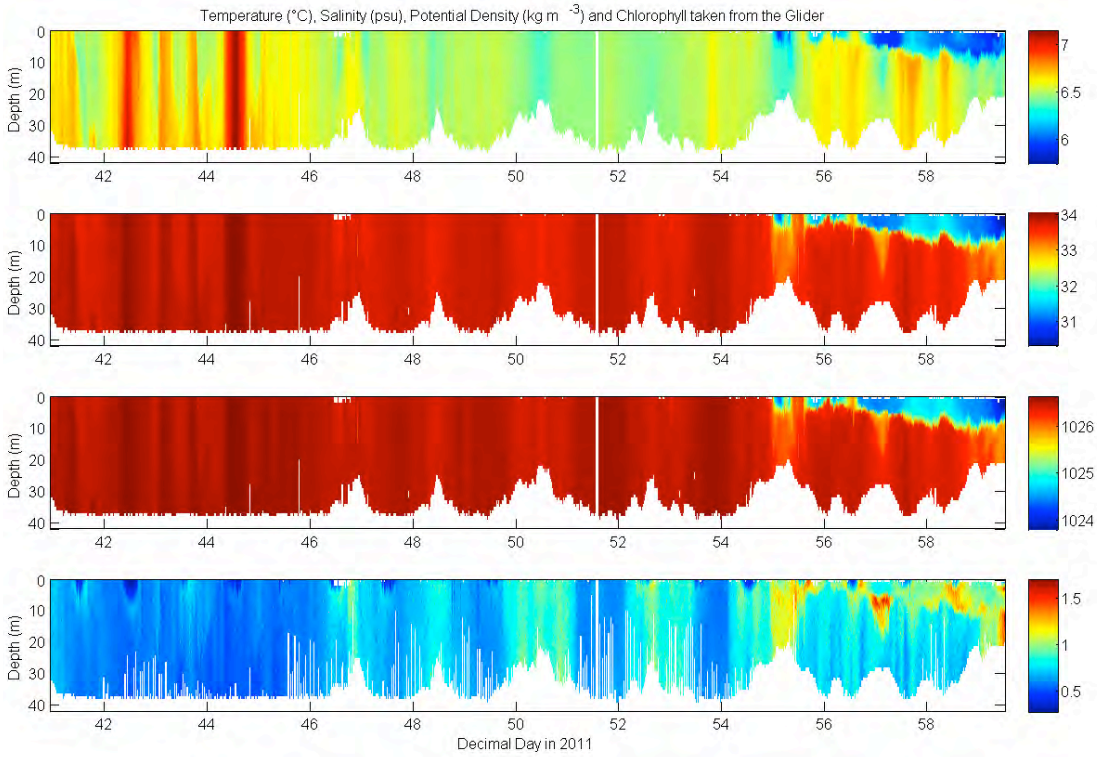

Figure CS4.15: Glider 194 data, from top to bottom; temperature (°C), salinity, density (kg.m^3) and chlorophyll concentration (mg.m^3).

The dominant signature within the time series is clearly the plume event following day 55. A cool, freshened lens of plume water persists from the near coast to beyond 45 km offshore. This plume promotes strong vertical density stratification of up to 2.5 salinity units. Associated with this fluvial input is a dramatic increase in chlorophyll biomass. At first, the Chl-a increase is associated with the front of the plume and affects the full water column for several hours. Following this, a Chl-a maximum is generally associated with the base of the strongly stratified layer, although some near surface increases are observed. While we are able to measure fluorescence over the majority of the water column it is clear that data is unreliable in the near surface regions due to a process termed 'fluorescence quenching', caused by the daily sunlight intensity cycle (e.g. Sackman et al, 2008).

Comparison with model data: The results of the 2011 Mersey Plume study are now compared with the output from the POLCOMS-ERSEM (Holt and James, 2001; Blackford et al, 2004; Fig. CS4.16). Data were extracted from the pre-operational model runs made at NOC-L, using the glider track to select appropriate data points to create a simulated glider dataset.

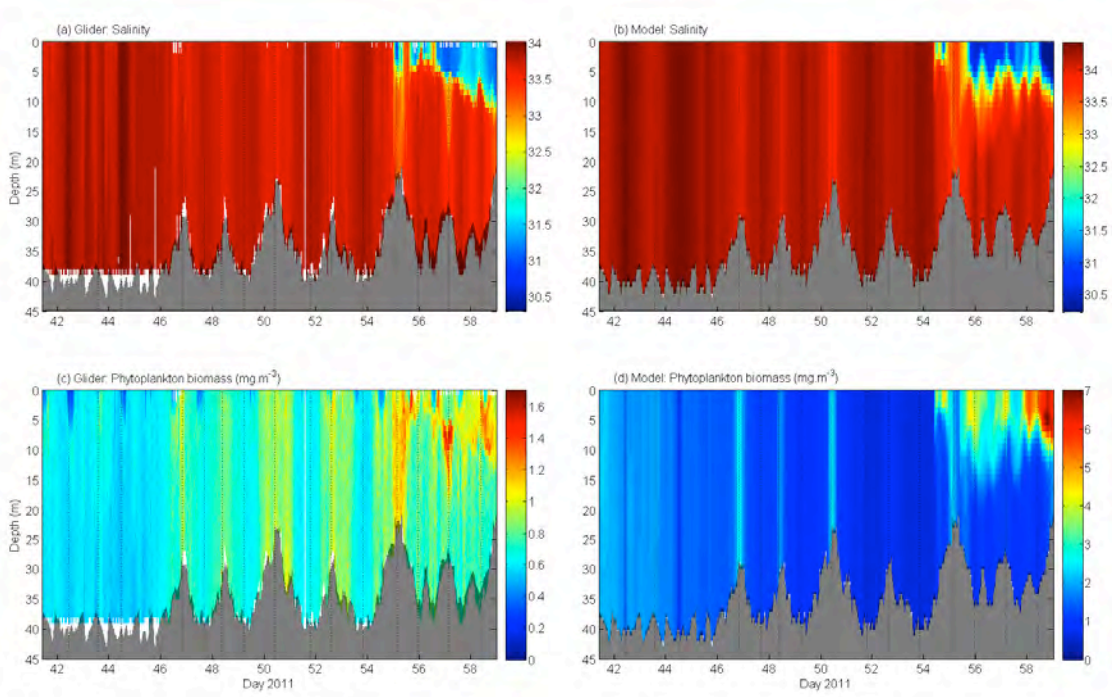

Figure CS4.16: Glider (a) salinity and (c) chlorophyll biomass are shown alongside model output data (b and d) for comparison.

A first-order comparison suggests the model does a good job in recreating the observed physical structure of the plume. The delivery of freshened water is well timed and density (and salinity) differences are similar. Small differences are observed in the pre-plume period; horizontal gradients appear too strong and vertical and horizontal structure display little of the observed natural variability. The plume itself is similarly less complex in structure than observations. The pycnocline is too abrupt for much of the time with little of the diffuse nature of the real plume.

The ecosystem component of the model is less successful than the physical component in recreating the natural variability. Although the model does predict near shore increases in pre-plume biomass, very little of the vertical or horizontal structure of the observed Chl-a concentration is simulated. During the plume event the model significantly over-predicts biomass concentration and fails to recreate the observed vertical structure and pycnocline maximum, instead predicting a 'bloom' which affects the entire surface mixed layer.

CS4.5. Summary

We have presented mission details and results from two very different glider studies in the Irish Sea. Both missions were highly successful, providing unique datasets that will provide greater understanding of shelf sea and coastal processes.

The Western Irish Sea mission demonstrates the suitability of ocean glider technology for monitoring long-term development of temporally and spatially variable features. This work also demonstrates how regions of busy shipping and fishing can be successfully monitored with these exciting new instrument platforms. We must, of course, acknowledge that the WIS mission was brought to an abrupt end by a suspected collision or entanglement, possibly with fishing gear. Whenever we aim to conduct research of this type in heavily fished regions this will always be a risk.

The WIS mission also demonstrates the ability to remotely deploy gliders within regions of convenience or safety, which are then subsequently 'flown' into the operational area. When considering this for financial reasons alone, the extra manpower required for piloting and lost survey time that this inevitably requires must be considered. The durability of glider sensors for up to seven weeks in a highly productive environment has been demonstrated. Both physical (CTD) and biological (fluorescence and oxygen) sensors have proved to be well constrained by *in situ* calibration.

The Mersey Plume mission has demonstrated how gliders are capable of several weeks deployment in high energy environments. The glider pilot effort for such missions is increased significantly due to the ever-present risk of collision or grounding and should be considered. The value of this relatively cheap platform, when compared to ships, is that events such as the observed plume (which are difficult to accurately predict) can be captured by having the appropriate instrumentation in place waiting for such an event. The equivalent cost for keeping a research vessel in place for the two weeks prior to the plume arriving would likely be at least an order of magnitude greater than the glider mission costs.

CS4.6. References

Blackford J.C., Allen J.I. and Gilbert F. J. (2004) Ecosystem dynamics at six contrasting sites: a generic model study. Journal of Marine Systems, 52, 191-215.

Dickey-Collas, M., Brown, J., Fernand, L., Hill, A. E., Horsburgh, K. J. and Garvine, R. W. (1997) Does the western Irish Sea gyre influence the distribution of pelagic juvenile fish? Journal of Fish Biology, 51, 206–229.

Greenwood, N., D. J. Hydes, C. Mahaffey, A. Wither, J. Barry, D. B. Sivyer, D. J. Pearce, S. E. Hartman, O. Andres, and H. E. Lees, (2011) Spatial and temporal variability in nutrient concentrations in Liverpool Bay, a temperate latitude region of freshwater influence. Ocean Dynamics, 61, (12), 2181-2199.

A.E. Hill, R. Durazo, D.A. Smeed (1994) Observations of a cyclonic gyre in the western Irish Sea. Continental Shelf Research, 14(5), 479-490.

Holt, J.T. and James, I.D. (2001) An s coordinate density evolving model of the northwest European continental shelf: 1, Model description and density structure. Journal of Geophysical Research, 106, 14,015–14,034.

Howarth, M. J. and M. R. Palmer (2011) The Liverpool Bay Coastal Observatory. Ocean Dynamics, 61 (11). 1917-1926.

Palmer M. R. (2010) The modification of current ellipses by stratification in the Liverpool Bay ROFI. Ocean Dynamics, 60 (2), 219-226.

Palmer, M. R. and J. A. Polton, (2011) A strain-induced freshwater pump in the Liverpool Bay ROFI. Ocean Dynamics, 61 (11). 1905-1915.

Sackmann, B. S., M. J. Perry, C. C. Eriksen (2008) Seaglider observations of variability in daytime fluorescence quenching of chlorophyll-a in Northeastern Pacific coastal waters. Biogeosciences Discussions, Vol. 5, pp 2839-2865.

T.J. Sherwin (1987) Inertial oscillations in the Irish Sea. Continental Shelf Research, 7(2), 191-211.

Simpson, J.H., Bos, W.G., F. Shirmer, A.J. Souza, T.P. Rippeth, S.E. Jones and D. Hydes (1993) Periodic stratification in the Rhine ROFI in the North Sea. Oceanologica Acta 16 (1): 23–32.

Simpson, J. H., C. M. Allen, and N. C. G. Morris (1978) Fronts on the Continental Shelf, J. Geophys. Res., 83(C9), 4607–4614.

Case Study 5: Deep-water boat-based mapping in Whittard Canyon

CS Leader: Dr Veerle Huvenne (NOC)

CS5.1. The CS5 task

As set out in the proposal this task's remit was as follows:

"*In June 2009, NOC staff on RRS James Cook undertook detailed mapping of the Whittard Canyon system along the Celtic Margin off SW UK. In 12 days, >700 km of track-lines were surveyed with the Towed Ocean Bottom Instrument (TOBI, carrying a 30 kHz sidescan sonar system with phase bathymetry capability, an 8 kHz chirp profiler and a magnetometer) and 6130 km^2 of shipborne multibeam data was acquired over the four main branches of the canyon. This comprehensive and highly detailed dataset is providing new insights into canyon morphology, formation, sediment transport processes and the resulting spatial distribution of benthic habitats. In addition, the data formed an indispensable base map for the planning of ROV dives and geological/biological sampling during the follow-on cruise JC036. This case study will illustrate the capability of shipborne and deep-towed instruments in deep-water habitat mapping. The full cruise report can be viewed at:* http://eprints.soton.ac.uk/69695/1/nocscr042.pdf

This Case Study will be compiled by NOC between 1 March and 31 May 2012."

CS5.2. Introduction

Canyons are the main sediment transport pathway between the shelf and the deep sea. Processes including dense shelf water cascading (DSWC, Canals et al., 2006), the capture of along-shelf sediment transport, resuspension by internal waves and tides (de Stigter et al., 2007) and turbidity currents may result in either canyon flushing or focussed deposition of sediments and organic matter (Masson et al, 2010). Canyons are complex environments that can harbour a significantly increased biodiversity and biomass compared to the open slope (Vetter & Dayton, 1998; de Leo et al., 2010), hence they are often considered as ecosystem and biodiversity hotspots. However, their extent and terrain heterogeneity also makes them challenging environments for study. Conventional shipboard mapping and sampling techniques cope poorly with the steep topography.

An extensive, nested, habitat-mapping programme was carried out in Whittard Canyon in the northern Bay of Biscay, in 2009 (Fig. CS5.1). The main aim was to identify the different habitats in the canyon, with emphasis on cold-water coral communities, and to assess their status, especially with respect to human impacts. Whittard Canyon is a dendritic system, connecting the broad shelf at ca. 200 m water depth with the Whittard Channel and Celtic Fan at 4000 m water depth (Zaragosi et al. 2006). Canyon incision, mainly by headward erosion and retrogressive slope failure, started in the Plio-Pleistocene and cut deeply into the underlying Miocene deltaic deposits and Cretaceous/Paleocene chalks. The developing canyon morphology was influenced by the location of existing NNW-SSE trending fault systems, older buried canyons, and natural depressions in the seafloor (Cunningham et al., 2005). The canyon was very active during sealevel lowstands, more particularly during deglaciation phases (Zaragosi et al., 2006; Toucanne et al., 2008). However, its present-day activity is much reduced: it is located far from terrestrial sources, and sediment input is limited to shelf spill-over (Cunningham et al., 2005).

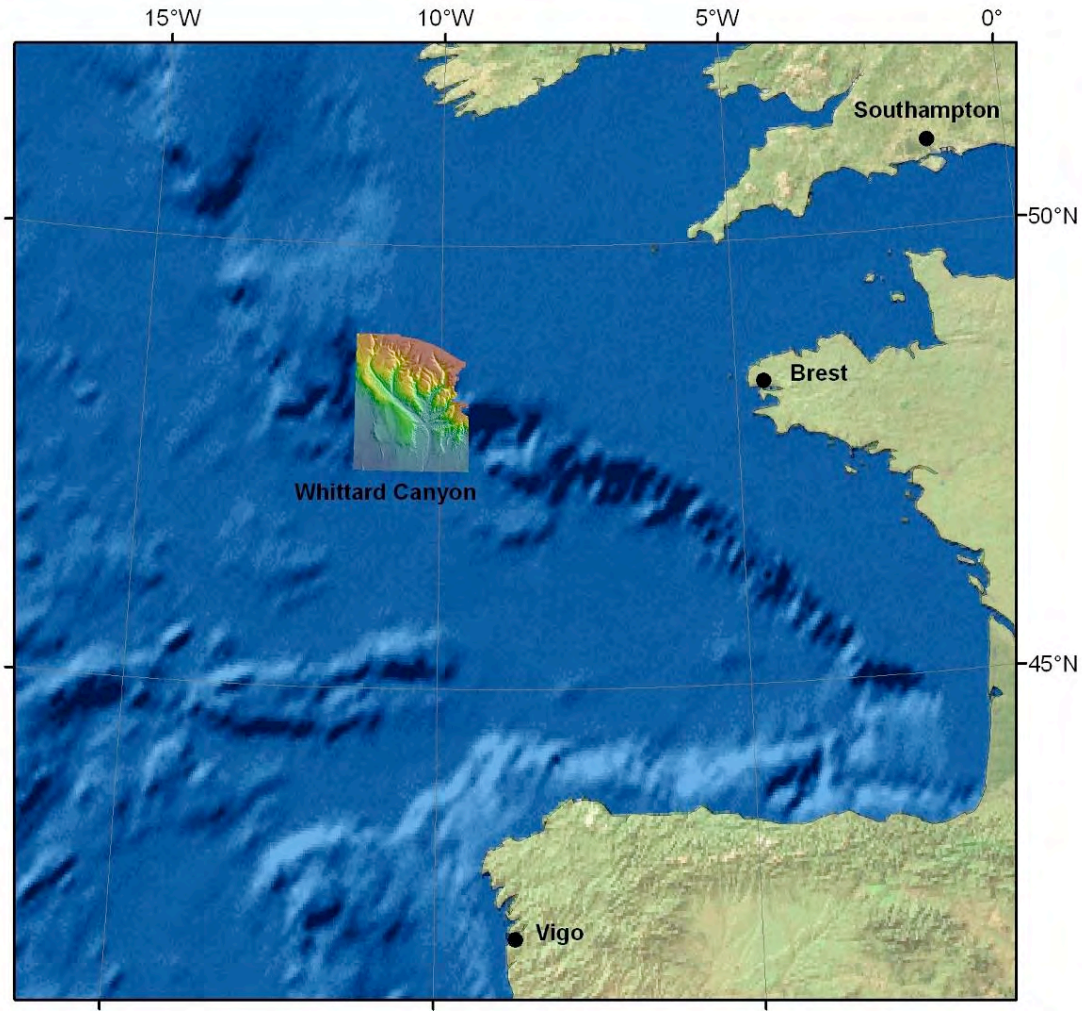

Figure CS5.1: Location map of the Whittard Canyon, Bay of Biscay, NE Atlantic.

CS5.3. Nested mapping methodology

The extent and complexity of submarine canyon systems demands a survey methodology that covers a number of spatial scales (levels of detail and extent). Insights obtained from the higher resolution data (with limited coverage) support the interpretation of the lower resolution data, which is covering a larger extent. Based on experience obtained over several expeditions in the canyons offshore Portugal (Huvenne et al., 2012), a nested habitat mapping approach was developed and subsequently applied to the Whittard Canyon. It consisted of the following methods, summarised in Table CS5.1.

The work in the Whittard Canyon was split over two cruises on board the RRS James Cook in June/July 2009: JC035 and JC036. The details of those two voyages are specified in Tables CS5.2 and 5.3 (full details can be found in the respective cruise reports: Huvenne et al. (2009) and Masson et al. (2009)). The first cruise ran for 12 days, and was fully dedicated to multibeam and TOBI sidescan sonar work (TOBI stands for Towed Ocean Bottom Instrument). The second cruise took 39 days, and comprised the ROV and sampling work. In addition to habitat mapping, a considerable part of the ROV time was also used to carry out in-situ ecological experiments on the seabed.

Equipment	Resolution	Total Extent	Survey time
EM120 (shipboard multibeam)	25x25 to 50x50 m pixels (depending on depth)	6128 km^2	200 h
TOBI 30kHz sidescan sonar	3 x 3 m pixels	3841 km^2	200 h
ROV ISIS multibeam	1 x 1 m pixels	~3.60 km^2	~50 h
Video/ photographs	Ca. 0.25 mm pixels	~29 km transect, ~0.044 km^2	~80 h of video-transecting (ROV time spent on the seabed)
Sampling	Real samples – full resolution	34 Megacores 18 Piston cores 3 Box cores 53 push cores 24 suction sample events 39 Biobox samples	134.6 h 81.4 h 10.0 h 343 h of ISIS ROV work, of which appr. 100 h for sampling

Table CS5.1: Summaryof survey activities in Whittard Canyon, according to resolution

Vessel	RRS James Cook
Start	7 June 2009
End	19 June 2009
Duration	12 days
Weather downtime/transit	0 days/2.5 days
Partner organisations involved in JC035 science	2
Scientists on board	6
Technicians on board	4
Ship's officers and crew	22
Cost of shiptime (NERC)	****
Cost of 'superstructure': equipment, technicians, mob/demob, shared by NERC + EC-HERMIONE	****
Cost of scientists (FEC), consumables, travel, paid from a variety of sources (NERC-OCEANS2025 and EC-HERMIONE)	Estimate: £17,000

Table CS5.2: Summary of JC035 metrics

Vessel	RRS James Cook
Start	19 June 2009
End	28 July 2009
Duration	39 days
Weather or equipment downtime/transit	8 days/3 days
Partner organisations involved in JC036 science	7
Scientists on board	20
Technicians on board	11
Ship's officers and crew	22
Cost of shiptime (NERC)	****
Cost of 'superstructure': equipment, technicians, mob/demob, shared by NERC + EC-HERMIONE	****
Cost of scientists (FEC), consumables, travel, paid from a variety of sources (NERC-OCEANS2025, EC-HERMIONE, university funds for the different partners…)	Difficult to estimate due to different partners organisations and variable costs for consumables and personnel. Estimate: £200,000

Table CS5.3: Summary of JC036 metrics

CS5.4. Results

The eight days of multibeam and TOBI work during cruise JC035 allowed the mapping of the four main branches of Whittard Canyon (Fig. CS5.2). This dataset provides very important regional information, and forms a solid basis for the geological and geomorphological interpretation of the area (e.g. Figs CS5.3-5.4). However, the ROV bathymetry and video data recorded during JC036 illustrate that, even with the 3x3 m pixel resolution of the TOBI sidescan sonar imagery, a lot of information is missed that might explain the relationship between benthic communities and their environment, especially in more complex areas of the canyon (Fig. CS5.5). Given that previous studies have shown that a more varied benthic community can be found in areas with a high availability of steep substrates (Tyler et al., 2009), this extra information is essential. On the other hand, the ground-truthing work is very time-consuming, which means that during the 39-day cruise JC036, only the eastern-most and western-most branch of the canyon could be surveyed in any detail (Fig. CS5.6).

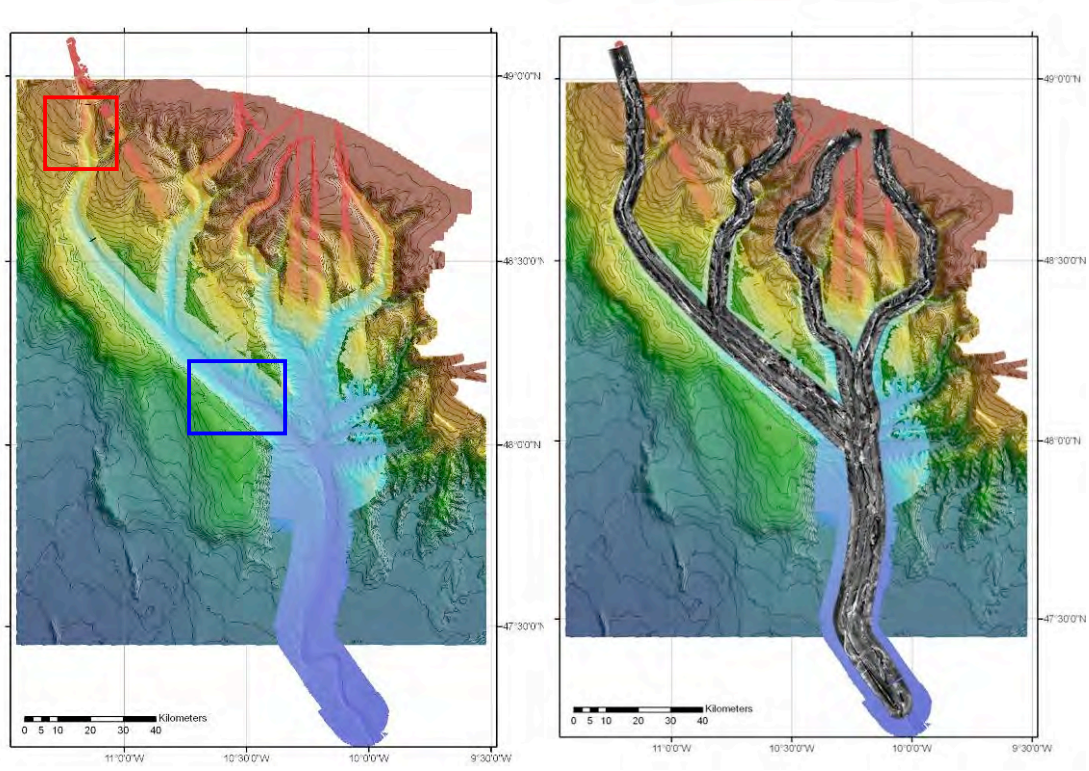

Figure CS5.2: Multibeam data coverage (left, light colours) and TOBI sidescan data coverage (right) obtained during JC035. Background: pre-existing bathymetry data used for cruise planning, 200x200 m grid from the Irish National Seabed Survey, courtesy of the Geological Survey Ireland, Dublin. Blue box indicates the approximate location of Fig. CS5.3; red box of Fig. CS5.4.

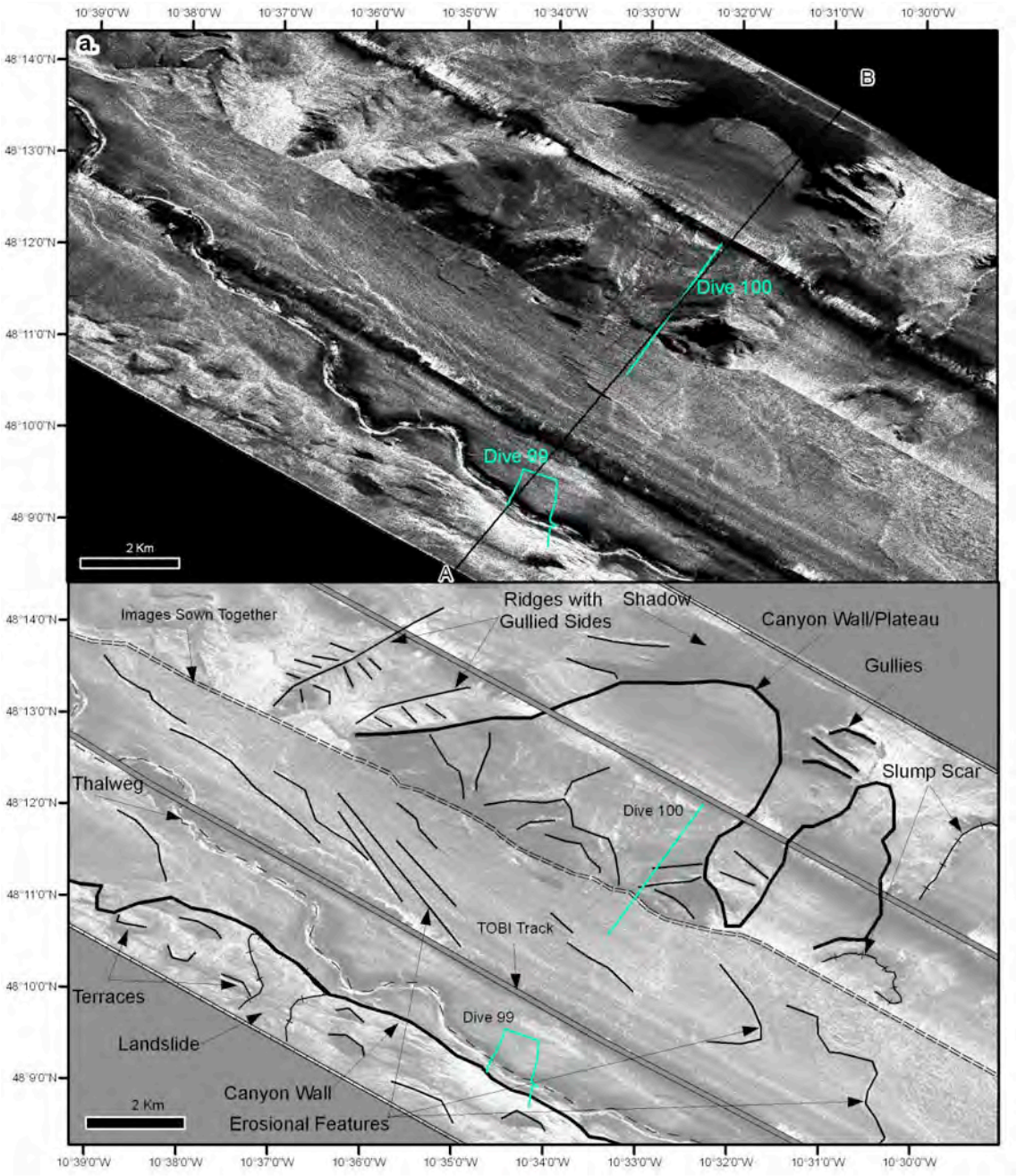

Figure CS5.3: TOBI sidescan sonar mosaic of the lower Whittard Canyon, western branch (top) and geomorphological interpretation (bottom, from Crowe (2010)).

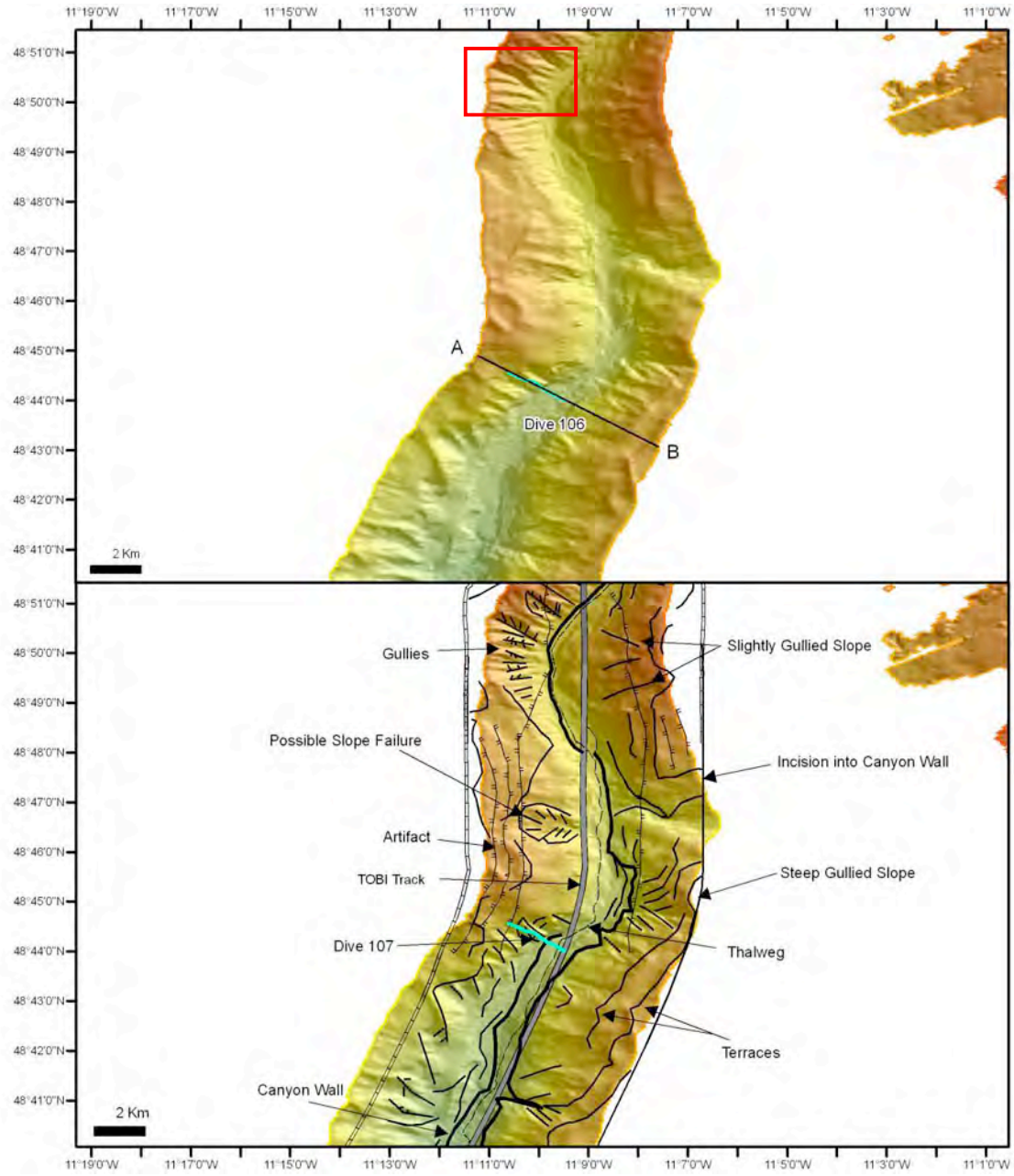

Figure CS5.4: Bathymetry and geomorphological interpretation of the upper Whittard Canyon, western branch (from Crowe (2010)). Red box indicates the approximate location of Fig. CS5.5.

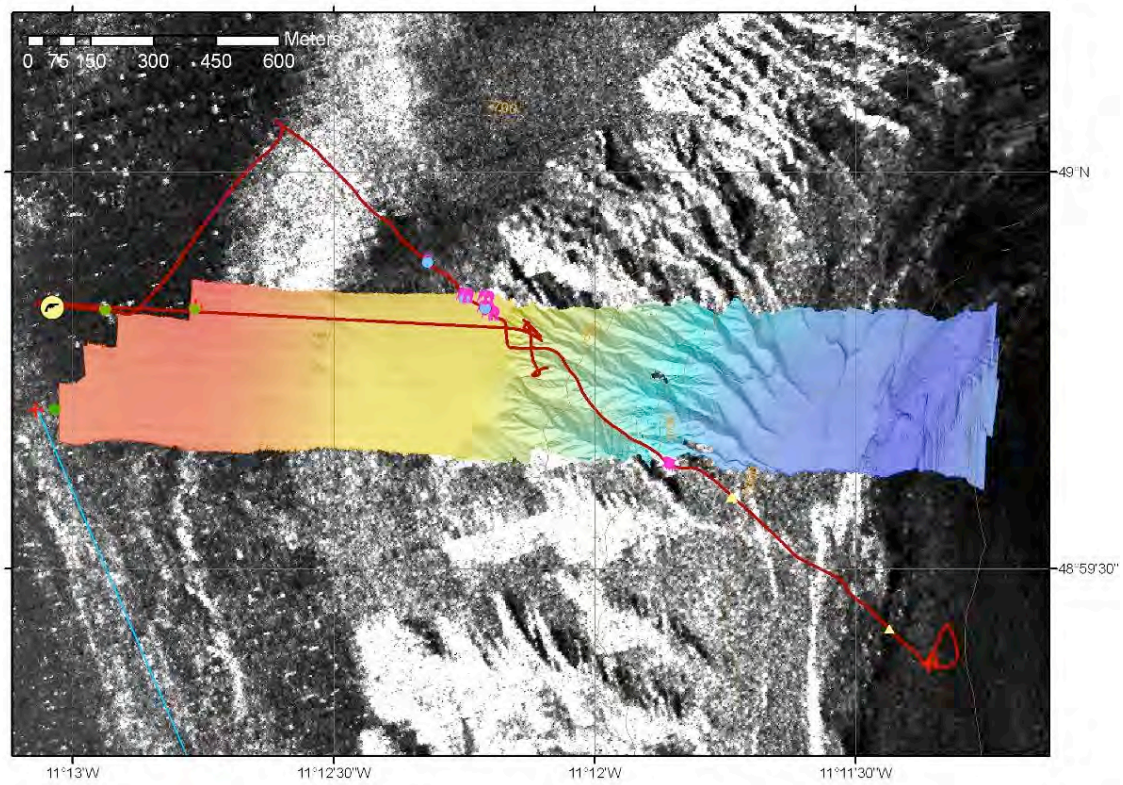

Figure CS5.5: ROV bathymetry of a gully system in upper Whittard Canyon, western branch. For location see Fig. CS5.4. Background: TOBI sidescan sonar mosaic. Compare the detail between the two datasets (1x1 m vs. 3x3 m pixel resolution). Insights obtained from the ROV bathymetry can now be transferred to locations on the TOBI mosaic, where similar gully patterns can be identified.

The observation that the richest benthic communities appear to occur in areas with steep topography in the Portuguese canyons (Tyler et al., 2009) underpinned the choice of some of the ground-truthing sites in Whittard Canyon. The eastern branch contains a higher proportion of steep substrates, either in the form of gully systems, or in the form of escarpments and submarine cliffs (Fig. CS5.7). Some of those areas provided terrain morphologies beyond expectation, such as the gully system at ca. 1800 m water depth, where the steep gullies are separated by knife-sharp ridges ending in walls of about 1m wide and 10 m high (Fig. CS5.8). A diverse community of filter feeders was found in this area (Fig. CS5.9), including the stony coral *Lophelia pertusa*, which is most commonly reported from shallower depths of ca. 700-1000m along the NE Atlantic margin (Roberts et al., 2009).

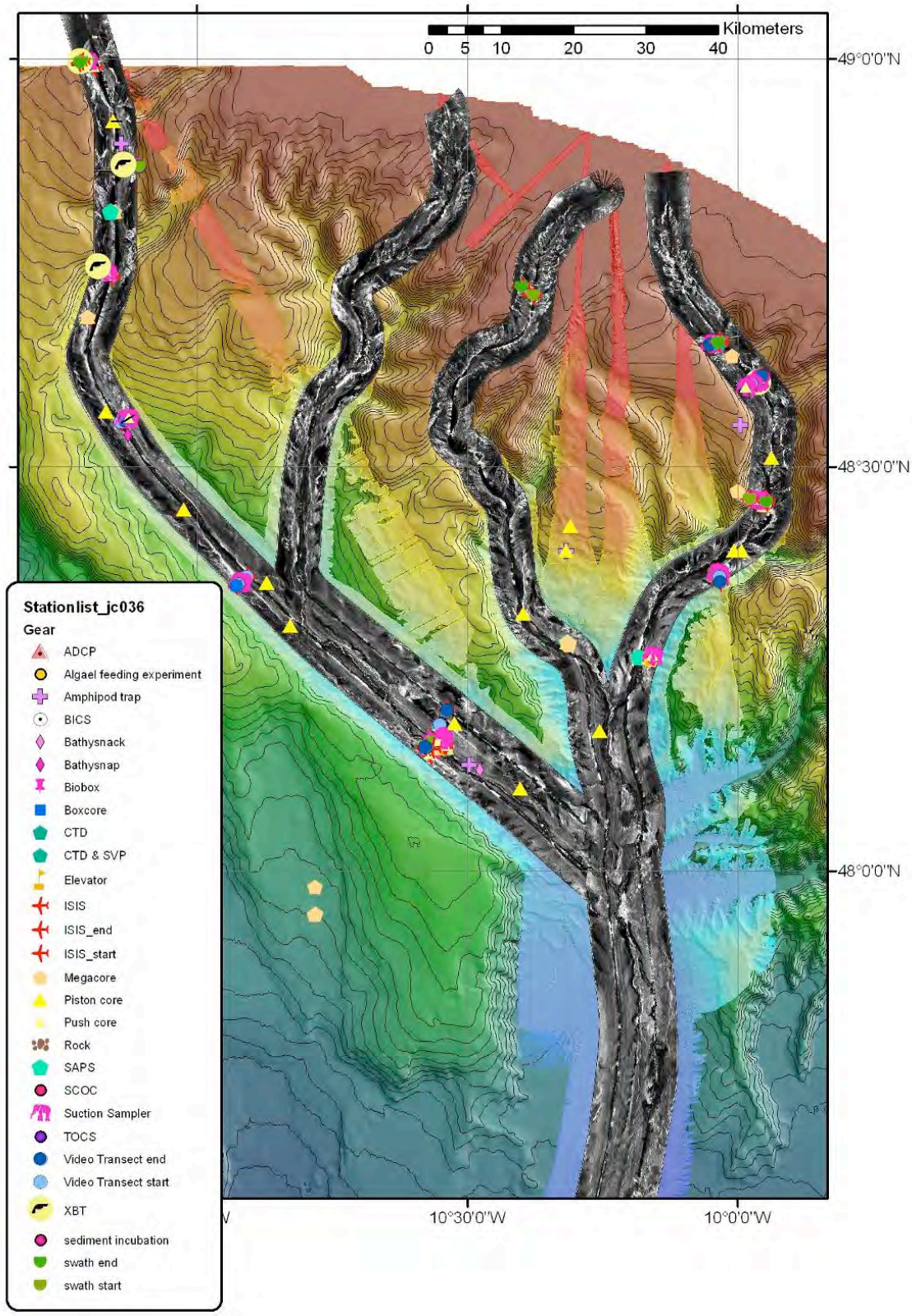

Figure CS5.6: Multibeam and TOBI sidescan sonar coverage map showing locations of all stations occupied during JC036. Note that a 39-day cruise only provided time for the ground-truthing of the eastern-most and western-most branch of the canyon system (although some time was also used for ROV-based in-situ experiments at the seabed).

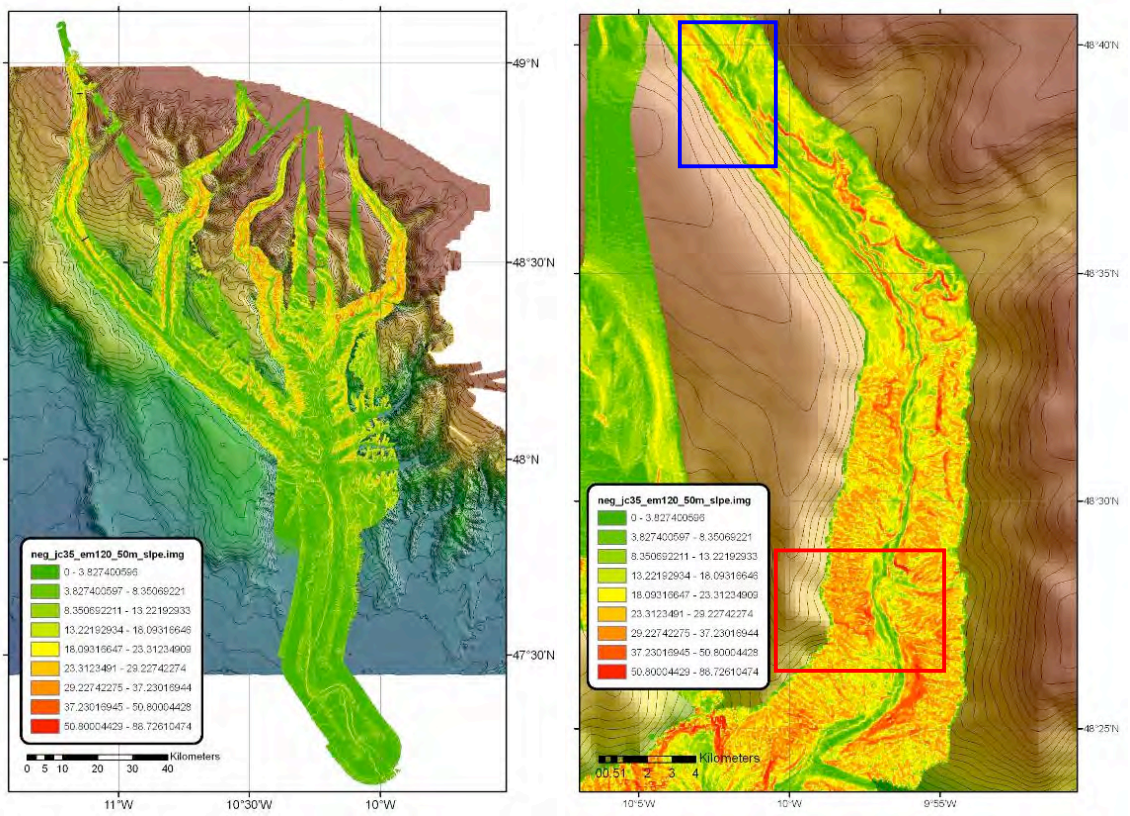

Figure CS5.7: Slope map of Whittard Canyon (left) with detail of the eastern branch (right), where the majority of the steep substrates are found. Red box is the approximate position of Fig. CS5.8; blue box that of Fig. CS5.10.

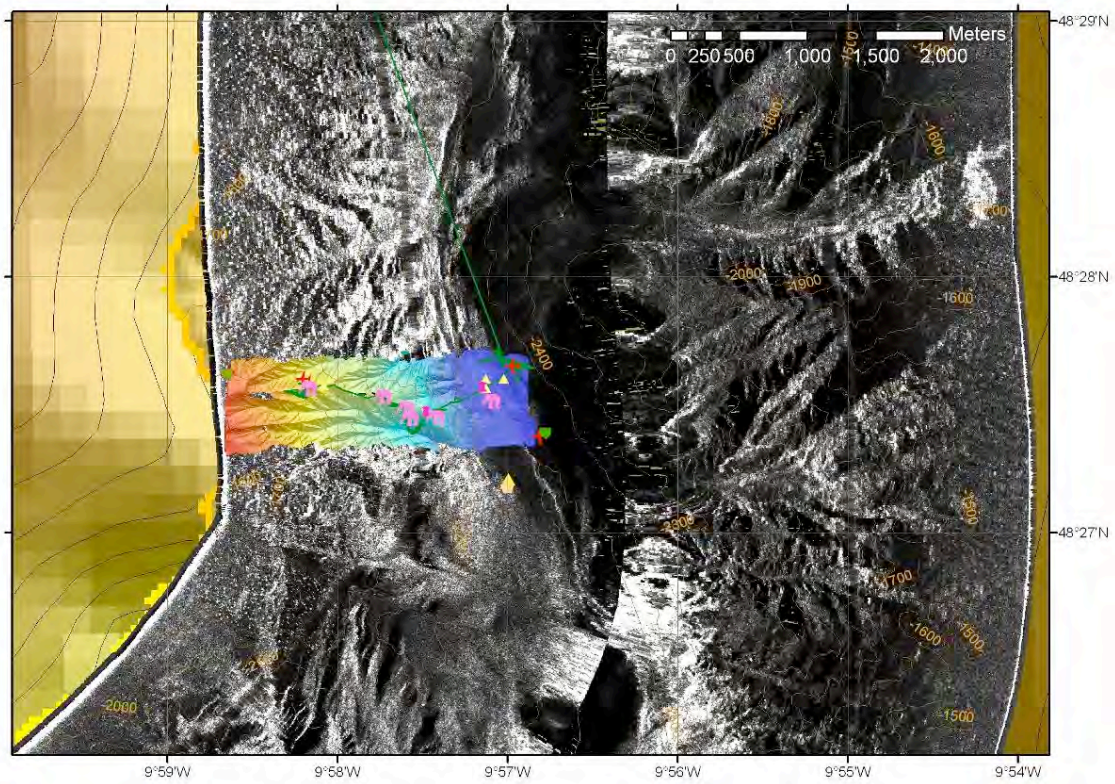

Figure CS5.8: TOBI sidescan sonar map and ROV bathymetry of a gully system in the Whittard Canyon, eastern branch. For location see Fig. CS5.7.

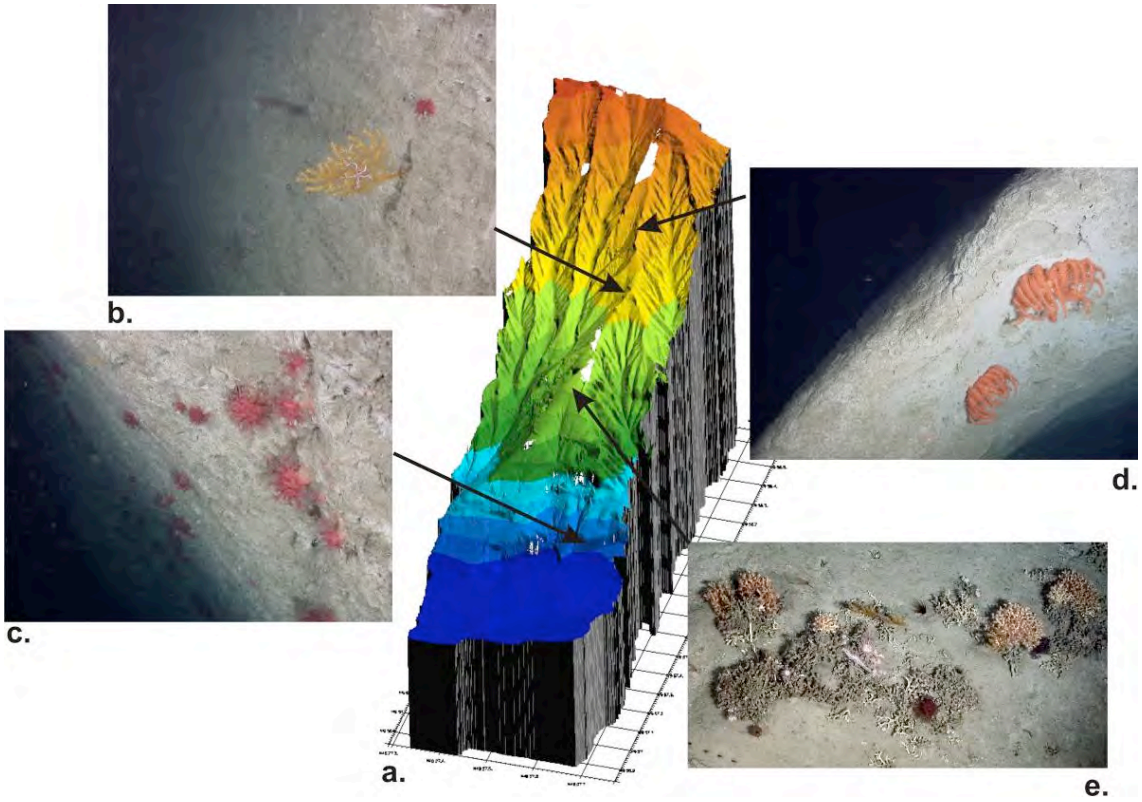

Figure CS5.9: Diversity of filter-feeder fauna around the steep terrains of the gully system at 1800m water depth, eastern Whittard Canyon. (a) 3D model of the ROV bathymetry, presented without vertical exaggeration; (b) Gorgonian coral with associated brittle star; (c) Anthomastus soft corals at the base of the gully system; (d) Illustration of the knife-sharp walls on the ridges separating the gullies. Substratum used by Brisingid *seastars; (e) patch of* Lophelia pertusa *and associated fauna. For location see Fig. CS5.8.*

The most illustrative example of the increased understanding of deep-sea terrain and habitat as a result of ROV use for habitat mapping was the discovery of an overhanging cliff in the eastern branch of the Whittard Canyon, at ca. 1350m water depth (Figs CS5.10-5.11). Although the shipboard bathymetry indeed indicated the presence of a scarp at that depth, downward looking multibeam systems and ship-deployed equipment (cores, video-frames) simply cannot detect this kind of setting. In order to map the cliff morphology in detail, the ROV multibeam system was mounted on the front of the vehicle, pointing forwards. With the ROV traveling sideways at several depths (and distances off the cliff), a series of maps of the cliff habitat could be made with different resolution and extent (Fig. CS5.12). These illustrate the geological framework of the substrate, and at higher resolution show individual bedding planes and biological cover. Subsequent video surveying of the cliff revealed that it was covered up to 70% with a rich cold-water coral-based community. The discovery and mapping method, together with the resulting interpretation and implications for deep-sea management are discussed in Huvenne et al. (2011).

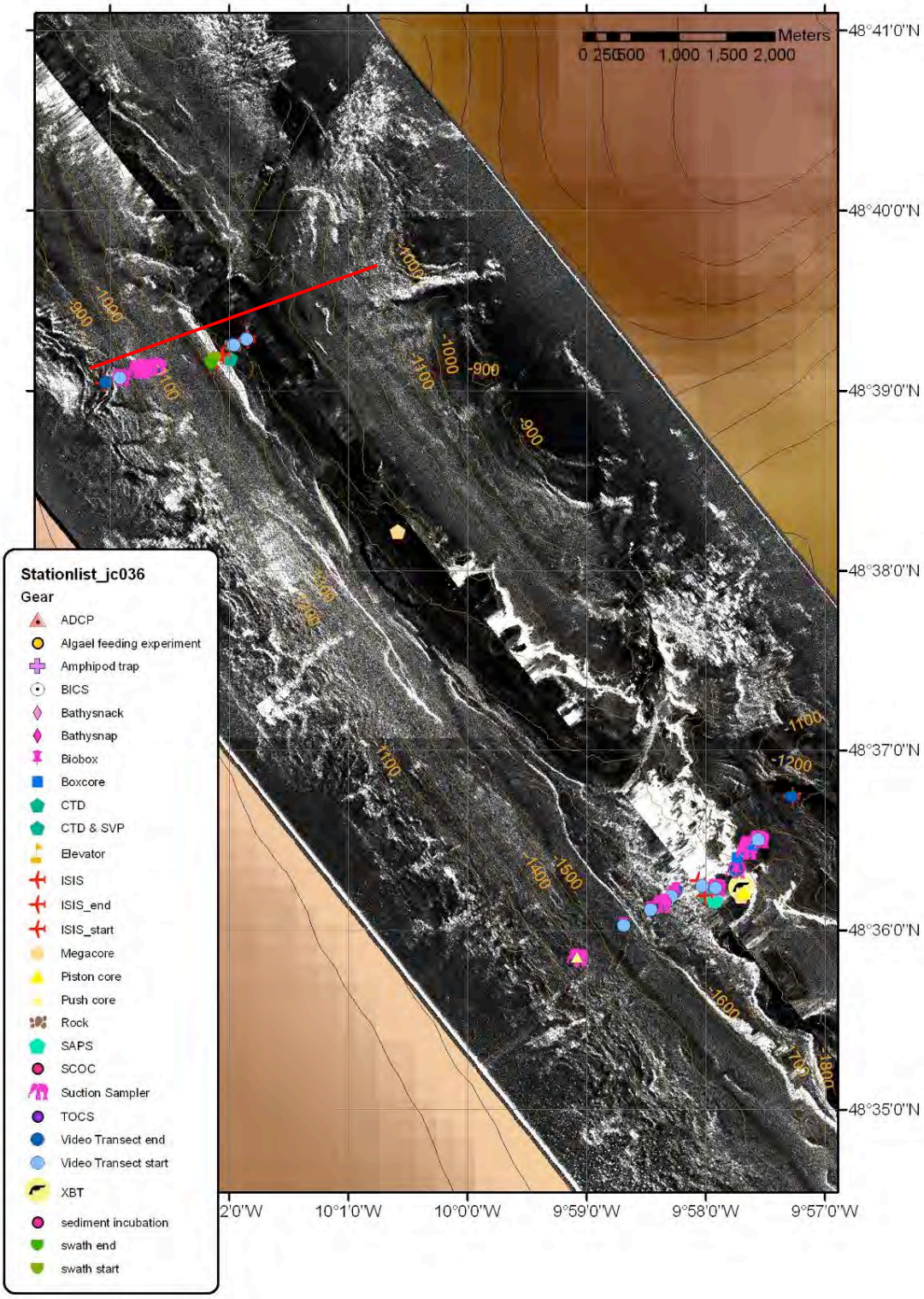

Figure CS5.10: Location map of the coral wall in Whittard Canyon, eastern branch. For location see Fig. CS5.7. The position of the depth profile presented in Fig. CS5.11 is indicated with a red line.

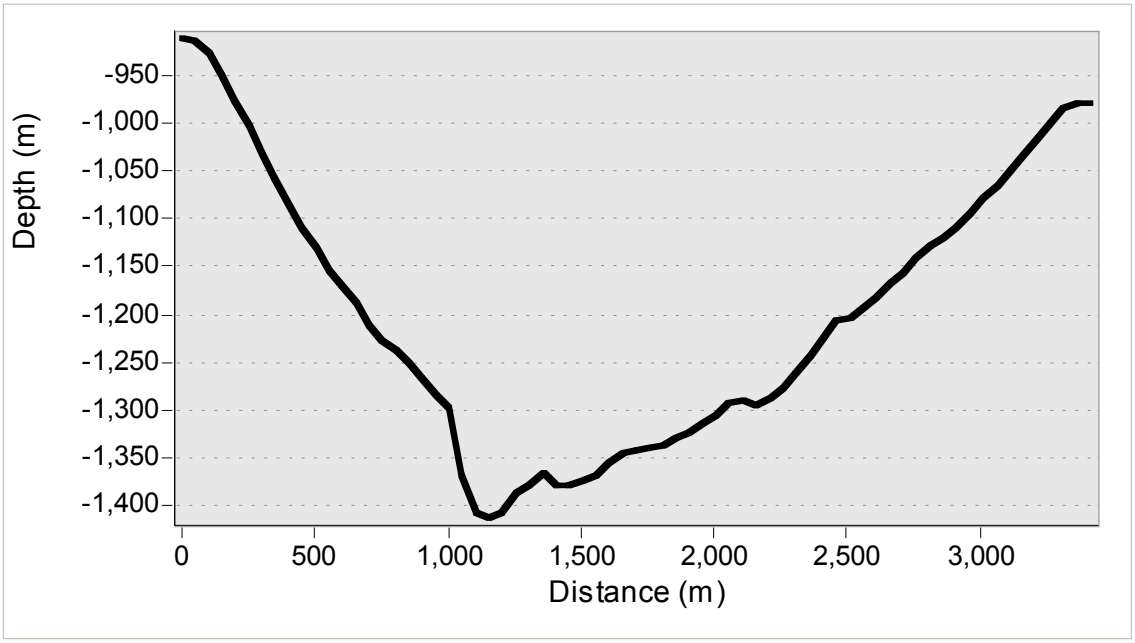

Figure CS5.11: Depth profile across the upper Whittard Canyon, eastern branch, illustrating the steep topography around the scarps in that area. Note the vertical exaggeration. For location see Fig. CS5.10.

CS5.5. Implications

The examples presented in this Case Study illustrate the necessity of collecting data at several levels of detail, extent and resolution. Further research is necessary to develop quantitative techniques to correlate these insights at each stage of the nested survey, and fractal theory is just one possible avenue of investigation with that respect (Fig. CS5.13). The ERC project CODEMAP, closely linked to the MAREMAP programme, is specifically aimed at covering these scale gaps in a quantitative way.

As stated before, the work in Whittard Canyon has provided an insight in the extreme complexity that can be found in certain deep-sea areas. This complexity forms a challenge for routine approaches to habitat mapping and marine surveying for the designation of Marine Protected Areas. The use of deep-water Robotic Vehicles is necessary to obtain sufficient detail, but even for those vehicles, the extreme terrain poses challenges. For example, collision avoidance and bottom tracking systems in AUVs may be pushed to their limits when surveying gullies such as those presented in Fig. CS5.9. In such cases, the use of manually steered ROVs is currently still the best survey method, although technology develops quickly and solutions are actively being pursued. For example, one of the aims of the ERC project CODEMAP is to transfer and perfect the ‘sideways mapping’ technique onto the Autosub6000 vehicle, which would provide a more stable and time-efficient way to map the scarps in Whittard Canyon.

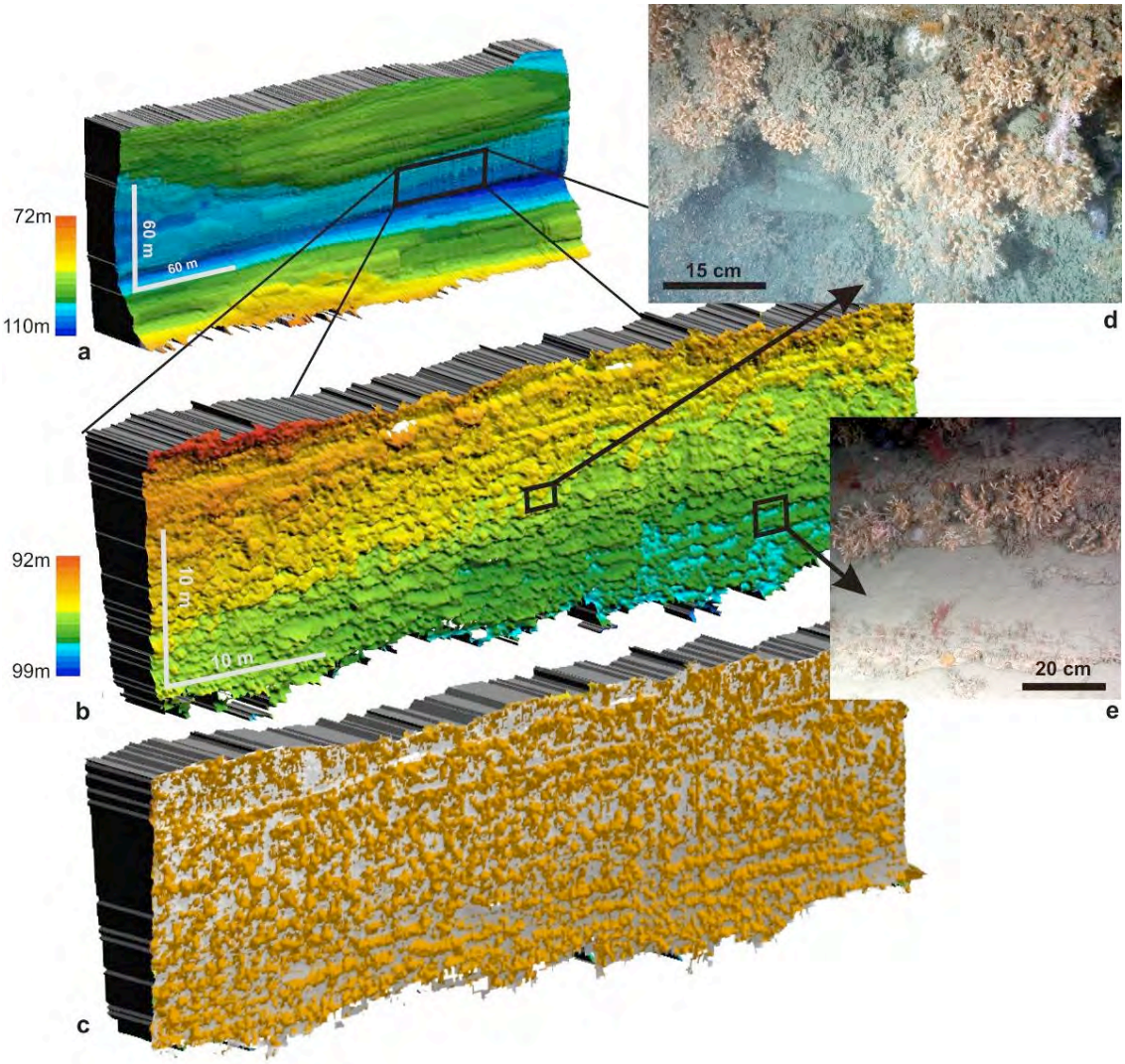

Figure CS5.12: Results of sideways ROV mapping of the coral wall in the upper Whittard Canyon. For location see Fig. CS5.10. (a) overall cliff morphology, mapped from 30 m distance (50 cm pixel size), illustrating the fact that the cliff is overhanging; (b) detailed map, acquired from 7 m distance (10cm pixel size), showing individual bedding planes and the shapes of the coral colonies; (c) top-hat transformation of the map above, illustrating the coral cover (~70%); (d) example of the rich and extensive coral framework attached to the geological strata; (e) illustration of the preference of the corals for specific types of strata, especially the more protruding and overhanging parts of the wall.

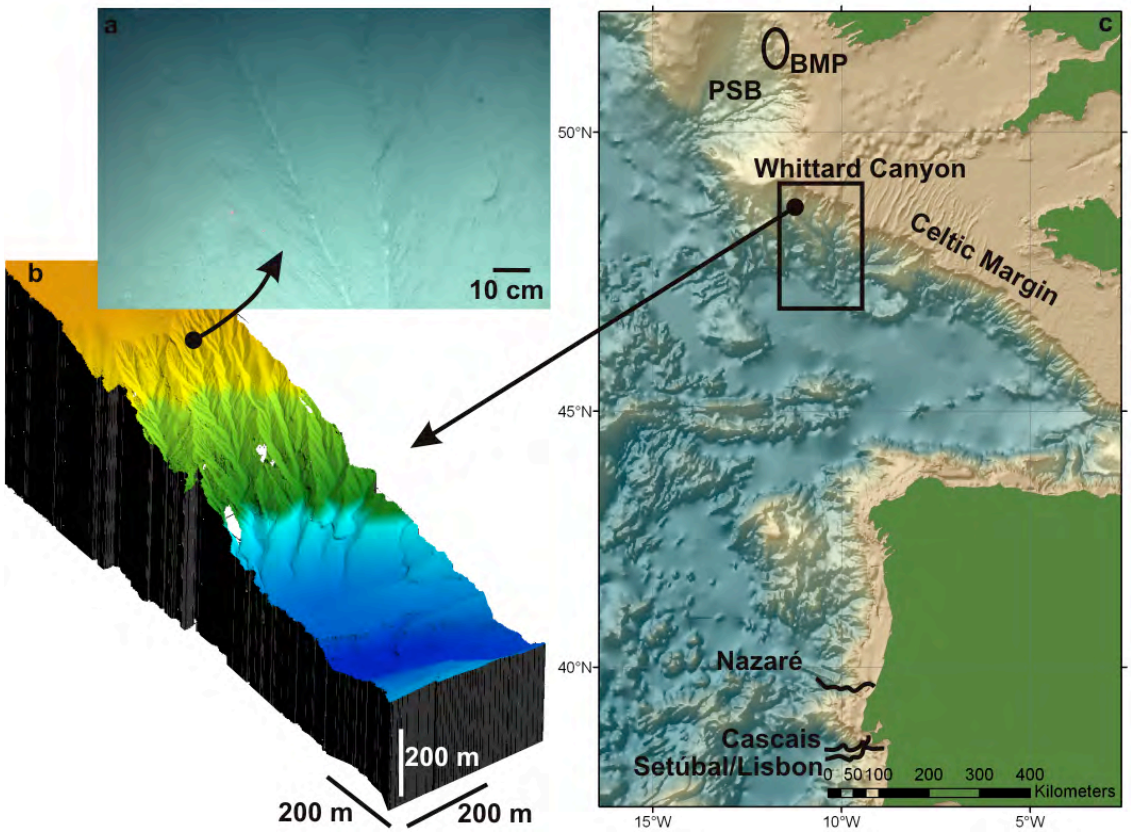

Figure CS5.13: Relationship between spatial scales in Whittard Canyon, illustrating gullies of cm-size, m-size and the km-size canyon itself.

CS5.6. References

Canals, M., Puig, P., Durrieu de Madron, X., Heussner, S., Palanques, A. & Fabres, J. (2006). Flushing submarine canyons. Nature 444, 354-357.

Crowe, B.M. (2010). An interpretation of the morphology and recent sedimentary processes of Whittard Submarine Canyon, Bay of Biscay, North-Eastern Approaches.BSc Honours Dissertation, University College Cork, Cork, 56pp + Appendices.

Cunningham, M. J., Hodgson, S., Masson, D. G. & Parson, L. M. (2005). An evaluation of along- and down-slope sediment transport processes between Goban Spur and Brenot Spur on the Celtic Margin of the Bay of Biscay. Sedimentary Geology 179, 99-116.

De Leo, F. C., Smith, C. R., Rowden, A. A., Bowden, D. A. & Clark, M. R. (2010). Submarine canyons: hotspots of benthic biomass and productivity in the deep sea. Proceedings of the Royal Society B-Biological Sciences 277, 2783-2792.

de Stigter, H. C., Boer, W., de Jesus Mendes, P. A., César Jesus, C., Thomsen, L., van den Bergh, G. D. & van Weering, T. C. E. (2007). Recent sediment transport and deposition in the Nazaré Canyon, Portuguese continental margin. Marine Geology 246, 144-164.

Huvenne, V.A.I. and et al RRS James Cook Cruise 35, 7-19 Jun 2009. Sidescan sonar mapping of the Whittard Canyon, Celtic Margin, Southampton, National Oceanography Centre Southampton, 2009, 35pp. (National Oceanography Centre Southampton Cruise Report, 42) http://eprints.soton.ac.uk/69695/

Huvenne, V.A.I., Tyler, P.A., Masson, D.G., Fisher, E.H., Hauton, C., Hühnerbach, V., Le Bas, T.P., Wolff, G.A. (2011) A picture on the wall: innovative mapping reveals cold-water coral refuge in submarine canyon. PLoS ONE, 6(12), e28755. Doi:10.1371/journal.pone.0028755.

Huvenne, V.A.I., Pattenden, A.D.C., Masson, D.G., Tyler, P.A. (2012). Habitat heterogeneity in the Nazaré deep-sea canyon offshore Portugal. In: Harris, P.T. & Baker E.K. (Eds.). Seafloor geomorphology as benthic habitat: GeoHab atlas of seafloor geomorphic features and benthic habitats. Elsevier, Amsterdam, 691-701. Doi: 10.1016/B978-0-12-385140-6.00050-5.

Masson, D.G. (2009). The geobiology of Whittard Submarine Canyon. Southampton, National Oceanography Centre Southampton, 2009, 53pp. (National Oceanography Centre Southampton Cruise Report, 41).

Roberts, J. M., Wheeler, A. J., Freiwald, A. & Cairns, S. D. (2009). Cold-water corals: the biology and geology of deep-sea coral habitats, Cambridge University Press, Cambridge.

Toucanne, S., Zaragosi, S., Bourillet, J.-F., Naughton, F., Cremer, M., Eynaud, F. & Dennielou, B. (2008). Activity of the turbidite levees of the Celtic-Armorican margin (Bay of Biscay) during the last 30,000 years: imprints of the last European deglaciation and Heinrich events. Marine Geology 247, 84-103.

Tyler, P., Amaro, T., Arzola, R., Cunha, M. R., de Stigter, H., Gooday, A. J., Huvenne, V., Ingels, J., Kiriakoulakis, K., Lastras, G., Masson, D., Oliveira, A., Pattenden, A., Vanreusel, A., van Weering, T., Vitorino, J., Witte, U. & Wolff, G. (2009). Europe's Grand Canyon: Nazare submarine canyon. Oceanography 22, 48-57.

Vetter, E. W. & Dayton, P. K. (1998). Macrofaunal communities within and adjacent to a detritus-rich submarine canyon system. Deep-Sea Research Part Ii-Topical Studies in Oceanography 45, 25-54.
Zaragosi, S., Bourillet, J.-F., Eynaud, F., Toucanne, S., Denhard, B., Van Toer, A. & Lanfumey, V. (2006). The impact of the last European deglaciation on the deep-sea turbidite systems of the Celtic-Armorican margin (Bay of Biscay). Geo-Marine Letters 26, 317-329.

Case Study 6: Shallow-water boat-based mapping off NW Scotland

CS Leader: Dr John Howe (SAMS)

CS6.1. The CS6 task

As set out in the proposal this task's remit was as follows:

"*In shallow-water environments on the continental shelf, seafloor mapping has traditionally been undertaken from small inshore vessels using hull-mounted multibeam bathymetry systems. Much of the existing high-resolution bathymetry data from the UK shelf has been collected by the MCA and partners to IHO Order 1a standard, in order to comply with 'Safety at Sea' requirements. This case study will provide examples of existing high-resolution hull-mounted multibeam bathymetry data from the NW UK shelf, with a focus on the rocky seafloor off NW Scotland.*

*This Case Study will be compiled by SAMS between 1 March and 31 May 2012***.**"

CS6.2. Introduction

This work package describes recent hydrographic surveys in the Sea of the Hebrides, the region of a number of proposed MPAs, and identifies the benefits, costs and risks of using vessel-mounted bathymetric observations for MPA work. The data described in this Case Study are derived from a number of sources. In particular most of the data was collected as part of the Civil Hydrography Program (CHP) instruction for the Maritime and Coastguard Agency, from Emergency Towing Vessel ETV Anglia Sovereign. In addition, some surveys were undertaken from the SAMS vessel R/V Calanus for the NERC's Oceans 2025 program, and finally for Marine Science Scotland from the Northern Lighthouse Board vessel NLV Pole Star for MPA and renewables.

Later in this report is an articulation of the variety of data types and products generated by vessel mounted multibeam sonar. It is important to outline here the datasets gathered in the Sea of the Hebrides. Since the 1980's SAMS have collected a wide variety of oceanographic data from this region, notably biological and physical data. The NERC-funded research programs of the late 1990's and more recently have provide a wealth of data. Multibeam sonar is a recent acquisition to SAMS capabilities, being bought for the Oceans 2025 program in 2007. The main source of bathymetry data in the UK is the UK Hydrographic Office, which licenses bathymetric data through SeaZone. The advent of the MAREMAP partnership has coincided with large datasets becoming accessible through data sharing agreements and other Memorandum of Understanding, whereby the UKHO and the MCA are interested in providing data to other users outwith of the data required simply for updating navigational charts. Given the wide uses of bathymetric data there are a number of approaches for data collection, which the Sea of the Hebrides nicely illustrates. Data collected by the R/V Calanus was principally collected using a pole-mounted system; this does not confirm to international data standards (International Hydrographic Organisation Order 1a) and thus have data errors and artefacts (see Fig. CS6.1), which, whilst not impairing the actual imagery (collected for geological investigations) does mean the data is not suitable for making navigational charts. SAMS have since updated its procedure to a hull-mounted system. The ETV Anglia Sovereign obtained the highest quality data on behalf of the Maritime and Coastguard Agency for purposes of updating navigational charts.

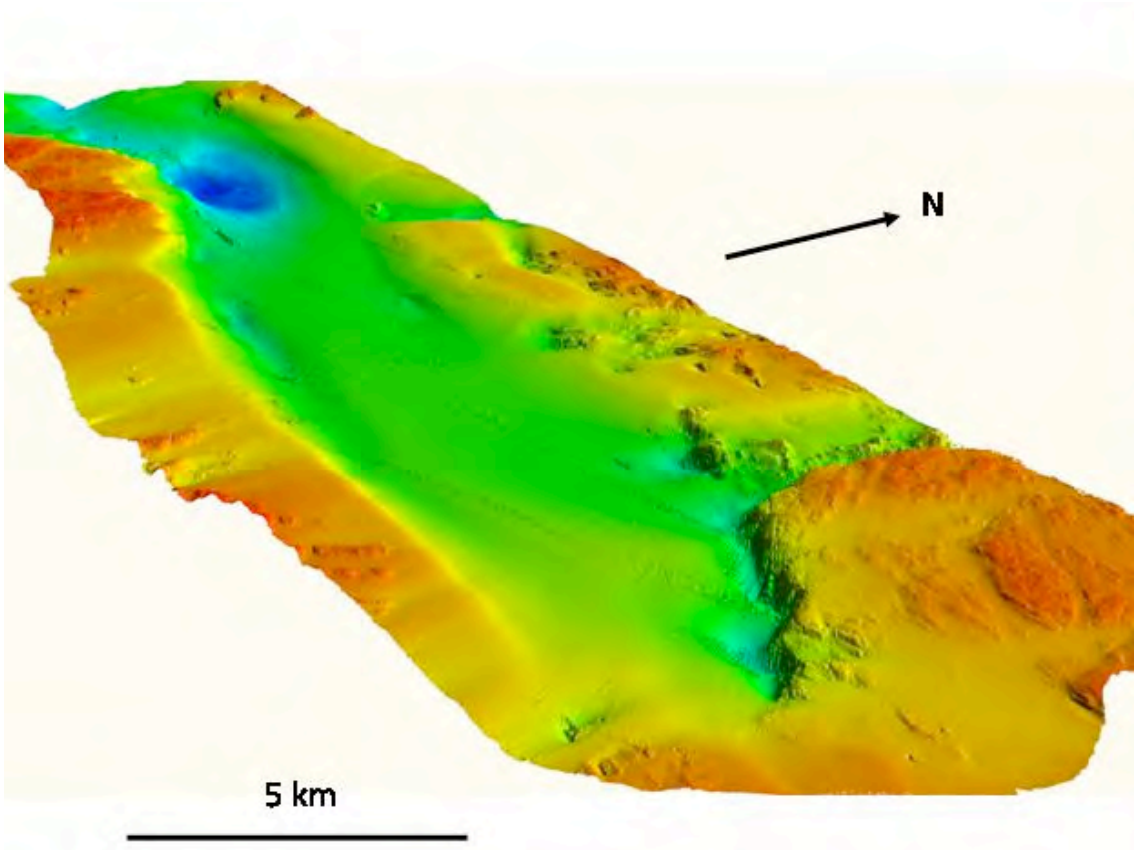

Figure CS6.1: A ~75 km^2 survey from the Muck Deep, Sea of the Hebrides, collected in 2009 from a pole-mounted 8124 Reson system from R/V Calanus. Note the data artefacts – visible as 'train-tracks' - showing data quality issues on the outer beams, a problem that is solved by more sturdy hull-mounted systems. For this project with a geological aim – these artefacts were acceptable.

Also collected alongside the bathymetric data is backscatter or (faux) side-scan data. This data is extremely useful in classifying the texture of the seabed. Data collected as part of the CHP routinely collect backscatter, although the priority is always Saving Life at Sea (SOLAS), this being the main driver, the backscatter data does not always get the attention it should, and is an essential requirement for MPA work.

CS6.2.1. The Sea of the Hebrides – geological and oceanographic setting

The Sea of the Hebrides is an area of bathymetrically complex seafloor west of the Scottish mainland, south of the Isle of Skye and including the Isles of Rum, Muck, Eigg and Canna (part of the 'Inner Hebrides' island group; Fig. CS6.2). The area is geologically notable containing a wide variety of lithologies including igneous rocks of the British Tertiary Igneous Province (BTIP) and numerous tectonic features relating to the geological evolution of the region, e.g. the Moine Thrust (Fyfe et al., 1993; Smith, in press). The most prevalent bedrock types at seabed and underlying the Quaternary within the study area include outcrops of undivided Torridonian, Triassic and Jurassic rocks within two NNE trending Mesozoic basins (Hebrides-Little Minch Trough and Inner Hebrides Trough), and the volcanic/volcaniclastic rocks of the BTIP (Fyfe et al., 1993). Within the study area the BTIP lavas from Skye, Eigg, and Mull are present, along with the more structurally complex volcanic centres of Ardnamurchan and Rum (Browne et al., 2009; Smith, in press).

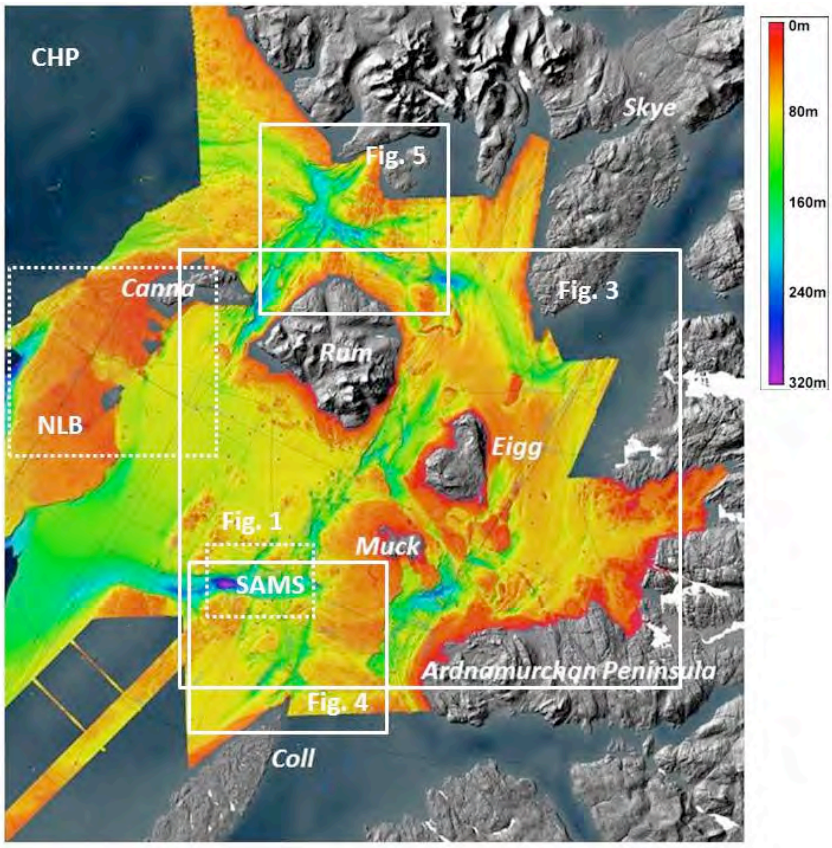

Figure CS6.2: Sea of Hebrides bathymetry, surveyed principally by ETV Anglia Sovereign, (CHP: Civil Hydrography Programme), with additional input from Northern Lighthouse Board (NLB) and SAMS. Main image used courtesy of the Maritime and Coastguard Agency. Adapted from Howe et al. (submitted). Location of Figs CS6.1 and 6.3-6.5 also shown.

During the Quaternary, it is assumed that the Sea of the Hebrides was overridden by the BIIS on numerous occasions (e.g. Boulton et al., 1991) although the incomplete marine sediment record precludes quantifying the number of ice sheet advance-retreat cycles. The evidence for glacial erosion and deposition is variable but deposits exist of Quaternary (largely glaciogenic) sediment, the thickness of which can locally exceed 300 m (Fyfe et al., 1993). The complex bathymetry of the region is also testament to the action of multiple glaciations, with elongate, over-deepened rock basins a character of the inshore continental shelf (Wingfield, 1989; Fig. CS6.1). Principally the deeps have formed in the structural lows (Mesozoic Basins) or areas of predisposed structural weakness (Evans et al., 1986) and their over-deepening and general orientation suggest ice-flow direction. The bedrock highs (Fig. CS6.3), between the rock basins have correspondingly been formed from the more resistant Pre-Cambrian and Tertiary rocks. The Quaternary deposits of the Sea of the Hebrides are highly variable, mostly comprising Devensian-age sediments and most confined to the basins. Earlier, Pre-Devensian age sediments are present, notably these are in the Canna Basin, but are eroded and incomplete (Fyfe et al., 1993).

The shelf has subsequently been shaped by sub-glacial and post-glacial processes. The Sea of the Hebrides has been postulated as the location of a Devensian-age (MIS-2) fast-flowing ice stream, sometimes referred to as the Barra (-Donegal) Fan Ice Stream (Dunlop et al., 2010), a south-flowing equivalent of the Minch Ice Stream (Bradwell et al., 2007). Since deglaciation, post-glacial and Holocene tidally dominated processes have modified sediment, reworking and transporting relict glacial deposits across the shelf (Pantin, 1991).

The Sea of the Hebrides is an area of outstanding natural beauty and a region that is presently the subject of interest from industry for both tidal and wind power sites and submarine cable routes. The Minch is a principle seaway for inshore shipping, whilst both the Minch and the Sea of the Hebrides are important areas for shellfish and finfish fisheries. A number of areas within this region are also proposed as Marine Protected Areas (e.g. the area around the Isle of Canna). The Isle of Rum is a nature reserve and a Special Area of Conservation. Given the considerable interest in this area, surprisingly little is known about the submarine landscape or the physical processes that operate within it. The multibeam surveys conducted so far in this region can be used for habitat mapping, especially when combined with video and ground-truthing such as grab samples to determine the benthic fauna.

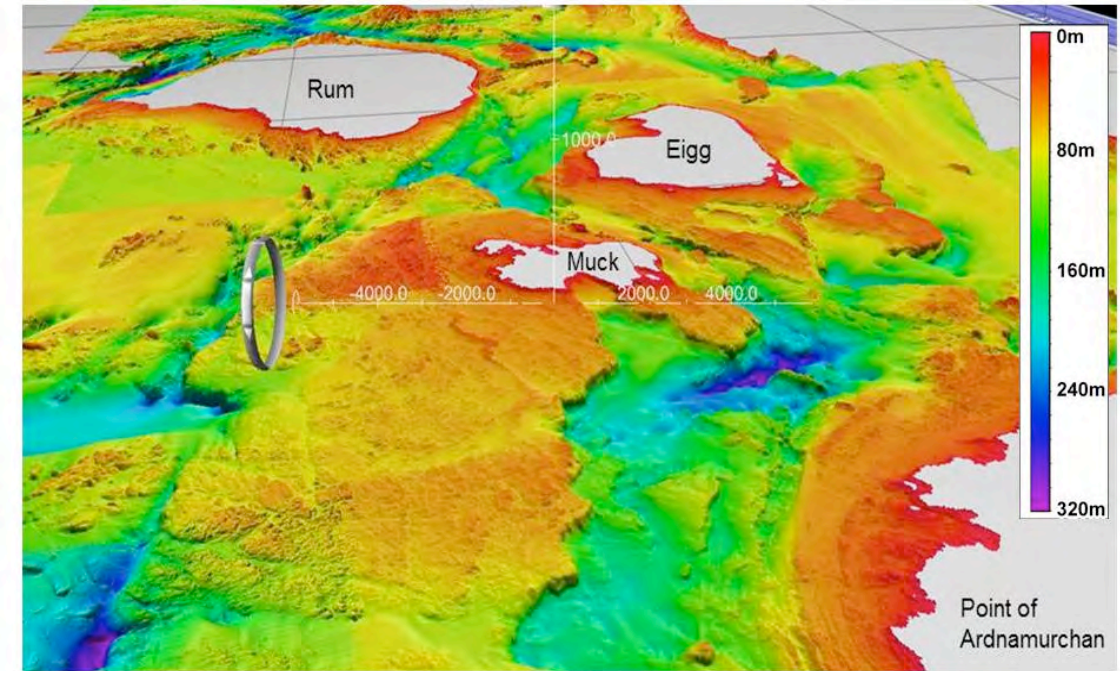

Figure CS6.3: A perspective view across the Sea of the Hebrides from the north of Coll toward Rum. The shallow water bedrock platforms (<50m) south of Muck are very well imaged in the data (iView4D image). For location see Fig. CS6.2.

Generally, the oceanography of the region is characterised by the inflow of Atlantic oceanic waters, and the role of a strong, dynamic tidal regime. Oceanic waters flow into the region between Tiree and Barra (Ellett and Edwards, 1983) although this inflow is highly variable between years (Inall et al., 2009). The Scottish Coastal Current (SCC) flows northwest through the Sea of Hebrides. Estimates of the transport volume of the SCC vary between ca. 11 x 10^4 m^3/s^{-1} to 9 x 10^4 m^3/s^{-1} (McKay et al., 1986; Inall et al., 2009).

The modern hydrography in the Sea of the Hebrides is tidally dominated where localised strong tidal flows (>1m/s^{-1}) can occur, notably between Eigg and Muck and Canna and Rum (UKHO, 2008). These enhanced flows may be the product of the restricted passage of water between the islands and the complex seafloor topography (Ellett and Edwards, 1983, Ellett, 1979). The water masses in the deeps (>200m) are isolated from lateral exchange and therefore not well mixed, especially during the quieter summer months. The role of internal waves are not well understood in this region, however, given the extent of mixing occurring in the winter, there is the possibility of an enhanced internal tide responding to a greater stratification of the water column in the summer.

CS6.3. Methods (techniques and time)

Seabed bathymetric data were collected by the Maritime and Coastguard Agency, Emergency Towing Vessel, ETV Anglia Sovereign, using a Reson 7125 Seabat dual frequency multibeam utilising 512 beams, at either 200 or 400kHz frequencies across a 165° swath; this provided data coverage approximately 5x water depth with a potential resolution of 0.6 cm*, in addition to grab samples and ancillary observations (e.g. weather, sea state, sea visibility, detailed focus on obstructions, wrecks). Surveys were conducted during 2008-2011 as part of the Civil Hydrography Programme (CHP) on behalf of the Maritime and Coastguard Agency (MCA). Most of the survey is identified as Hydrographic Instructions 1257, 1297 and 1299, and covers an area of approximately 2200 km^2 from the Ardnamuchan Peninsula in the south and south of the Isle of Skye in the north and from the Scottish mainland to 7^o west (see Fig. CS6.2). Surveys southwest of Canna were subsequently collected by the Northern Lighthouse Board vessel, NLV Pole Star for Scottish Natural Heritage on behalf of the Scottish Government (Marine Science Scotland) in 2010. NLV Pole Star surveyed using a Kongsberg EM3002 multiple frequency (293, 300, 3007kHz) with 130-200° beam angles providing a swath coverage of approximately 7x water depth with a resolution of 1cm*. Additional data were provided by SAMS vessel R/V Calanus (2009) using a pole-mounted Reson Seabat 8124 200 kHz multibeam. The system utilises 80 beams across a 120° swath providing data coverage approximately 3x water depth with a potential resolution of 20 cms*. Sound velocity data were collected from a hull-mounted Reson SVP 71 sound velocity probe. Attitude, heading and positional data were collected using a DMS-05 motion sensor, a TSS Meridian surveyor gyro compass and an Ashtech ADU3 Dynamic Global Positional System (DGPS). All data were compiled on board using Triton Isis software. Conductivity, Temperature and Density (CTD) dips were obtained during the survey using a Seabird 19+ instrument. Water column velocity profiles were prepared using SeaTerm software and converted into ASCII files. As described below weather downtime in this region can be up to 30% of a survey and needs to be factored into surveying planning.

Post-acquisition data processing was conducted by the UK Hydrographic Office. The data were imported, cleaned and basic mean bathymetric and CUBE (Combined Uncertainty Bathymetric Evaluation) grids were prepared. Subsequent data manipulation and visualisation was conducted by the British Geological Survey using Caris HIPS and SIPS and Fledermaus software (Figs CS6.3-6.5). GeoTiff's of the data layers were imported into ArcGIS v.9 where geomorphological classification and mapping were conducted, via direct digitising of features.

*Although these figures look impressive they are theoretical and very rarely achieved. The variables of data density and data processing mean that only very small amounts of data can be utilised to provide these sorts of resolution – a survey the size of the Sea of the Hebrides will be gridded at >5m resolution – in order to be able to be represented on a desktop computer.

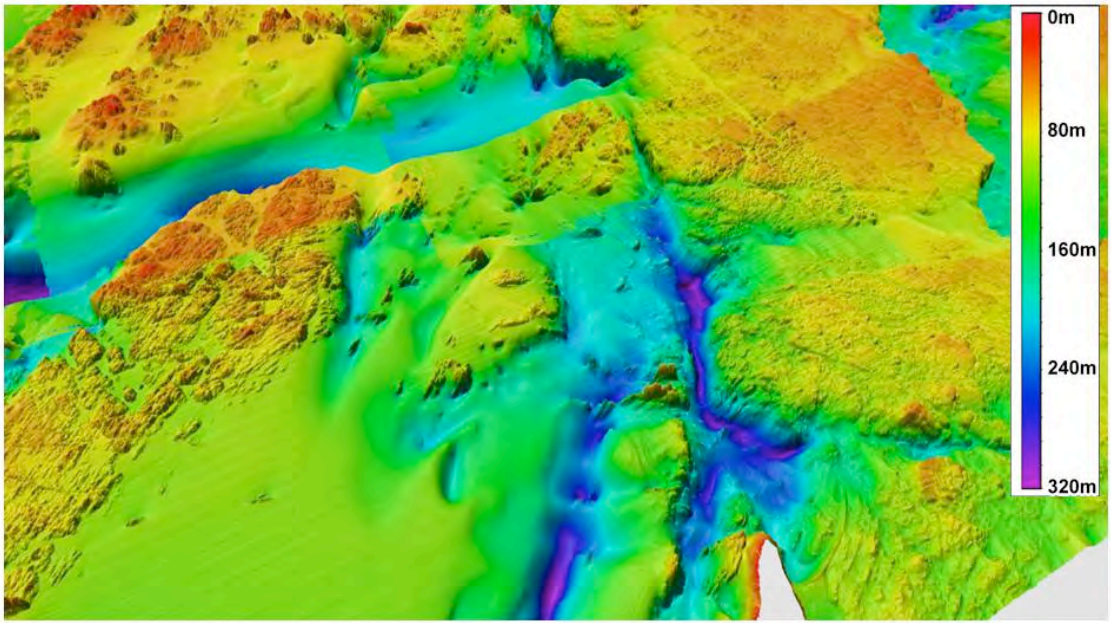

Figure CS6.4: Perspective (looking N) of seabed imagery north of the Isle of Coll. For location see Fig. CS6.2. Note the overlap (at left hand side of image) between datasets, and the faintly visible track lines in the foreground showing the density of line spacing. Figure is approximately 15 km wide (iView4D image).

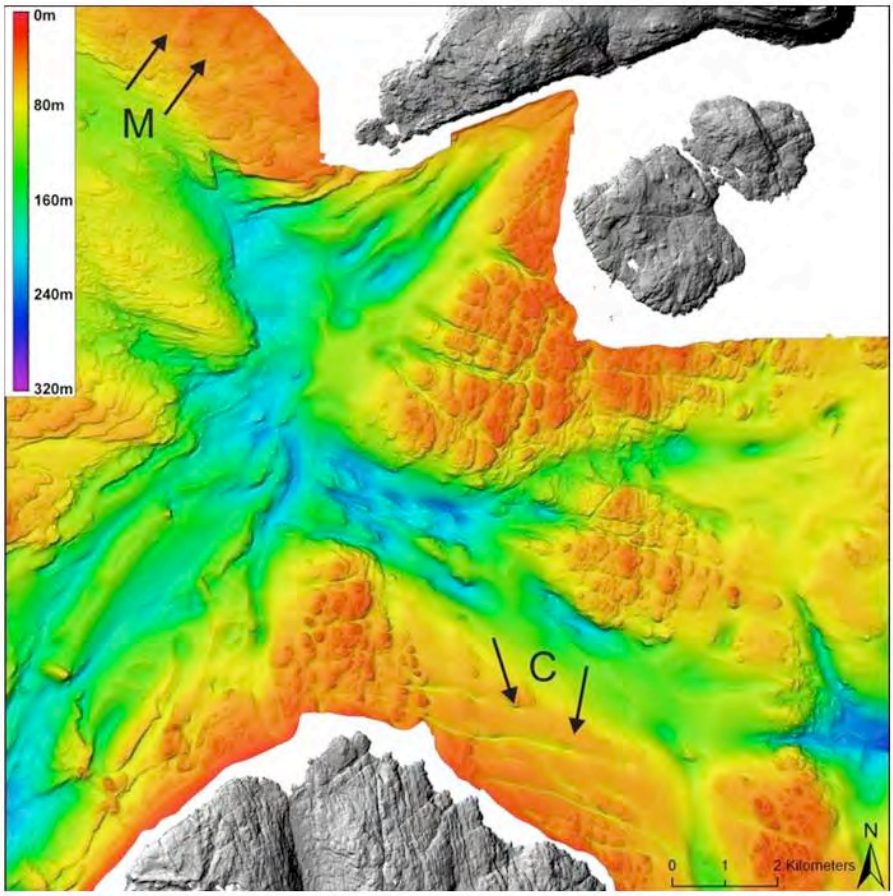

Figure CS6.5: The glaciated seabed north of the Isle of Rum, showing the incised Mesozoic bedrock to below 200 m water depth. For location see Fig. CS6.2. Northeast of the island

the seabed has been eroded into channels (C) and faint moraines also occur west of Skye (M). This image was gridded at 7 m, producing the smooth 'plastic' appearance.

Detail on considerations of survey methodology can be found below. The duration of a survey can be readily estimate based on the vessel used, an approximation of the water depth and the multibeam system to be used. For example, for the Sea of the Hebrides, a coverage area of 2200 km^2 based on the ETV Anglian Sovereign and using a Reson 7125 system with swath coverage of 5x water depth is based on the following assumptions: 24hr working, with water depths of 5-300m and perhaps a 30% downtime (or less) from using a larger (60m) vessel with the capability to survey in poorer weather. Using these assumptions an estimate of 202 days survey time for the Sea of the Hebrides survey is arrived at. This estimate requires further fine-tuning (see below) but is a realistic estimate of the vessel effort required for a survey of the extent discussed here.

Item	Value	Effort
ETV Anglia Sovereign (60m)	Larger vessel reduces weather downtime	24hr working
Reson 7125	x5 water depth reduces survey time	Seabed coverage
Bad weather downtime	30% estimate	Reduced with larger vessels

Table CS6.1: Parameters used to estimate vessel effort

A further consideration when estimating survey time is the effort required for processing the data. A good rule of thumb to allow an equivalent time to process the data as was taken with data collection. A day spent surveying will require a day spent processing. For a survey the size of the Sea of the Hebrides nearly a year was spent by the UKHO in preparing the data. This lag from collection to data product can be reduced by employing onboard data processors, who can process the data as the survey is underway. The considerable advantage in this is to allow any data acquisition problems to be identified whilst the vessel is in the area. Any problem lines can be resurveyed at limited cost to the project, other than time.

A wide variety of both data acquisition and processing software are available: typically there is no real difference in terms of data quality or time spent, but there are very real issues with the importing of data between software. The most commonly used systems are Hypack, SYS, PDS2000, QINSy and Triton Isis with processing in Caris HIPS and SIPS, Fledermaus or Neptune.

CS6.4: Benefits and risks of ship-based observations in the Sea of the Hebrides

For discrete monitoring of MPAs in the Sea of the Hebrides, vessel mounted operations are effective. The real benefit comes from the additional applications of having a small inshore survey in the area enabling other observations to be made (although in the case of bathymetric surveying there are only limited data gathering exercises that can be made, as the vessel is understandably underway all the time). For the Sea of the Hebrides, most of the survey has now been undertaken by ETV Anglia Sovereign – sadly now decommissioned. The question is what can be achieved by repeated surveys? The use of backscatter might reveal impacts of trawling – possibly annual surveys with high-resolution backscatter (<2m) may show recent activity in an MPA and show any seabed disturbance. A combination of backscatter and drop down video would be highly beneficial as a monitoring tool. The use of repeated bathymetric surveys is questionable in this area. However, in regions of high sediment (bedload) transport such as inshore estuaries (e.g. Thames

estuary) and over tidally-influenced sandbanks (e.g. Southern North Sea) this is an invaluable tool. The Sea of Hebrides is only locally influenced by tides and the principle bathymetric control being the bedrock. In this respect, once a survey has been achieved to the highest standard (order 1a) there is little benefit to repeating expensive, time-consuming surveys.

As stated, the impressive amount of data collected in the Sea of the Hebrides is a reflection of the dedicated surveys aimed at the Civil Hydrography Programme. The use of MCA standby Emergency Towing Vessels is invaluable. However, given that this is public funded work, this service is at risk and cannot be relied upon, which points to sub-contracting the work to a survey company (e.g. MMT or EMU both operate multibeam equipped vessels in the area), the advantage of this is a quick turnaround of data but the disadvantage is cost. Other vessels tend of be opportunistic e.g. Northern Lighthouse Board vessel NLV Pole Star and SAMS vessel R/V Calanus. Other vessels with multibeam in Scotland include, Alba Na Mara (Marine Science Scotland, Aberdeen), FRS Scotia (Marine Science Scotland, Aberdeen). For a survey as large as the Sea of the Hebrides, ideally a number of months need to be dedicated to the surveys, and a dedicated vessel provided for the surveys. Smaller areas could be surveyed or resurveyed as required by smaller vessels, possibly with temporary pole-mounted, over the side multibeam systems. This would reduce cost but might have data quality issues if not carefully set up.

CS6.5. References

Boulton, G.S., Peacock, J.D. & Sutherland, D.G. 1991. Quaternary. In: Craig, G.Y. Geology of Scotland. 3rd Edition. Geological Society of London.

Bradwell, T., Stoker, M.S. & Larter, R. 2007. Geomorphological signature of and flow dynamics of The Minch palaeo-ice stream, northwest Scotland. Journal of Quaternary Science, 22, 609-617.

Browne, D.J., Holohan, E.P. & Bell, B.R. 2009. Sedimentary and volcano-tectonic processes in the British Paleocene Igneous Province: a review. Geological Magazine. 146 (3), 2009, pp. 326–352.

Dunlop, P., Shannon, R., McCabe, M., Quinn, R., Doyle, E. 2010. Marine geophysical evidence for ice sheet extension and recession on the Malin Shelf: New evidence for the western limits of the British-Irish Ice Sheet. Marine Geology, 276: 86-99.

Ellett, D.J. 1979. Some oceanographic features of Hebridean waters. Proceedings of the Royal Society of Edinburgh, 77B, 61-74.

Ellett, D.J. and Edwards, A. 1983. Oceanography and inshore hydrography of the Inner Hebrides. Proceedings of the Royal Society of Edinburgh, 83B. 143-160.

Fyfe, J.A., Long, D. and Evans, D. 1993. The geology of the Malin-Hebrides sea area. London: HMSO for the British Geological Survey .

Howe, J.A., Dove, D., Bradwell, T & Gafera, J. Submitted. Submarine geomorphology and the glacial history of the Sea of the Hebrides, UK. Marine Geology.

Inall, M., Gillibrand, P., Griffiths, C., MacDougal, N. & Blackwell, K. 2009. On the oceanographic variability of the North-West European Shelf to the West of Scotland. Journal of Marine Systems, 77, 210-226.

McKay, W.A., Baxter, J.M., Ellett, D.J. & Meldrum, D.T. 1986. Radiocaesium and circulation patterns west of Scotland. Journal of Environmental Radioactivity, 4, 205-232.

Pantin, H.M. 1991. The sea-bed sediments around the United Kingdom; their bathymetric and physical environment, grain-size, mineral composition and associated bedforms. British Geological Survey Research Report, SB/90/1.

Smith, K. In Press. The Fascadale fault: A tectonic link between the Cenozoic volcanic centres of Rum and Ardnamurchan, Scotland, revealed by multibeam survey. Scottish Journal of Geology.

Wingfield, R. 1989. Glacial incisions indicating Middle and Upper Pleistocene ice limits off Britain. Terra Nova, 1, 538-548

Case Study 7: Multiple resolution boat-based seafloor mapping in the outer Firth of Forth, Scotland

CS Leader: Dr Dayton Dove (BGS) with input from Nick Smart (BGS), Rhys Cooper (BGS), Daniel Buscombe (University of Plymouth), Alan Stevenson (BGS), Sophie Green (BGS) and Francis Daunt (CEH)

CS7.1. The CS7 task

As set out in the proposal this task's remit was as follows:

"*This case study will focus on shallow-water nearshore and estuarine environments off NE Scotland, in areas typically characterised by muddy or sandy substrates, e.g. Firth of Forth, Moray Firth. New high-resolution multibeam bathymetry and backscatter data will be collected on the BGS vessel RV White Ribbon, during 15 days of survey effort in spring-summer 2012. Some of these data will be in areas covered by existing protection measures, e.g. SACs, and are therefore likely to feed into the ongoing MPA identification process in Scottish waters. BGS are currently investigating options to include a hull-mounted camera system on the RV White Ribbon, and if available to this study would provide useful comparison with AUV-mounted camera systems.*

CS7.2. Introduction and survey overview

The BGS survey vessel *White Ribbon* was used to conduct a seabed survey in the outer Firth of Forth, offshore Fife Ness and around the Isle of May (Figs. CS7.1 and CS7.2), from 23 May through 11 June 2012 (Table CS7.1), incorporating 16 potential days of survey.

Figure CS7.1: Bottom Left: BGS survey vessel White Ribbon. Top Right: Isle of May from the back deck of the White Ribbon.

The *White Ribbon* is a 7.9 m, purpose-built survey catamaran equipped with a Kongsberg EM3002D multibeam echo sounder for the purpose of high-resolution bathymetry mapping. The boat is capable of conducting geophysical surveys requiring towed equipment e.g. surface-tow boomer, side-scan sonar, and magnetometer. It was also recently used for shallow coring, and in this survey, seabed photography.

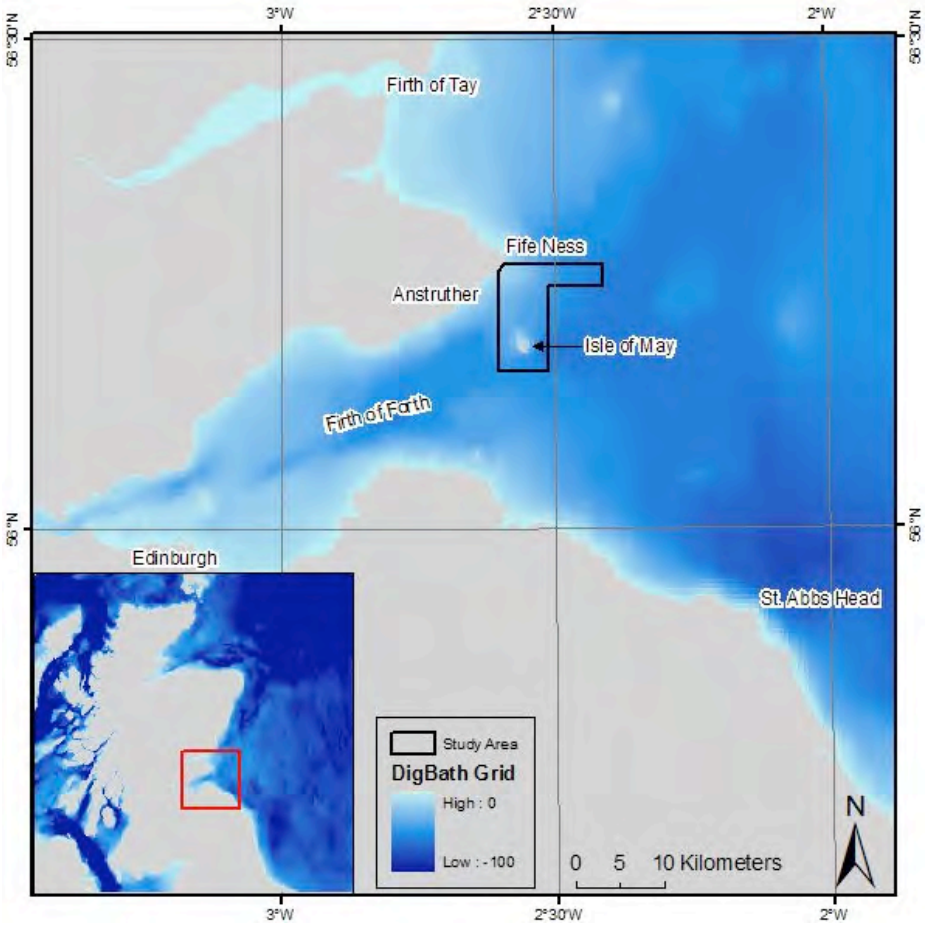

Figure CS7.2: Outer Firth of Forth study area and regional bathymetry.

The survey had several objectives: 1) To test the suitability of a small boat to map and monitor Marine Protected Areas (MPA) within inshore waters. The fundamental dataset for this mapping is multibeam echo-sounder (MBES) data, which yields bathymetry (seabed surface), and backscatter (reflected energy providing a measure of seabed character e.g. sediment distribution); 2) Collect progressively higher resolution datasets, i.e. high-resolution side-scan sonar (SSS) and seabed photography, to examine the feasibility, and potential benefit, of acquiring these data for inshore and MPA mapping; 3) Test a novel data analysis technique which calculates grain-size statistics from seabed photographs (if proven, this computational approach would allow a campaign of seabed 'sampling' to characterise the seabed in areas where collecting physical sediment samples on a small boat would be impossible; also, there is potential for significant time and cost savings for the process of analysing and mapping regional distributions of seabed sediment); 4) Conduct a repeat MBES survey in an area offshore Fife Ness, where the Maritime Coastguard Agency (MCA) has previously surveyed, to investigate the utility of repeat surveying for studying and monitoring sediment mobility; 5) Collect bathymetric and seabed character data around the Isle of May, a proposed marine Special Area of Conservation (SAC), for the use of biological researchers and marine planners (Fig. CS7.3).

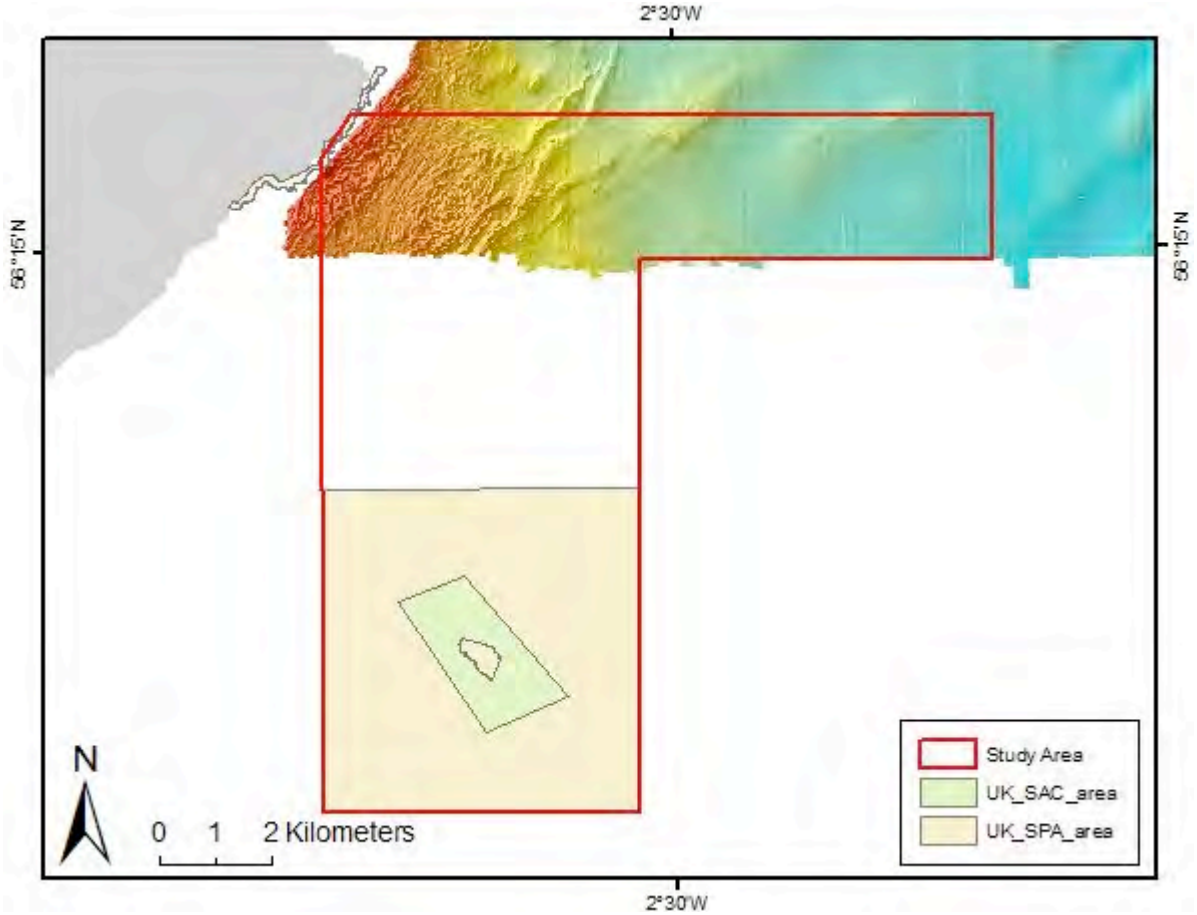

Figure CS7.3: Map showing the study area for this Case Study (red outline). Locations of the Isle of May Special Area of Conservation (SAC) and Special Protection Area (SPA) are shown. MBES data in the north (survey-HI1152) was acquired by the UK Civil Hydrography Programme and was partially re-surveyed, to test the utility of repeat surveys.

The MBES data was acquired first as it is considered the primary dataset for both its scientific utility, but also because the acquisition areas of the SSS data and seabed photography were dependent on a quick, preliminary interpretation of the MBES data. The Isle of May SSS survey area was chosen within the Isle of May SAC, in an area where MBES had previously been collected. The SSS was also collected in the repeat-survey area off Fife Ness, to compare its functionality in assessing seabed change with that of the MBES. The seabed photograph sites were chosen by analysing both the MBES bathymetry and backscatter data around the Isle of May, ensuring a spread both geographically, and across predicted sediment types/environments.

Survey Activity Log				
Day	**MBES**	**SSS**	**Drop-Camera**	**Comment**
23/05/2012				surveyors arrive in Anstruther
24/05/2012				
25/05/2012				
26/05/2012				
27/05/2012				
28/05/2012				
29/05/2012				mobilise and test SSS
30/05/2012				down on weather-no survey
31/05/2012				
01/06/2012				
02/06/2012				no-survey
03/06/2012				no-survey
04/06/2012				mobilise and test camera
05/06/2012				
06/06/2012				
07/06/2012				
08/06/2012				poor weather; Demob camera and remobilise SSS
09/06/2012				
10/06/2012				SSS cable damaged, end SSS survey
11/06/2012				survey complete-return to Port Edgar

Table CS7.1: BGS White Ribbon Survey in the outer Firth of Forth; Activity Log

CS 7.2.1. Geological history

The outer Firth of Forth survey area falls within the Midland Valley of Scotland, a large WSW-ENE trending Palaeozoic sedimentary basin. The survey area includes outcrops of intensely folded sedimentary rocks and igneous intrusions, both Carboniferous in age (Ritchie et al. 2003; Underhill et al. 2008). The sedimentary rocks (mudstones, sandstones, and limestones) outcrop along the Fife coastline where the deformation is interpreted to have resulted from strike-slip faulting on intra-basinal faults. The Isle of May itself is an outcropping of an easterly dipping sill of fine-grained greenstone (Chesher et al., 1986) There has been recent interest in these Carboniferous sedimentary rocks farther offshore, as potential reservoirs for CO^2 sequestration (Monaghan et al., 2012)

Due to the limited amount of high-resolution data within the Firth of Forth, we do not have a clear understanding of the more recent geological history, which will have influenced the present-day geomorphology. BGS mapping in the 1980s identified two late-Pleistocene glacial formations in the study area, the St. Abbs Formation (pebbly, glaciomarine muds), and the Wee Bankie Formation (sandy, gravelly sub-glacial till) (Stoker, 1987; Gatliff et al., 1994). Further to the west, the Holocene St. Andrews Bay member (muddy, pebbly estuarine and fluviomarine sands) of the Forth Formation is more representative of modern conditions.

There is ample evidence from terrestrial studies that the Firth of Forth served as a conduit for streaming-ice sourced from the Southern Uplands of Scotland during the last glacial maximum (LGM) (Finlayson et al., 2010). Provenance studies conducted offshore also suggest that sub-glacial tills are derived from rocks of the Midland Valley, the Firth of Forth serving as the obvious conduit (Davies et al., 2011). Further high-resolution data acquired in the region will be key to understanding what role the Firth of Forth played in ice-sheet drainage over the Quaternary glacial cycles, how it interacted with the better known ice-streams to the north and south e.g. Tweed ice-stream, and how these relict sedimentary deposits along with the Carboniferous rock outcrops constrain biological habitats.

The seabed sediment cover of the Firth of Forth (with the exception of the coastlines and margins of islands) is largely muddy, due largely in part to the low-energy environment, and the relatively low sediment supply (Graham, 1986). The headland of Fife Ness and the Isle of May experience stronger tidal forces, which on top of a relatively shallow seabed results in seabed with coarser-grained sediments or the absence of sediments (Green et al., *in prep*) (Fig. CS7.4).

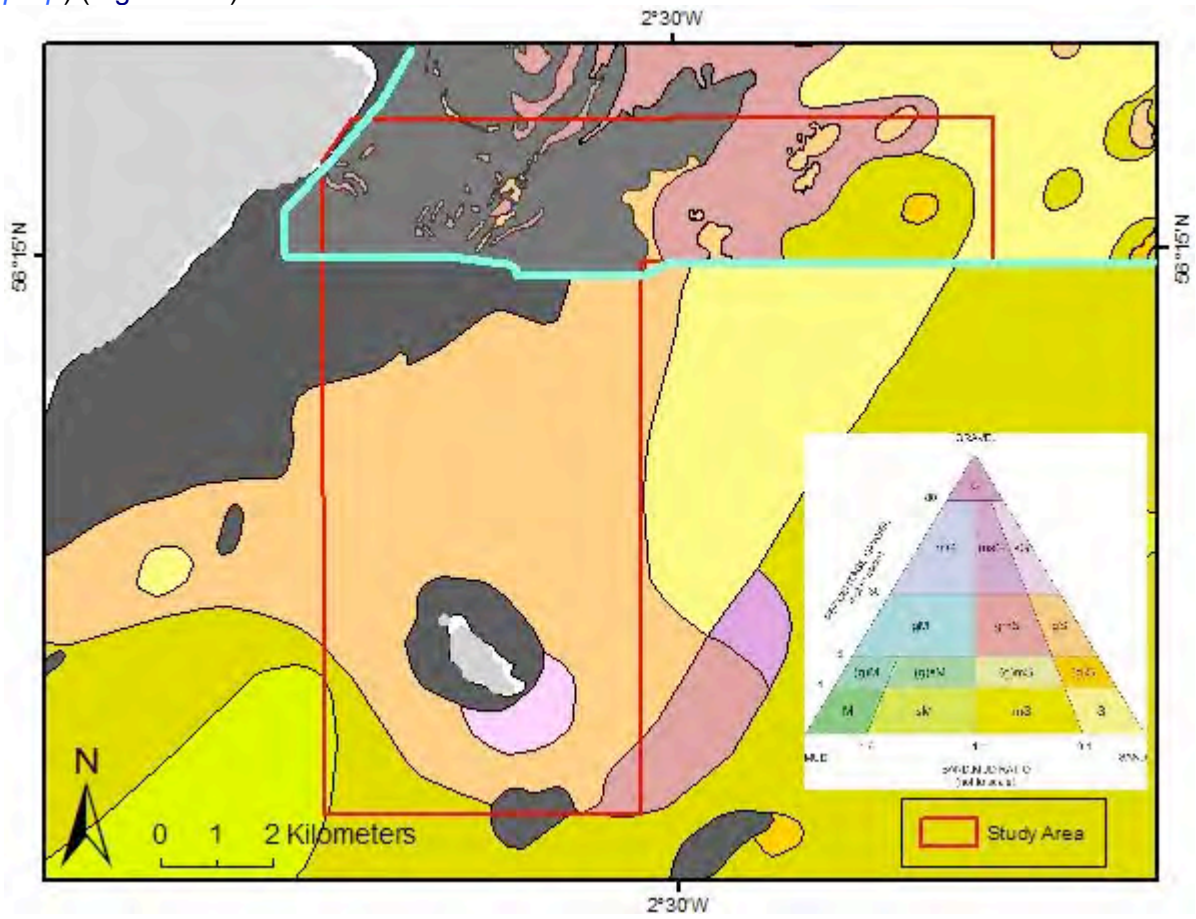

Figure CS7.4: BGS seabed sediment maps based on MBES data (north of the blue line) (Green et al., in prep), and compiled without MBES data (south of the blue line) (Stoker, 1987). Folk sediment classes in bottom right; Pre-Quaternary rock outcrop in grey.

CS 7.2.2. Habitat studies

The Isle of May case-study area was chosen largely due to its significance as an important habitat for both marine mammals (Special Area of Conservation (SAC) as designated by the EU Habitat's Directive) and seabirds (Special Protection Area (SPA) as designated by the European Commission's Directive on the Conservation of Wild Birds). We have taken guidance from biological researchers from both Scottish Natural Heritage (SNH) (marine

mammals) and the Centre for Ecology and Hydrology (CEH) (seabirds), and will collaborate on future survey efforts in the area.

The Isle of May SAC was established due to the large breeding colony of grey seals, as well as the rocky reef surrounding the island. SNH commissioned previous research assessing the rocky reef habitat of the Isle of May. Their research incorporated a video survey of the sublitoral reef biotopes, which identified 34 distinct biotopes supporting up to 102 recorded taxa (Moore et al., 2009).

The Isle of May is also a National Nature Reserve, attracting thousands of tourists each year who travel to the island with commercial boat operators. Other human impacts and risks in the area include bottom fishing and the potential for marine pollution in the form of oil spillages in the Firth of Forth. In assessing whether anthropogenic activities have negatively impacted the area, the authors found no 'adverse changes in diversity, composition, or distribution of biotopes' between a previous survey in 2002, and 2007. Along with future observations of biotope composition and distribution, it is recommended that 'reef extent' is monitored (Moore et al., 2009). For the purposes of mapping the reef, the acquisition of MBES data (this report) vastly improves this objective. The recently collected MBES data will be extremely useful in improving our knowledge of the geographic distribution of defined biotopes, as well as aiding the assessment of potential anthropogenic impacts.

The Isle of May SPA was established due to the importance of the area for breeding seabirds. The Isle of May seabird study is one of the longest (started 1973) and most comprehensive (five species, data on demography, diet, physiology, behaviour) of its kind in the world, with a number of science highlights, e.g. Reed et al. (2008) revolving around the extrinsic drivers of seabird populations and the use of seabirds as indicators of environmental change. CEH and other academic collaborators regularly monitor the seabird populations of the Isle of May, including the European shag, black-legged kittiwake, northern fulmars, Atlantic puffins, and razorbills (Newell et al., 2011). The lesser sandeel is a shoaling fish closely associated with sandy sediments and is the primary food for puffins, shags, and guillemots (Daunt et al., 2008).

Biological researchers have relied on the BGS 1:250k seabed-sediment maps of the region (Graham, 1986) to understand the distribution of the sandeel, and in turn the foraging habits of seabirds. There is a demand from the biological community to improve these maps, and the new MBES, SSS, and camera data will lead to a significant improvement in defining the distribution of sediment in the area.

CS7.3. Survey equipment

CS7.3.1. MultiBeam Echo-Sounder (MBES)

The EM3002D is a dual-headed system capable of producing up to 508 dynamically focused beams; this produces a swath width of up to 200° operable in depths of up to 150 m. The system operates in the 300 kHz frequency range, which ensures narrow beams and a small acoustic footprint, and is also robust under conditions with high particle content in the water column. Swath width is approximately four times the water depth. Navigation is acquired using a Trimble 461 Real-time Kinematic (RTK) GPS, and QINSy navigation software was used for survey planning. All data were collected as geographic coordinates with reference to the WGS-84 datum.

Post-Processing: The raw .ALL MBES files were imported into CARIS HIPS for processing. Data were reduced for tide and corrected to Chart Datum using GPS ellipsoid height obtained from real kinematic position (RTK). The UKHO's VORF (Vertical Offshore Reference Frame) was used to correct ETRF89 ellipsoid height to Chart Datum. The GPS height had to be smoothed using a combination of the 'Moving Average function' and the 'Fast-Fourier transformation' low pass filter to ensure vessel movement wasn't present in the derived GPS tide value and to mask/cover random drop outs of the RTK GPS corrections.

A Total Propagated Uncertainty (TPU) was calculated using vessel offsets and equipment specifications. This enables the initial cleaning of data and creation of a preliminary QC data surface using CUBE (Combined Uncertainty and Bathymetry Estimator). This surface/data was then visually inspected using CARIS subset and swath editors. Any artefacts were manually removed/cleaned prior to the final surface interpolation.

The final CARIS .csar base surface was exported to an XYZ file and imported to DMagic for final surface and data product creation (XYZ, ESRI ArcGrids, Fledermaus SD) at 2 m resolution. Backscatter mosaics (2 m resolution) were created using Fledermaus FMGT. GeoTiffs of both the MBES bathymetry and backscatter data were imported into ESRI ArcGIS for interpretation.

CS7.3.2. Side-Scan Sonar (SSS)

An Edgetech 4125 dual-frequency (400/900kHz) system was used to collect the SSS within the survey area (Fig. CS7.5). Both frequencies were acquired. The across-track range for the 400kHz data was 150m per channel (300m full swath width), and the 900kHz data was 75m (150m full swath width). The recorded data yield a maximum horizontal resolution of less than 10cm.

The sonar fish was deployed from the centre-stern of the boat with an electrically-driven winch, and controlled using the EdgeTech Discover acquisition software. An Ultra-short baseline (USBL) beacon was used to constrain underwater positioning of the sonar fish, though the beacon was damaged mid-way through the survey and was not functional, at which point a static layback was used.

Post-Processing: The SSS data were post-processed in Coda Geosurvey software, where Time-Varying Gain (TVG), swell filtering, and slant-range corrections were applied. We have not produced SSS mosaics for this report as a hardware error in the rented equipment produced navigation errors in some of the final data. The error can be rectified, though we have not had sufficient time to fix this in time for reporting.

Figure CS7.5: Edgetech 4125 dual-frequency side-scan sonar system

CS7.3.3. Seabed camera

It is not practical to obtain a large number of sediment grab-samples from the *White Ribbon,* as there is inadequate sample processing and storage space aboard the boat. As it is necessary to recover samples to ground truth the MBES and geophysical data, we decided to test a novel sampling approach using seabed photographs, as an alternative to physical sediment samples. We have used Digital Grain Size (DGS), a semi-automated program which calculates grain-size statistics from sediment photographs (Buscombe et al. 2010; Buscombe, 2012).

To obtain the seabed photographs, a Kongsberg OE14-208, 5 MP digital stills camera was mounted on an aluminium drop-frame along with a Seatronics LED lamp, and three lasers for image rectification and scaling. The camera system was deployed from the starboard davit of the *White Ribbon* (Fig. CS7.6). Video footage was taken at each photo station, and at each station a total of 3-5 digital stills were taken to ensure a high-quality image was recovered. The deployment was very successful, even in moderate sea-state conditions. Strong tidal currents were the most inhibitive variable, and thus sampling was primarily conducted during periods of slack tide in the most vulnerable areas.

Figure CS7.1: Seabed camera system. Camera, light, and lasers mounted on drop-frame at deployment position on the White Ribbon.

Post-Processing: DGS is written and operated within MATLAB. As the program is sensitive to the image quality, the first step was to filter out images of poor quality, e.g. out of focus, turbid water, excessive biological cover. The next step was to use the program to crop the photos if necessary. The images were then scaled according to the measured distance between the two parallel lasers, converting the images from pixel to mm dimensions. At this stage, DGS is run on all images within a specified directory, outputting for each image the arithmetic mean grain size, skewness, standard deviation, kurtosis, and the complete grain-size distribution.

To produce a sediment classification (Folk) for each sample, which will be used in the future to map the distribution of seabed sediments, the complete grain-size distribution is input into the program GRADISTAT (Blott and Pye, 2001) in order to calculate a more complete suite of grain size statistics, including the textural (Folk) group (future versions of DGS will produce these further statistics, removing the GRADISTAT step). The resulting sediment classifications of each photo sample were imported into ESRI ArcGIS where they may be assessed together with the bathymetry and backscatter data.

CS7.4. Results and Assessment

CS7.4.1. MBES bathymetry

Over approximately one week of MBES surveying, the *White Ribbon* surveyed the majority of the Isle of May SPA area, and re-surveyed a section of the UKHO CHP area HI1152 (Fig. CS7.7). The survey of the northeast sector of the SAC area could not be conducted due to adverse weather conditions. The data (gridded at 2m resolution) are generally of good quality, although noise from heave is apparent.

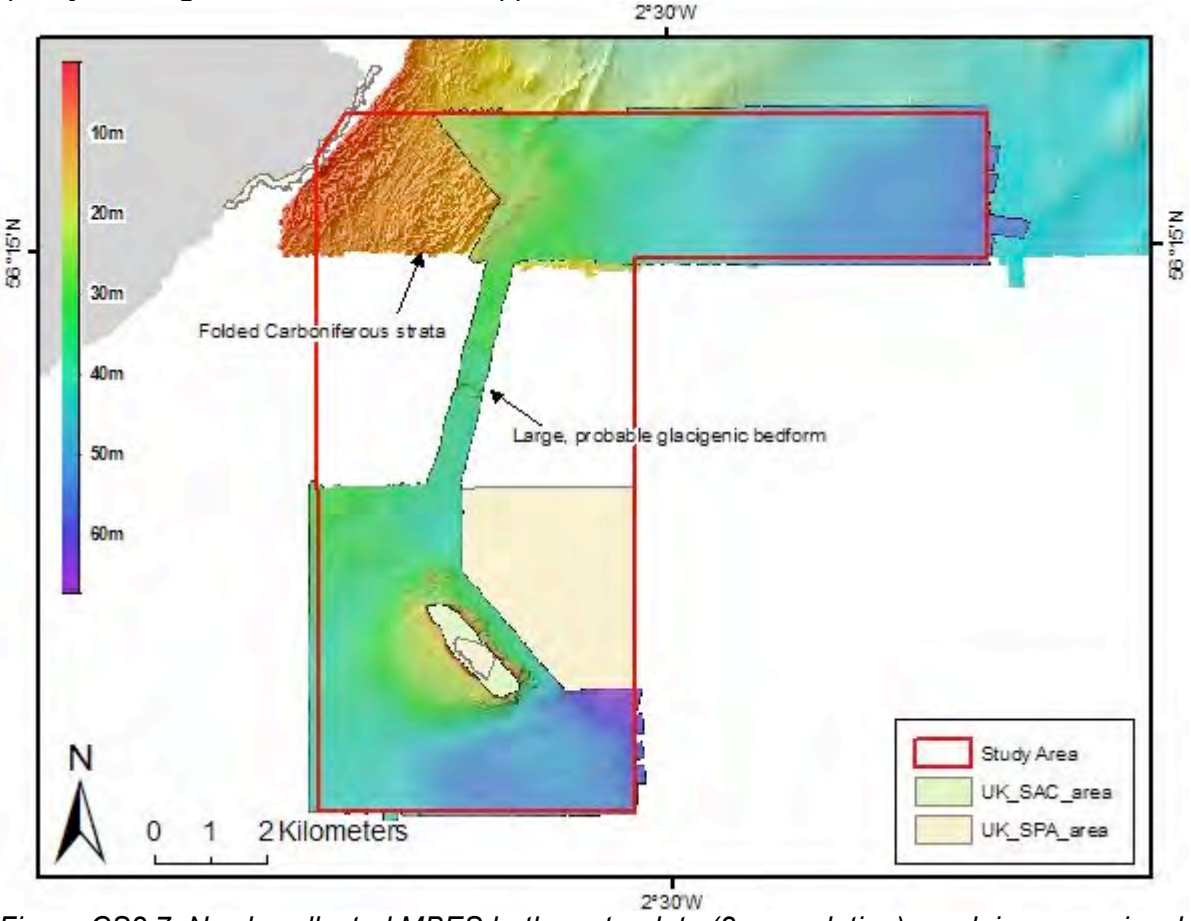

Figure CS2.7: Newly collected MBES bathymetry data (2m resolution) overlain on previously collected UKHO data-HI1152 (7m resolution).

The newly collected MBES data around the Isle of May reveal a diverse suite of bedforms, from probable moraines to outcrops of igneous rock (Fig. CS7.8). The Isle of May area is characterized by a broad, shallow platform associated with the Isle of May sill, and rock outcrops surround the majority of the island (Fig. CS7.9). On the west of the island there are a series of ridges that may be moraines, which were pinned against the Isle of May during glacial retreat. Hummocky terrain to the northwest of the island is also likely glacial in origin. To the southeast of the island, the seabed slopes to a basin at least 60m deep.

The northern surveyed area (repeat survey) reveals the intensely folded Carboniferous strata, and possibly superimposed glacial bedforms. Away from the rock exposures, the seabed slopes gently to the east where there are several broad, low-relief mounds. A transit line between the two survey areas gives a glimpse of a larger, probably glaciogenic bedform (Fig. CS7.7).

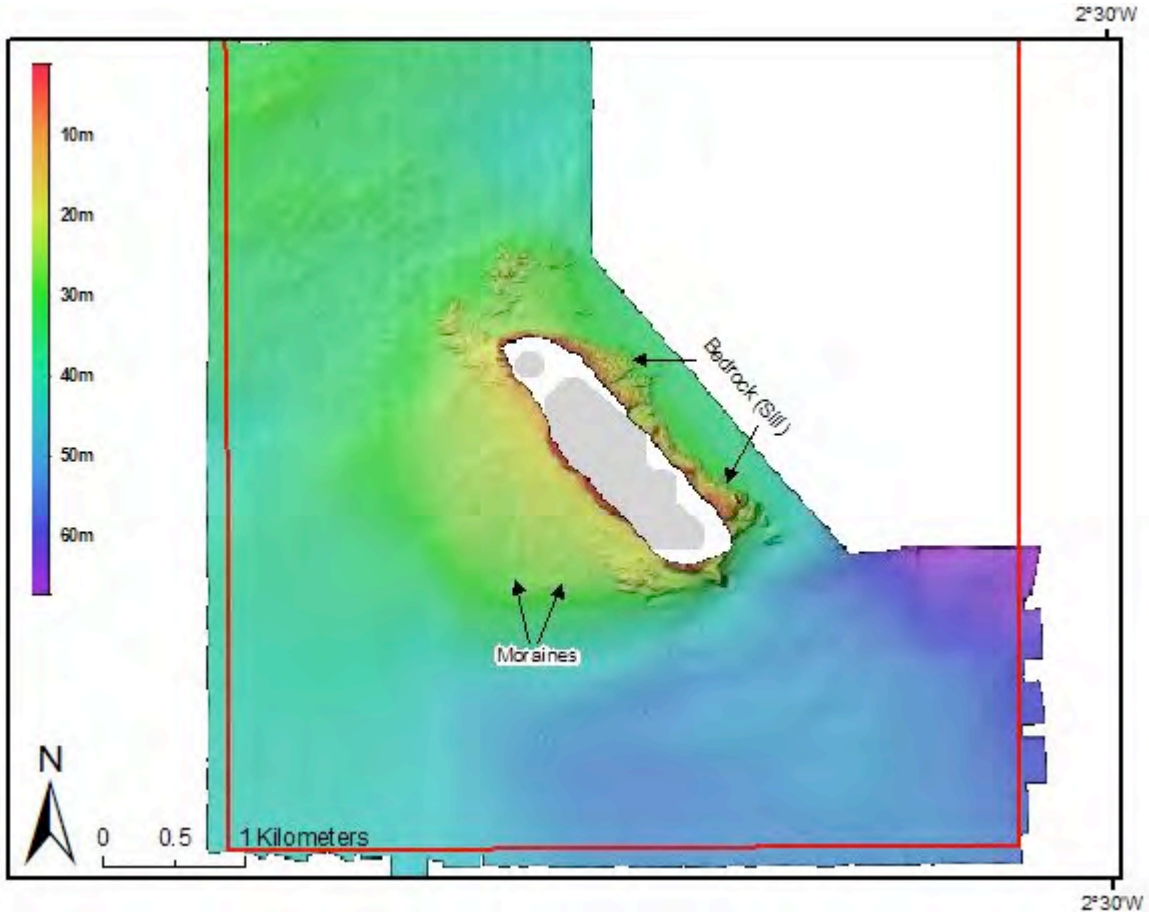

Figure CS7.3: Newly collected MBES data surrounding the Isle of May

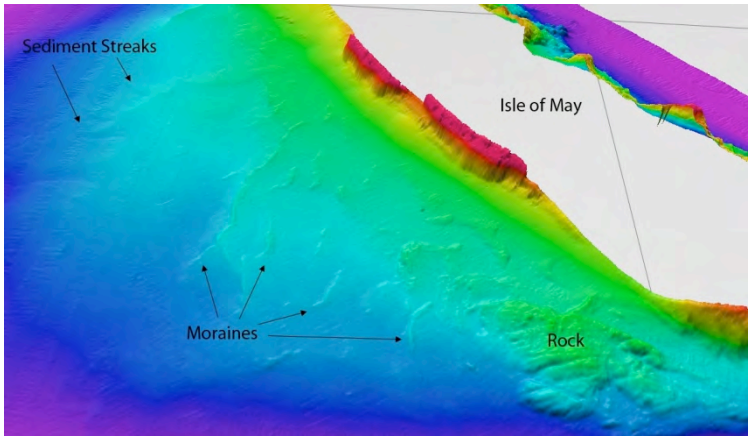

Figure CS7.4: Oblique view of bathymetry west of Isle of May showing rock outcrops, probable moraines, and the low-relief gully/furrow system associated with sediment streaks observed in backscatter data.

CS7.4.2. MBES backscatter

The MBES derived backscatter data reveal a complex pattern of sediment distribution as well as the rock outcrops surrounding the Isle of May (Fig. CS7.10). The variation in backscatter intensity is used in conjunction with bathymetry data (and physical samples if available) to produce maps of sediment distribution. In simplest terms, high intensity returns (lighter tone) are associated with coarser-grained sediments, poorly sorted sediments and rock, whereas low intensity returns (darker tones) are associated with finer-grained, well-sorted sediments.

Much of the survey area surrounding the Isle of May comprises coarse-grained sediments (later confirmed with seabed photography). Poorly sorted, gravel-rich sediments dominate much of the area. The rock exposures are characterised by extremely 'bright' backscatter, but also darker areas resulting from acoustic shadows. There is a marked fining of sediments in the southwest, where mud is dominant. Interestingly, this pattern is not reflected in the bathymetry (Fig. CS7.8), which gradually deepens from west to east. This decoupling suggests that hydrodynamics largely influence sediment distribution in the south of the study area.

The glaciogenic bedforms observed in the bathymetry have only a minor expression in the backscatter data, and tend to be relatively coarser than surrounding seabed. Other interesting features are the curvilinear, streak-like features to the west of the Isle May. These bathymetrically controlled sediment streaks show coarser-grained sediment flowing (SE to NW) through low-relief gullies or furrows (Fig. CS7.9).

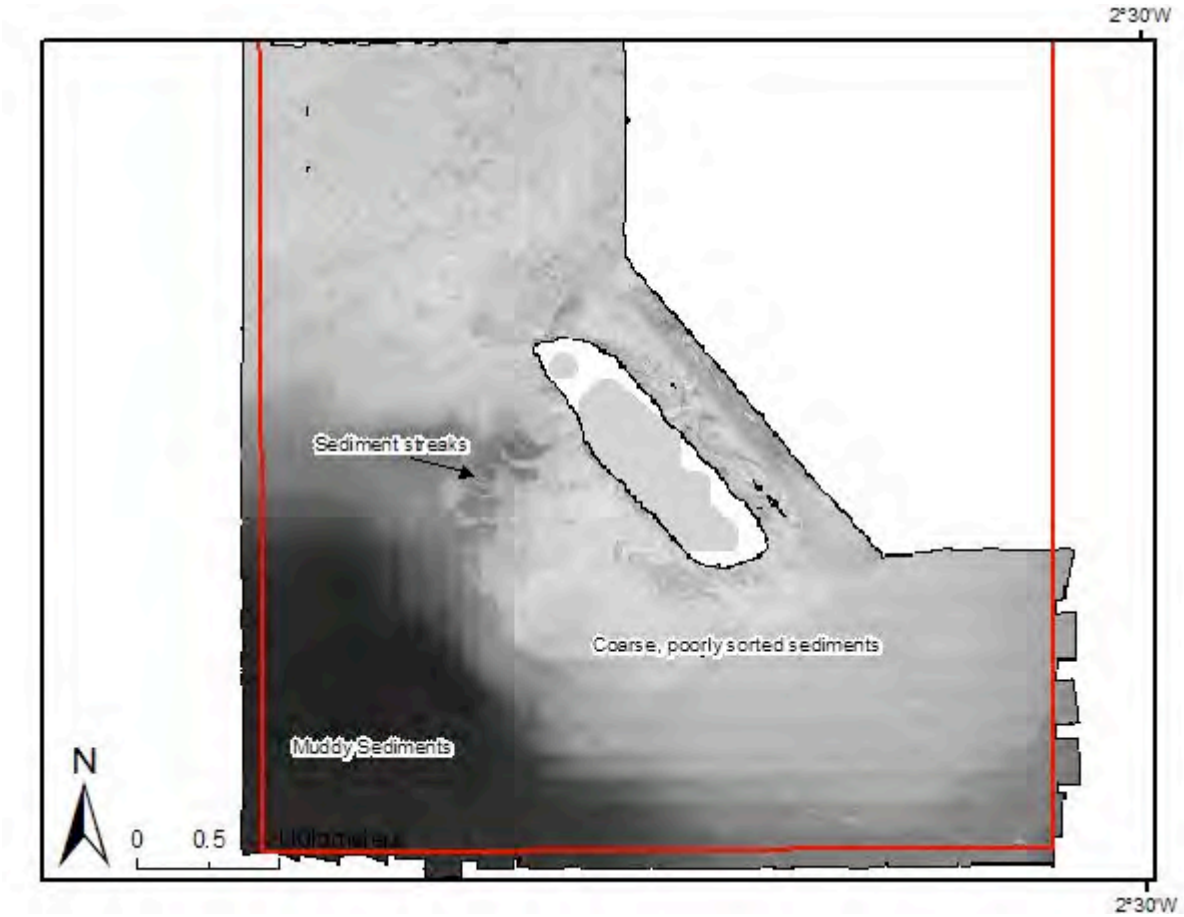

Figure CS7.5: MBES backscatter data surrounding the Isle of May. High intensity returns (lighter tone) are associated with coarser-grained sediments, poorly sorted sediments and rock, whereas low intensity returns (darker tones) are associated with finer-grained, well-sorted sediments.

CS7.4.3. MBES repeat survey

The MBES bathymetry and backscatter data from the recent *White Ribbon* survey have been qualitatively compared with the UKHO CHP survey area HI1152 where data were collected in 2007 and 2008. The comparison is biased, as the recent data are gridded to 2m whereas the CHP bathymetry data are gridded to 7m, and the backscatter to 2.5m. Both datasets were processed using different processing routines, which for the backscatter in particular causes significant variability in the final imagery (Figs. CS7.11c and d). The bathymetry data have been prepared with the same colour scale and shading to improve the visual comparison (Figs. CS7.11a and b).

There are no appreciable differences between the two bathymetric datasets that cannot be explained by the change in resolution. This is due to the area having significant bedrock outcrops and lack of obvious mobile sediment features. A change in seabed character was more likely to be observed in the distribution of sediments as exhibited by the backscatter data. In this case we also see no apparent difference that can't be explained by the different processing methods applied to the two datasets. The large-scale variation is similar in both datasets, but the significant difference in the two backscatter images indicates that care should be taken in setting up consistent backscatter acquisition and processing routines for the purposes of MPA monitoring (repeat surveys).

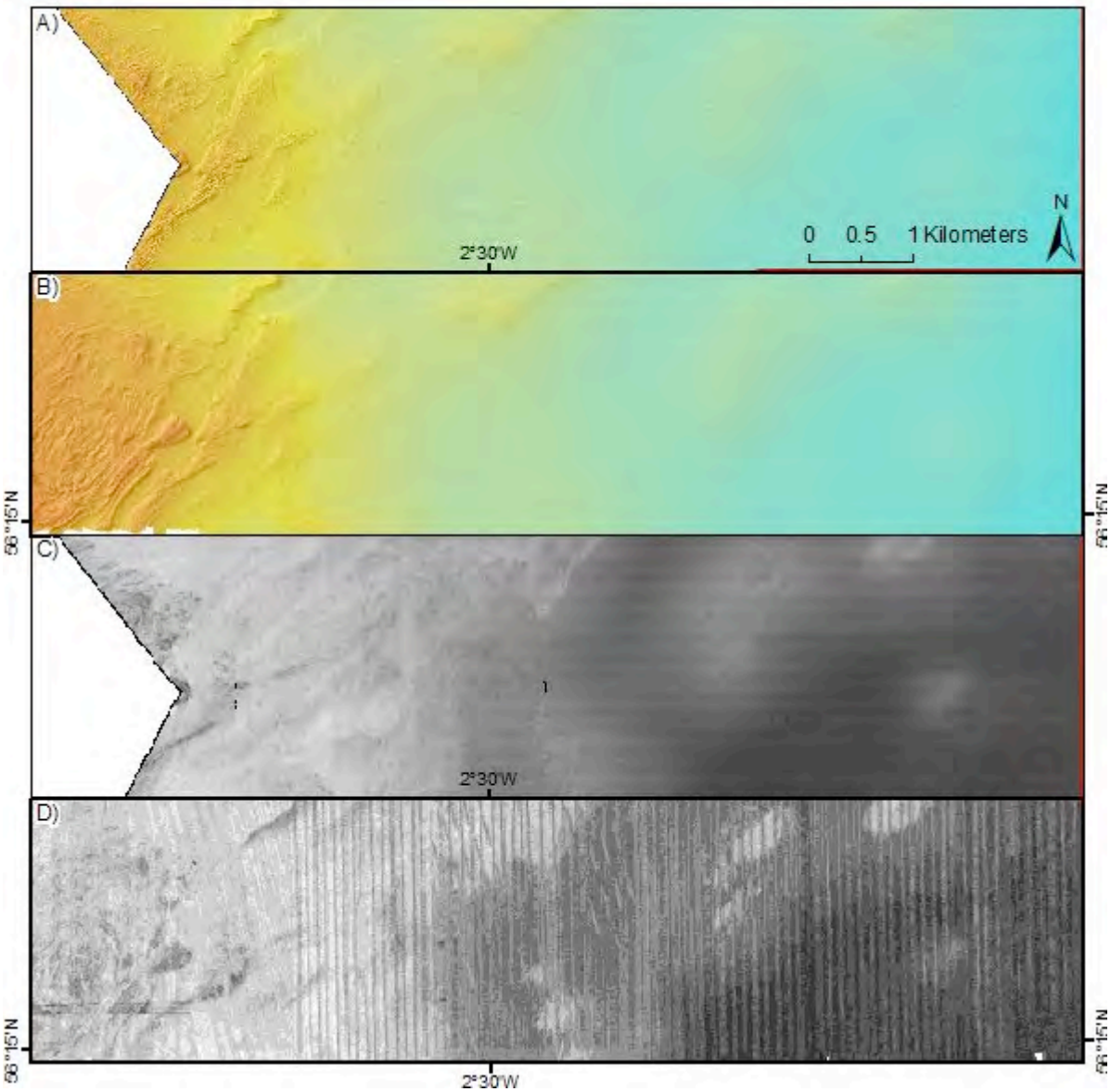

Figure CS7.6: Data comparison between the MBES bathymetry and backscatter datasets of this survey (panels A, C) and the UKHO CHP area HI1152 (panels B, D). Bathymetry data from this survey are gridded at 2m (panel A) compared to HI1152 data gridded at 7m resolution (panel B), and reveal no appreciable morphological change between 2008 and 2012. Backscatter data from this survey gridded at 2m (panel C) compared with HI1152 data gridded at 2.5m resolution (panel D) reveals how different processing protocols yield significantly different imagery.

CS7.4.4. MBES equipment advantages

- MBES bathymetry data (here with a resolution of 2m) is the fundamental dataset for mapping the seafloor, as seabed morphology influences all benthic processes/phenomena;
- MBES bathymetry compliments many other data types, e.g. backscatter and physical samples;
- MBES backscatter data reveal the 'texture' of the seabed, allowing for the mapping of rock outcrops, the distribution of seabed sediments, the presence of large-scale biogenic structures, and anthropogenic features e.g. pipelines. Seabed character maps are fundamental for the purposes of regional biotope mapping;

- The acquisition MBES bathymetry and backscatter data is not labour intensive and, as this data is so widely collected, there is a large knowledge/skills base for acquiring and processing the data;
- Positioning of MBES bathymetry and backscatter is accurate to within centimetres;
- As the bathymetry and backscatter simply exploit two aspects of the same signal, the positioning is identical, allowing for accurate integrated interpretations;
- Processing of both datasets is now routine and efficient, though still moderately labour intensive;
- High quality data may be collected from small survey boat such as the *White Ribbon.*

CS7.4.4. MBES equipment disadvantages

- MBES systems are expensive;
- While boat-based data are generally high resolution (~1-5m), the resolution is not as high as SSS (centimetre-scale), thus sub metre-scale objects cannot be identified;
- Different processing methods for backscatter data may produce significantly different results.

CS7.5. Side-Scan Sonar

Depending on seafloor conditions, the side-scan sonar (SSS) was towed between 5m and 20m above the seabed. The data are of good to poor quality, with snatch (intermittent cable tension resulting in a striping noise in final data) affecting much of the data (Fig. CS7.12). While the sea state was typically slight to moderate, the small dimensions of the *White Ribbon* make it more susceptible to this problem.

The dual-frequency SSS backscatter data provide a higher resolution (<10cm) record than the MBES backscatter. As with the MBES backscatter, clear sediment boundaries were observed, as were fields of mega-ripples/small sand waves, boulder fields, and trawl-marks from fishing activity (Fig. CS7.12). Because of the side-on perspective of the SSS, it is also more effective at feature detection, so rock outcrops and high-relief biogenic structures are more easily observed in SSS backscatter data.

CS7.5.1. SSS equipment advantages

- SSS data may be very high resolution, in this case less then 10cm. This allows for detection of small geomorphological features and biogenic structures, as well as anthropogenic features such as trawl marks;
- SSS systems are commonly used, and post-processing is generally not labour intensive;
- SSS systems are portable and data may be acquired from a small boat.

CS7.5.2. SSS equipment disadvantages

- Positioning of SSS data is not linked directly to the bathymetry, therefore introducing potential errors in integrated interpretation;
- Despite the use of USBL, SSS data is vulnerable to errors in positioning as it is a towed instrument. Using standard equipment, position errors can be assumed to be at least ±5m;
- Acquisition of SSS data from a small boat is more sensitive to poor weather than the MBES, resulting in poor quality data;
- Acquisition of SSS data is more labour intensive than the MBES.

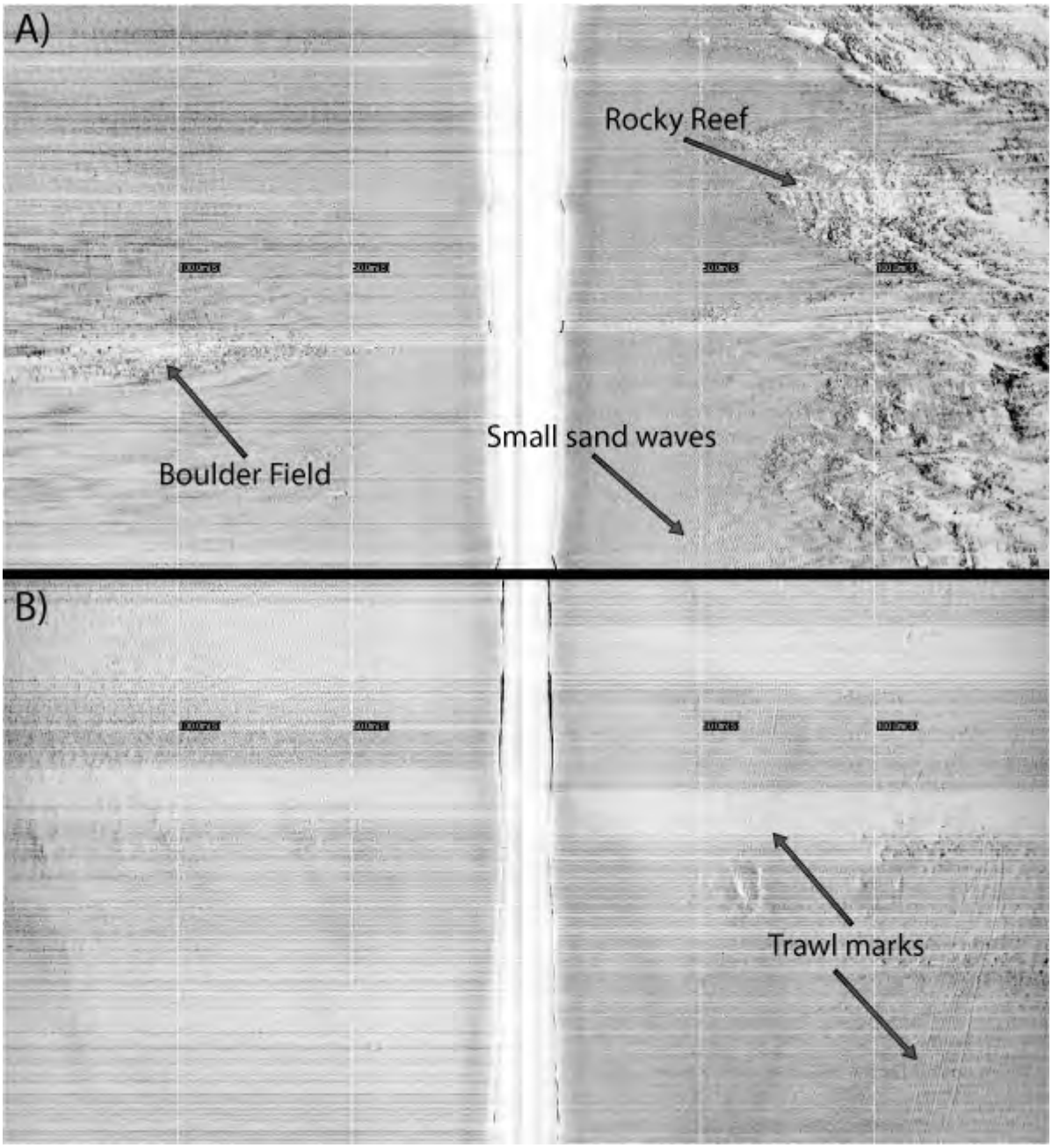

Figure CS7.7: SSS data (400kHz) examples. Snatch (striping) apparent in both images.

CS7.6. Seabed Camera

A total of 256 photographs were acquired from 69 sample sites surrounding the Isle of May (Fig. CS7.13), providing ground-truthing of the MBES and SSS backscatter data. Video recording was activated as the camera frame approached the seabed at each site and not deactivated until leaving the site. Several high-resolution digital stills were captured at each site, once the camera frame had settled on the seabed. The images are generally of high quality (Fig. CS7.14). Strong tidal currents prevented acquisition at some sites, where the camera frame was unable to settle on the seabed. Turbidity in the water column resulting from the camera frame landing on the seabed also resulted in some poor imagery, though typically the water column cleared quickly which allowed high quality images to be captured.

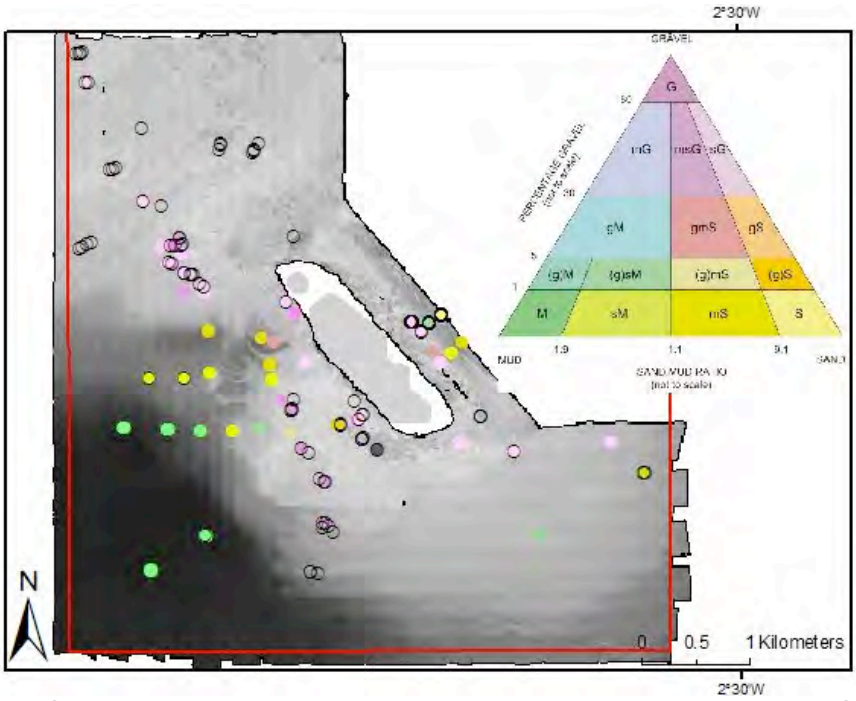

Figure CS7.8: Seabed photograph sample locations overlain on MBES bathymetry. Symbology: Folk classification of the qualitative interpretation (hollow circles indicate photographs unsuitable for interpretation).

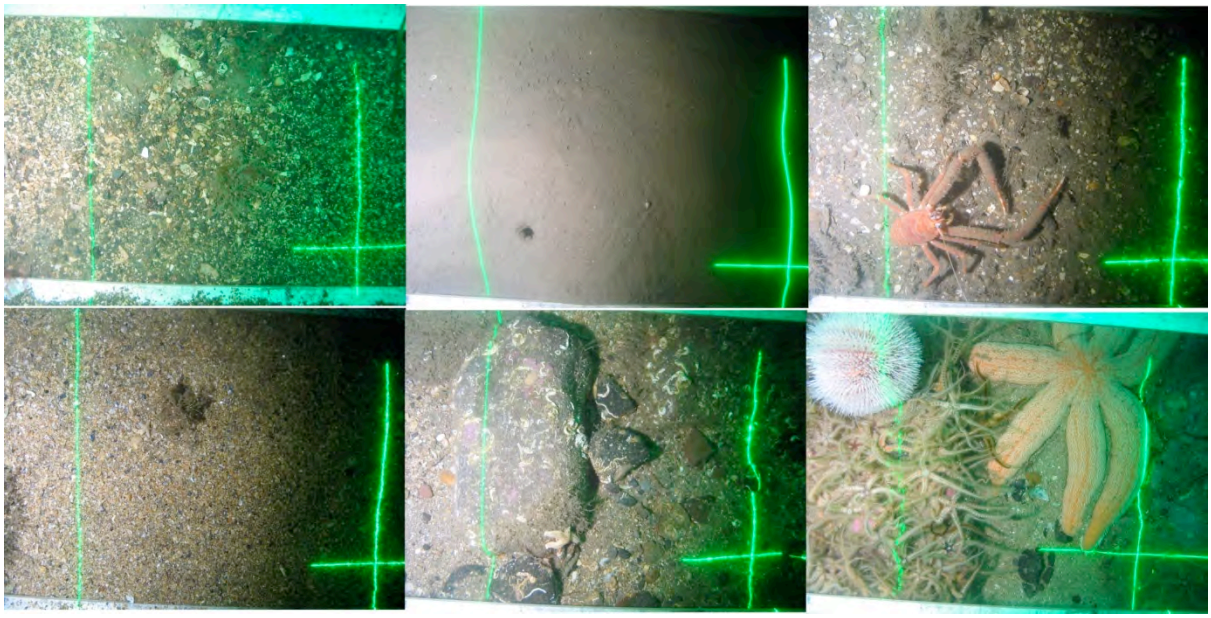

Figure CS7.9: Example photographs show diverse seabed environments around the Isle of May (parallel lasers offset by ~25cm). Seabed character observed on millimetre-scale photographs may be extrapolated with backscatter and bathymetry data for the purposes of regional biotope mapping and monitoring.

CS7.6.1. Qualitative interpretation

198 of the photographs were suitable for qualitative interpretation. Each image has been visually examined, and assigned a sediment class according to the Folk grain-size classification (Folk, 1954) (Fig. CS7.13). Further environmental observations and the extent of benthos in each image were also recorded. The characterization of the broader seabed character was aided by viewing the video imagery.

The following Folk classes have been identified through the visual interpretation photographs: Mud, Sandy Mud, Sand, Gravelly Muddy Sand, Muddy Sandy Gravel, Sandy Gravel, Gravel, as well as Rock. While a sediment distribution map has not been produced for this project, the photographic samples appear consistent with the variations within the backscatter data.

The common co-occurrence in much of the area of mud and coarser sediment (gravel, cobbles, boulders) suggests that this is a low-energy hydrodynamic environment, with low sedimentation rates. The coarser grained sediments are likely derived from relict glacial deposits. The mud component is most likely derived from both the glacial tills and the more modern Holocene sedimentation. As predicted by the backscatter data, the southwest of the study area is characterized by mud, which is Holocene in origin.

Benthos is present in many images, and in several cases, entirely obscure the underlying geology. Commonly observed organisms include brittle stars, urchins, starfish, sponges, soft corals (dead man's fingers), anemones, crabs, lobsters, algae, and shrimp, most showing an affiliation with coarse-grained sediment and the rocky reefs (brittle stars). Abundant burrows are observed finer-grained sediments. The future production of sediment distribution maps will aid in refining the biotope maps of the area.

CS7.7. Digital Grain Size Analysis

Digital Grain Size (DGS) software was tested for the purposes of extracting grain-size statistics from the seabed photographs (Buscombe, 2012). Of the 198 images that were visually interpreted, 109 were suitable (e.g. precisely focused, sufficient light, etc) for DGS processing (Fig. CS7.15). The photographs have an image scale of 0.135mm/pixel. As the software requires each grain to be at least 1-2 pixels to resolve, the smallest grain size that could be assessed was fine to medium sand. DGS is therefore unable to operate on the mud component observed in many of the images.

DGS was run (semi-automated cropping, scaling, processing of image statistics) successfully on all 109 samples (Fig. CS7.16). Once the operator is proficient in the program, processing the images is extremely efficient. While the cropping and scaling steps take some time (~30secs per image), the automated image processing requires only seconds per image.

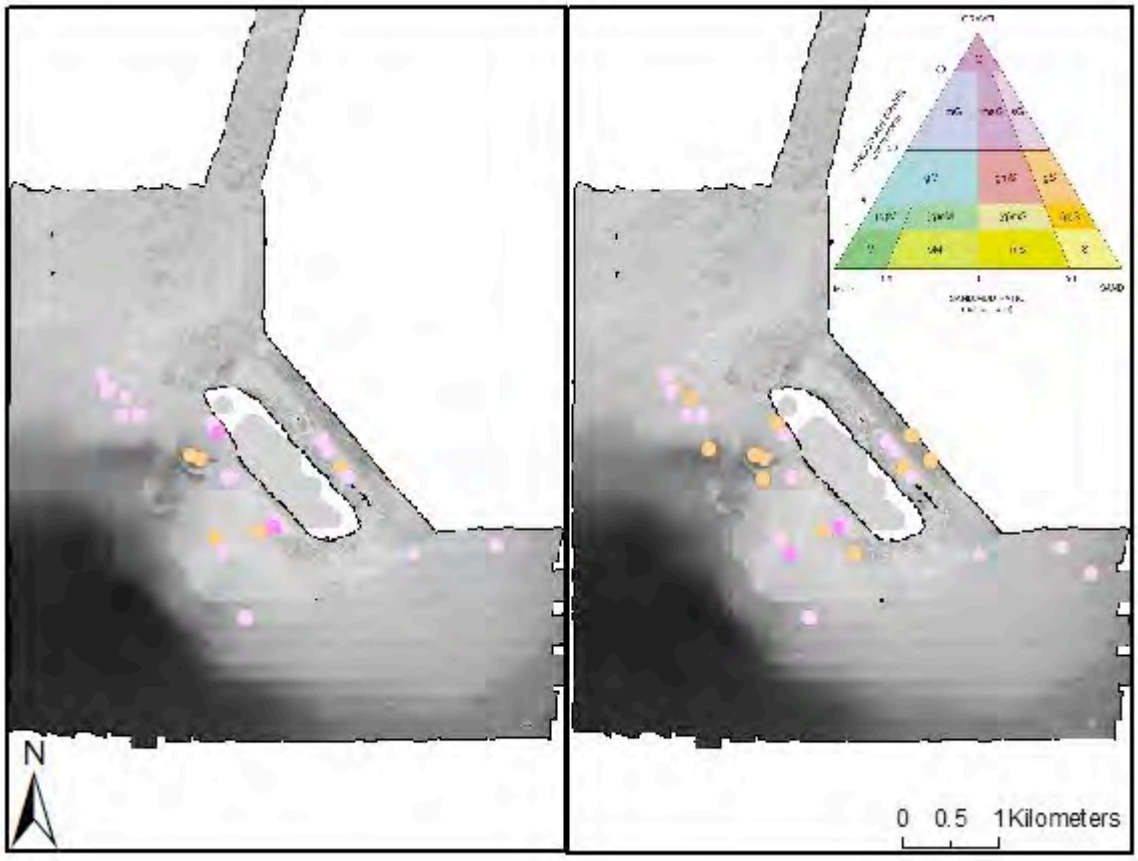

Figure CS7.10: Comparing qualitative interpretation (left panel) with Digital Grain Size (DGS) analysis (right panel). Note that many samples (out of 83 total) are within metres of one another from the same 'site', thus overlapping in the figure. With the mud component removed, the two techniques produced identical classification 60% of the time. Discrepancies are primarily due to the way in which each method measured shell fragments.

To compare the results from the DGS analysis to our qualitative assessment, the mud component was removed from the qualitative Folk classification. Samples where mud was the primary component were removed entirely, and the term 'muddy' (e.g. Muddy Sandy Gravel) was removed where mud was a secondary or tertiary component. This left 83 seabed photographs that were suitable for comparison. To test the similarity between the two analyses a value of '1' was assigned for identical matches, and a value of '0' for those which were not identical. This test showed that the two separate analyses yielded an identical classification 60% of the time (Fig. CS7.15). This is clearly a simple comparison as DGS fails to 'see' the mud, but it does demonstrate where the technique succeeds, and where it is less successful.

Where the two analyses failed to predict the same sediment class is primarily explained by the way shell fragments were interpreted by both techniques. DGS probably overestimates grain size where there is a large fraction of shell fragments in sand. For example, where visual interpretations described a sample as 'Sand', DGS classified it as either 'Gravelly Sand', or even 'Sandy Gravel' depending on the amount of shell present. This occurs as DGS operates on a 2D image of the seabed, and shells tend to lie flat on the surface. However, in retrospect it also seems we underestimated grain size, failing to account sufficiently for the shell fraction during the qualitative interpretation. This highlights one of the pit-falls in visual interpretation, user error. Errors may also have resulted from the uneven lighting in the images, although this does not have so large an effect as one might think (D. Buscombe, pers. comm.)

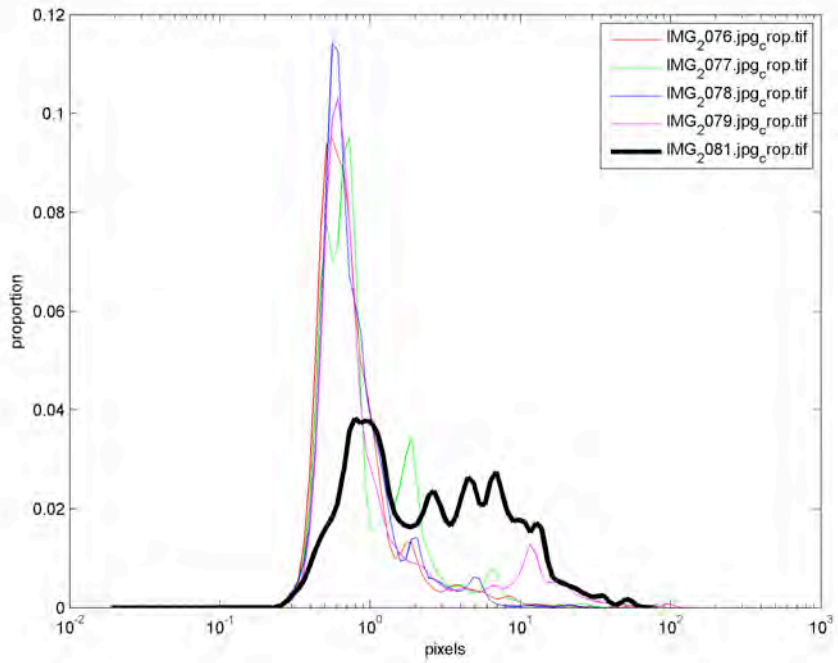

Figure CS7.11: Grain size distribution: Graphical example of DGS output from processing run of five images. The x-axis is grain size in pixel dimensions; the y-axis is proportions per grain size.

CS7.7.1. Seabed Camera equipment advantages

- Video and digital stills give millimetre-scale resolution images of the seabed, allowing for both a qualitative and quantitative assessment of the seabed environment;
- Acquiring seabed photographs is more time and space efficient than collecting physical grab-samples, ideal for a small boat. This efficiency can also be improved (see below);
- The Digital Grain Size (DGS) software has been shown to accurately predict sediment grain size from seabed photographs. This software has the potential to be broadly applied across a range of platforms. With a camera system that can resolve the mud fraction, this protocol would be applicable in any sediment environment;
- The qualitative and quantitative analyses are complimentary, and observations are easily extrapolated using geophysical data (MBES and SSS).

Note that BGS is designing a bespoke camera system that will be lighter in weight, and be capable of resolving the mud fraction. A lighter system will be safer to handle, and will allow for significantly faster acquisition.

CS7.7.2. Seabed Camera equipment disadvantages

- A small boat is vulnerable to drift in currents, which can inhibit camera system from settling on the seabed. Small boats are also vulnerable to heave, increasing the chances that the camera frame may experience collisions with the seabed. The camera system must therefore be robust;
- At present the DGS software likely over-estimates coarseness where broken shell is ubiquitous. Future work with the developer will aim to improve this;

- While the errors are not as great as SSS, this tethered system will have some positioning error (±1-2m) if using some form of underwater acoustic positioning;
- A large, heavy camera system may be impractical to deploy from a small boat;
- A photograph remains a 2D representation of the seabed, potentially biasing the assessment of sediment composition by not capturing the variation of the top centimetres of material sampled by sediment grabs (though one may conversely argue that sediment grabs return deeper material which is not necessarily representative of the seabed);
- DGS software is not commonly used, therefore it is less likely to be employed for routine mapping and monitoring.

CS7.8. Conclusions and future work

With the capacity to collect high-quality data with equipment operating at multiple resolutions, a small day-survey boat like the BGS *White Ribbon* is suitable for the purposes of MPA mapping and monitoring in the near-shore environment. Such a platform is cost-effective, and offers significantly more flexibility than larger vessels e.g. rapid deployment to exploit weather windows.

Several equipment types were employed to map the seabed in the outer Firth of Forth. This report demonstrates the effectiveness of each instrument with respect to data resolution, assessing data quality, ease of acquisition and processing, and the resulting applicability of the acquired data. MBES bathymetry data (2m resolution) are fundamental for the purposes of habitat mapping. Acquisition is efficient and not labour intensive, post-processing is routine, and the resulting data compliment many other physical and biological assessments of the seabed. MBES backscatter data (2m) provide the 'character' of the seabed, e.g. the distribution of seabed sediments and the presence of large-scale biogenic structures as well as anthropogenic features. The MBES backscatter data are co-registered with the bathymetry allowing for accurate integrated interpretations.

Higher-resolution SSS backscatter data (<10cm) give the ability to image small geomorphological features and biogenic structures, as well as anthropogenic features such as trawl marks caused by fishing. Positioning errors are more inherent with SSS data, the equipment itself is more labour intensive to operate, and the data quality deteriorates faster (than MBES) when collected in poor weather from a small vessel.

The seabed camera (mm scale) provides an alternative to grab sampling, which is particularly useful on a small survey vessel. With seabed photography, the seabed environment may be assessed both qualitatively and quantitatively. Digital Grain Size (DGS) software was shown to be a good predictor of grain-size from seabed photographs, ground-truthing the lower resolution geophysical datasets. Future modifications to the camera system and the software will only improve this approach.

As requested by the Scottish Natural Heritage (SNH), the acquired survey data will be used to compile sediment distribution maps in the area. These substrate maps will be used to upgrade the regional biotope maps, improving the ongoing monitoring of the Isle of May SAC.

There is also demand (CEH) to conduct further seabed mapping in the outer Firth of Forth. Improved maps would be used by CEH and others involved in the long-term Isle of May seabird study to better understand the behaviour and foraging habits of seabirds.

CS7.9. References

Blott, S., Pye, K., 2001. GRADISTAT: a grain size distribution and statistics package for the analysis of unconsolidated sediments, Earth Surface Processes and Landforms, Vol. 26, 11, p. 1236-1248.

Buscombe, D., Rubin, D.M., and Warrick, J.A., 2010 Universal Approximation of Grain Size from Images of Non-Cohesive Sediment, Journal of Geophysical Research - Earth Surface Vol. 115, F02015.

Buscombe, D. (submitted) Universal Approximation to Grain-Size Distribution from Images of Sediment, Thin Sections, and Other Granular Patterns. Geology

Chesher, J., Fanin, N., Thomson, M., 1986. Tay Forth: Solid Geology, 1:250 000 Series (British Geological Survey).

Davies, B., Roberts, D., Bridgland, D., Cofaigh, C., Riding, J., 2011. Provenance and depositional environments of Quaternary sediments from the western North Sea Basin. Journal of Quaternary Science, Vol. 26, 1, p. 59-75.

Daunt, F., Wanless, S., Greenstreet, S., Jensen, H., Hamer, K., Harris, M. 2008.The impact of the sandeel fisher closure on seabird food consumption, distribution, and productivity in the northwestern North Sea. Can. J. Fish. Aquat. Sci., Vol.65, p. 362-381.

Finlayson, A., Merrit, Jon., Browne, M., Merrit, J., McMillan, A., Whitbread, K., 2010. Ice sheet advance, dynamics, and decay configurations: evidence from west central Scotland. Quaternary Science Reviews, Vol 29, 7-8, p. 969-988.

Folk, R L. 1954. The distinction between grain size and mineral composition in sedimentary rock nomenclature. Journal of Geology, Vol. 62 344–359.

Gatliff et al., 1994. The geology of the central North Sea. UK Offshore Regional Report, British Geological Survey.

Graham, C., 1986. Tay-Forth: Sea Bed sediments, 1:250 000 Series (British Geological Survey).

Monaghan, A., Ford, J., Milodowski, A., McInroy, D., Pharaoh, T., Rushton, J., Browne, M., Cooper, A., Hulbert, A., Napier, B. 2012. New insights from 3D geological models at analogue CO2 storage sites in Lincolnshire and eastern Scotland, UK. Proceedings of the Yorkshire Geological Society, Vol. 59, p. 53-76.

Moore, C., Edwards, D. C., Harries, D.,Lyndon, A., 2009. The establishment of site condition monitoring of the rocky reefs of the Isle of May Special Area of Conservation. Scottish Natural Heritage Commissioned Report No. 301.

Newell, M., Harris, M., Burthe, S., Wanless, S., Daunt, F., 2011-submitted. Isle of May seabird studies in 2011. CEH commissioned report for JNCC.

Reed, T., Daunt, F., Hall, M., Phillips, R., Wanless, S., Cunningham, E., 2008. Parasite Treatment Affects Maternal Investment in Sons. Science, Vol. 321, p. 1681-1682.

Ritchie, J., Johnson, H., Browne, M., Monaghan, A., 2003. Late Devonian-Carboniferous tectonic evolution within the Firth of Forth, Midland Valley; as revealed from 2D seismic reflection data, Scottish Journal of Geology, Vol. 39, p. 121-134.

Stoker, M., 1987. Tay-Forth: Quaternary Geology, 1:250 000 Series (British Geological Survey).

Underhill, J., Monaghan, A., Browne, M., 2008. Controls on structural styles, basin development and petroleum prospectivity in the Midland Valley of Scotland, Marine and Petroleum Geology, Vol 25, p. 1000-1022.

Work Package 5: Comparison of different survey methods

WP Leader: Dr Russell Wynn (NOC) with input from Case Study Leaders

5.1. The WP5 task

As set out in the proposal this task's remit was as follows:

"*The key component of this WP will be a cost-benefit comparison of AUV and Glider technology compared to conventional boat-based mapping and monitoring techniques. This comparison will be achieved through collation of quantifiable parameters such as cost per unit area (e.g. £ per km^2 of mapped seafloor) or time per unit area (e.g. hours per km^2 of mapped seafloor). This WP will also pull together existing and new case study to assess the advantages and disadvantages of different survey methods, in terms of data quality and resolution, operational risks (e.g. equipment failure, weather downtime), and the overall fit with MCZ/MPA mapping/monitoring requirements. Comparison will be made with data recently acquired by contractors in priority rMCZ areas (it is anticipated that this will be undertaken in collaboration with CEFAS). Post-acquisition data processing and storage requirements will also be outlined in economic terms.*

This WP will be undertaken by NOC (with input from BGS and SAMS) between 1 March and 31 May 2012."

5.2. Introduction

A key aspect of this study is a cost-benefit analysis of different survey techniques. Here, we specifically discuss the costs associated with each method, i.e. AUV, Glider and research vessel. Information on the advantages and disadvantages of different survey methods can be found within each of the Case Studies, and are summarised in Sections CS1.5, CS2.5, CS3.8, CS4.5, CS5.5, CS6.4 and CS7.8.

5.3. AUV costs

In Case Studies 1 and 2 a 6000 m depth-rated AUV (Autosub6000) was deployed, in both cases as part of ocean-going scientific research expeditions. However, this makes it hard to assess the true costs of using such instruments for specific MPA-oriented work in UK waters. The full cost of an ocean-going research vessel such as RRS *James Cook* or RRS *Discovery* is in the region of £20-25k per day, but this varies widely depending upon mobilisation and demobilisation costs, and the number of technicians required to support large equipment such as AUVs. It only took about 18 hours to collect the AUV dataset from the Haig Fras rMCZ that is shown in Case Study 2, but it would not have been economic to have undertaken this as a stand-alone cruise, due to the significant mobilisation costs and moderately long passage to/from a suitable port. The full cost for a one-month research cruise on a large research vessel such is likely to be in the order of £1M, but several deep-water sites could be mapped or monitored in high resolution over this period.

Future mapping and monitoring of a UK MPA network would likely be carried out much more efficiently through use of smaller AUVs, better suited to shallow-water shelf environments, that could potentially be deployed and recovered from shore (or from smaller, cheaper vessels). It may be economically viable to deploy larger AUVs for survey of more distant and/or deep-water sites, where high-resolution data are required, e.g. areas of complex habitats. In the future, it is likely that new instruments such as Autosub Long Range will have a major part to play in mapping and monitoring of such sites.

5.4. Glider costs

5.4.1. Glider costs during Case Study 3 deployments off northwest UK

Tim Boyd has provided comprehensive information on the costs associated with Glider deployment during data collection for Case Study 3. The operational costs for mission 1 are itemised below in Table 5.1. Iridium communication/data telemetry costs are based on PSTN transmission. The total cost for Iridium transmission was £3524 (about £700 per month or £4.46 per dive). A RUDICS-based connection for Iridium communications existed, but was not used during mission 1 due to technical problems.

Activity	Contractor	Date	Cost (£)	Comment
Deployment	Coastal Connection	12 Oct 2009	625.77	
Recovery	Northern Lighthouse Board '*NLV Pole Star*'	9 Mar 2010	3030.97	Fuel costs for opportunistic recovery
Iridium communications and data telemetry	NAL Research	13 Oct 2009 -12 Mar 2010	3524.30	Dives 15:789
Shipping to the US service centre			671.00	
Post mission servicing / calibration	iRobot and Seaglider Fabrication Center, Univ. Washington	Autumn 2010	7083.00	including VAT but not transportation
Total cost			**14,935.04**	£15.6k with estimated shipping of £671 to UK

Table 5.1: Operational costs associated with Talisker mission 1. Note that NAL Research, iRobot, and the U. W. Seaglider Fabrication Center, are based in the USA. Costs shown were converted to GBP at the rate of $1.6 to £1.

Note that the sum of deployment and recovery costs for mission 1 amounted to about £3.7k, with the bulk of that amount going for the fuel required to divert the Northern Lighthouse Board *NLV Pole Star* to conduct an unplanned, but not completely unanticipated, recovery. The total costs for end-of-mission calibration, new batteries, servicing and testing of the Seaglider by the manufacturer amounted to about £7.7k, including the cost of shipping to, but not from, Seattle. Assuming similar costs for shipping to the UK, we estimate the total mission cost at £15.6k.

Due to abnormal pitting during mission 1, the anodized aluminium pressure hull was replaced during the post-mission servicing. This cost was not included in the above table, as it is viewed as a 'one-off' cost rather than an operational cost. Reviewing the data from mission 1, it was apparent that the un-pumped SBE 43 dissolved oxygen sensor was reporting values of about 1 ml l^{-1} less than expected (Sherwin and Dumont, 2012a). Based on the experience of other users (Nicholson et al., 2008; Perry et al., 2008), an Aanderaa Optode dissolved oxygen sensor was added to the Seaglider sensor suite for mission 2. The costs shown here do not include cost of the new Optode sensor, which is also viewed as a one-off capital cost rather than an operational cost. Table 5.1 also does not include labour costs for piloting, deploying, and recovering the Seaglider or managing its maintenance. Some of these costs are discussed below.

The operational costs for Mission 2 are itemised in Table 5.2. Iridium costs for mission 2 are based on RUDICS transmission using TCP/IP. The total cost for RUDICS-based Iridium transmission for the period including the mission was about £290 per month, or about £1.39 per dive. In comparison, Iridium costs for mission 1, during which PSTN-based communication was used throughout, amounted to about £4.46 per dive. The mission 2

RUDICS-based transmissions were about 41% of the mission 1 PSTN-based monthly costs, or about 31% of the PSTN-based per dive costs.

Activity	Contractor	Date	Cost (£)	Comment
Deployment	Coastal Connection	3 May	861.82	
Recovery	Faroe Marine Research Institute, '*FRV Magnus Heinason*'	3 Sept	0.00	Goodwill gesture
Iridium communications and data telemetry	JouBeh Technologies	May-Sept usage	1165.75	Dives 1-841
Shipping to/from US service centre	Included below	June 2012	1770.57	Faroes to US; US customs clearance; US to Scotland
Post mission servicing / calibration	Seaglider Fabrication Center, Univ. Washington	Spring 2012	6909.54	Not including VAT
Total cost			**10,404.68**	

Table 5.2: Operational costs associated with Talisker mission 2. Note that JouBeh Technologies, and the U. W. Seaglider Fabrication Center, are based in the USA. Costs shown were converted to GBP at the rate of $1.6 to £1.

The sum of deployment and recovery costs for mission 2 were considerably lower than for mission 1, due to the generosity of the Faroe Marine Research Institute, which recovered Seaglider 'Talisker' using the research vessel *FRV Magnus Heinason* without any charge despite unanticipated diversion from her scheduled cruise plan. The total costs for end-of-mission calibration, new batteries, and manufacturer servicing and testing of the Seaglider amounted to £6.9k, with shipping to and from the US amounting to £1.8k, so the total operational costs for mission 2 amount to about £10.4k, substantially lower than the total of £15.6k for mission 1, but without UK VAT added to the US servicing fees. As with mission 1, the costs shown for mission 2 in Table 5.2 do not include labour costs for piloting, deploying, and recovering the Seaglider or managing its maintenance, some of which are discussed below.

5.4.2. Comparison with hydrographic cruise costs

For this report a rough comparison can be made between Glider and vessel-based hydrographic surveys, based solely on the time required to conduct the hydrographic casts over a given transect both by ship and by Glider. In the case of the Extended Ellett Line hydrographic sampling, conducted during *RRS Discovery* cruise D365 in May-June 2011, it took nearly two full days to conduct 19 CTD casts between Rockall Bank (13.63°W) and the Sea of Hebrides (8.78°W), over a distance of about 290 km (at 57.5°N). In comparison, 21 days were required for Talisker to complete roughly the same transect, during which time 314 profiles (157 dives) were conducted.

The Ellet Line is normally undertaken by the NERC vessels RRS *James Cook* or RRS *Discovery*. At a day rate of £24k the Rockall Trough CTD transect would cost roughly £46k in ship time alone. Additional cost elements include labour for scientific and technical staff, preparation and shipping of scientific equipment, costs for mobilisation, and additional ship time for steaming time from port to the study region; therefore the costs discussed here are minima. Considering only the cost of ship time, the cost of the conventional hydrographic line amounts to £46k/19 CTD casts = £2.4k/CTD cast or £46k/290km = **£158/km of hydrographic transect**.

Using the total mission 2 operational costs shown in Table 5.2, prorated for the duration of the 21 days of the Ellett Line segment (relative to mission 2 sampling from 3 May – 24 August), the Seaglider transect costs are £10.4k*21/119 = £1.8k = 4% of the cost of the conventional hydrographic transect. The cost per Seaglider profile was £1.8k/314 = £5.8 (= 0.2% of the cost of a CTD cast), or £1.8k/290km = **£6.3/km of hydrographic transect**. In sampling along the nominal Ellett Line, Talisker actually covered 536 km over the ground during mission 2, yielding a cost of £1.8k/536km = £3.4/km.

In addition to data transmission and other (fixed) operational costs (e.g. for deployment and recovery), glider operations require regular monitoring as well as intermittent intervention by a trained pilot. Review of the Talisker logs for mission 1 reveals that pilots reviewed glider performance more thoroughly and/or intervened with the glider's existing mission program every 1-1.5 days. Assuming up to one hour of pilot effort per intervention, this would result in 4.5-7 hours (or approximately 1 day) of pilot time per week of glider deployment, some of which would be after normal work hours (evenings and weekends). For the Ellett Line segment, this would amount to a total of 12-21 hours of pilot time for operation of the vehicle, or a net cost of £0.8k-1.3k, at a typical current PDRA (Post-Doctoral Research Associate) salary rate, including overheads. For the Ellett Line, as sampled during mission 2, this amounts to about £4.1 per profile or £4.5 per km of hydrographic transect. Although this is a very rough estimate, it is clear that the pilot costs, while low, are comparable to the sum of all other operational costs for the Seaglider. Nevertheless, even when piloting costs are taken into account, the glider cost is over an order of magnitude cheaper than the research vessel cost for the same amount of survey work.

Over the course of the entire 120 days (4 months) of a typical deployment, pilot labour would amount to about 80-120 hours of pilot time, or approximately £5k-7.5k, at current PDRA rates. This estimate is in addition to the glider deployment and recovery efforts, which are variable. In both missions discussed here, the recovery was conducted through a collaborative effort between SAMS and the colleagues shown in Tables 5.1 and 5.2, with a SAMS pilot accessing near-real time position data via the Iridium link and directing the colleague's ship to the recovery site. At the conclusion of mission 1, Talisker was returned via the *NLV Pole Star* to the NLB base in Oban, Scotland. At the conclusion of mission 2, Talisker was returned by the *FRV Magnus Heinason* to the DAMRI lab in Torshavn, Faroe Islands, from where it was recovered by SAMS staff, an effort which required three days including travel.

5.5. Deep-water vessel-based surveys

The deep-water vessel-based survey outlined in Case Study 5 was undertaken on the NERC vessel RRS *James Cook*. This survey was actually undertaken over two back-to-back research expeditions that lasted 51 days. As discussed above, it is not appropriate to evaluate typical costs based upon a long and highly specialised scientific research expedition such as this. The day rate mentioned above of £20-25 k for ocean-going research vessels still applies, although costs associated with mobilisation and technical support are inevitably higher for cruises involving a deep-water ROV.

5.6. Shallow-water vessel-based surveys

More appropriate details of costs can be obtained from the two shallow-water vessel-based surveys, outlined in Case Studies 6 and 7. Survey costs for small vessels can vary considerably, depending on the vessel(s) used and the extent of the area being surveyed and the water depth. Generally, the deeper the water, the easier and quicker the survey is achieved, due to the wider multibeam swath width (see Table 5.3). Shallow waters (<30m) take much more time to survey, but much higher seabed resolution can be obtained.

Water Depth (m)	Swath width (m)
25	87
50	173
75	260
100	346
125	434
150	520
175	606
200	692
225	779
250	866
275	952
300	1039
325	1126
350	1212

Table 5.3: Seabed coverage (swath width) and water depth, based on a 120^{o} beam angle.

An additional consideration is the survey specification; typically this follows International Hydrographic Organisation (IHO), which can be detailed and requires careful planning in order to achieve the specification. The Sea of the Hebrides dataset in Case Study 6 was principally undertaken to IHO order 1a standard, providing data of the highest quality.

Typically, the costs of a 20-100 m survey vessel vary from anywhere from £7000-£25,000 per day (+VAT and fuel costs), the higher cost vessels being fitted out with a full complement of oceanographic equipment and working 24 hours per day. Additional costs need to be found for hydrographers and technical support staff to collect and process the data. Typically a hydrographer can expect about £500-£750 per day plus expenses when at sea.

Using the example of a moderate sized MPA in the Sea of the Hebrides, perhaps the Muck Deep area, using a small inshore 20 m vessel with a hull-mounted MBES; an estimate of the cost of the 75 km^2 survey can be made as follows:

Survey Time estimate =	*5 days (assuming 12 hour working)*
Vessel Cost @£7900 per day =	*£39,500*
Hydrographer Cost@ £600 per day x2 =	*£6,000*
Total Survey Cost =	***£48,500 (excl VAT and fuel costs)***

Additional costs may be incurred if other products (e.g. contour maps, backscatter geotiffs, GSF data formats etc) are required. It can be assumed that a per diem rate of £500 is used. Extrapolating these estimates to a survey the size of the Sea of the Hebrides (2200 km^2) reveals the cost of extensive surveys in the relatively shallow waters of the UKCS.

Survey Time estimate =	*198 days**
Vessel Cost@ £7900 per day =	*£1,564,200 (assume 24hr working)*
Hydrographer Cost@ £600 per day x4 =	*£484,800*
Total Survey Cost =	***£2,049,000 (excl VAT and fuel costs)***

*Using an assumption of 45 days for approx. 500km^2 using a 7125 system and 24hr working.

For comparison, below is a summary of costs from the 2012 *White Ribbon* survey in the Isle of May area, which covered about 60 km^2 over a period of about one week. The *White Ribbon* is owned by BGS and is a day-survey boat, so the crew returned to port at Anstruther each evening where accommodation was pre-arranged. Surveying times differed from day-to-day according to tides and weather conditions. There were 16 days of potential survey, and only two days of full weather-down time. Considering weather down time,

surveying occupied approximately six hours per day, excluding transit times (~1hr/day). Some of the costs are known exactly e.g. equipment hire, whereas some have been estimated (e.g. Travel and Subsistence), therefore this table is a simplification of the exact expenditure. However, having also accounted for staff time, and various minor costs, this can be taken as a generally accurate statement of the full cost of the survey.

Costs: BGS *White Ribbon* - 17 day survey			
Equipment	**Days**	**Daily cost (GBP)**	**Cost (GBP)**
Hire: Side-Scan Sonar (SSS)			8300
Hire: Drop-frame Camera			2500
Hire: Sound Velocity Profiler (SVP)			500
Insurance for hired equipment			1500
Misc Consumables			500
Fuel			
Average fuel consumption was ~75litres/day	17	90	1530
Travel and Subsistence			
Avgerage daily cost of travel, accommodation, and subsistence per person was ~£90. Two to three people were active at any given time. Average daily cost = £225	17	225	3825
Staff Costs			
A total of five staff members participated in the survey, two or three at a time depending on what data were being acquired. The cost estimate includes cruise planning and data post-processing.			30000
Total			**48655**

Table 5.4: Summary of Costs; BGS White Ribbon Isle of May survey

In summary, the two examples provided here indicate that total costs for shallow-water vessel-based MBES surveys are likely to be in the range of £600-£800 per km^2, and that about 15 km^2 of daily (24 hr) coverage can be achieved totalling £9,000-12,000 per day.

5.7. Summary of AUV operations

Comparing costs of AUVs and research vessels is challenging due to the many variables associated with large marine infrastructure. Deploying a large AUV such as Autosub6000 requires a large vessel, and such vessels cost up to £25k per day to run (note that a large AUV with significant battery capacity is needed if power-hungry systems such as sidescan sonar are being run). However, it has to be remembered that the AUV is of course autonomous and, once deployed, the mother ship can then carry out other operations, e.g. sampling or geophysical surveys. In addition, Autosub can simultaneously collect a number

of data streams simultaneously, e.g. high-resolution sidescan sonar and colour seafloor photography.

Flying at a height of 50 m the Autosub6000 AUV can cover about 20-25 km^2 with multibeam bathymetry in a day. In deep water, the resolution that can be achieved (2 m or better) is far greater than is attainable using hull-mounted systems on a research vessel. The data presented in Case Study 1 demonstrate how the high quality of AUV data is of particular benefit in complex deep-water habitats, such as rocky reefs, canyons, or areas of deep-water coral communities.

In summary, it seems that the typical cost of AUV-based multibeam mapping is about £1000 per km^2, compared to similar vessel-based mapping that costs about £600-800 per km^2. However, it should again be stressed that AUV-based mapping includes the cost of the mother ship, which can be used for other tasks while the AUV is in operation. Other tasks, such as high-resolution sidescan sonar or seafloor photography over large areas, are likely to be more cost-effective with an AUV.

5.8. Summary of Glider operations

This study has shown that Gliders are significantly cheaper than research vessels for hydrographic and biological surveying of offshore sites, potentially over an order of magnitude cheaper. The ability to launch and deploy from relatively small vessels, and for missions to last for several weeks, also helps make these a highly cost-effective alternative for routine water column and pelagic biological monitoring. They are particularly useful for collecting repeat transect data over temporal scales of several days to weeks, which is expensive to undertake using a vessel. Another key advantage of Gliders is their ability to operate at all seasons and in all weathers (see Case Study 3), which is obviously not feasible for most research vessels.

As with AUVs, Gliders are vulnerable to entanglement in fishing gears or impacts from vessels, and this has to be considered during mission planning. Their small size and relatively low velocity does make them prone to drift in tidal currents, but their frequent surfacing means this can be corrected ‘on-mission’.

Further discussion on the pros and cons of AUVs and Gliders is included in WP6.

Work Package 6: Conclusions and Recommendations

WP Leader: Dr Russell Wynn (NOC)

6.1. The WP6 task

As set out in the proposal this task's remit was as follows:

"*This WP will pull together all of the above information into a series of concluding remarks about the feasibility of utilizing AUV and Glider technology for mapping and monitoring of the UK MPA/MCZ network. In addition, a series of recommendations for future work will be included. These recommendations will take account of new and emerging technology, e.g. the ability to undertake integrated bio-physical AUV or Glider surveys using traditional sensors for abiotic parameters and plankton biomass, as well as additional sensors for higher trophic levels (e.g. EK60 fish-finders and cetacean Passive Acoustic Monitors). Such developments are highly relevant to future MCZ mapping and monitoring work.*

This WP will be undertaken by NOC (with input from BGS and SAMS) between 1 March and 31 May 2012."

6.2. Conclusions and Recommendations

6.2.1. Recommendations based upon current AUV and Glider capabilities
This study has shown that AUVs are particularly well suited to high-resolution acoustic and photographic surveys, with the ability to collect accurately positioned data that is not affected by issues (e.g. pitch and heave) associated with towed platforms. New developments such as Autosub Long Range and air-launched AUVs will expand these capabilities and will have direct relevance to Defra monitoring requirements.

Gliders are a highly cost-effective and fit-for-purpose platform for water column survey and monitoring. Ongoing development of new sensors means that their capabilities are continually increasing, and multi-trophic-level monitoring is now feasible. They are particularly valuable for routine transects that might need to be repeated on a monthly or annual basis, and are able to operate in hostile environments that are difficult to access using research vessels, e.g. northwest UK in winter.

However, it should be noted that AUV and Glider operations can potentially be affected by adverse conditions, such as extreme tidal flows, high turbidity, and high density of shipping and/or fishing activity. In some regions, such as nearshore tidally dominated environments, research vessels are likely to remain a more cost-effective and efficient platform. In addition, research vessels are still necessary for direct water column and seafloor/sub-seafloor sampling.

In conclusion, it is recommended that future mapping and monitoring of the UK MPA network will benefit both financially and scientifically from the increased application of AUV and Glider platforms, particularly if vessel fuel costs continue to increase. A combination of commercial and Government operators will likely be required to carry out routine operations in an efficient and cost-effective manner (see Section 1.7.2 and 1.7.3). Research vessels will remain as the optimal platform for survey of certain environments and where direct sampling is required. Further proof-of-concept studies will be required to validate methodologies and assess the repeatability of specific surveys undertaken with AUVs and Gliders (see below).

6.2.2. Defra SEPF project
Since starting this study, the project team have subsequently developed another research project with Defra entitled '*Novel AUV and Glider deployments to inform future MPA and*

MSFD monitoring strategy in UK shelf waters'. The SEPF proposal document is copied below, as it is highly relevant to this WP. The project has been approved and is due to start in 2013.

Introduction
The UK is committed to developing an ecologically coherent network of Marine Protected Areas (MPAs) as part of the UK Marine and Coastal Access Act 2009. In English waters a total of 127 Marine Conservation Zones (rMCZs) have recently been recommended as high priorities for protection, although the long-term strategy (and cost) of monitoring this network has yet to be determined. In addition, the UK will also have to devote significant resource to monitoring programmes that contribute to our obligations under MSFD.

Rapid advances in Autonomous Underwater Vehicle (AUV) and Glider technology are providing the UK research community with opportunities to test novel sensors and methodologies in increasingly complex and hostile offshore environments. These platforms generate datasets that are of higher spatial and temporal resolution than traditional ship-based datasets, and can be highly cost-effective. Here, we propose two 'proof-of-concept' studies involving the application of novel sensors and innovative methodologies to the mapping and monitoring of complex, temporally variable, and commercially and biologically important shelf habitats in UK waters. This proposal is timely as it brings together existing expertise within DEFRA (CEFAS, JNCC) and NERC (NOC, PML and SMRU) to form a multi-disciplinary partnership that benefits from significant leveraged resource through the £5M NERC Ocean Shelf-Edge Exchange Research Programme (RP), the £11M NERC-DEFRA Shelf Sea Biogeochemistry RP and the £1M pa NERC-led UK Marine Environmental Mapping Programme (MAREMAP). Although the SEPF contribution is relatively small, it will support additional ship-time and equipment trials specifically targeted at DEFRA's strategic requirements as outlined below.

Aims/objectives
This project has two main aims:

1) *To undertake Glider deployments in a region of the UK shelf characterised by tidal-mixing fronts*. Tidal-mixing fronts are boundaries between seasonally stratified and tidally mixed waters. Satellite-based front maps[1] are already being used as a data layer in the regional MCZ projects (project MB0102), with the assumption that these fronts are pelagic 'biodiversity hotspots' for multiple trophic levels (from plankton through to fish and cetaceans) due to a variety of physical processes. However, this assumption is not supported by adequate data in UK waters due to the logistical and economic challenges associated with ship-based monitoring of these environments. Gliders are able to monitor dynamic environments across multiple trophic levels for periods of several weeks, which is beyond the capabilities of the UK research vessel fleet. ***SEPF funding will, for the first time, enable Gliders carrying innovative sensors to be deployed in dynamic frontal regions in UK shelf waters***. The objective is to deploy Gliders carrying Echosounder and Passive Acoustic Monitoring instruments to assess fish and cetacean abundance either side of major frontal features, as well as at the front itself (which will be identified on real-time satellite imagery). The results will help determine the future role of Gliders for monitoring a broader range of hydrographic features as required for MPA and MSFD monitoring.

2) *To undertake hi-res mapping of benthic habitats in areas of mobile substrate characterised by significant temporal variability, in order to test both the repeatability of the survey methods and the biological response to the changing habitat*. Benthic habitats in UK waters are drastically under-sampled due to the logistical and financial challenges associated with ship-based data collection in these environments. Assessment of key MSFD indicators (e.g. seafloor integrity) will therefore continue to be difficult and expensive. However, developments in AUV technology mean it is now possible to undertake high-

resolution seafloor mapping and photographic transects simultaneously, and independently of the host vessel. Trial deployments in selected areas are vital if we are to assess the cost-effectiveness of these tools, and to separate variability introduced by survey methodology/equipment and natural variability in seafloor habitats (across different temporal scales) from future management measures, e.g. restrictions on bottom trawling. ***SEPF funding will, for the first time, enable repeat AUV surveys over several weeks to be undertaken in mobile benthic habitats in UK shelf waters***. An example target area could be the extensive zone of mobile bedforms off southwest UK that are included within at least one large rMCZ. Long-term MAREMAP funding will then be used to undertake repeat AUV mapping in the surveyed area one or two years later, in order to assess inter-annual variability in both the substrate (habitat) and the benthos.

Specific research questions
The key research questions to be addressed are:

1) Can tidal-mixing fronts in UK shelf waters be identified as biodiversity hotspots, holding higher densities of plankton, fish and cetaceans than adjacent stratified or mixed waters?
2) Is the near-surface expression of tidal-mixing fronts (as viewed from satellite imagery) representative of the whole water column, or do we need other methods to adequately map and monitor these features in three dimensions?
3) Is it feasible to use AUVs to undertake repeated high-resolution surveys over selected sections of seafloor, and does the extra resolution significantly alter interpretations of habitats and biodiversity?
4) How do benthic habitats and species vary in areas of mobile substrate, both in the short-term (weeks) and the longer term (years)? Can this natural variability be separated from changes induced by management measures?

Policy context
This project will deliver results that will inform future mapping and monitoring strategy in DEFRA, specifically related to the UK MPA network and MSFD obligations. Linking the project with the NERC Ocean-Shelf Edge Exchange RP will also provide access to novel biogeochemical sensors on Gliders (e.g. nitrates) that will provide important environmental context for the higher trophic level monitoring being undertaken in this project. Management of threats to mobile species, e.g. fisheries bycatch of cetaceans, is challenging in large-scale and mobile habitats such as tidal-mixing fronts (which are often important sites for commercial pelagic fisheries); proving the relationship between fronts and mobile species will therefore also inform the future Common Fisheries Policy and the large-scale SCANS surveys.

Alignment with essential criteria and suitability for the SEPF
This multi-disciplinary project (involving oceanographers, geoscientists, biologists and technologists) is closely aligned with SEPF objectives as 1) it cuts across several components of the DEFRA marine research programme, including marine environment, marine biodiversity and marine fisheries, 2) it brings together multiple partners to tackle research questions that will inform future MPA and MSFD monitoring strategy, 3) the proposed research is linked to a new NERC RP (see below), but SEPF funds will be specifically targeted at DEFRA's strategic long-term requirements, 4) the project will further strengthen links between the DEFRA and NERC community, building upon synergies recently developed within the £11M NERC-DEFRA Shelf Seas Biogeochemistry RP, and 5) the proposed 'proof-of-concept' studies requiring SEPF support could significantly influence the nature of future marine monitoring in UK shelf waters.

Leverage
SEPF funds will gain significant leverage from the NERC Ocean Shelf-Edge Exchange RP[2], which has a major field programme with combined ship-based and AUV studies in UK outer

shelf waters in 2013. Specifically, the work will complement the activities of the NERC FASTNET project[3] (Fluxes Across the Sloping Topography of the North East Atlantic), and four sub-projects that have been funded under the Sensors on Autonomous Underwater Gliders call. Although FASTNET is focussed on relatively distal shelf edge locations, leverage will be provided for this proposed project in the form of shared ship-time and Glider resources, as well as NERC staff and PhD students. Linkage to FASTNET will provide important physical and biogeochemical context for the proposed Glider deployments (as will the linkage with the ongoing Shelf Seas Biogeochemistry RP). Finally, the long-term MAREMAP programme will support further AUV monitoring at the selected site(s) beyond the one-year period of SEPF funding, i.e. in 2014/15.

References

1) Miller, P.I. (2009) Composite front maps for improved visibility of dynamic sea-surface features on cloudy SeaWiFS and AVHRR data. Journal of Marine Systems, 78(3), 327-336.
2) http://www.nerc.ac.uk/research/programmes/shelfedge/
3) http://www.nerc.ac.uk/research/programmes/shelfedge/documents/fastnet-summary.pdf

Appendix 1: Summary table of known UK AUV and gliders within the scope of the report

Capabilities existing as of 4/2012 in black and, where known, planned are in red. Total is 40 vehicles as of April 2012.

Type	Owner	Manuf	No.	Vehicle	Depth (m)	Endurance (days)	CTD	O_2	CHl CDOM OBS	PAR	µStruct	Camera	N & P	Acoustics
AUV	NOC	NOC	1	Autosub3	1600	3	X	X	X		X		X	ADCPx2, Swath
			1	Autosub6000	6000	1	X	X	X			X	X	ADCPx1, Swath, SBP, SS
			1	Autosub LR	6000	Up to 180	X	X	X		X	X		
	SAMS	Hydroid	1	REMUS 600	600	<3	X		Chl		X			ADCP
	HWU	Hydroid	1	REMUS 100	100	<1	X							ADCP
	MOD	Hydroid	12	REMUS 100	100	<1								µBathymetry and swath
			~4?	REMUS 600	600	<3	X?							?
Glider	NOC	WRC	4	Deep Slocums	1000	Typ 86	X							
			2	Slocum 117 & 194	200	~42	X	X	X					
			1	Slocum 175	200		X				X			
		iRobot	1	SG Bellatrix	1000	Up to 180	X	X	X	X			X	Passive
			1	SG Canopus	1000	Up to 180	X	X	X	X				
			1	SG Denebola	1000	Up to 180	X	X	X				X	Passive
			1	SG Eltanin	1000	Up to 180	X	X	X					
	BAS	WRC	2	Deep Slocums	1000	Typ 86	X	X	X					
		iRobot	1	Seaglider	1000	Up to 180	X	X	X					Imagenex 853
	SAMS	iRobot	2	Seaglider	1000	Up to 180	X	X	X					
	UEA	iRobot	1	Seaglider	1000	Up to 180	X	X	X					
			1	Seaglider	1000	Up to 180	X	X	X	X				
			1	Seaglider	1000	Up to 180	X	X	X					Imagenex 853

KEY

CTD: Conductivity Temperature and Depth
OBS: Optical Basckscatter
N&P: Nitrate and Phosphate nutrients
SBP: Sub-Bottom Profiler
CHL: Chlorophyll via Fluorescence
PAR: Photosynthetically Available Radiation
ADCP: Acoustic Dopper Current Profiler
SS: Sidescan sonar
CDOM: Coloured Dissolved Organic Matter
mStruct: Microstructure (Temperature and Velocity)
Swath: Multibeam swath bathymetric echo sounder
853: Short range 120kHz zooplankton echo sounder

Appendix 2: Why do Gliders have a much longer endurance than propeller-driven AUVs?

The answer is straightforward. But when confronted with this question, very many scientists and engineers provide woolly or wrong answers. The following may help remove confusion over the propulsion of undersea gliders.

Start with some simple mechanics: Work Done is Force times Distance Moved. It is the work done that we are interested in for propulsion. It is measured in Joules (J), and the batteries will have a declared capacity in Joules.

Think about where in the trajectory of a glider the batteries are called on to do work: at the inflexion between dive and climb at the very bottom of the profile. An electric motor drives a pump that moves a volume of fluid from an internal to an external reservoir against the hydrostatic pressure. As Pressure is Force divided by Area, and Volume can be written as Distance times Area, the Work Done is simply Pressure times Volume.

For example, a Slocum electric glider diving to 1000 m, would typically need to pump 500 cm^3 ($5x10^{-4}$ m^3) of oil against a pressure of 1010 dBar (10.1 MPa), giving a work done of 5050 J. *However*, this is for a 100% efficient system. For a Slocum, we can calculate the actual work done at 1000 m by multiplying the power into the electric motor (Watts, or Js^{-1}) by the time the pump is on (s). Typically, this will be of the order of 9000 J, ignoring the energy converted to heat in the battery internal resistance. The efficiency is simply the theoretical work done divided by the actual, in this case about 56%. The equivalent efficiency of the motor and controller within an Autosub AUV is about 70%. Consequently, glider endurance is <u>not</u> because of higher propulsion engine efficiency.

All well and good, but this does not actually answer the question. To do that we have to look at an alternative expression for the Work Done. In this case we consider the Force due to drag on the glider as it moves through the water. This is a far more complex problem that calculating the work done as set out above, and is fraught with assumptions. In a simplified form the Force due to drag is: $F = 0.5\ C_d\ A\ r\ V^2$, where F is the Force in Newtons (N), C_d is a drag coefficient (difficult to get right, and it should account for all the imperfections on an actual glider and AUV), A is the frontal area of the glider, r is the seawater density, V the glider velocity. In one second the work done is this Force times the Velocity (distance divided by time) of the glider, hence the work done each second is $0.5\ C_d\ A\ r$ V3.

Let us now compare this glider with an Autosub AUV. The glider travels at ~0.4 ms^{-1}, compared with 1.8 ms^{-1} for Autosub. The cubic dependence on speed of rate of work done means that the glider, on this factor alone, requires only one 90^{th} of the propulsion power of the Autosub. But, if we assume similar drag coefficients (in reality they are different but of same order), the frontal area of the glider at 0.036 m^2 is about one 18^{th} that of Autosub at 0.64 m^2. Thus, overall, the glider propulsion power is some one-1620^{th} that of Autosub. Hence, although Autosub3, for example, carries a total battery capacity of about 180 MJ for propulsion (and everything else) and a glider may only carry 12 MJ for propulsion (and everything else), the glider endurance is very approximately (12/180) times 1620 that of Autosub 3, or just over 100 times. The answer is, therefore, the slow speed, the small size, and, assumed here, the low power expended on the control systems and sensors within the glider.

Appendix 3: Autosub missions during research cruise JC060 (Case Study 1). EDM Eastern Darwin Mounds; WDM Western Darwin Mounds; PFA Polygonal Fault Area; RB Rockall Bank; LFSSS low frequency sidescan sonar (120kHz); HFSSS high frequency sidescan sonar (410kHz).

#	Start date & time [GMT]	Duration Hrs	Loc.	Start	Max Depth [m]	km travelled surveying	Survey Mode	Area Surveyed [km^2]	Notes on mission
37	12/05/2011 11:39	3.8	EDM	59.8678 N 7.0580 W	1036	n/a	n/a	n/a	Initial shakedown test mission. On first attempt at dive the AUV headed off in the wrong direction – rudder installed incorrectly. Noise affecting the obstacle avoidance caused erratic depth control. Tail lifting lines had come out before recovery.
38	13/05/2011 19:13	22.8	WDM	59.8143 N 7.3806 W	943	83.3	EM2000 LFSSS	14.4	Sternplane failure near the end of mission causing large depth excursions
39	15/05/2011 20:01	17.2	EDM	59.8502 N 7.1151 W	1015	66.6	EM2000 LFSSS	25.2	Multibeam and side scan survey of the Darwin mounds.
40	22/05/2011 01:30	19.8	WDM	59.8252 N 7.3995 W	969	79.9	EM2000 HFSSS	15.5	The AUV ran out of power while circling at the end of the mission dropping abort weights and then surfaced.
41	25/05/2011 19:03	17.9	PFA	58.1747 N 16.4458 W	1163	77.3	EM2000 HFSSS	16.8	AUV ran out of energy and aborted during surfacing
42	30/05/2011 19:55	10.5	RB	56.6689 N 14.0124 W	405	43	HFSSS	6.9	Concerns that one battery was not discharging caused us to reduce the mission length. In practice the battery functioned normally.
43	01/06/2011 21:15	15.6	RB	57.9669 N 13.9982 W	219	69	HFSSS	12.0	All ok.
44	03/06/2011 06:38	15.0	RB	58.0863 N 14.1754 W	319	68.9	HFSSS	12.0	All ok.
45	04/06/2011 07:02	16.5	RB	57.8504 N 13.9704 W	179	70.7	HFSSS	13.0	All ok.
46	05/06/2011 09:26	15.6	RB	58.0708 N 14.1790 W	322	60.7	EM2000 HFSSS	n/a	Hires SS, camera and multibeam evaluation mission for the CODEMAP project.
47	08/06/2011 21:59	0.8	EDM	59.8430 N 7.0442 W	789	N/A mission was terminated	HFSSS	N/A mission was terminated	The mission was terminated due to the control plane failing in a similar fashion to Mission 38.
48	09/06/2011 10:16	17.2	EDM	59.8491 N 7.1143 W	1053	65.7	HFSSS	10.8	All ok.

Appendix 4: Abbreviated mission diary, showing the main events of mission 1. Highlighted comments refer to transect endpoints (magenta), interactions with ocean currents (red), and eddy investigation timeline (cyan). From Sherwin and Dumont (2012a).

Date (2009-10)	Dive no.	Location	Comment
12 Oct	1	56.56 N, 7.48 W	First dive completed at 13:44 h. 24v 1.12 Ah
14 Oct	77	56.47 N, 7.84 W	Porpoising started
17 Oct	200	56.49 N, 9.02 W	At shelf edge 24v: 18.67 Ah
18 Oct	235	56.60 N, 9.39 W	Porpoising ended
19 Oct	241	56.63 N, 9.68 W	First deep dive in RT
26 Oct	283	57.26 N, 11.14 W	Anton Dohrn Seamount
30 Oct	301	57.35 N, 12.72 W	Bad GPS fix (58.22 N, 12.43 W) - false drift current
31 Oct	304	57.35 N, 12.82 W	At ROCK (Rockall Bank). 24v: 33.88 Ah
12 Nov	353	56.66 N, 9.02 W	At SHELFE (shelf edge). Round trip 1 completed. 40.63 Ah
19 Nov	380	57.13 N, 10.25 W	Arrested by strong eastward current S of Anton Dohrn Seamount
26 Nov	408	57.42 N, 10.82 W	On the Anton Dohrn Seamount
28 Nov	415	57.33 N, 10.74 W	Westward travel resumed just S of Anton Dohrn
7 Dec	449	57.26 N, 10.51 W	Switched off cap file upload to reduce power consumption and transmission costs
9 Dec	458	57.30 N, 10.69 W	Arrested by impenetrable eastward current S of Anton Dohrn. Allowed to continue without interference.
10 - 14 Dec	459 - 480	just S of Anton Dohrn	Experiment to see what happens with passive piloting in a strong opposing current. Result - no westward progress!
15 Dec	481	57.32 N, 10.67 W	Decide to go south to the HEBRIDE (Hebrides Terrace Seamount) to avoid eastward current
16 Dec	486		Communication lost due to basestation being switched off. Unable to command Talisker to go west
17 - 19 Dec	487 - 499	eastern Rockall Trough	Problems restoring communication. Strong current carries Talisker too far south.
20 Dec	500	56.64 N, 9.96 W	Finally picked up new target of ROCK (Rockall)
21 Dec	503	56.54 N, 10.25 W	Hebrides Terrace Seamount, now going west
29 Dec	532	57.39 N, 12.80 W	At ROCK (Rockall Bank). 24v: 63.26 Ah
13 Jan	592	56.68 N, 9.02 W	At SHELFE (shelf edge). Round trip 2 completed. 69.98 Ah
14 Jan	593	56.69 N, 9.04 W	Stuck on bottom at 545 m - emergency surfacing
25 Jan	636	57.28 N, 12.90 W	At ROCK (Rockall Bank). 24v: 75.15 Ah
28 Jan	647	56.84 N, 12.09 W	Broke off return trip to track through eddy
31 Jan	659	57.63 N, 12.13 W	Northernmost point of eddy investigation
04 Feb	673	57.24 N, 12.18 W	End of eddy investigation
14 Feb	708	56.69 N, 9.08 W	At SHELFE (shelf edge). Round trip 3 completed. 83.32 Ah
22-23 Feb	740 - 745	approaching Rockall	NAL Research disconnected Talisker for supposed non-payment of bills. No transmission
23 Feb	742	57.33 N, 12.78 W	At ROCK (Rockall Bank). 24v: 87.46 Ah
5 Mar	780	56.66 N, 9.14 W	At SHELFE (shelf edge). Round trip 4 completed. 92.13 Ah
8 Mar	789	56.58 N, 9.78 W	Final dive at 05:22 h. Roll motor failure.
9 Mar		56.72 N, 9.51 W	Recovered by NLB Pole Star

Appendix 5: Abbreviated mission diary, showing the main events of mission 2. Highlighted comments refer to transect endpoints (magenta), interactions with ocean currents (red), and eddy investigation timeline (cyan). From Sherwin and Dumont (2012b).

Date (2011)	Dive	Location	Comment
3 May	1	56.67 N, 7.12 W	First dive completed at 14:21 h. 23.9v 8.39 Ah; 10.3v 11.07 Ah
11 May	302	56.99 N, 9.19 W	First deep dive in RT 22.2 v: 23.98 Ah. 1.7v drop in main battery. Unusual wiggle in the climb first noticed.
13 May	311	57.26 N, 10.17 W	Furthest N before encountering cyclonic eddy drive towards the south
17 May	328	56.75 N, 10.80 W	Furthest S in large mesoscale feature (is it an eddy?)
19 May	332		Sent towards the Anton Dohrn Seamount
23 May	354	57.40 N, 11.13 W	On top of Anton Dohrn Seamount. New target ICE_BAS in the Iceland Basin at 60° N 20° W.
23 to 28 May	353	56.66 N, 9.02 W	Encountered very strong NE currents that backed NW and then W as Talisker crossed the western side of the Trough. This obstructed her from reaching Rockall
2 June	398	58.82 N, 14.44 W	Crossing southern side of the George Bligh Bank. Front encountered with cooler water towards the west.
9 June	428	59.19 N, 16.51 W	Reached the western side of the Hatton-Rockall Plateau. Very weak (tidal) currents on the plateau, but speeds increasing on southern flank of Hatton Bank
14 June	450	59.58 N 17.87 W	Over 990 m on N side of Hatton Bank in Iceland Basin. Website now shows NRL global NCOM model predictions
19 June	469	60.05 N, 18.97 W	In Iceland Basin, struggling to get to ICE_BAS. NCOM model shows opposing currents in a front. Cut losses and decided to make directly for the Iceland Shelf.
23 June	486	60.77 N, 18.64 W	Encountered intense anti-cyclonic eddy pushing Talisker south. Invoked some novel commands to get her out. In so doing managed to drive Talisker round in circles!
25 June	492	60.68 N, 18.68 W	Heading north again. Problems with understanding the relationship between $NAV_MODE and $HEADING.
30 June	513	61.43 N, 18.61 W	24v battery reading 20.5 v. This is a cause for concern and sent emails to Fritz etc and have contacted Hedinn Valdimarsson in case an Icelandic recovery is necessary.
	after 514		Thereafter the condition of the 24 v battery is an on going concern
12 July	561	63.25 N, 19.68 W	Reaches ICE_SHELF2 at the Icelandic shelf edge
13 July	565	63.31 N, 19.70 W	Furthest north position. Problems with navigating because of strong currents and variable topography. Much discussion in log book.
14 July	571	63.20 N, 19.59 W	Start to fly eastward along Icelandic Shelf edge with $HEADING,100 (and $NAV_MODE,0)
17 July	597	63.22 N, 18.49 W	Hit bottom at 182 m. Move S into deeper water.
20 July	611	63.07 N, 17.95 W	Hit bottom at 911 m. Low salinities near the surface. High backscatter values causing concern.
30 July	650	62.35 N, 15.09 W	Turned off Wetlabs puck because all frequencies appear contaminated
31 July	655	62.27 N, 14.75 W	Reached ICE_BAS_NE, now heading for Iceland-Faroe Ridge (IFR).
1 Aug to 5 Aug	666 - 676		Strong southwards currents preventing northward progress
16 Aug	727	62.99 N, 12.20 W	Furthest point on ridge. Strong tides. Bottom at 482 m. Redirected

Date (2011)	Dive	Location	Comment
			towards ICE_BAS_NE
18 Aug	740	62.39 N, 11.53 W	Bottom temperature < 2° C at 825 m.
to 22 Aug	744 - 755	62.23 N, 11.38 W 62.02 N, 11.29 W	24v battery voltage declined from 20.6 v (744) to 19.9 v (748) to 19.6 v (755). Contacted Bogi Hansen to see if FFL can rescue Talisker.
24 Aug	763		Turned off all sensors and altimeter. Set dive depth to 700 m.
25 Aug to 2 Sept	764 - 841		Variously put Talisker on surface or got her to dive to shallow depths depending on wind drift conditions
3 Sept		61.33 N, 9.78 W	0617 GMT: Talisker finally on board Magnus Heinasen. Set $T_RSLEEP to 1 day to save Iridium charges.
Finally			
26 Jan 2012		FIMR lab Torshavn	Batteries 23.42 v and 8.81 v on external power, 22.73 v and 10.22 v on own power. OK for shipping.